Gold(I) *N*-Heterocyclic Carbene Complexes: a Chemical and Biological Study of their Therapeutic Potential as New Anticancer Agents

Von der Fakultät für Lebenswissenschaften

der Technischen Universität Carolo-Wilhelmina

zu Braunschweig

zur Erlangung des Grades eines

Doktors der Naturwissenschaften

(Dr.rer.nat.)

genehmigte

D i s s e r t a t i o n

Von Riccardo Rubbiani

Aus Modena / Italien

1. Referent: Professor Dr Ingo Ott

2. Referent: Professor Dr. Conrad Kunick

3. Referent: Professor Dr. Luigi Messori

eingereicht am: 08.10.2012

mündliche Prüfung (Disputation) am: 17.01.2013

Druckjahr 2013

Vorveröffentlichungen der Dissertation

Teilergebnisse aus dieser Arbeit wurden mit Genehmigung der Fakultät für Lebenswissenschaften, vertreten durch den Mentor der Arbeit, in folgenden Beiträgen vorab veröffentlicht:*

Publikationen

Rubbiani R., Can S., Kitanovic I., Alborzinia H., Stefanopoulou M., Kokoschka M., Mönchgesang S., Sheldrick W. S., Wölfl S., Ott I., *Comparative in-vitro evaluation of N-heterocyclic carbene gold(I) complexes of the benzimidazolidene type*, Journal of Medicinal Chemistry, *54*, (**2011**), 8646-8657

Rubbiani R., Kitanovic I., Alborzinia H., Can S., Kitanovic A., Onambele L. A., Stefanopoulou M., Geldmacher Y., Sheldrick W. S., Wolber G., Prokop A., Wölfl S., Ott I., *Benzimidazol-2-ylidene gold(I) complexes are thioredoxin reductase inhibitors with multiple antitumor properties*, Journal of Medicinal Chemistry**,** *53*, (**2010**)**,** 8608–8618

Tagungsbeiträge

Rubbiani R., *"Gold(I) carbene complexes: from design to bioactivity"* (Oral presentation), Universitá degli studi di Firenze, grad-school invited seminar, Firenze, Italy (2012)

Rubbiani R., Can S., Alborzinia H., Stefanopoulou M., Kokoschka M., Sheldrick W. S., Wölfl S., Ott I., 10th Ferrocene Colloqium,: *"Gold(I) NHC complexes: TrxR inhibition and influence on cancer cell metabolism",* (Poster), Braunschweig, Germany (2012)

Rubbiani R., "*From chemistry to biology: rational design, biodistribution and bioactivity of new gold(I) N-heterocyclic carbene complexes*" (Oral presentation), East China University of Science and Technology, institute seminar, Shanghai, China (2011)

Rubbiani R., Can S., Kitanovic I., Alborzinia H., Stefanopoulou M., Kokoschka M., Sheldrick W. S., Wölfl S., Ott I., International Conference of Bioinorganic Chemistry15: *"Drug design, inhibition of thioredoxin reductase and in-vitro biological activity of a series of gold(I) NHC complexes"*, (Poster), Vancouver, Canada (2011)

Rubbiani R., "*Benzimidazol-2-ylidene gold(I) complexes as antiproliferative thioredoxin reductase inhibitors with multiple antitumor properties*" (Oral presentation), Pharmazie Seminar TU-Braunschweig, Braunschweig, Germany (2011)

Rubbiani R., "*Gold(I) NHC complexes: a class of compound with a high biological potential*", (Oral presentation), East China University of Science and Technology, institute seminar, Shanghai, China (2010)

Rubbiani R., Kitanovic I., Alborzinia H., Can S., Kitanovic A., Onambele L. A., Wolber G., Prokop A., Wölfl S., Ott I., Asian Bioinorganic Conference 05, *"Benzimidazol-2-ylidene gold(I) complexes as antiproliferative TrxR inhibitors"* (Poster), Kaohsiung, Taiwan (2010)

Rubbiani R., Kitanovic I., Alborzinia H., Can S., Kitanovic A., Onambele L. A., Wolber G., Prokop A., Wölfl S., Ott I., Tagung der Deutschen Pharmazeutischen Gesellschaft: *"Gold(I) carbene complexes: a class of compounds with a high biological potential"*, (Poster) Braunschweig, Germany (2010)

Rubbiani R., Kitanovic I., Alborzinia H., Can S., Kitanovic A., Onambele L. A., Wolber G., Prokop A., Wölfl S., Ott I., International Symposium of Bioorganometallic Chemistry 11, *"Glutathione reductase/thioredoxin reductase systems as molecular target for antiproliferative gold(I) carbene complexes"* (Poster) Bochum, Germany (2010)

Rubbiani R., Symposium of Bioinorganic Chemistry: "*Glutathione/thioredoxin reductase system as molecular target for antiproliferative gold(I) carbene complexes*" (Oral presentation) Goslar, Germany (2010)

Time of accomplishment

The present work was accomplished between May 2009 and October 2012 at the Faculty of Pharmacy, Institute of Medicinal and Pharmaceutical Chemistry, of the Technische Universität Braunschweig

Financial acknowledgement

Financial support and research collaboration of this work by “Deutsche Forschungsgemeinschaft” (DFG) with the research group FOR630 “Biological Function of Organometallic Compounds” and Volkswagen Stiftung are gratefully acknowledged.

Thanks

I want really to thank my mentor Prof. Dr. Ingo Ott for the innovative and interesting theme, the constructive discussion, the constant supervision and the freedom to develop my ideas.

I want to thank all the collaboration partners with whom I worked in these years. Especially, I want to mention Prof. Dr. Stefan Wölfl for the possibility to spend some days working in his laboratory in Heidelberg; Prof. Dr. William S. Sheldrick for the intensive collaboration; Prof. Dr. Luigi Messori for his willingness in being my reviewer, correcting my thesis and his invitation to Florence; Prof. Dr. Qian and Prof. Dr. Xu for the possibility to spend several week and work in their laboratories in Shanghai and Prof. Dr. Conrad Kunick to accept in being my reviewer and commission member.

A key contribute to my whole work has been supplied by my research group. I definitely have to thank the LabManager, Luciano, Julia, Kely, Laura and Vincent to build a beautiful atmosphere that encouraged scientific discussion as well as important “social moments”.

I have to thank all the people at the Institute of Medicinal and Pharmaceutical Chemistry of the Technische Universität Braunschweig and especially Magnus Matz.

I must mention also Suzan Can, Hamed Alborzinia, Igor Kitanovic and Pavlo Holenya from Heidelberg, Liliane Olambele and Prof. Dr. Aram Prokop from Köln, Yvonne Geldmacher, Malte Kokoschka, David Koster, Jan Dittrich, Johanna Niesel, Jessica Lemke and Marilena Stefanopoulou from Bochum, Prof. Dr. Gerard Wolber from Berlin, Tanyu Cheng and Wang Xin from Shanghai. Their collaboration was an important contribute for my work.

Finally I want to thank Franziska and my family for the imperishable support.

a Franziska

List of Abbreviations

5',5'-Dithionitrobenzoic acid = DTNB

5`-Adenosine monophosphate kinase = AMPK

5'-Thionitrobenzoic acid = TNB

Atomic Absorption Spectroscopy = AAS

ATP binding cassette = ABC

Before Christ = b.C.

Bond dissociation energy = BDE

Bovine serum albumin = BSA

Camptothecin = CMPT

Carbonyl cyanide 3-chlorophenylhydrazone = CCCP

Coupling costant = J

Density functional theory = DFT

Delocalized lipophilic cation = DLC

Deoxyribonucleic acid = DNA

Dimethylformamide = DMF

Dimethylsulfoxide = DMSO

Dulbeco minimum essential medium = DMEM

Electronspray ionization = ESI

Electron impact = EI

Ethyl-diamino-tetraacetic acid = EDTA

Extracellular signal-regulated kinase = ERK

Fast atomic bombardment = FAB

Fetal calf serum = FCS

Food and drug administration = FDA

Fluorescence-activated cell sorting = FACS

Focal adhesion associated protein kinase = FAK

Gas chromatography = GC

Glycogen synthase kinase beta 3 = GSK-3β

Gold phosphole inhibitor = GoPI

Glutaredoxin = GTR

Glutathione = Glu

Glutathione peroxidase = GPx

Glutathione reductase = GR

Glutathione-S-transferase = GST

Half inhibitory concentration = IC_{50}

Heat shock protein 27 = Hsp27

Hertz = Hz

High performance liquid chromatography = HPLC

Hour = h

Human serum albumin = HSA

Inductively coupled plasma mass specrometry = ICP-MS

Interleukin 1 = IL-1

Lactate dehydrogenase = LDH

Mitochondria membrane potential = MMP

Mitogen activated protein kinase = MAPK

Mammalian target of raptamycin = mTOR

MAPK-ERK kinase 1/2 = MEK1/2

Mass spectrometry = MS

Molecular weight = MW

Multidimensional protein identification technique = MudPIT

Multi resistance protein = MRP

N-heterocyclic carbene = NHC

Nicotinamide adenine dinucleotide (phosphate) / reduced = $NAD(P)^+$ / NAD(P)H

Nuclear Magnetic Resonance = NMR

Phosphate buffer saline = PBS

Propidium iodide = PI

Proto-oncogene protein tyrosine kinase = Src

Reactive oxygen species = ROS

Roswell Park Memorial Institute = RPMI

Structure activity relationships = SAR

Thioredoxin = Trx

Thioredoxin reductase = TrxR

Tolman electronic parameter = TEP

Triethyl phosphine gold chloride = TEPG

Triisopropyl phosphine gold chloride = TiPrPG

Trimethyl phosphine gold chloride = TMPG

Triphenyl phosphine gold chloride = TPPG

Tumor necrosis factor alpha = TNFα

Ultraviolet = UV

World Health Organization = WHO

List of Tables

List of Figures

List of Schemes

List of Equations

Table of Contents

1. Introduction

1.1 Historic notes, cancer insurgence and pathology

A neoplasm or tumor is a fluid or solid cell alteration caused by a change in metabolism or genetic mutation and abnormal growth. When the regulation and control of the normal cell cycle and cellular role fails and the neoplasm is correlated with the insurgence of peripheral damage, migration and organism life risk the tumor is defined malignant and the pathology is called cancer. The word *cancer* derives from the Greek *carcinos* (crab) used by Hippocrates to describe the macroscopic features of the pathology (similar to the body of a crab with the appendages that represented the blood vessels). Thus, the disease was analyzed since ancient times, with the earliest cancer report going up to the Egyptians, more than 5000 years ago.[1] Around the 16th century B.C. it is possible to find reports about cancer and its cure in both old medicine *papyri* (*Ebers Papyrus*, *Leyde Papyrus* and *Edwin Smith Papyrus*).[1,2] In India, early information about this malignancy could even be found in the epic poem *Ramayana*. In the early century A.C., Aurelius Cornelius Celsius observed the formation of secondary tumor after removal of the primary one and Claudius Galenus correlated psychosomatic symptoms to cancer progression, assessing the black bile theory (body humors) of Hippocrates as cancer origin. In the same period, Pedanius Dioscorides drew up a list of botanical remedies for cancer disease that was in use for the following 15 centuries. Between the 11th and 12th century the Arabian physicians Avenzoar and Averrhoes employed esophageal sounds for cancer diagnostic while the pharmacologist Ibn Sina made use of arsenium for systemic therapy. During the Renaissance, Gabriele Falloppio made use of caustic pastes to treat malignant tumors. Since the 16th untill the end of the 19th century chemotherapy was mainly abandoned and surgery became the first line solution for cancer treatment.[1,2]

Even if the affection is known for several centuries and a lot of research has been performed, nowadays cancer diseases represent the second most frequent cause of death worldwide, with approximately 13 million of deaths per year (data from World Health

Organization, WHO).[3,4] This rate is always increasing due mainly to incidental factors. In fact, cancer development has been particularly related to aging and life conditions.[5] The increase in life expectancy and new factors or pathologies (like organ transplantation, obesity, diabetes, working conditions, tobacco, etc.) make the human body more susceptible to cancer. However, because just 5% of the malignant tumors have a hereditary source, a concrete reason for the development of the disease is hard to find.[5] Cancer has been described as an environment linked illness since most of the cases are strictly connected with the life style or the origin of the single person. Bad life attitudes (smoke, alcohol), uncontrolled work conditions (e.g. asbestos contact, heavy metal powder, benzene inhalation) provoke several hundred thousand cancer cases per year. An unbalance diet (e.g. high salt diet, low fruits and vegetables) is also the cause of the development of different forms of tumors.[6] There are more than 200 different cancers affecting the human body from the most common lung cancer to the less common throat, kidney or pancreatic malignancy. They are classified on the basis of the tissue that they are affecting or the primary tumor from which they developed. There are 5 main malignant tumor classes: *carcinomas* (the most common one, from epithelial cells), sarcomas (from the connective tissue), lymphoma (also called leukemia and most common in children, from hematopoietic tissue), blastoma (from not fully differentiated or developed cells, like embryos) and germ cell tumor (from pluripotent cells). Despite the localization and characteristic of the mother cell, all of them present similar symptoms and proliferation stages. In a first phase no referable symptoms could be normally noticed. However, once that the malignancy achieves a further development stage cancer is often associated with ulceration, local pain and bleeding. The tumor mass can provoke narrowing or blockage of organs or blood vessels resulting in function failure.[7]

Carcinogenesis and cancer development can be subdivided in three main phases. In the time the cell will encounter a mutation that will divert the cell from the normal cell cycle and modify the proliferative internal control. This mutation could be provoked just by a failure in DNA replication or by external induction. Alterations in the regulation of two

species of genes can be observed: expression of oncogenes which enhance the growth and repression of tumor suppressors which control the entrance of the cell into apoptosis.[6,7] Cells in this status are tumorigenetic but still not cancer. A second phase is represented by the replication of the mutant cells, which assess and multiply their oncogenes and tumor suppressor inhibition genes. This process will create what is called a primary malignant tumor or primary cancer. During this phase an enlargement of the tumor mass is noticed parallel to the formation of new blood vessels (angiogenesis) to provide more nutrients to the cancer cell agglomerate. The last phase and most dangerous for the human body is characterized by the possible migration of cancer cells from one tissue to another, even quite distant, through blood vessels and the lymphatic system. This displacement is called metastasis and is one of the main causes of therapy failure and death produced by cancer.[6]

Beside the symptoms, a number of screenings and tests are used to diagnose cancer. The most common methods are X-ray, blood or histological analysis or computer tomography (CT). X-ray and CT are non invasive techniques that determine the proliferation grade and tumor mass. Histological analysis determines genetic mutations or cell abnormalities by direct tissue extraction. Blood tests investigate specific tumor markers (cancer antigens like CA15-3, CA 125, beta-2-microglobulin B2M, prostate specific antigen PSA, alpha fetoprotein AFP, human chrorionic gonadotropin HCG, etc.) to individuate and possibly prevent the tumor development.[8-11]

Also at cellular level, cancer presents characteristic features, assessing the loss of differentiation and genetic mutation. Enzymes (like lactate dehydrogenase LDH), specific receptors (like epidermal growth factor receptor EGFR) or hormone receptors (in some cell lines, such as MCF-7 breast adenocarcinoma) are just some examples of over-expressed elements in cancer cells.[12,13]

During the long history of malignant tumor many remedies have been proposed, screened and involved in therapy. In 1955 the United State Congress founded the National Cancer Chemotherapy Service Center in response to the first therapeutic successes. It was one

of the first organizations in charge to promote and control anticancer research. In 1971, following the scientific rush, Richard Nixon declared “war against cancer” (“National Cancer Act”, 1971) and since that moment the fundings as well as the therapeutic solutions drastically increased.[14]

For a non metastatic solid malignancy, surgery represents one of the main solutions to cure cancer. The ablation of the tumor mass is a first choice treatment to increase life expectancy. The discovery of X-Rays in 1895 by Wilhelm Conrad Röntgen followed by the implementation with the radium ray by Pierre and Marie Curie opened the era of the radiation for diagnostic.[15] Because the radiations demonstrated dangerous cellular effects and good penetration capacity, many researchers (e.g. Curie, Abbe) applied ionized radiation in cancer therapy. The good result arose the treatment to elective therapy involved in half of the cases, in combination with surgery and chemotherapy. Chemotherapy is based on active molecules able to penetrate the tissue, reach the cancer and induce apoptosis. They are broadly used in different therapeutic cycle phases with an efficacy strictly linked to the toxicity of the drug involved. All these prophylaxis just in the U.S. cost huge amount of money (for example a pilot study on a possible genome atlas in 2007 cost more than 100 million dollar).[16,17] Despite the various strategies and treatments, cancer is nowadays still a deadly pathology representing 13% of the death causes worldwide (data from WHO). Even if the antitumor therapy results successful the patient who overcomes cancer has an increased risk to develop a secondary tumor. All the common therapies are aggressive and characterized by a lack of selectivity. Often the therapy in itself is another cause of tumor death.

1.2 Origin and state of the organic modern anticancer research

Despite the great number of efforts done, until the 18th century a stable strategy against cancer was still missing. At the end of the 1700 Burrows argued "that whatever has been proposed for the curing of cancers, are merely palliative medicines; and that no real specific has been hitherto discovered for that fatal disorder, although the physicians of all

nations, from the time of Hippocrates to the present, have, by numberless researches and experiments, made trial of everything in nature, from the most innocent drug, to the most virulent poison, both in the mineral and vegetable kingdoms; yet the disease still baffles the power of physic".[1] However, starting with the middle of the last century anticancer research drastically advanced. Especially in the field of chemotherapy many research groups dedicated their work to study the tumor cell physiology and synthesized new effective anticancer drugs.

The efforts, that during several centuries did not produce effective progress, achieved undoubted results by the study of the chemical warfare during the World War I and World War II. In consequence of the massive use of mustard gas bombs a large number of the civil population died. The autopsies confirmed a drastic reduction of the proliferation of somatic cells, especially in lymphoid tissue. The pharmacologists Frederick S. Philips, Louis S. Goodman and Alfred Gilman (see figure 1.1) applied this discovery to an animal model with lymphoma and observed substantial tumor suppression. Moreover, in collaboration with Gustav Linskog they treated a human patient with mustine (a mustard derivate) and noticed a reduction of tumor mass in the first days of treatment, proving the possible efficacy of the molecule and performing the first step in chemotherapy.[18]

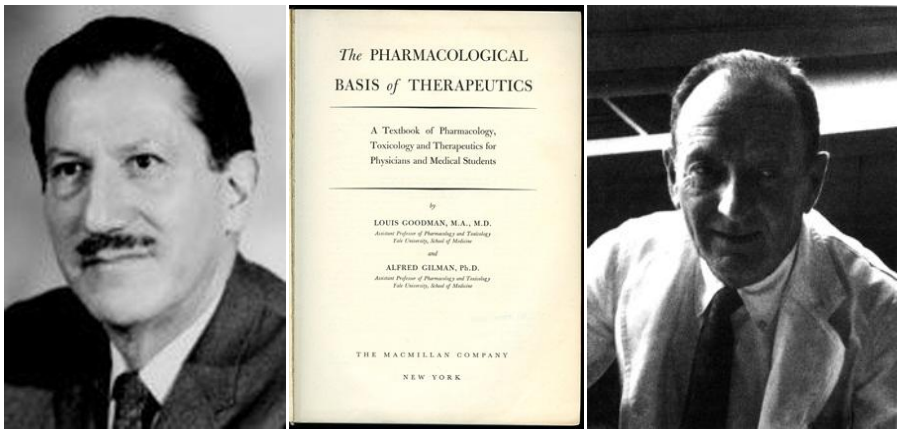

Figure 1.1: Louis S. Goodman (left), Alfred Gilman (right) and their work on therapeutics (center); picture obtained from *http://medicine.yale.edu/pharm/about/index.aspx* and from "biographical memoirs", The National academy Press *http://www.nap.edu/openbook.php?record_id=5406&page=59*

Almost simultaneously, in 1950s, Sidney Farber (see figure 1.2) observed that folic acid (vitamin B9, essential for DNA that in this time was still not discovered) stimulated the proliferation of acute lymphoblastic leukemia (ALL). Performing probably the first structure activity relationship and drug targeting, Farber treated ALL cells with folic acid antagonists such as aminopterin and amethopterin and observed a regression of the tumor.[19] Although the resistances opposed to the Farber´s study by the scientific community, the pathologist involved amethopterin (now known under the name methotrexate) in the cure of children ALL and published its results in the 1948. Just 10 years afterwards methotrexate was successfully involved in the treatment of choriocarcinoma, representing the first case of cancer cured by a chemotherapeutic and Farber was acknowledged with the name of "father of the anticancer chemotherapy".

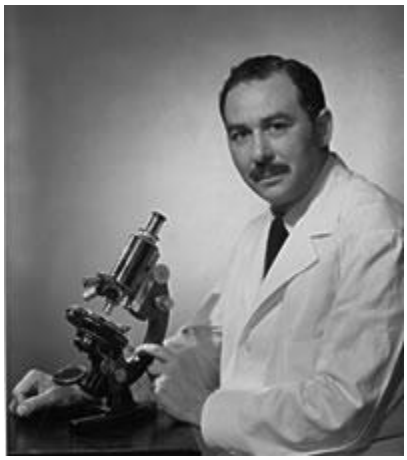

Figure 1.2: Sidney Farber father of the modern anticancer chemotherapy and founder of pediatric pathology; picture from DANA-FARBER Cancer Institute, *http://www.dana-farber.org/about-us.aspx*

As a direct consequence of the work of Farber many metabolites and chemical analogues of vital molecules have been investigated for their anticancer activity. A good example is the discovery in 1954 of the anti-cancer properties of 6-mercaptopurine or of of 5-fluorouracil, both the drugs simulating DNA nucleotides.[20,21] The anticancer research output grew up significantly and different strategies to achieve potent medicines or an

effective therapy have been proposed. An increasing number of studies started to test all the chemical and natural drugs for their possible anticancer properties. Between 1954 and 1996 a great number of natural drugs have been involved in cancer treatment like extracts from *Vinca Rosea* (e.g. vincristine), from *Taxus* (e.g. paclitaxel) and from *Camptotheca Acuminata* (e.g. topotecan).[22] The total synthesis of drugs like nitrosoureas derivates (e.g. fludarabine phosphate) or anthracycline compounds (e.g. daunorubicine, doxorubicine) was performed.[23,24] Combined therapy with different anticancer drugs and / or with the ablation of the most part of the tumor followed by the chemotherapeutic treatment resulted to be successful for the cure of ALL, Hodgkin and non-Hodgkin lymphomas as well as for some sarcomas. In 1966, in the ambit of contraceptive research, Dora Richardson synthesized for the first time an estrogen receptor antagonist called tamoxifen.[25,26] The link between breast cancer and contraception was already known and the following clinical trials established tamoxifen and its derivates as anticancer agents approved by the Food and Drugs Administration (FDA). Between the end of 19th and begin of the 20th century many advances have been made to understand the cell physiology. Scientists like Matthias Schleiden, Theodor Schwann, Franz Bauer, Richard Altman, Keith Robert Porter and many others put the cell at the base of organism life and characterized their organelles.[27] Especially in the second half of the 20th century cellular pathways comprehension drastically increased. The advent of advanced microscopy (fluorescent, confocal), mass spectrometry applied to biological system (proteomics, metabolomics and genomics) found specific pathways, processes or proteins present in cancer cells. All those discoveries contributed to the development of the targeted therapy in which chemotherapeutics interact selectively with vital cancer processes. For example, during 1990s the study of the oncogene Abl-Bcr highlighted the production of an analogous of the protein tyrosine kinase in tumors. The selective inhibition of this protein has been investigated starting from the screening of a large number of molecules, improved by a rational drug design. The results led to the nowadays

first line treatment for chronic myelogenous leukemia: Imatinib and its derivates.[28] A selection of anticancer molecules is shown in figure 1.3.

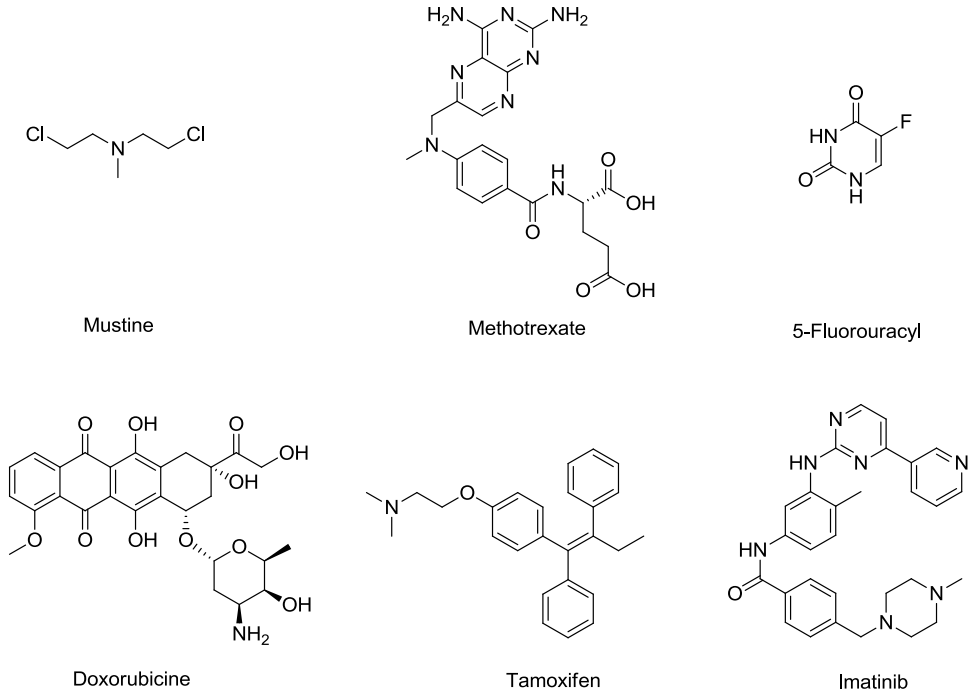

Figure 1.3: organic anticancer compounds

1.3 Metal complexes in cancer therapy: history and advantages

Metals play a central role in human life as well as in scientific research. In total 14 metals (four of the main groups: Na, K, Ca and Mg; ten of the transition group: Fe, Co, V, Cr, Zn, Mo, Cd, Cu and Ni) have a key role in the human body to control osmotic pressure, as regulators or messengers and are involved like stabilizers or enzyme cofactors.[29] Metals have been used by humans since ancient times. Beside the implication of their good conductivity (both for heat and electricity), malleability and ductility our forefathers employed them also as medicinal remedies. Examples are transcriptions of gold preparations dated at 2500 B.C and mercury ointments used by the Pharaohs or in alchemical healing preparations.[30]

The advent of modern metal based chemotherapy is dated at 1865 when potassium arsenite demonstrated anti-leukemia properties.[1] In 1870 Jorgensen synthesized the first

metal conjugates and in 1893 the Nobel Prize laureate Werner helped in clarifying their chemical configuration.[29] Metal based medicines have been prescribed for various pathologies until 1950 under the name of Fowler´s water. In 1909 Paul Ehrlich and co-workers discovered from a drug screening of several new molecules the anti-syphilitic properties of an arsenium based compound: arsphenamide or compound 606, an organo-arsenamide commercialized in 1910 under the name "Salvarsan".[31] This was the first attempt of drug discovery starting from a large set of substances. Salvarsan was used intensively during the first half of the 20th century and contributed extremely to eradicate dangerous pathologies. In 1927 Merthiolate (Thiomersal), an organo-mercury compound, demonstrated high antibacterial profile. In 1935 Forestier published the first study on gold compounds with anti-rheumatic properties.[32] Gold based drugs like Aurothiomalate, Aurothiosulfate or the oral administrable Auranofin are still nowadays benchmark drugs in that treatment.[33]

In 1965, Barnett Rosenberg, observing the similarity between the mitotic fuse and an electric field assumed that bacteria could also be influenced by it. The serendipitous results showed a block in the replication of the microorganism and opened the era of metal complexes in anticancer therapy. The following experiments proved that electrolysis at the electrode formed an active platinum species responsible of the cytostatic effects.[34] The obtained molecule, Cisplatin, was involved successfully in the therapy against testicular and ovarian cancer, neck cancer as well as lung cancer.[35,36] Since that day many research groups focused on the platinum medicinal chemistry and the main mode of action of Cisplatin has been probably disclosed.[37-40] Outside of the cell the concentration of chloride anions do not allow exchange reaction between water molecules and the chlorido ligands of Cisplatin. When the molecule penetrates into the cell, the low Cl^- concentration promotes the formation of aqua complexes, replacing the chloride. This adduct is the active form of the platinum derivate that penetrating into the nucleus interacts with the minor groove of DNA, especially with nucleotide guanine, inducing cross-linking of the bases with consequent loss of functionality and arrest in replication.

Unfortunately, Cisplatin demonstrated also severe damage to nerves and kidney. Side effects included nephrotoxicity and neurotoxicity, nausea vomiting, and hair loss etc.[41,42] To try to reduce these problems at the end of the 20th century two other platinum derivatives started to be involved in therapy: Carboplatin and Oxaliplatin.[40] Beside the side effects another main problem characterized the platinum anticancer category: the development of resistance phenomena. Cisplatin and its derivates undergo a high metabolization. For example, their reaction with glutathione promotes the drug-extrusion by over-expressed specific efflux channels. The new generation of platinum derivatives proposed in the last decade many possible solutions to overcome both the problems and to find another action mechanism. The coordination of key molecules (like hormones or long alkylic backbones) or the use of other oxidation state (Pt(IV)) or configuration (transplatinum derivatives) showed the broad patterns pool at researchers disposal in bioinorganic chemistry.[43]

Cisplatin was the first extremely successful bioinorganic drug and nowadays it (or its derivatives) is involved in almost 50% of the cancer treatments. Following the affirmation of the platinum complexes the scientific world started to put interest in the medicinal applications of inorganic chemistry. Preliminary screenings of Cisplatin analogues with different metals have been reported. Almost all the atoms between the 4th and the 12th group of the periodic table have been used to synthesize new potent drugs.[44] Currently, it is established that a single mode of action for a single metal is far to exist. Very often even different oxidation states correlate with different modes of action.[43,45-47]

Ruthenium is the most investigated metal, after platinum, in medicinal chemistry. Many reports are already attesting the capacity of this metal in cancer therapy. There are 2 ruthenium based compounds actually in clinical trials (KP1019 or its more soluble Na derivate KP1339 and NAMI-A).[48] Ruthenium complexes are a large and different family of compounds with a broad bioactive spectra, from valuable cytotoxic potency to less side effects and strong antimetastatic effects (NAMI-A, RAPTA-series).[42] The mode of action of ruthenium compounds is still not completely understood, indeed inhibition of enzymes

containing a cysteine in the active site (cathepsin B, glutathione reductase) has been observed. Some ruthenium complexes can cover more than 30 stereo isomeric configurations enabling the drug to interact or bring an opportune functional group to appropriate region. This revolutionary concept was used by Meggers and co-workers to design kinase inhibitors that manage to reach picomolar IC_{50} values.[48,49]

Metal derivatives of a well established drug were also successful in the field of medicinal chemistry. Especially, the use of metallocene moieties (e.g. ferrocene) resulted in overcome of the standard drug resistance. That was observed for drugs like ferrocifen (the metallocenyl derivative of tamoxifen) able to influence various cancer cell lines, estrogen receptor positive as well as negative (ER(-) and ER(+)), and for ferroquine (the metallocenyl derivative of chloroquine) active on chloroquine resistant malaria strains.[50,51] Promising results have been also obtained with titanium complexes.[52] Dichlorido titanocene and its more soluble derivative titanocene Y demonstrated strong antiproliferative properties and reached also the clinical trials but failed because of metabolization problems.[53] Some of the key molecules witnessing the importance of metal complexes in medicine are reported in figure 1.4.

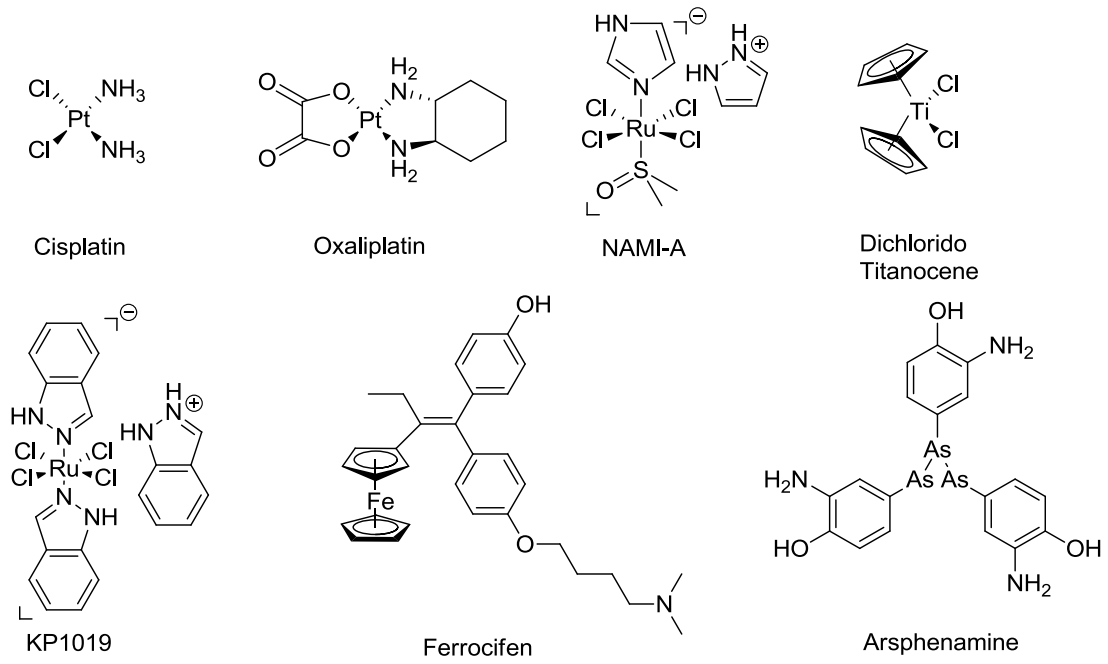

Figure 1.4: examples of metal complexes involved in therapy and research or undergone clinical trials

These are just few examples of the efficacy of metal complexes in cancer therapy. Many molecules (e.g. chromocene platensimicyne derivate, silver(I) theobromin, iridium and rhodium phenantroline or bisphenantroline, metal porphyrin, carbene complexes, cobalt ruthenium and iron bio-conjugates etc.) underwent preliminary studies.[45,54-57] This great capability of metal complexes is mainly due to the special features offered by these species. Metal complexes present different characteristics being very adaptable and effective drugs. Metals possess a multi electron orbital sphere with access to d orbitals and a modular stable configuration. The steady state is reached when the environment of the metal has 18 electrons (18 VE, e.g. iron). Sometimes when the bond presents an increased distance the metal can lose ligands and be stable with a minor number of electrons (16 VE, e.g. rhodium) or an increased one (19 VE, e.g. cobalt). They are characterized by different oxidation states with different reactivity. In a physiological environment there is the presence of many possible substituents and many studies describe a typical metal reaction called: ligand exchange reaction.[58,59]

The ligand exchange reactions confer to the metal the capacity to answer to specific chemical environment modification due to their electronic configuration. It is known for example that the formation of an aqua complex of Cisplatin is the activation step required to achieve antitumor activity. Meanwhile glutathione (a tripeptide present in high concentration in the cell) reacts with Cisplatin too, but the product represents one of the main processes of intra-cellular drug elimination.[59]

As reported above the various configurations, hybridization and the inert character of some metals suggested the possibility to work with them as molecule scaffold. The pioneer work of Meggers and co-workers demonstrated the suitability of the ruthenium or iridium stereochemistry to achieve and optimize the enzyme – drug interaction, reaching extraordinary inhibition potency.[60]

Third peculiarity of the metals reactivity is their catalytic properties. During the 19th and 20th century the chemistry research and industry produced a huge number of catalysts to

perform a great number of reactions. Most of them included a metal center carrying the activity. This concept can be also applied in the medicinal field when the reactive center of the drug is a metal. Examples of a metal complex with an interesting catalytic profile are the aminoferrocenyl derivates of Mokhir and co-workers in which cytotoxicity is obtained by the catalytic conversion of Fe^{3+} in Fe^{2+} self-reproducing in biological conditions and inducing reactive oxygen species (ROS) production.[61] Examples of the listed metal advantages are reported in figure 1.5.

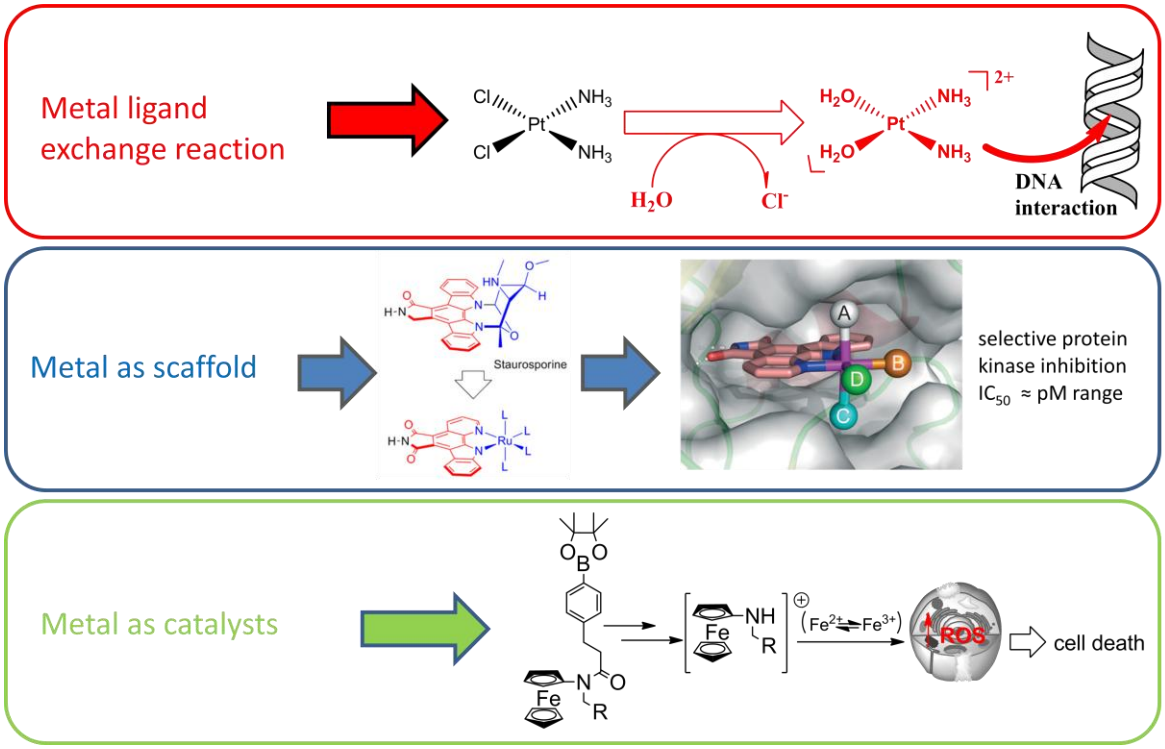

Figure 1.5: reactions and advantages of metal based molecules (blue and green pictures from references 60 and 61)

The first generation of metallodrugs have been characterized by platinum derivates, their DNA targeting activity and the efforts of the researchers to achieve better compounds with the same mechanism of action. However, an increasing number of reports assess that DNA targeting therapy is resulting inadequate.[48,62] Cells with high metabolism (e.g. hairs, skin) present the same DNA replication rate as cancer and the genetic material in itself is

one of the most controlled cellular macrostructures. With the improvement in technology output always more information on cancer metabolism are nowadays available. Fields as proteomics, genomics and metabolomics changed the approach of many researchers. Mapping the different cellular pathways enables the scientist to pick up crucial elements like siRNA, or kinases with a key role for signal translation and cellular counteraction. Immuno-techniques discovered characteristic proteins over-expressed in cancer cells as a possible new target for drug design. These new findings represent a begin of a second generation of metallodrugs that will aim specificity, selectivity towards cancer cells and potency.

1.4 A new gold rush

Gold played a central role in human life since the ancient time and it is probably between the first metal discovered by the mankind. It is an inert material with a good ductility and conductivity and it is spread in most of the regions of the world. Elaborate gold mining techniques have been developed by almost all our forefathers, from Alaska to the South African Republic. Reports of gold mines and gold manufactures go back to the Cro-Magnon era and in the Turin *Museum of Old Art* there is an official Egyptians map of a gold mine site of more than 4000 years ago.[63] Its excellent malleability, price / traceability ratio and impressive colors made of gold an excellent ornament material. From the pharaohs to the popes and sovereigns of all the times, the royal families and upper class carried gold weapons, decoration or clothes.

During the civilization development gold became also a potent symbol. In the Bible, in the Iliad and Odyssey poems gold is associated to immortality and fecundity. In the Chinese tradition the gold and yellow were the colors that represented the Emperor of the Sky and even in the Incas old transcription gold traces symbolized the tears of the god Sun (from “Gold in the Ancient World” by John Hiller).[63,64]

Starting in 5th century B.C. in Greece under Philipp II of Macedon, gold was employed in coinage of currency and this remained its main role through many centuries. Still

nowadays, the gold price has a relative stable value independently by wars, bourse depressions or financial crisis (see figure 1.6).

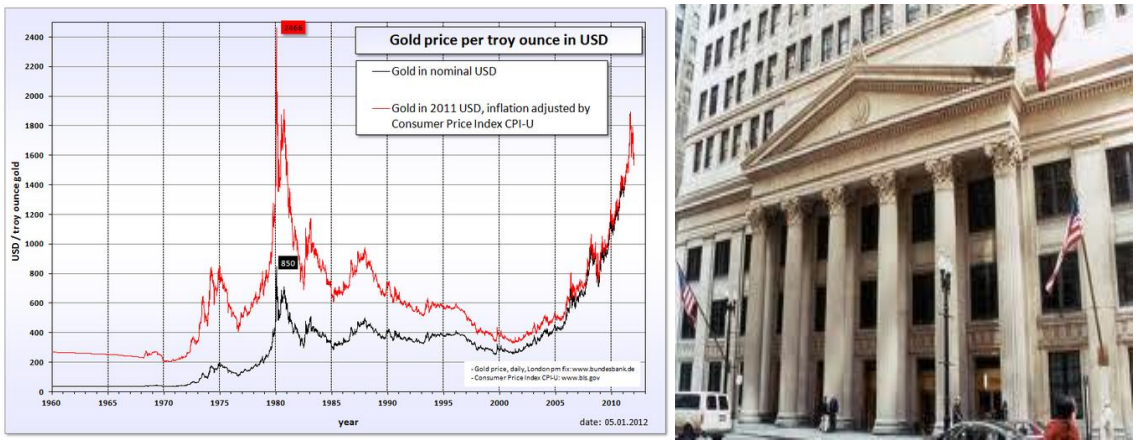

Figure 1.6: left) gold price fluctuation over the last 50 years; right) the federal reserve bank USA; source *Wikipedia common*

Alchemy considered gold as the noblest of all the elements and one of the mystical powers of the philosopher stone was to convert other metals to gold. The atomic number of gold is 79 and in the periodic table is placed beside mercury. Mercury is found liquid in nature and its chemical transformation it was considered to have the capacity to transcend different states and parallel to overcome the border between earth and heaven as well as the one between life and death. Gold was thought to be the end step of mercury transformations.[65]

Gold has been considered catalytically inactive for a long time with the exception of some sporadic studies that were in any case not showing advantages in comparison with other catalysts. Surprisingly within the second half of the 20th century gold industrial chemistry increased drastically. The activity of gold is mostly based on the size of the gold catalytic particles. The traditional preparation method for catalysts was the “impregnation method” which produced, in the case of gold, particles too large or bulky, impeding a good chemi-sorbtion of the reactant compounds.[66] Haruta and co-workers firstly started to work on the particles size. In 1980s they established new preparative methods called “deposition precipitation” and “co-precipitation” that enabled to

produce gold nano-particles of 2-4 nm of diameter (with the impregnation precipitation method they were > 10 nm). Together with this finding they discovered that with such particles gold molecules are able to selective catalyze the oxidation of carbon monoxide (CO) at drastic low temperature (-76°C) as well as epoxidation.[67] In 1973 Bond and co-workers published a milestone study that reported the hydrogenation of olefins over gold catalyst.[68] They demonstrated that even at not extreme temperatures (127-217°C) an efficient and chemo-selective mono-hydrogenation of alkene and alkyne was possible. They found that the catalytic capacity was influenced not just by the particle size of gold but also by the supporting material, changing from γ-Al_2O_3 to SiO_2 support (see scheme 1.1).

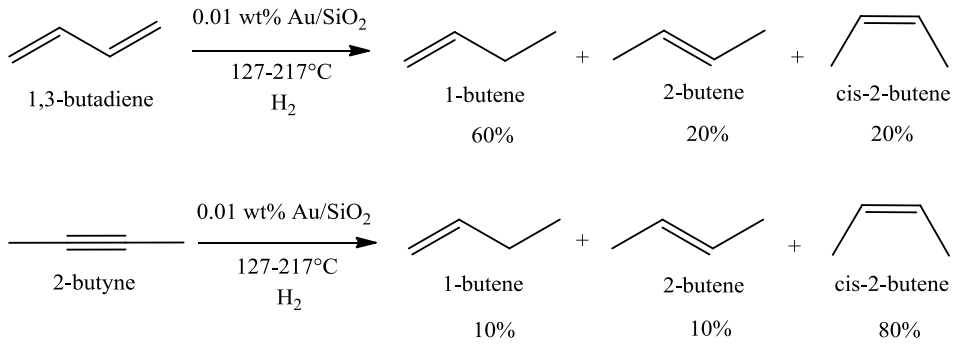

Scheme 1.1: chemo-selective alchyl mono-hydrogenation performed by Bond and co-workers (scheme taken from reference 66)

Stimulated by these discoveries, in the following years many research groups investigated gold catalytic properties and extended the application field to different carbonic structures (both aliphatic and aromatic) as even to functional groups. Gold has been found capable to catalyze hydrogenation reactions of α,β-unsaturated aldheyds, alcohols and polyols and C-H bond activation. Especially for nucleophilic attack Hutchings and co-workers described the hydrochlorination of ethyne to vinyl chloride, demonstrating gold(III) to be the most potent catalyst for such reactions.[66,69] Since 1990s, gold started to play an important role also in homogeneous catalysis. Especially, at the begin of the 21th century

effective generation of gold homogeneous catalysts have been synthesized by Corma and co-workers (e. g. Au-Me-duphos) or by Hosomi and co-workers ($ClAuPPh_3$) enabling complexes functional groups as alkenes, ketones, alkynes, alkyl halides, tertiary alcohols, aldehyds and carbamates to be processed.[70,71]

Gold has been also involved in healing remedies since 2500 B.C. It was probably the product of the simple deduction that something so rare and precious must also have extraordinary healing properties. Phoenicians, pharaohs as well as Incas population reported in their texts about gold preparations. Gold as medicament was also reported in "*De Materia Medica*" edited by Pedanius Dioscorides in the first century B.C. In the alchemy gold played also a central role such as important medicine (see figure 1.7). *Tinctura Aurii*, *Oleum Aurii* or *Essentia Aurii* were gold based remedies for cutaneous as well as *per os* application.[72,73]

Figure 1.7: alchemic representation of the gold working process with the 7 steps of metal elaboration, the patched alchemist and the rabbit as a guide (picture from ref. 74)

Although gold based therapies (also called aurotherapy or chrysotherapy in the case of rheumatoid arthritis) have been known since the ancient times, the real mechanisms of action are still not fully understood. Elemental gold is an inert material and just its salts or radioisotopes could have been involved in aurotherapy. Gold can be found in all oxidation states (between –I to +IV) but just two forms are better suitable for medicinal applications: gold(I) and gold(III).[33] Gold(I) is a soft Lewis acid with affinity for soft ligands (like thiolates) and presents a d^{10} close shell configuration enabling it to assume the trigonal three-coordination, tetrahedral four-coordination and the most important (for medicinal purposes) linear planar two-coordination. Gold(III) is harder than gold(I) and presents a d^8 close shell configuration with a classical square planar tetra coordination and analogies with platinum.[33,75]

Similarly to its catalytic properties, because of their instability medicinal research on gold drugs was quite rare until the last centuries. Parallel to the innovations in catalysis, a real new gold rush started also in medicinal chemistry. The first scientific studies about medicinal gold have been published at the end of the 19th century.[32] Gold compounds provided evidences to have an effect as anti-bacterial agents. In 1920 they were tested for tubercolosis treatment but did not show any relevant activity.[76] In 1935 Forestier studied their salts as possible anti-inflammatory drugs and demonstrated a disease regression due to the action of the gold(I) salts.[32] Afterwards, we have to wait almost 40 years to see another medicinal gold study.

At the end of the 20th century some derivatives of gold(I) started to be involved in anti-rheumatic therapy. Aurothiomalate, Aurothioglucose and Auranofin are registered marks.[76,77] Nowadays chrysotherapy is an established strategy to cure rheumatoid arthritis, with 50% to 70% chance of disease suppression and 20% of complete remission.[64] Despite the mode of action is still not understood, some dominant hypothesis have been postulated. The curative potential of gold complexes is mainly the result of the action of the different metabolized gold salts (Au(III), Au(I), Au^0). Au(III) can oxidize proteins and be reduced to Au(I). Gold(I) acts as chelating agent

forming a stable bond between cysteine residues. It inhibits key steps of the inflammatory answer such as the T-cell mediated antigen recognition, oxidative burst in the synovial fluid of the inflamed joints, the leukocytes migration and adhesion.[64,78] Some data reported the formation of Au^0 from Au(I) and postulated it to be responsible of the activity. Overall, the action of gold salts proved to be strictly linked to the immune-modulatory answer, inhibiting the protein kinase C and the protein tyrosine phosphatase, suppressing relevant cytokines (tumor necrosis factor α, interleukin-6) and lowering the maturation and circulation of lymphocites.[64,78] Other evidences assessed that gold drugs should be able to block COX-2 expression and prostaglandin production by destabilizing COX-2 mRNA.[79]

Research on gold based therapy has been applied to all the branches of medicine. In 1996 Shapiro and Masci investigated the effect of Auranofin on a HIV patient who was also affected by psoriatic arthritis.[80] Her skin lesions and arthritis resolved after Auranofin treatment and she has remained free of opportunistic infections during the following 24 months. Her $CD4^+$ count during oral gold therapy showed a significant increase in $CD4^+$ cells. Many research groups presented evidence of a reverse transcriptase inhibition by gold complexes. The main gold anticancer and anti-rheumatic drugs were tested and showed to have a therapeutic value against HIV.[80-82]

Since the discoveries of the influence of gold chloroquine derivates on *Plasmodium Falciparum* (*PF*) made by Navarro in the late 1990s many research groups started to investigate the anti-malarial and anti-parasitic properties of gold complexes.[73,74,226] The inhibition β-hematin formation, that provokes a mysfunction in heme aggregation, or the inhibition of falcipain 2 kinase, providing vital monomers (e.g. aminoacids) and the intercalation with DNA (against the malaria pigment formation) produced a essential reduction of the *PF* proliferation *in vitro* and *in vivo*.[83-86] The gold derivative resulted to be effective also on two chloroquine resistant strains of *PF*.[86] The successes achieved against malaria stimulated the researchers to investigate more in detail the effects of gold complexes as anti-parasitic agents. Gold(III) demonstrated to be potent inhibitor of

Leishmaniasis, with LD_{50} in the nano-molar range.[83,86] The trypanosomiasis family presented some metabolic analogies with cancer cells, especially for the anticancer drug response with inhibition concentration in the low micro-molar range, comparable with established drugs.[86] Gold(I) complexes have been recently also tested as anti-schistosomiasis agents. These parasites possess a thioredoxin reductase / glutathione reductase system, essential for the worm life.[83,86] Established drugs such as Auranofin and Aurothiomalate have been investigated and demonstrated to inhibit the extracted enzyme in the low nano-molar range provoking the worm death.

The interesting activity of a silver complex (Ag-sulphadiazine[87]) as anti-microbic stimulated many research groups to apply bioinorganic chemistry for the development of new anti-bacterial agents. Gold derivatives with ibuprofen or carbene ligands have been synthesized and demonstrated to be active towards some bacteria (e.g. *E. Coli*, *S. Aereus*).[88,89] Recently Cui and co-workers proposed two possible mechanism of action for gold as anti-bacterial agent. Gold complexes alter the membrane potential interfering with the ATP production. Concurrently, they inhibit the subunit of ribosome from binding tRNA.[90]

In 1985 Mirabelli and co-workers studied the anticancer properties of Auranofin and opened a new interesting horizon for gold based therapy.[77] Also for the anticancer effect the mode of action is still a debate point but a main target for gold complexes inside the cell has been found. Thioredoxin reductase (TrxR) is a key enzyme over-expressed in tumor cells that present in the active site a selenocysteine / cysteine pair.[91-96] Gold complexes reacted selectivity with the selenium, building a covalent adduct and inhibiting the enzyme activity as proved by biochemical as well as mass spectrometry investigations.[97-99] The inhibition of TrxR leads to an onset in cell homeostasis, reactive oxygen species production and apoptosis induction.[97] Gold(I) and gold(III) compounds resulted to be the most potent inhibitors for this key enzyme. Especially for this therapeutic category, the activity and selectivity of gold seems to be in close relation with the specificity and properties of the ligand. A good drug design will lead to an

effective structure activity relationship and more predictable results. Following this trend many possible ligands have been synthesized and tested (see figure 1.8).[100]

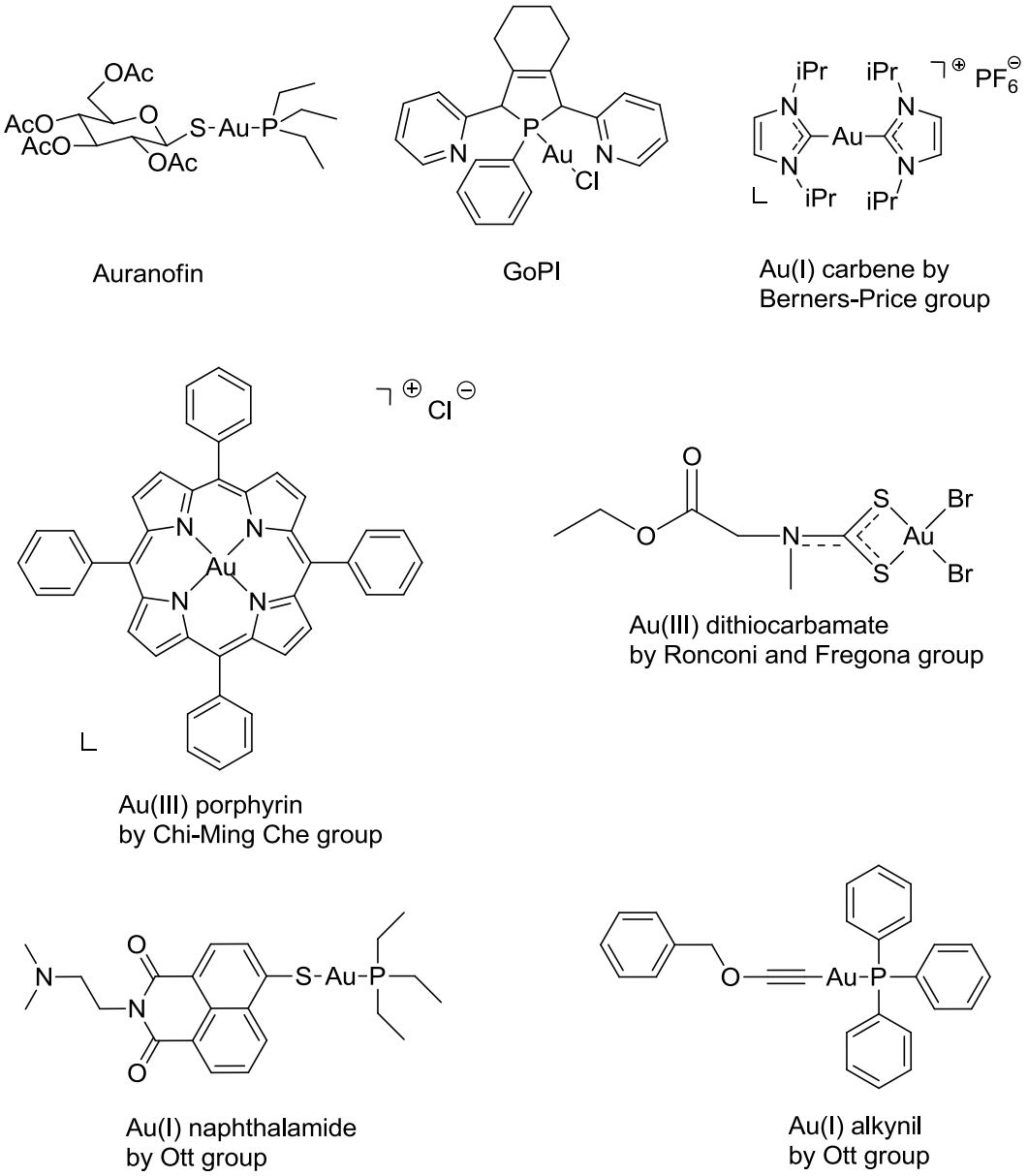

Figure 1.8: representative gold complexes

The main group of gold based anticancer agents is represented by the phosphines. Their ligands have been already diffusely used in catalysts because of their good coordination capacity. Gold(I) phosphine derivatives have been studied by many research groups and demonstrated outstanding biological properties and represent the most common example of gold(I) complexes.[101-104] They inhibit potently and

selectively the target enzyme TrxR possessing also a good profile towards other components of the antioxidant network (glutathione reductase, glutathione peroxidase), inhibit the 26S proteasome activity, block angiogenesis, induce apoptosis and have strong antiproliferative effects.[101-106] The variation of the second ligand at the gold center (e.g. naphtalimide, alkyn, thiol) influenced deeply the stability as well as the overall pharmacodynamic. It is important to mention that belonging to this class are the two most potent TrxR inhibitors nowadays discovered: auranofin and gold phosphol inhibitor (GoPI).[107] Until 2008 few studies also reported the activity of gold(I) carbene complexes.[108-111] In 2006 Berners-Price and co-workers published a milestone report on the interaction of this species with the TrxR system, the influence on mitochondria and the selectivity of a gold *N*-heterocyclic carbene (NHC) towards cancer cells.[110,112] Gold(III) class of compounds has been also investigated.[113,114] Examples of bioactive gold(III) complexes are represented by porphyrins, phenantroline or in general halides or nitrogen bonded derivates.[115-117] The biological data proved a strong interaction with the mitochondria membrane potential, induction of mitochondrial membrane pores, reactive oxygen species stimulation, interaction with DNA and apoptosis induction.[116,118] Recently gold(III) dithiocarbamate complexes resulted to be good TrxR inhibitors and trigger apoptosis through mitogen activated protein kinase ERK mediated pathway.[119]

Others interesting target enzymes have been recently discovered.[120,121] Casini and co-workers tested the activity of some different gold complexes on PARP-1, a key enzyme involved in the protection of DNA and in combinatorial therapies. They demonstrated that gold derivatives are more effective than the traditional organic inhibitor (3-aminobenzamide). A gold complex (Auphen) showed also a potent activity inhibition of the aquaglyceroporin-3 with IC_{50} value in the submicromolar range.[121,122] Recently the strong inhibition by Auranofin of the enzyme glutathione-S-transferase has also been proved.[123]

Very limited *in vivo* data are available for gold compounds. A partial success was obtained in the treatment of mice inoculated with lymphocytic P388 leukemia cells with Auranofin.

The therapy resulted in a dose dependent increase in survival up to a maximum of 22 days (more than 200 %). However the data could just be partially reproduced in another experiment with the same animal tumor model. Although less data are available for gold(III) species, very recent reports described the encouraging *in vivo* activity of gold(III) porphyrins and dithiocarbamates that respectively increase the survival rate of hepatocarcinoma up to 42 days (against 30 days for the control) and inhibition of tumor growth in invasive breast adenocarcinoma in nude mice and no toxicity was noticed up to 29 days.[75]

Although until nowadays no clinical trials are running for gold complexes the above reported data stand for the great potential of this class of therapeutics. Especially in the anticancer field always new promising drugs are required. Gold based therapy like in the past as nowadays demonstrated a great medicinal potential.

2. Aim of the project

As reported in the introduction metal complexes and especially platinum derivates represent nowadays a first line treatment against cancer and are involved in therapy (alone or in combination with surgery, radiation or other chemotherapeutics) in more than 50% of the cases. Despite the incredible success of platinum therapy, two main concerns about the use of cisplatin, carboplatin and oxaliplatin remain. First of all, platinum based drugs provoke severe side effects, sometimes ending up in death cases. Secondly, already after few treatments the cancer develops resistance to these drugs, defeating the therapeutic value but preserving the hard side effects for the patients.

The bioinorganic chemistry arsenal offers many solutions to correct these problems and to obtain efficient and selective anticancer agents. Among the different metals tested in the last decades, gold presents some interesting features. Gold has been involved in therapy since ancient times. Nowadays gold complexes are benchmark products against rheumatoid arthritis. Gold based therapy does not produce severe side effects during short time treatment (examples of them are just cutaneous rash, proteinuria or diarrhoea).[124] The main target of gold compounds is not DNA but proteins (like TrxR, GR, GPx, GST, 26S proteasome, etc.) enabling a broad range of medical targets and modes of action.

Aim of this PhD thesis was to synthesize, characterize and biologically evaluate a series of new gold complexes, suitable for anticancer therapy. The oxidation state I of gold was chosen because it enables a more stable complex coordination and it is borne by some of the most effective gold therapeutics. Carbene complexes of the Arduengo type (*N*-heterocyclic carbene, NHC) have been selected to be the core ligand of the new molecules. The direct σ coordination of the carbene carbon with the gold(I) atom should provide stability and remarkable bioactivity due to previous reports. Opportune modification at the NHC core (e.g. side chains) or at the second ligand (e.g. chlorido,

phosphine) will result in an essential change of the physical-chemical properties of the molecules and will lead to different bioactivity.

An intensive biological evaluation will assess the anticancer potential of the new gold(I) NHCs. Key point of the screening will be the interaction with the target enzyme TrxR. Since the complexes are expected to be good inhibitors, all the possible metabolic onsets provoked by their influence on TrxR will be observed (ROS stimulation, apoptosis induction, etc.). Selectivity will be established between TrxR and other enzymes belonging to the antioxidant network (e.g. GR, GPx). The carbene moiety is also expected to confer an overall good stability to the compounds. Therefore, the gold NHCs will undergo stability test in buffer as well as under relevant biological conditions (serum protein, small intracellular thiols). Anti-proliferative effects of the gold carbenes will be tested in different cancer cell lines as well as in resistant and healthy cell lines. The presence of gold will enable to trace the uptake of the compounds into the cell by a convenient and sensitive technique (atomic absorption spectroscopy, AAS). For a schematic representation of the target complexes see figure 2.1.

The overall data output of the present PhD project will contribute to enforce and improve the medicinal application of gold complexes.

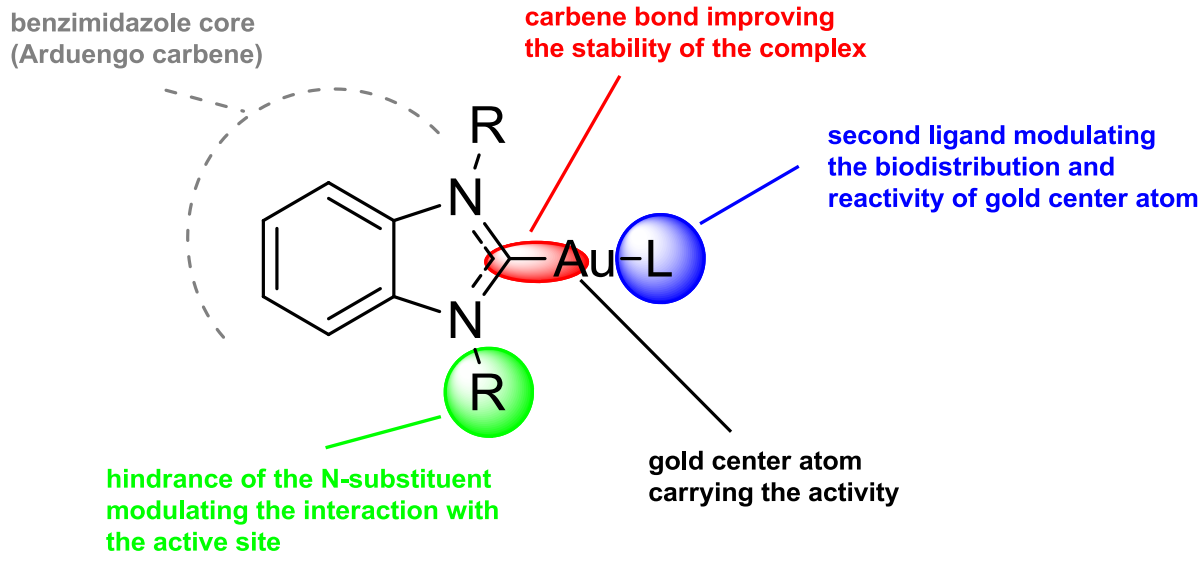

Figure 2.1: drug design of target gold(I) NHC complexes

3 Synthesis

3.1.1 Chemical consideration on series I

A steadily increasing number of reports assessed the suitability of gold molecules for medicinal implications.[33,96,100,125,126] The main problem affecting the benchmark gold based drugs (Auranofin, Aurothiomalate and Aurothiosulfate) is the high metabolization inside of the body once administered.[127,128] The binding to thiol shuttles (serum proteins), inactivation by small molecules (glutathione, ascorbic acid) and loss of the ligands defeated trustable drug designs and the study of possible structure activity relationships. An efficient investigation of the properties of different functional groups will contribute to optimize the drug design and stimulate the synthesis of more effective substances.

Metallic gold is an inert ductile material but its other oxidation states possess interesting chemical properties and biological profile. Au has a stable 18 electron configuration. The ionic chemical compounds of gold are soft Lewis acids and are present in nature almost in all the oxidation states between +I and +IV but specific medicinal interest lie in gold(I) and gold(III). Gold(I) can assume a trigonal three-coordination, tetrahedral four-coordination or linear planar two-coordination configuration geometry while gold(III) has just a classical square planar tetra coordination configuration geometry.[33,75] Gold(III) salts (e.g. $AuCl_4$) presented also a high metabolization under biological conditions and are easily reduced to gold(I). Recently, gold(III) thiocarbamates demonstrated outstanding biological properties.[115,116,119,129,130]

Since the discovery of the anticancer properties of Auranofin, gold(I) complexes started to be intensively investigated. Especially, Auranofin became the lead structure and activity comparison parameter for anticancer aurotherapy. The easy substitution of the thioglucosidic rest and the redox instability of the phosphine ligand direct the attention of the researchers to find other new stable coordinative solutions. The hypothesized mode of action of gold complexes involved a direct interaction between the metal center and cysteine or selenocysteine containing enzymes.[97,100,131-133] To trigger bioactivity, the

presence of gold in the molecule as well as a good leaving group is required. Since many of the most efficient gold complexes are phosphine derivatives, a detailed analysis of the phosphine ligand chemical properties and metal interactions would clarify the role of that residue and would allow a rational improvement with other ligand solutions.

A phosphorus atom containing three different alkyl residues (PR_3, phosphine ligand) possesses favorable coordinative properties.[134,135] The electron repulsion between the alkyl rests and the phosphorus decreases in presence of a metal coordination. This is due to the sequestration of the P lone pair engaged in the P-M bonding. This push forward and backward compensation effect stabilizes the length of the P-C bonds. The same electron lone pair attributes to the phosphorus atom Lewis base properties and, thus, affinity for Lewis acids (like gold). Phosphorus establishes a convenient σ coordination with the metal atom which locates also (though without the formation of a particular strong bond) electron density from the p and d metal orbitals to the phosphorus symmetrical p and s antibonding orbitals, giving the formation of a backbonding (see figure 3.1).[134,135]

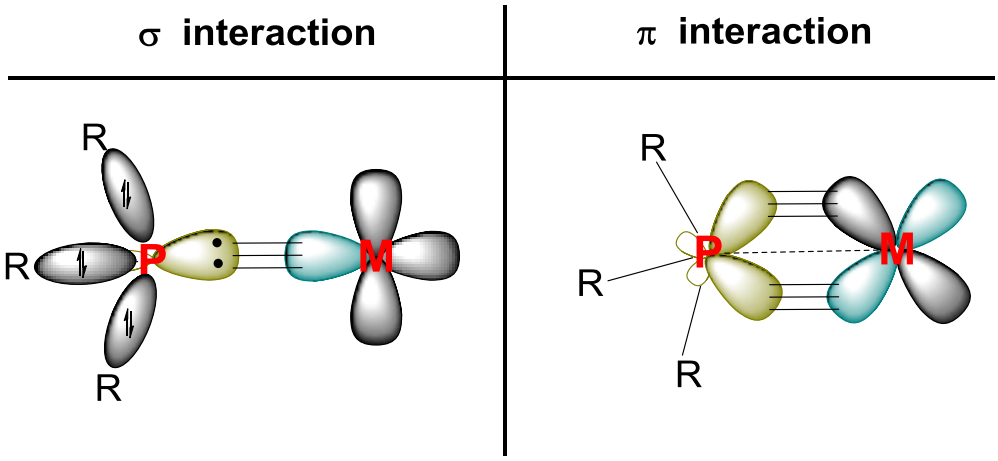

Figure 3.1: phosphine – metal interaction: left) σ binding orbitals and P electron lone pairs interactions, right) σ P and metal d bonding orbitals and d metal and p P antibonding orbitals interaction

The electron donor capacity of a single atom or a specific chemical environment could be described using the Tolman electronic parameter (TEP, ν).[134,135] TEP indicates the frequency or vibrational mobility of the carbonyl residue ($\nu_{CO}(A_1)$) of a complex containing

the electron donor ligand (in this case a phosphine ligand) binding to a nickel tricarbonyl moiety, measured with infrared spectroscopy. The higher the freedom degree of CO groups (see blue part in figure 3.2, with e^- representing the electrons), the weaker will be the CO triple bond, the higher the donor character of the ligand at the Ni atom.[136]

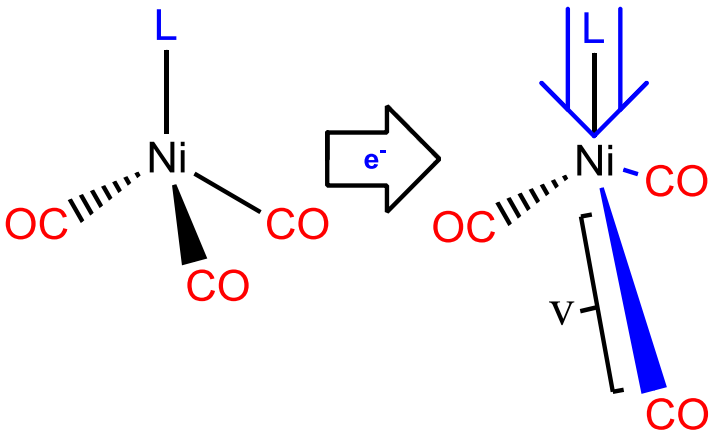

Figure 3.2: schematic representation of the CO vibration influenced by the ligand electron donor properties

The implication of a strong donor ligand according with $\nu_{CO}(A_1)$ could be a convenient starting point for the drug design of new stable metal complexes. TEP could be also implicated in the characterization of another emerging class of compounds with interesting properties: the carbene compounds.

A carbene is a molecule containing a central carbon with a valence II and an unshared electron pair.[133,137] They are classified in 2 categories depending on the electronic configuration: singlet or triplet. Singlet carbenes possess a spin-paired moment with a sp^2 hybrid orbital configuration, a total spin of zero (ħ) and represent the excited state of the carbene structures. Triplet carbenes present a paramagnetic character, two unpaired electrons with a total spin of one (ħ) and can adopt either *sp* or sp^2 hybridization. Unsubstituted hydrocarbon molecules assume often a triplet carbene with sp^2 hybrid configuration that represent the energy ground state of the compounds. Generally, triplet carbenes are more stable than singlet ones. However, the presence of geminal donor, like hetero-atoms, that delocalizes electrons in the empty p orbital of the carbene carbon

offers a compensation effect on the molecule and enables the singlet carbene to become the new energy ground state. There are no reported data about a similar effect for triplet carbenes. Overall, unstabilized carbenes possess a very short half-life.[133,137-139]

Carbene carbon could also be categorized for their intrinsic reactivity when they are coordinated to a metal. Fischer carbenes are described like electrophilic carbenoids due to the impoverishing effect of the bonded metal possessing an electron withdrawing ligand. Schrock carbenes are described like nucleophilic carbenoids due to the enriching effect of the bonded metal possessing an electron donating ligand. A third category is represented by the persistent carbenes that show a relative long half-life, stability and low reactivity. The *N*-heterocyclic carbene (NHC or Arduengo´s carbene) belong to that group and they found in the last decade broad use in catalysis as ancillary ligands (see figure 3.3).[140,141]

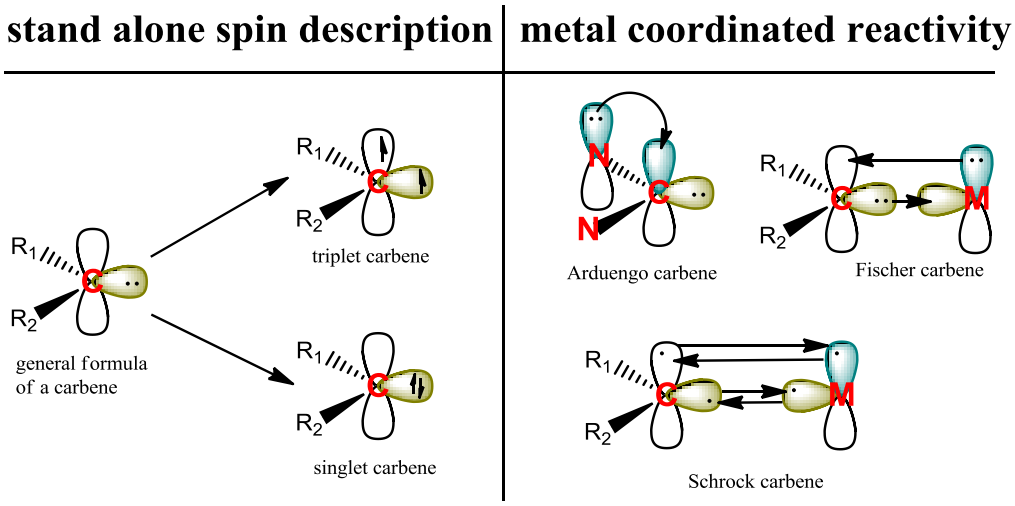

Figure 3.3: carbene classification: left) spin configuration, right) reactivity coordinated to a metal

The presence of two nitrogens and the aromatic ring (imidazole ring) enforces furtherly the half-life of the NHC through a *M*+ / *M*+ stabilization effect of the α-groups which compensate the p orbitals electrons lack and simplify the π conjugations (of the N) and molecule stabilization.[98]

Based on these properties it results clear to understand the strong TEP similarity between NHC and phosphine ligands. Furthermore, the class of the NHC resulted in a lower $\nu_{CO}(A_1)$ and thus in a stronger metal electron donor capacity (see figure 3.4).[135,136]

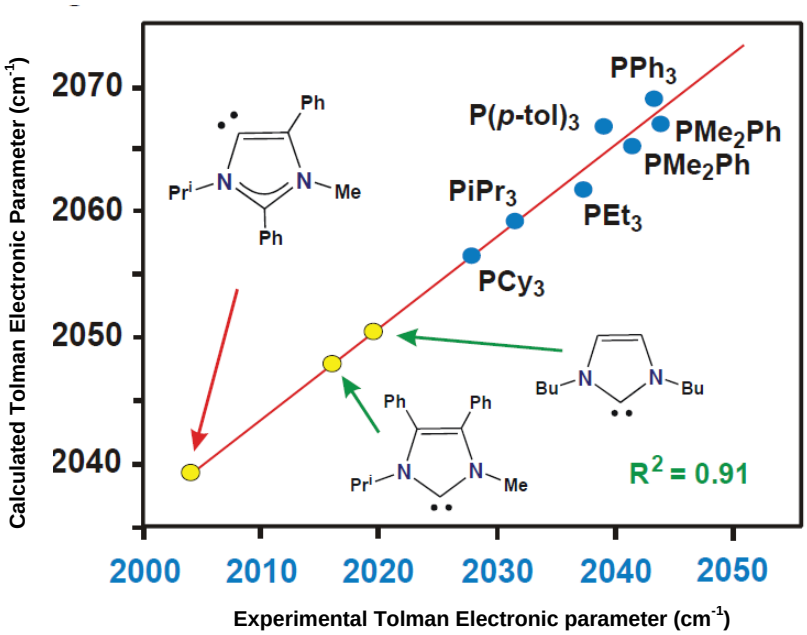

Figure 3.4: graphic representation of the TEP of some NHCs and phosphine ligands performed with an $Ir(CO)_3$ complex; figure taken from reference 136

3.1.2 Drug design of series I

Considering the extended analogies between phosphine and NHC ligands, an Arduengo carbene seemed a suitable organic scaffold for the synthesis of the new target molecules.[142,143] Since the starting concept of the project was to synthesize stable complexes that would allow proper structure activity relationship (SAR), gold(I) has been preferred over gold(III). One of the most potent thioredoxin reductase inhibitor has been chosen as lead structure. The gold phosphol inhibitor (GoPI, see chapter 4) has the gold center atom binding to tertiary phosphorus and outstanding biological properties (see figure 3.5).[107]

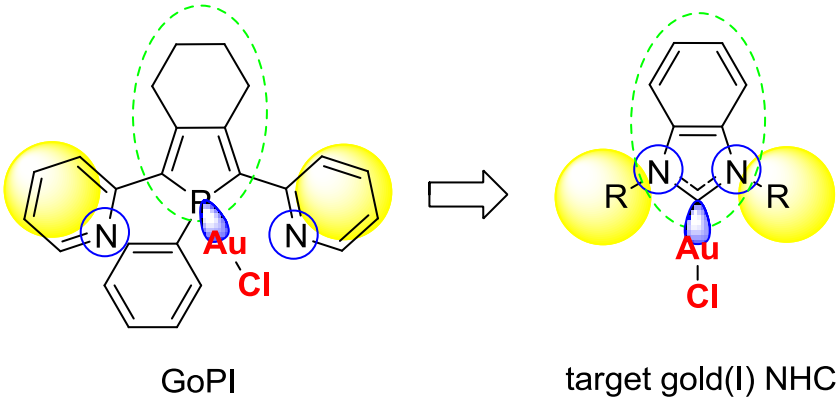

Figure 3.5: drug design and analogies between gold phosphol inhibitor and the new carbene gold(I) complexes

As core structure of the molecules we chose the benzimidazol-2-ylidene ligand (green dotted line in figure 3.5). The benzimidazol-2-ylidene is similar to the GoPI condensed ring system. Furthermore, the imidazole group possesses intrinsic biological properties (antiprotozoal, antibacterial) and could contribute to the overall activity of the substances.[144]

The position and chemical properties of the two nitrogens (blue circle) are similar to those present in GoPI. They represented a typical Arduengo NHC and together with their position in a core structure conferred to the complexes a strong electron donor capacity, similarity to the phosphine bond (blue electron cloud) and a remarkable stability.[133]

The lipophilic residues (yellow spheres), that in the leading structure are two pyridin rests, will be replaced by a series of lipophilic substituents. The increase in hindrance would afford a first drug design and the influence on the bioactivity of the complexes will be monitored.

The gold center atom is carrying the activity and the chlorido ligand represents the leaving group of the molecule (both Au and Cl red marked).

3.1.3 Synthesis of series I[145]

The new gold(I) NHC complexes of the benzimidazol-2-ylidene type were prepared according to a convenient established procedure starting from benzimidazole (see scheme 3.1 A).[146,147] Alkylation of the aromatic nitrogens was achieved by heating under reflux condition (~100°-120°C) treating the benzimidazole with an excess (1 : 3) of the respective alkyl halogenide in the presence of a mild base under vigorous stirring with acetonitrile as solvent. The reaction time was dependent on the structure of the residues. Good results were obtained for 6 - 10 h reactions. K_2CO_3 deprotonated the hydrogen in position N^3, forming bicarbonate, that precipitated in the reaction mixture and was then filtered off. The obtained benzimidazolium halides were recrystallized in ethylacetate / dichloromethane. All the yields were above 75%.

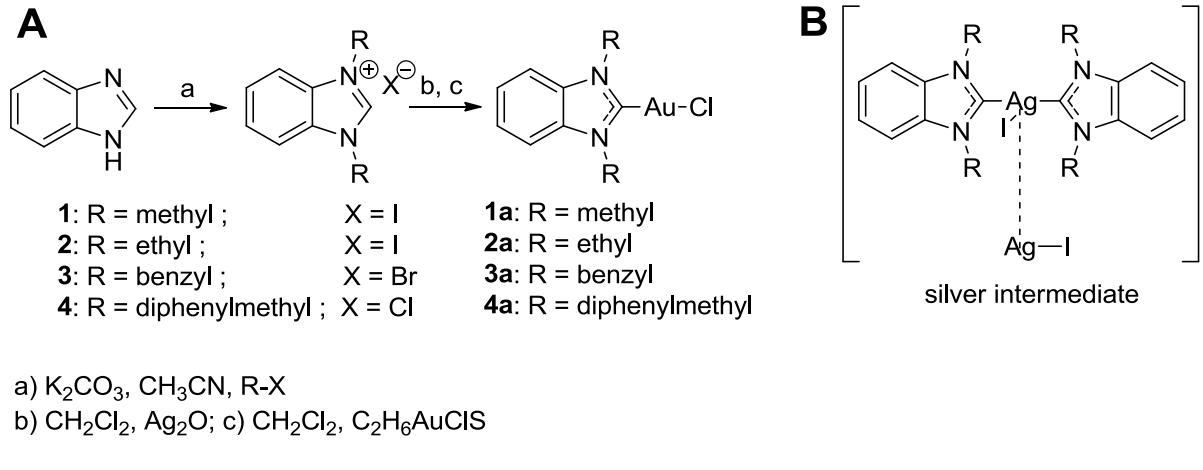

Scheme 3.1: synthesis of the benzimidazol-2-ylidene gold(I) chloride complexes

To obtain the target gold complexes, benzimidazolium halides were reacted with Ag_2O in dichloromethane at room temperature under vigorous stirring. The reaction led to the formation of a light instable silver-NHC intermediate (see scheme 3.1 A and B)[148] after at least 2 h. The first step of the complex formation reaction was followed by evident color change of the mixture and by TLC. Once the silver intermediate was achieved, chlorido dimethylsulfide gold(I) was added. The following reaction (also named trans-metallation)

led to the formation of the target gold(I) NHCs and precipitation of silver halogens. The compounds were finally purified by filtration over Celite-281 with a 45.3 µm particles diameter using dichloromethane as eluent. The gold complexes were characterized by ^{1}H NMR, electron ionization mass spectrometry (EI-MS), and elemental analysis with a deviation from the theoretic value lower than 0.4 %. Complex **2a** was also characterized by ^{13}C NMR. The complexes presented an interesting substituent-dependent color. For small residues (methyl, ethyl) the color resulted intense or pale yellow (respectively), while large and lipophilic substituent gave a white coloration. All the yields were between 25 % and 55 %.

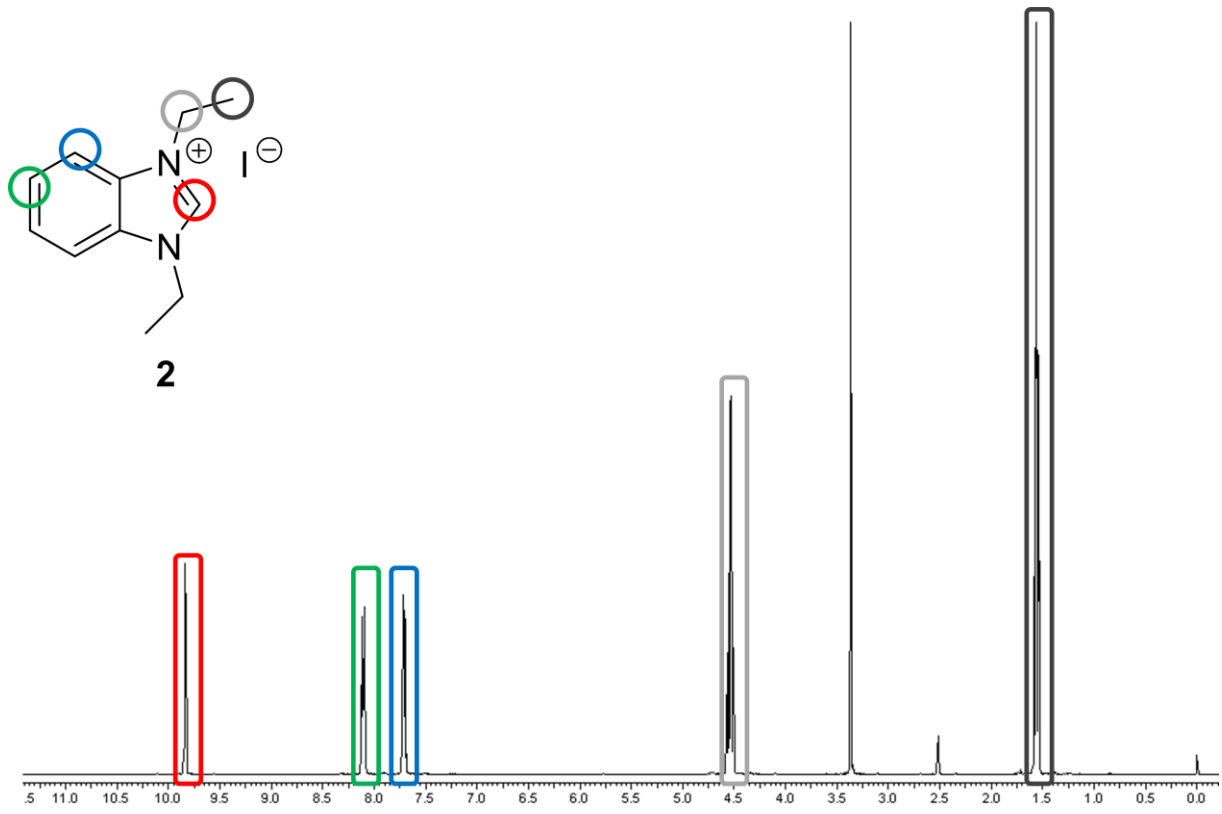

Figure 3.6: ^{1}H NMR spectrum in DMSO-d_6 of compound **2**

Characteristic spectroscopic features of the benzimidazolium halides formation included the disappearing of the proton signal at N-H at 12.4 ppm of the benzimidazole core in the

^{1}H NMR spectra and the strong downfield shift of the proton at the C^{2} carbon from 8.21 ppm to 9 – 10 ppm (example provided in figure 3.6).

Also the aromatic signals presented an interesting behavior. In the ^{1}H NMR of the benzimidazole the protons at the C^{4} and C^{5} gave a broad signal at 7.59 ppm and a double duplet at 7.19 ppm respectively. The aromatic proton signals of the benzimidazolium halides have been revealed between 7.0 and 7.5 ppm and gave a characteristic two double-duplet signals.

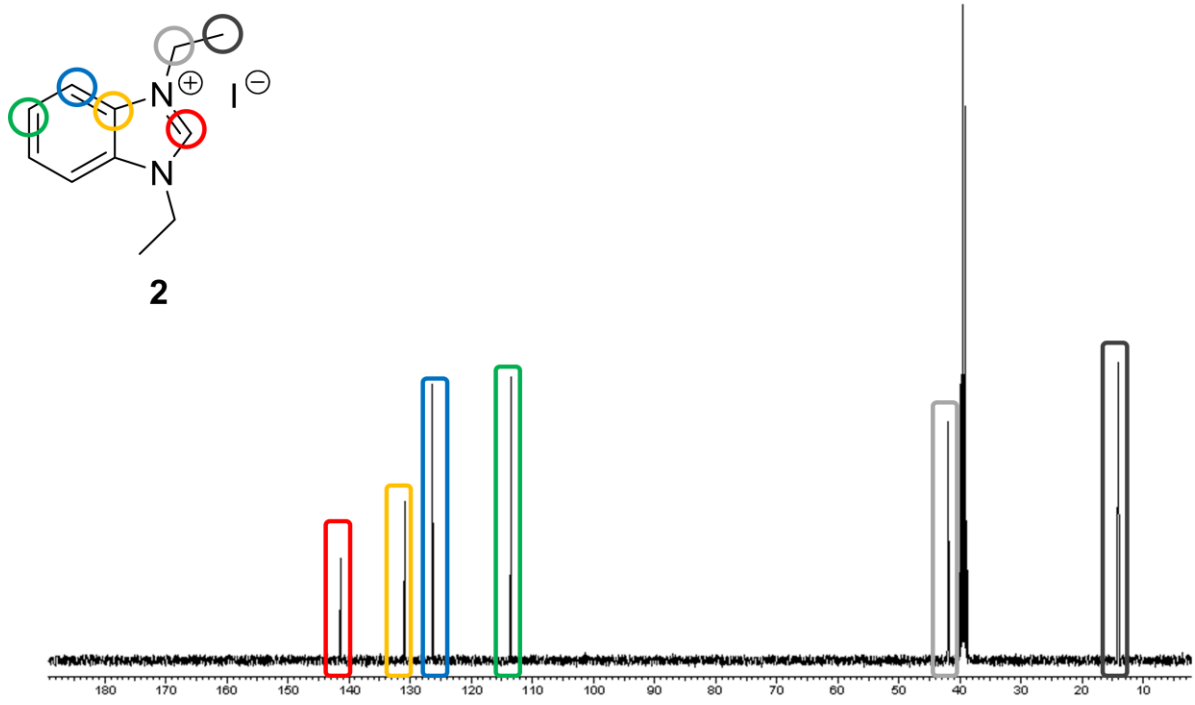

Figure 3.7: ^{13}C NMR in DMSO-d_6 of compound **2**

Characteristic spectroscopic features of the gold(I) NHC complexes formation included the disappearing of the proton signal at C^{2} of compounds **1** - **4** in the ^{1}H NMR spectra (expected at 9 - 10 ppm) and a strong downfield shift of the C^{2} carbon signal from 141 ppm (for benzimidazolium halide) to 177 ppm (for the gold NHCs) in ^{13}C NMR spectra (see figure 3.7 and 3.8 for an example). The aromatic signals resulted in a double-duplet with the two signals shifting towards each other. EI-MS coupled with gas chromatography

as injection method confirmed the presence of the molecular ion peak and the M^+-Cl as one of the main fragments.

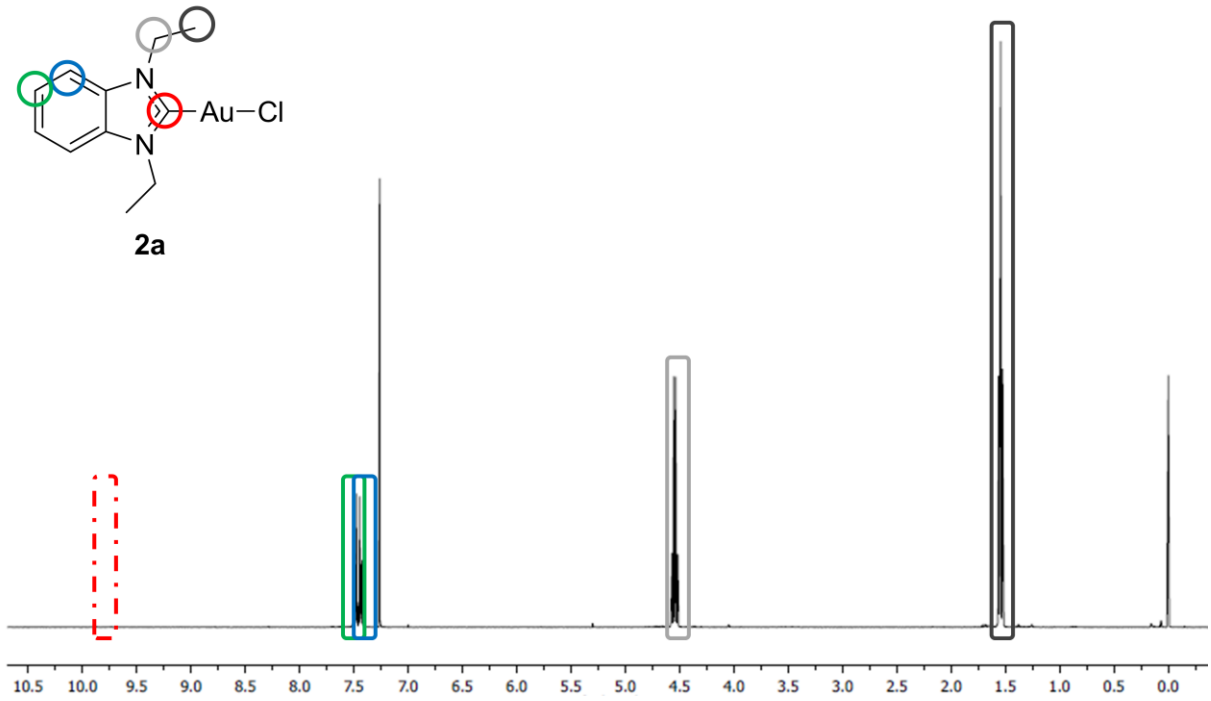

Figure 3.8: ^{1}H NMR spectrum in $CDCl_3$ of compound **2a**

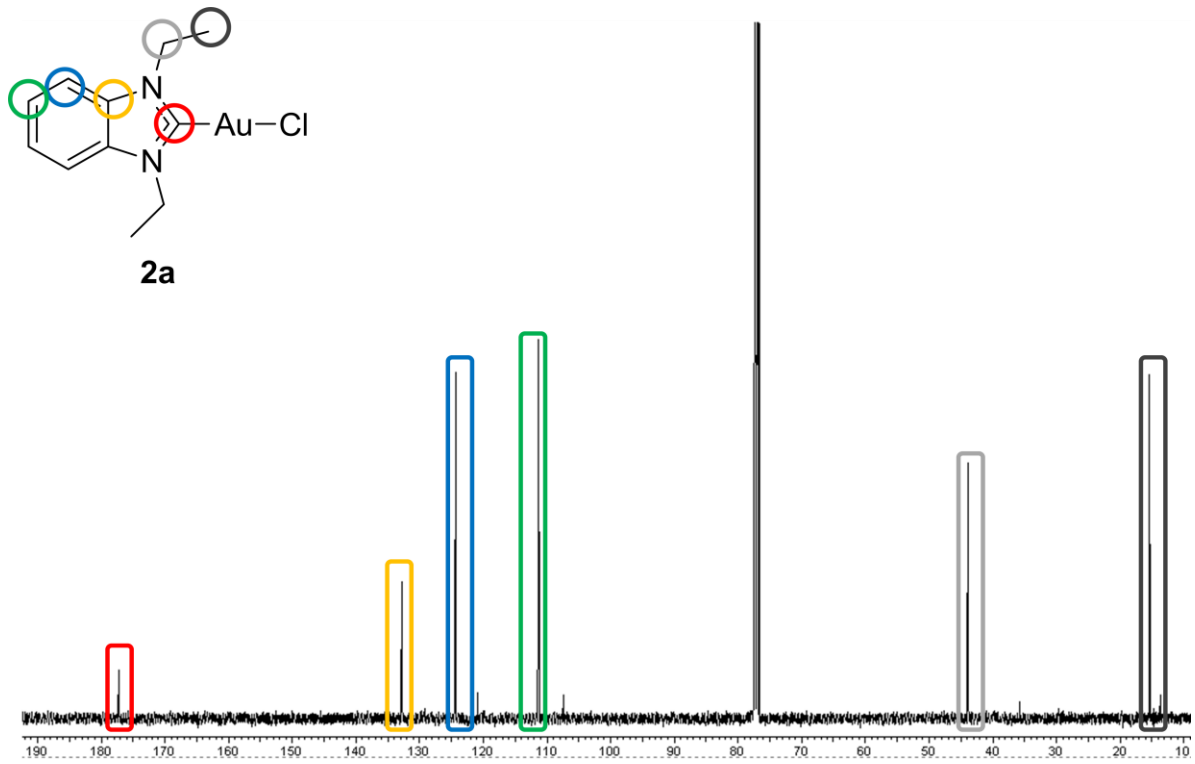

Figure 3.9: ^{13}C NMR spectrum in $CDCl_3$ of compound **2a**

3.2.1 Chemical consideration on series II

The variation of the side chains at the nitrogen atom of the benzimidazole core represented one of the possible modifications to induce a proper biological activity. The increase in steric hindrance of bulky alkyl chains resulted in an increased lipophilicity of the gold complexes. However, the modification did not lead to significant modulation of the bioactivity pointing out the minor influence of the side chains in the overall pharmacodynamic profile (for more information see chapters 6 and 8).

Since the gold atom demonstrated to carry the activity, substantial variation in its electronic environment or ligand dissociation energies could be expected to mirror a deep impact in the biological target interactions. The NHC structure showed useful chemical features coupled with bioactivity. Thus, a modification at the second ligand of the gold center atom (the chlorido ligand) could be rationally investigated.

While the gold center atom established a stable interaction with the NHC system through a strong σ coordination and π backbonding, the electronic configuration of the chloride group did not allow broad electron shell interactions. The introduction of a ligand possessing a major level of orbitals could influence the molecule properties, increasing the complex stability, weakening the carbene-gold coordination and having a deep impact on the overall biological profile. Furthermore, the possible involvement of a neutral ligand would allow the formation of positively charged complexes. The gold atom enables the molecule to set electrons on the third electronic shell, reaching the 18 electron configuration. The formal aligned positive charge would be surrounded by a great number of negatively charged electrons that could be delocalized on the whole structure due to the extended orbital interactions. Nevertheless, the introduction of a cationic species on a broad lipophilic system could attribute to the complexes a feature known as delocalized lipophilic cation (DLC) with relevant biological importance.[149]

3.2.2 Drug design of series II

Based on the results obtained with the first series (complexes **1a** – **4a**) of gold(I) NHC complexes, it was of interest to develop a new series of complexes positively charged and with a broad lipophilic system and compare their chemistry and bioactivity.

The coordination of other strong electron donors will increase the overall stability of the gold complexes. An increment in bond energy and stability will defeat possible cellular inactivation reactions and decrease undesirable drug efflux.

Many reports attested promising results concerning the biological potential of DLC substances.[110,112,149] While lipophilic structures penetrate through cellular membranes mainly by simple diffusion, DLCs possess an improved accumulation capacity. One of the main systems developed by the cell to regulate the nutrients and ion traffic between the outer and inner layer of the double phospholipidic strand is the electrochemical gradient (see chapter 9). Since the efflux of ions plays an important role for homeostasis and inter – intracellular communication, potassium, sodium and chloride ions level are highly controlled. The high concentration of Cl^- kept in the cytosol will provoke a migration of these anions to the peripheral part of the cell to compensate the osmotic gradient. This partial negative charge is balanced by an accumulation of potassium or sodium cations outside of the membrane. This configuration behaves like a simple capacitor and will determine the electrochemical gradient.[150] A lipophilic cationic compound, that would normally be taken up by simple diffusion, would be influenced by the field and synergistically increase its accumulation. Furthermore, it has been reported that there is a difference of 60 mV in the electrochemical field of healthy and cancer cells.[149] The difference is expected to confer selectivity to DLC molecules. Once penetrated into the cell, the substances will be directed to the peripheral parts of the cytosol and to the mitochondria. Consequently, the analogy between the two membranes could also stimulate a selective uptake into mitochondria (see figure 3.10).

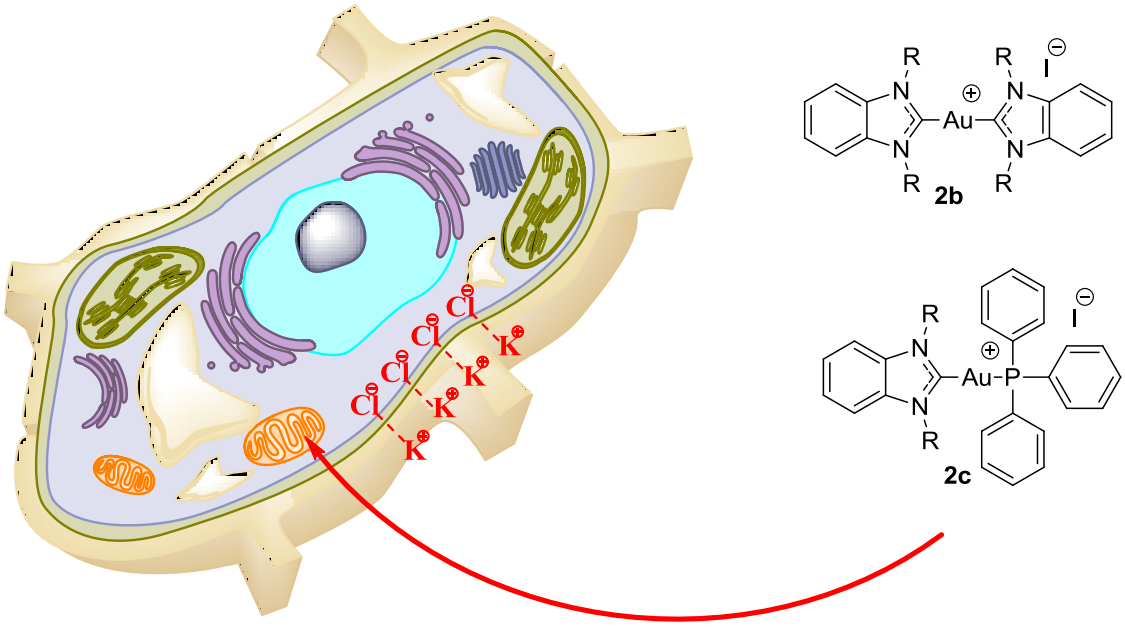

Figure 3.10: lipophilic cations and uptake into the cell of the target complexes **2b** and **2c**

Encouraged by data already present in literature and by our promising results, as first rational modification, the chlorido ligand has been replaced by another NHC moiety.[112,151,152] The complex so obtained will present a positive charge on a lipophilic system and a significant increase in bond stability between the residues and the gold central atom could be expected.

Since the gold phosphine complexes have been largely investigated with good results, the coordination of a phosphine moiety to the gold(I) NHC core will be performed.

The resulting complex will show similar chemical properties and will present a broader charge displacement due to the increased conjugation system and an incremented lipophilicity. Both the derivatives are expected to still present a good biological profile (enzyme inhibition, cytotoxicity) with an improved cellular membrane penetration and mitochondria selective delivery.

3.2.3 Synthesis of series II[153]

The target complexes were obtained starting from 1,3-diethylbenzimidazolium iodide (compound **2**, synthesis presented above). The C^2 possesses a proton with a pk_a of ~25.[154] This feature could be used to "increment" the reactivity of this position by simple deprotonation. For the preparation of the di-carbene derivative (complex **2b**), the benzimidazolium halide was reacted with chlorido 1,3-diethyl-benzimidazol-2-ylidene gold(I) (complex **2a**, synthesis presented above) at room temperature under vigorous stirring in dichloromethane : methanol (1 :1) and in presence of a mild base (K_2CO_3 deprotonating at the C^2 position) for 8 – 12 h (see scheme 3.2). The choice of a weak base incremented the time needed to complete the reaction but avoided undesirable cross-side reactions (for example between the base and the gold atom). The formed bicarbonate was then easily filtered off.

For the synthesis of the triphenylphosphine derivative (complex **2c**) the benzimidazolium halide was reacted with chlorido triphenylphosphine gold(I) (TPPG) at room temperature under vigorous stirring in dichloromethane and in presence of a K_2CO_3.

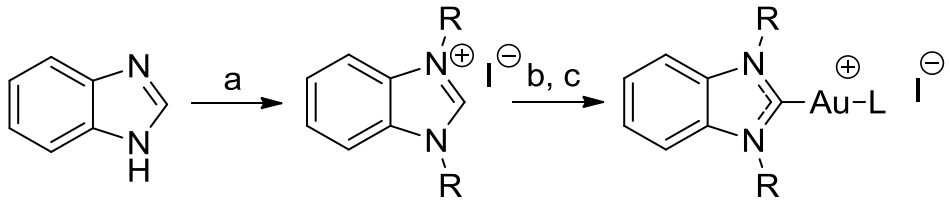

2: R = ethyl

2b: L = 1,3-diethylbenzimidazole
2c: L = triphenylphosphine

a) K_2CO_3, CH_3CN, CH_3CH_2I
b) CH_2Cl_2, K_2CO_3, complex **2a**; c) CH_2Cl_2, K_2CO_3, $C_{18}H_{15}AuClP$

Scheme 3.2: synthesis of the DLCs benzimidazol-2-ylidene gold(I) complexes

The products were isolated and purified by solvent extraction (bidistilled water / dichloromethane) or by column chromatography (with dichloromethane as eluent). The

obtained molecules were characterized by ^{1}H NMR, ^{13}C NMR, ^{31}P NMR (concerning complex **2c**) and elemental analysis with an accepted deviation from the theoretic values ≤ 0.4 %. Electron spray ionization or fast atom bombardment mass spectrometry were involved in the determination of the molecular ion and confirmed the presence of M^{+} and $M^{+} - I^{-}$.

Characteristic spectroscopic features of the complex formation included the disappearing of the proton signal at C^{2} of benzimidazolium halide in ^{1}H NMR spectra and a strong shift of the C^{2} carbon signal from 141 ppm (compound **2**) to 177 ppm (complex **2a**) to 190 ppm (complex **2b** and **2c**) in ^{13}C NMR spectra (see figure 3.11). ^{31}P NMR measurements of complex **2c** showed an upfield shift of approximately 2 ppm for the phosphorus signal when compared to TPPG (see figure 3.12).

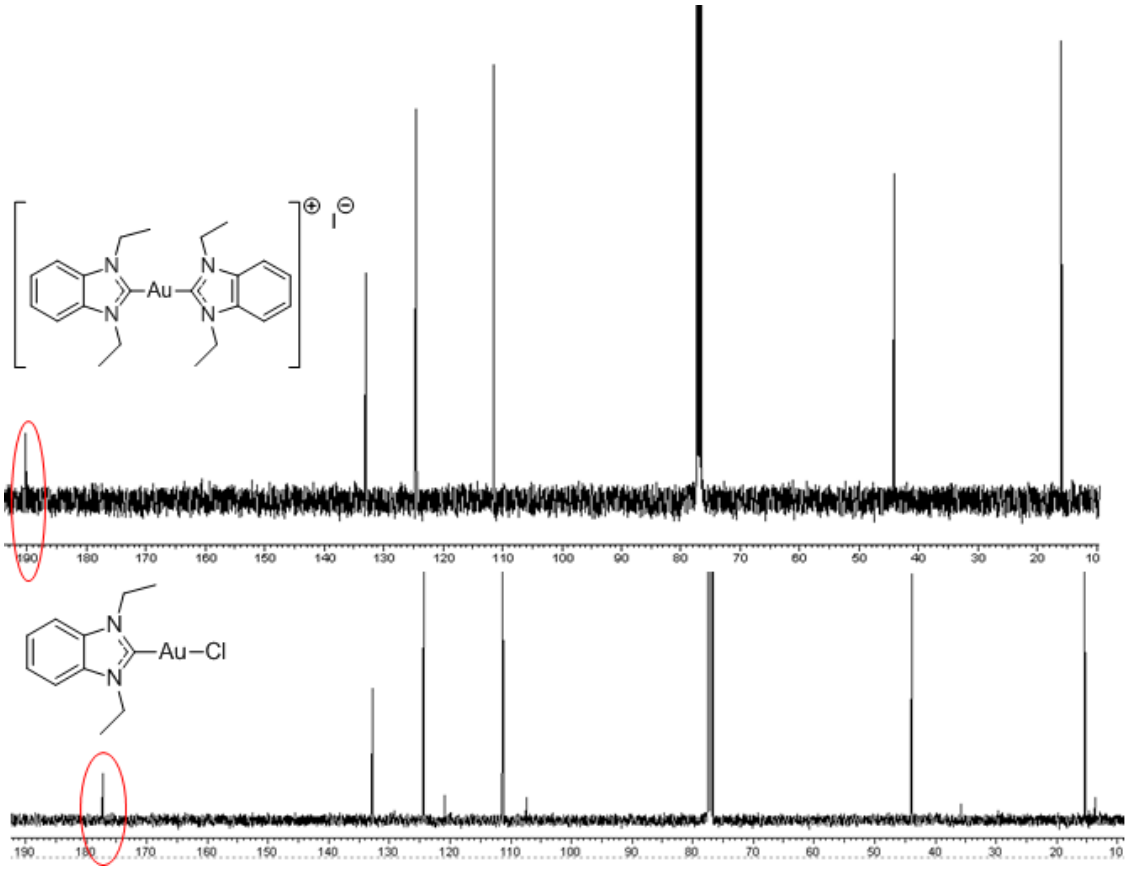

Figure 3.11: downfield shift of the C^{2} carbon signal in ^{13}C NMR spectra in $CDCl_3$ for complex **2a** and **2b**

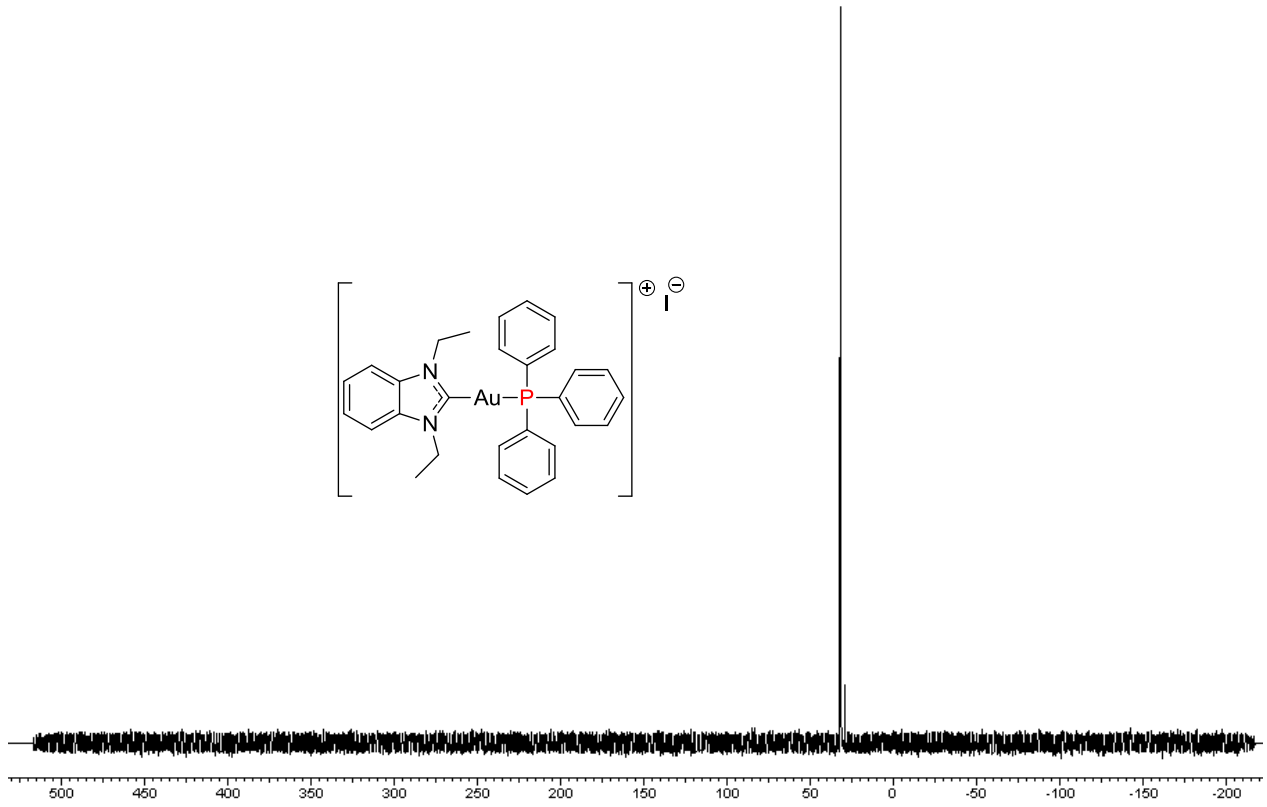

Figure 3.12: phosphorus signal in ^{31}P NMR spectrum in $CDCl_3$ of complex **2c**

3.3.1 Chemical consideration on series III

The presence of a positive charge on a broad lipophilic system resulted to be a key feature enabling a substantial uptake improvement and could lead to an efficient delivery of the compounds into mitochondria (see chapter 9). The strong coordinative properties of NHC or phosphine ligands had an essential influence on the complexes bioactivity from enzyme inhibition to the interaction with cellular metabolic processes. The results overall indicated that modification of the chemical properties of the ligands at the gold center atom altered the pharmacodynamic profile of the molecules (see chapters 8, 9 and 10).

Other functional groups with an electron-donor / electron-acceptor character could be added to the NHC scaffold in order to evaluate their influence on the overall stability and bioactivity.

From another perspective, modification of the phosphine could put in relation the coordinative potential (following the TEP) and the steric hindrance (from methyl to isopropyl R substituent) with the bioactivity of the compounds.[135,136]

In table 3.1 characteristic TEP values of substituted carbenes and phosphines presenting different rests are indicated.

NHC	TEP (v)	PR_3	TEP (v)
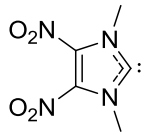	2068		2064
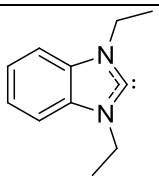	2055	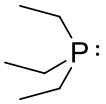	2061
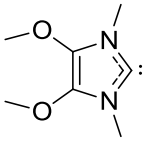	2052	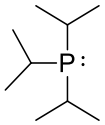	2059
		PPh_3	2068

Table 3.1: Tolman electronic parameter for different phosphine and carbene ligands (values taken from ref. 135 and 136)

3.3.2 Drug design of series III

Different TEPs stand for different chemical properties of the metal - ligand bond. The alteration of the bond energy and electronic configuration resulted in a variation of bioactivity. As represented in table 3.1 even internal molecule modifications like functional group insertion contribute to the overall chemistry of the gold – ligand interactions. To investigate such properties in detail a new series of gold(I) NHC complexes has been synthesized. The maintenance of the benzimidazol-2-ylidene

core as well as the lipophilic cationic structure represented a consequent choice to complete the ligand-dependent variations, SAR and biological profile studies.

Two main modifications have been carried out: NHC functionalization and phosphine modification. The insertion of an electron donor (methoxy) group in position C^6 has been performed. The enriching effect is expected to influence the kinetics of the gold atom towards biological targets. Two phosphines were coordinated to the methoxy-NHC: triethylphosphine as examples of short chain (**5e**), and triphenylphosphine as example of bulky aromatic residue (**5c**).

Moreover, the variation of the phosphine residue in relation with TEP and hindrance is expected to dominate the solubility as well as the cellular uptake of the molecules. Three phosphines have been chosen as second ligand and represent a gradual increment in hindrance, lipophilicity and decrease in TEP: trimethylphosphine (**2d**), triethylphosphine (**2e**) and triisopropylphosphine (**2f**).

3.3.3 Synthesis of series III

The target complexes were obtained starting from 1,3-diethylbenzimidazolium iodide (compound **2**, synthesis presented above). Compound **2** was dissolved in dichloromethane in presence of a mild base (Na_2CO_3), the suspension heated at 50°C for 10 minutes under vigorous stirring, the opportune chlorido phosphine gold(I) added and reacted at room temperature for 60 h (see scheme 3.3). The formed sodium bicarbonate was filtered off and the obtained powder washed with dichloromethane and water, dried and recrystallized in dichloromethane / hexane or purified by column chromatography with dichloromethane : methanol (2.5 %).

Characteristic features of the complexes formation included the disappearing of the C^2 proton signal at 8 - 10 ppm (NHC signal) in ^1H NMR and the shift of the C^2 signal from 141 ppm to 190 ppm in ^{13}C NMR such as already observed for the previous series (**1a** - **4a**, **2b** and **2c**). Electron spray ionization mass spectrometry (ESI-MS) confirmed the presence of the M^+ - I^-. The phosphine residues were confirmed by ^{31}P NMR and the

iodide counter-anion by elemental analysis with a maximal accepted deviation from the theoretic value of carbon, hydrogen and nitrogen ≤ 0.4 %.

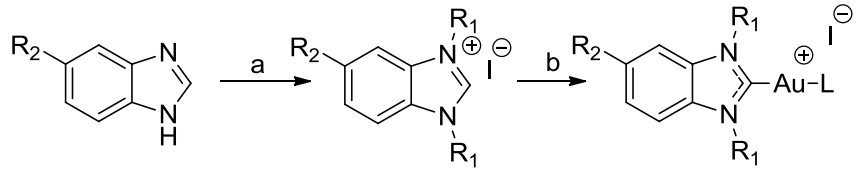

2: R_1 = ethyl ; R_2 = H
5: R_1 = ethyl ; R_2 = OCH_3

2d: L = trimethylphosphine
2e: L = triethylphopshine
2f: L = triisopropylphosphine
5c: L = triphenylphosphine
5e: L = triethylphosphine

a) alkyl halogenide in CH_3CN under reflux for 8-10 h
b) trialkylphosphine gold(I) chloride, Na_2CO_3 in CH_2Cl_2 at rt for 60 h

Scheme 3.3: synthesis of the carbene / phosphine variation gold(I) complexes

4. Computational chemistry

Computational studies with LigandScout 3.0 were performed by Prof. Dr. Gerhard Wolber, Institute of Pharmacy, Freie Universität Berlin, Königin-Luise-Strasse 2þ4, 14195 Berlin, Germany

DFT calculations were performed by Dr. Malte Kokoschka in the group of Prof. Dr. William Sheldrick, Lehrstuhl für Analytische Chemie, Ruhr-Universität Bochum, 44780 Bochum, Germany

4.1 Computational studies with LigandScout[145]

In the last decades many highly promising results concerning the involvement of novel gold(I) species in medicine have been reported.[100,155,156] The data progressively shed more light on the issue of drug design. In 2006 Becker and co-workers synthesized a new gold(I) phosphol complex [1-phenyl-2,5-di(2-pyridyl)-phosphole]AuCl (GoPI), which showed one of the strongest TrxR inhibition potential and IC_{50} values in the low nanomolar range either against TrxR and GR.[155] A crystal structure of GoPI with human GR was published. This provided an experimental proof for the covalent binding of gold to relevant cysteine residues in GR and thereby opened also some options for a more rational design of bioactive gold species.

For the drug design of new bioactive gold(I) NHC coordination compounds, the recently published crystal structure of human GR containing GoPI was used as a starting point. An initial overlay of human TrxR with human GR (see figure 4.1) had confirmed the close structural analogy of both protein structures, indicating that the observed binding sites of GoPI in GR could also be used to design potent inhibitors of TrxR.

TrxR shares with GR many crucial characteristics. Both the enzymes are ubiquitous NADPH dependent flavoproteins with the same folding configuration (with a conformation

analogy > 75%) and are involved in the cell homeostasis. They belong to the disulfide reductases antioxidant network. Moreover, the active site of the enzymes is characterized by a highly specific and similar motif that differs just for one amino acid: GR has Cys-aa-Cys (where aa represent 4 aminoacids) and in TrxR the second cysteine is replaced by a selenocysteine (Cys-aa-Sec).[157]

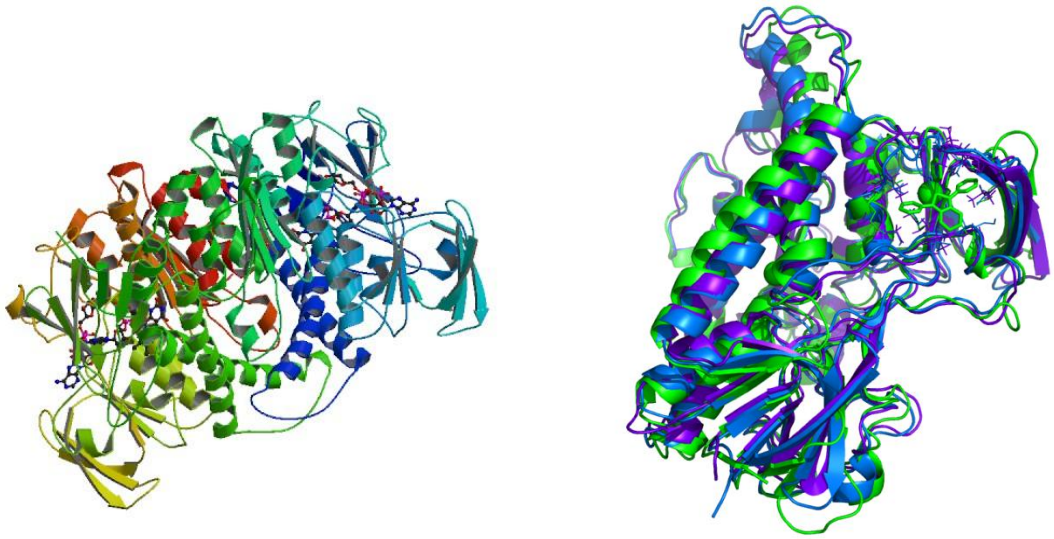

Figure 4.1: left) TrxR crystal structure (figure obtained from ref. 158); right) overlay between TrxR (blue) and GR (green); experiments performed by Prof. Dr. Gerard Wolber at the Freie Universität Berlin

The interaction of GoPI with the active site of glutathione reductase has been investigated and some striking features could be observed. The chlorido ligand represented the leaving group of the complex allowing the formation of a covalent bond between the gold center atom and the cysteine 63 in the enzyme active site (Cys63 has an enhanced Lewis base property due to the favored deprotonation assisted by the presence of a proximal hystidine). Interestingly, also the organic backbone of the molecule seemed to play an important role for the molecule-GR interaction and selectivity. The lipophilic residues of GoPI could interact with three hydrophobic residues in the proximity of the catalytic site: the isoleucine 175, the leucine 183 and 261 (see figure 4.2).

The study clearly demonstrated how the drug-enzyme interaction is influenced by the ligands of the complex. A rational drug design that will take in consideration such properties will lead to a strong improvement in activity and selectivity.

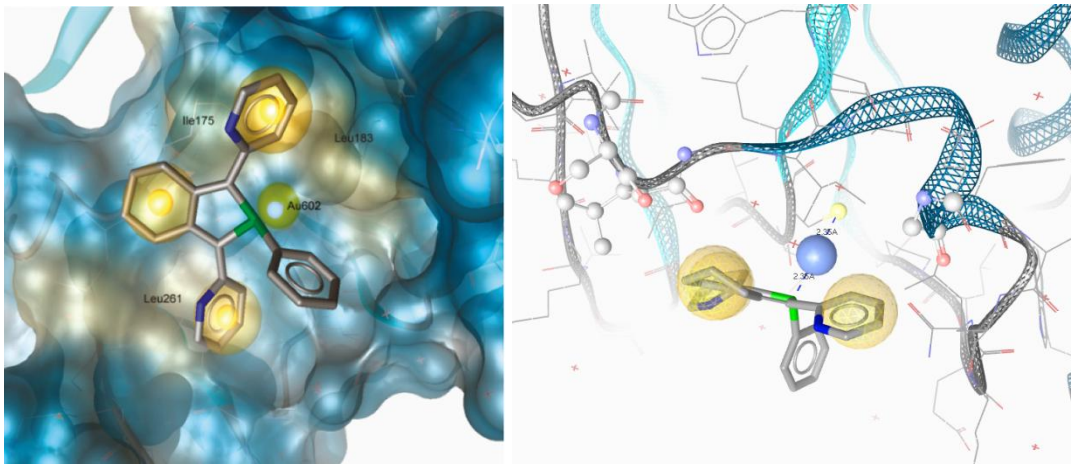

Figure 4.2: left) electron cloud and chemical interactions of GoPI with GR; right) P-Au and Au-Cl bond distances of the GoPI; experiments perfomed by Prof. Dr. Gerard Wolber at the Freie Universität Berlin

4.2 Density functional theory calculations

Density functional theory (DFT) developed in the late of the 20th century raised to routine method to calculate ground state, electron density and binding length or conformations of organometallic molecules.[159-162]

The many-body systems started to be considered for their electron density, as a measure of the ground state, depending just on three spatial coordinates (Hohenberg–Kohn theorem). By introducing the time variable it was possible to describe also the excited state. Inverting the external conditions, from interactive electron in a static environment to not-interacting electrons in a dynamic potential (Kohn-Sham theorem), refined the DFT calculation method. To determine the exchange and correlation interaction of the external potential the Thomas-Fermi model together with the local density approximation (LDA) has been involved.[159]

During the past decade, density functional theory and Becke´s three parameter (Lee, Yang, Parr) hybrid functional (B3LYP) in particular have evolved to be the workhorse in

the field of molecular structure calculations. Key feature of B3LYP theory is the description of the system energy. Its exchange correlation (xc) energy formula is written below and represents a measurement of the electron density and of the electron-gradient of a multi-electron system.

$$E_{xc}^{\mathrm{B3LYP}} = E_{xc}^{LDA} + a_0(E_x^{HF} - E^{LDA}) + a_x(E^{GGA} - E^{LDA}) + a_c(E_c^{GGA} - E_c^{LDA})$$

a_0 = 0.20, a_x = 0.72, and a_c = 0.81

Equation 4.1: exchange correlation energy in DFT B3LYP function

The three "*a*" parameter are an external correction derived from a Becke´s original fitting. The GGA energy parameters represented the generalized gradient. In the B3LYP the exchange energy is calculated as the combination of Becke´s parameter and exact Hartree-Fock energy. They minimized the many-body problem simplifying the Û term of the Schrödinger equation (electron-electron interaction) attributing to the particle density a central role.[159]

The low demand of density functional methods on computational resources is complemented by a high accuracy for many applications. Bond dissociation energies of systems containing transition metals, obtained with B3LYP were found to be of good quality.

The results derived from the first series of synthesis stimulated the variation of the chemical properties of the molecules through ligand modification. Since that change has been supposed to have a deep impact on the complex profile, it was of interest to study the geometry and bond dissociation energy of the selected compounds.

4.2.1 Molecules geometry[153]

The geometrical configuration of the gold(I) NHC complexes has been investigated in order to get information about the spatial conformation and ligand hindrance. All the

calculations were performed using Gaussian 03 (Rev. E.01) employing density functional theory (B3LYP). Geometries and zero point corrections were calculated using the Stuttgart RSC 1997 ECP (SDD) basis set on Au and the 6-31G (d) basis set on all other atoms. An ultrafine grid had to be employed for PPh_3-containing molecules to reach convergence. The calculations confirmed the expected linear planar coordination geometry of the complexes **2a** – **2c** (see figure 4.3).

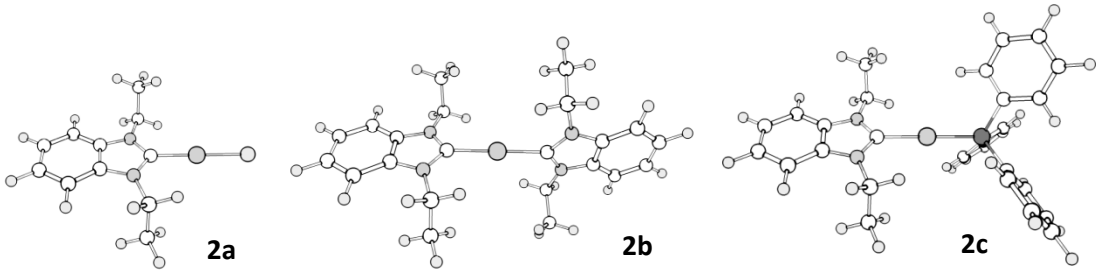

Figure 4.3: molecular representation of complexes **2a** - **2c**; experiments performed by Dr. Malte Kokoschka at the University of Bochum

4.2.2 Bond dissociation energy

Bond dissociation energies (BDEs) and geometry of the synthesized compounds have been investigated using density functional theory (B3LYP).

For a set of a neutral and two cationic gold(I) complexes, results obtained with B3LYP were shown to be in agreement with post Hartree-Fock methods like CCSD (T) or second order Møller-Plesset (MP2) theory. Due to the nature of the resulting fragments the employment of a diffuse basis set and the inclusion of solvent effects were vital. Solvent effects were introduced via the polarizable continuum model (PCM), the basis set superposition error was reduced to less than 4% by using the diffuse basis set aug-cc-pVDZ and corrected for by the counterpoise correction. The calculated BDE around the gold central atoms are summarized in table 4.1. The higher the BDE, the stronger will be the coordinative bond.

As expected, the carbene-gold bond presented a really high intrinsic stability with values always larger than 200 kJ / mol. The variation in the ligand induced a different electron density on the gold and consequently a different stability. The chlorido ligand of complex **2a** presented the lower BDE (concerning the Au-Cl bond), well according with its leaving group character. The dicarbene derivative (**2b**) showed an enhanced BDE over 225 kJ / mol resulting in being the more stable complex of the series (concerning the NHC-Au bond). Complex **2c** demonstrated an interesting behavior. Although still having a high Au-NHC BDE, the value is the lowest of the series. The PPH_3 did not reach the stability of the carbene ligand but presented a higher BDE than the chlorido. The BDE is expected to dominate the reactivity of the compound. The higher the BDE, the more stable the bond and the lower would be the reactivity. The overall order of reactivity **2b** < **2c** < **2a** is supposed to be reflected in the biological profile of the molecules.

Complex NHC-Au-L	BDE (kJ/mol) NHC-Au	BDE (kJ/mol) Au-L
2a (NHC-Au-Cl)	267.07	118.80
2b (NHC-Au-NHC)	225.39	225.39
2c (NHC-Au-PPh_3)	207.59	158.48

Table 4.1: bond dissociation energy calculation of the gold(I) NHC complexes **2a**, **2b** and **2c**; experiments performed by Dr. Malte Kokoschka at the University of Bochum

5. Thiol interaction and stability

5.1 General

As described in the introduction, despite the good results achieved by metal complexes in medicinal chemistry a large number of promising drugs have been dismissed due to high metabolization problems.

For example in aurotherapy, gold compounds demonstrated a significant interaction with small molecules present in serum or in the cell. Even before to penetrate the plasma membranes Auranofin is hydrolyzed at the acetyl groups and the whole thioglucosidic rest is replaced in a ligand exchange reaction forming thiol-shuttles with serum proteins (e.g. albumin, transferrin).[127] Once that Auranofin is taken up into the cell some reports proved the occurrence of a non enzymatic reaction between cytosolic small molecules (glutathione Glu, ascorbic acid) and the phosphine ligand leading to oxidation at the phosphorus atom (see figure 5.1).[163]

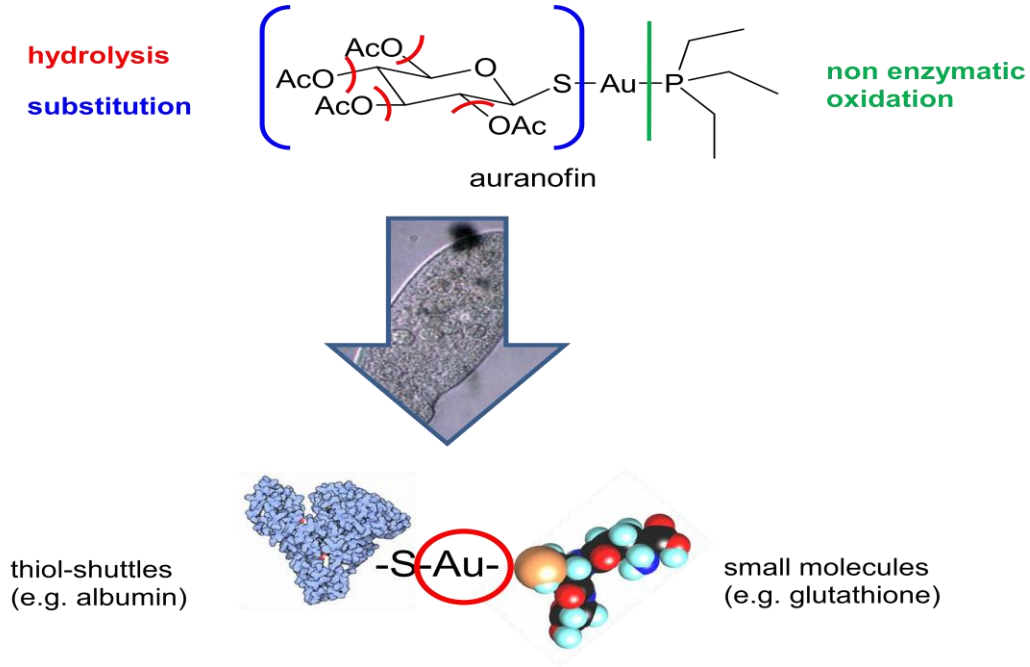

Figure 5.1: schematic representation of the Auranofin metabolization

Although its biological potential, the evidences are attesting that Auranofin is not the real therapeutic agent but is just a pro-drug of gold(I). This consideration has a deep impact on pharmaceutical chemistry and defeats rational drug design based on the organic backbone of Auranofin. Since the model showed to be unreliable for efficient structure activity relationships, new stable substances are strongly required.

The target gold(I) NHC carbene demonstrated already a considerably theoretical stability of the Au-NHC bond, enabling valuable drug design considerations (see chapter 4).

5.2 Glutathione interaction study

For inactivation of the anticancer drug cisplatin and many other metal based drugs, thiols such as the tripeptide Glu (γ-glutamyl-cysteinyl-glycine) play an important role. Glu depletion induces cancer cell sensitizing to xenobiotics, increase of reactive oxygen species (ROS) concentration and mitochondria permeability alteration, leading to apoptosis.[164] Glu binds with dangerous cellular molecules or xenobiotics and facilitates their extrusion through an ATP-dependent efflux channel system. P-glycoprotein families like the ATP binding cassette (ABC) or the multidrug resistance protein (MRP) are involved in Glu adducts or reduced Glu (GSSG) disposal process.[165,166] Compounds avoiding glutathione inactivation and extrusion (e.g. through an increase in internal bond energy) are required for a more effective therapy.

The gold(I) phosphine lead compound Auranofin is biologically processed and metabolized in thiol ligand exchange processes. As metal NHC complexes supposedly represent biologically stable coordination compounds, it was of interest to study their interaction with glutathione under physiological conditions in comparison to relevant gold(I) phosphine complexes.

5.2.1 Photometric assay[145]

To investigate the possible interactions between Glu and the gold(I) NHC complexes, 5,5-dithiobis-(2-nitrobenzoic acid) (DTNB, also known as the Ellmans reagent) has been

involved. DTNB can be used to quantify the thiol content of biological samples based on a rapid and stoichiometric reaction which also allows to monitor the activity of NADPH metabolizing enzymes such as TrxR.[167,168] In contrast to enzymatic reduction assays where one equivalent of DTNB is reduced under formation of two equivalents of 2-nitro-5-thiobenzoic acid (TNB), DTNB reacts with a thiol to a mixed disulfide and one equivalent of TNB, which can finally be measured photometrically (see scheme 5.1). The binding of gold complexes at the cysteine thiol of reduced glutathione (or a metal mediated oxidation of the tripeptide) would lower the available amount of free thiol able to react with DTNB. This assay thus provides an efficient tool to screen the stability of gold complexes against inactivation by glutathione.

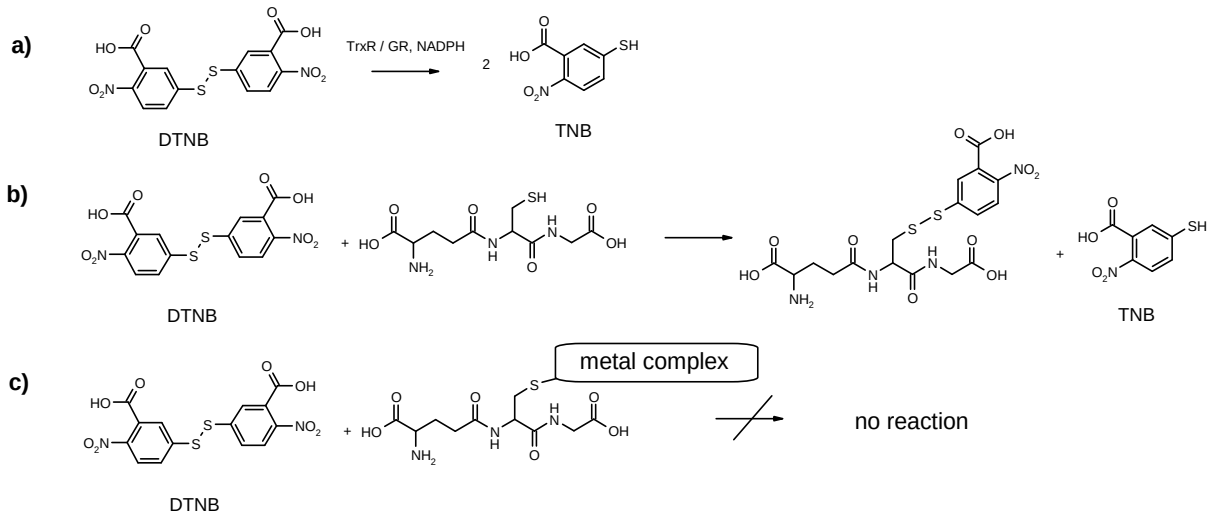

Scheme 5.1: a) DTNB enzymatic reaction; b) DTNB – glutathione reaction; c) metal complexes interference with the DTNB - glutathione reaction

To run off the experiments an excess of the respective gold complex (1 : 2 ratio) has been incubated with reduced glutathione at 37 °C for 20 and 60 min. Chlorido (dimethylsulfide)gold(I) was used as a gold positive control. $CuCl_2$, Hg-acetate (group 1), Auranofin and chlorido triphenylphosphine gold(I) (TPPG) (group 2) were involved as other comparative positive controls. As expected, all the standards of group 1 led to an

almost complete reduction of TNB product formation under the chosen conditions (see figure 5.2 - 5.4 for chlorido (dimethylsulfide)gold(I), figure 5.4 for $CuCl_2$, Auranofin and Hg-acetate). Instead lowering the TNB concentration, group 2 significantly increased the TNB level over 100% (see figure 5.4).

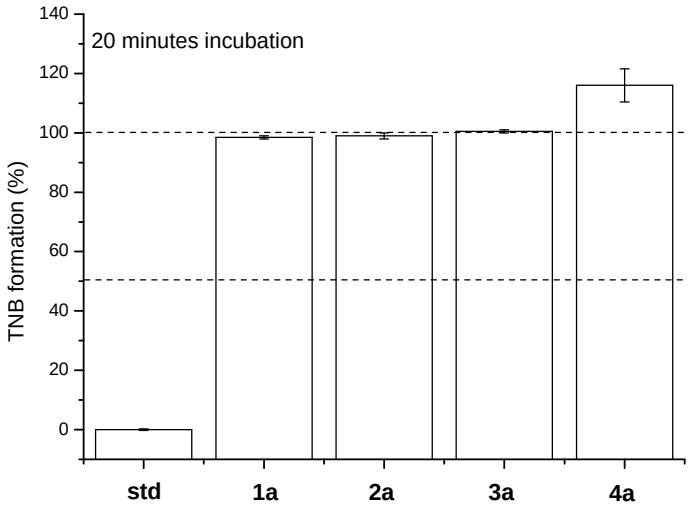

Figure 5.2: interactions of the gold(I) NHC complexes **1a** – **4a** with glutathione, incubation time 20 minutes, where std represents C_2H_6AuClS

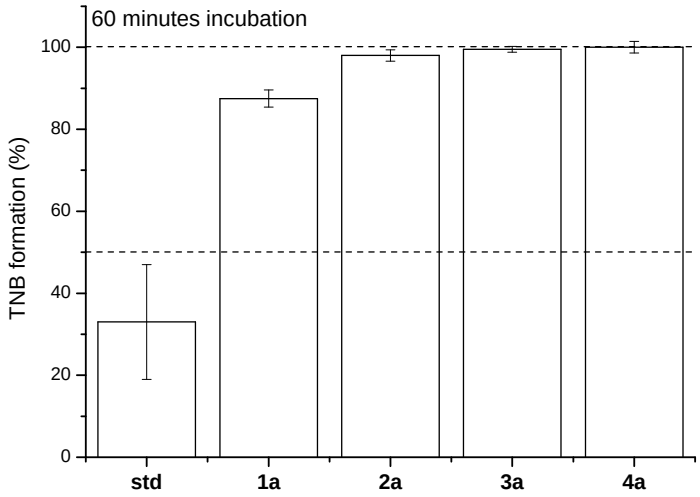

Figure 5.3: interactions of the gold(I) NHC complexes **1a** – **4a** with glutathione, incubation time 60 minutes, where std represents C_2H_6AuClS

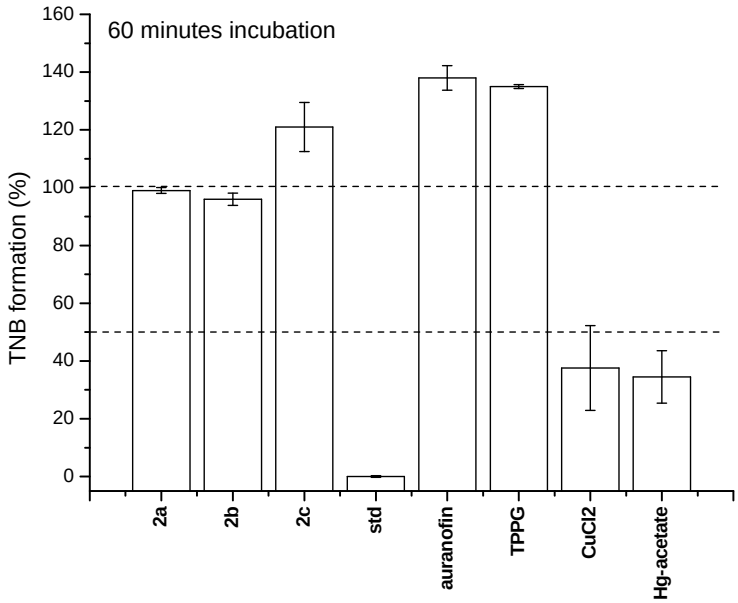

Figure 5.4: interactions of the gold(I) NHC complexes **2a** – **2c** and various positive controls with glutathione, incubation time 60 minutes; std = C_2H_6AuClS, TPPG = chlorido triphenylphosphine gold(I)

Quite astonishingly, the gold(I) NHC species **1a** - **4a**, and **2b** did not influence the reaction significantly and can thus be considered as sufficiently stable against thiols under biologically relevant conditions, a property highly desirable in the drug development of novel metal coordination compounds (see figure 5.2 - 5.4). Only **1a** showed a minor inhibition of approximately 10% after 60 min. This might be attributed to the lower steric hindrance of an attack at the gold center by the less bulky methyl side chains. In fact, ligand replacement processes upon reaction with cysteine over an extended period of time have been reported for gold(I) NHC derivatives.[112]

Unexpectedly, gold(I) phosphine complexes (e.g. Auranofin, TPPG or complex **2c**) led to an increase in TNB release during the reaction. Due to stoichiometric reasons, an exceeding of 100% is not possible and therefore the occurrence of an additional breaking / reduction of the DTNB disulfide bond had to be taken into account. For Auranofin, it had been reported that after an initial formation of an albumin-auranofin adduct, in which the thiocarbohydrate was replaced by a cysteine of albumin, the phosphine neutral ligand dissociated off the gold atom and was oxidized non enzymatically to the respective

phosphine oxide. Thus, an analogous “activation” by glutathione and subsequent oxidation of the phosphine moiety might in turn lead to the reduction of DTNB, resulting in the observed “overshot” of TNB. The formation of several intermediates related to a breakage of the DTNB disulfide bond (as well as coordinative bonds) in experiments on chlorido triphenylphosphine gold(I) (TPPG) could be expected.

5.2.2 NMR study of the interaction between TPPG and glutathione[145]

In order to study the reaction of gold(I) phosphines with glutathione and DTNB in more detail, ^{31}P-NMR spectra were taken and TPPG has been used as phosphine standard. TPPG and glutathione (1 : 1) have been incubated at 40 °C for 2 h and the different phosphorus-containing products were monitored. The ^{31}P-NMR spectrum showed four signals corresponding to Cl-Au-PPh_3, triphenylphosphineoxide and two other P-containing products (P-Au-R_1 and P-Au-R_2, see figure 5.5).

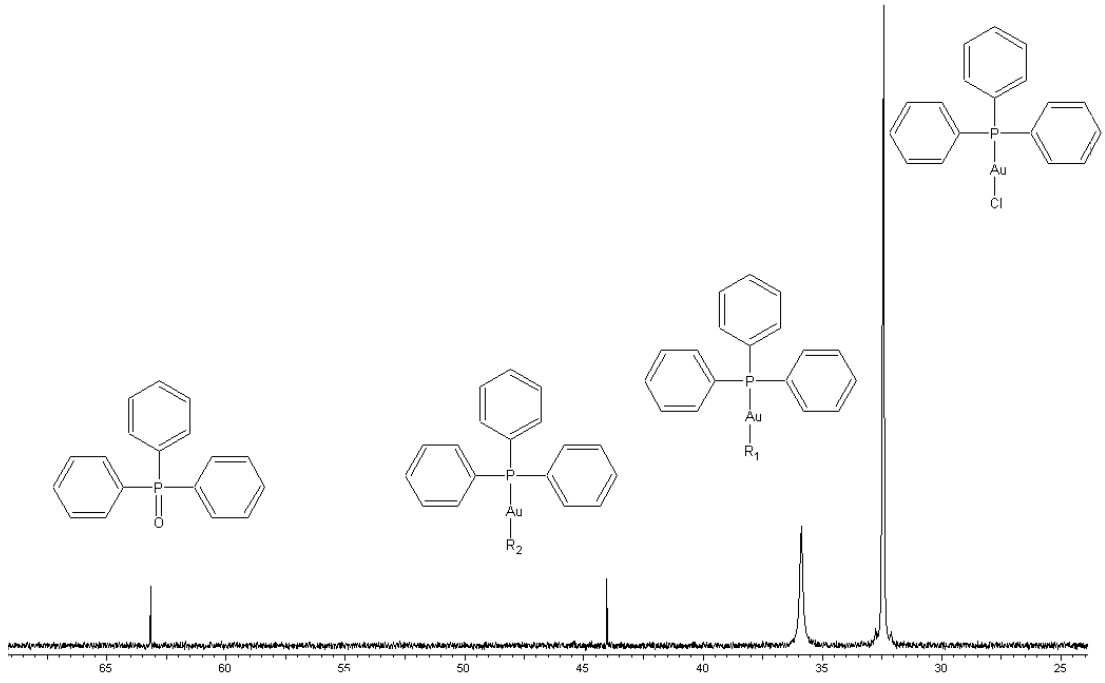

Figure 5.5: ^{31}P-NMR spectra of the reaction between glutathione and TPPG; R_1, R_2 and triphenylphosphine oxide (TPPO) are represented in scheme 5.2

The suggested reaction mechanism resulting from these observations is depicted in scheme 5.2. Supposedly an initially formed gold complex with glutathione and TPPG reacts with DTNB in two different ways. On the one hand cleavage of the gold sulfur bond leads to release of TNB, glutathione and TNB-Au-PPh_3. On the other hand cleavage of the gold phosphor bond causes the formation of TNB, triphenylphosphine and glutathione-gold-TNB. Both the glutathione and triphenylphosphine products can undergo further reactions (disulfide exchange or oxidation / reduction) with DTNB under release of further equivalents of TNB. Overall these mechanisms explain the observed increase of TNB formation in the stability experiments with gold(I) phosphines.

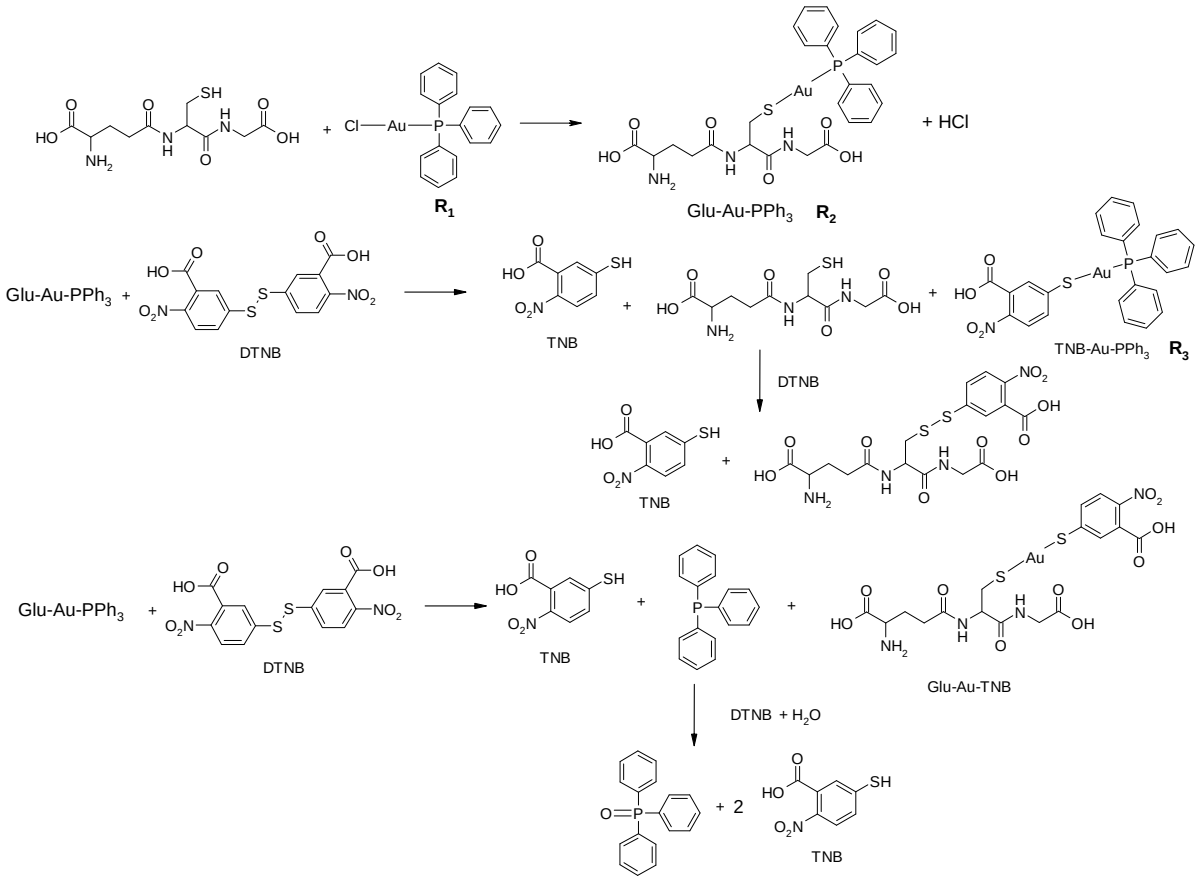

Scheme 5.2: suggested ongoing reactions for the glutathione gold(I) phosphine interactions; R_1 and R_2 are represented in the scheme by the Glu-Au-PPh_3 and the TNB-Au-PPh_3 adducts

5.3 Binding with serum albumin[153]

While intracellular thiols such as glutathione take part in the inactivation and elimination of dangerous species, extracellular thiols have a main carrier function facilitating the uptake or helping in the clearance.

Between the serum proteins, albumin is the most common one (representing 60% of the plasma proteins) and plays a central role for the osmotic regulation and oncotic pressure of interstitial fluids, blood vessels and connective tissues. Serum albumin is a monomeric 65 kDa protein, involved in the transport of lipophilic molecules such as fatty acids and steroids.[170] It is also capable to bind and carry cofactors such as hemin. Serum albumin tertiary structure is characterized by 17 disulfide bridges that are representing a main feature for the overall protein role and reactivity.[171] Many studies reported that the two domains, acting as binding regions, are highly hydrophobic pockets. The main reactive site of serum albumin has been found in a free cysteine residue (Cys-34) present in the hydrophobic pocket. Cys34 possesses two proximal lysines (Lys-195 and Lys-199) and a conformation vicinal histidine (His-39), which are hindering the water diffusion in the pocket. Biological relevant thiols have a normal pk_a around 8 – 9 (e.g. glutathione has a pk_a 8.7).[172] The extreme accessibility of the Cys-34 (located at the entrance of the domain) and the basic amino acid environment decrease the pk_a of the cysteinic sulphur to ~ 5. Such acidity is comparable to that expected for a selenocysteine (pk_a ~ 5.3). The hydrophobic environment and specific character of the Cys-34 create suitable conditions for the binding between albumin and metal drugs (see schematic representation in figure 5.6).[172]

It was shown that gold can be bound to the surface exposed Cys-34 of serum albumin and a thiol shuttle-model describing many thiol exchange processes has been proposed.[127]

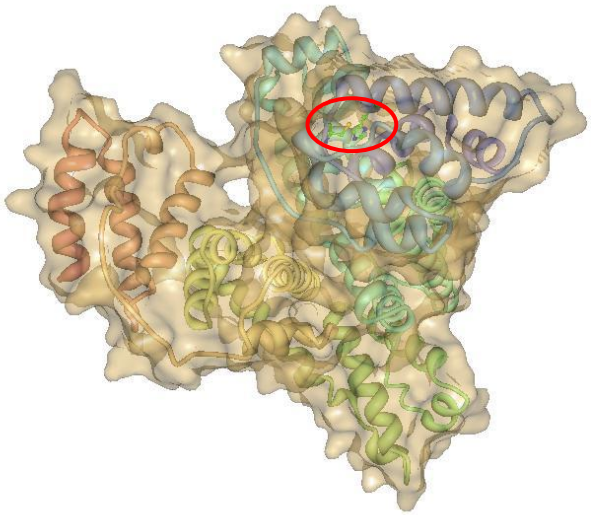

Figure 5.6: albumin domains and Cys-34 – His39 configuration (red circle: location, green: carbon backbone, blue: nitrogen, yellow: sulphur); imagine taken from ref. 173 and worked out with Protein-Workshop

Since the occurrence of binding with serum proteins reflects a first step metabolization of the complexes and could defeat structure activity relationship models, it was of interest to study the binding of **2a** - **2c** to bovine serum albumin by a precipitation method over a period of 24 h in order to evaluate the reactivity towards another biologically relevant thiol over an extended time frame (see figure 5.7). This data, implemented with the glutathione inactivation experiments, provide a good characterization of the interaction between biological thiols and the gold(I) NHC complexes.

Auranofin was used as a reference. In good agreement with the published literature[163] Auranofin showed a fast reaction (after 1 h binding of gold was almost complete) with 73 % of the available gold binding to the protein after 6 h. Complex **2a** reacted somewhat slower but overall protein binding was very similar to that of Auranofin (66 % after 6 h). Interestingly, **2b** showed a comparably low protein binding, which was still below 20 % after 6 h and did not exceed 50 % after 24 h. For **2c**, initial protein binding was 40 – 60 % and increased to 87 % over time. Whereas for Auranofin and **2a** stable values were reached within 1 - 2 h, binding continuously increased with the exposure time in the case

of **2b** and **2c**. This indicates that the expected ligand exchange processes between the cysteine residue of albumin and the gold center are slowed down for the latter two complexes. All together these results are in excellent agreement with the theoretical calculations (see chapter 4) and glutathione interaction.

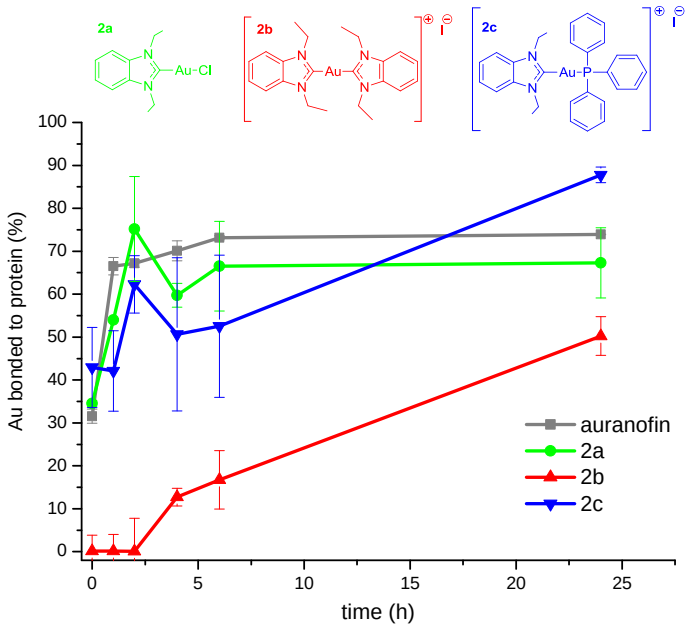

Figure 5.7: binding between bovine serum albumin and gold(I) NHC complexes **2a**, **2b** and **2c**; Auranofin as reference

5.4 Stability in buffer solution

In the cell Cisplatin allows a ligand exchange reaction replacing the chlorido ligands with water molecules forming an aqua complex.[174,175] The strong destabilization effect provoked by that metabolization challenged the research and concurred to the discovery of the nowadays commercialized platinum compounds carboplatin and oxaliplatin.

Since the carbene demonstrated to be more stable than the phosphine ligand (see results presented above), it was of interest to study their behavior under physiological conditions. Stock solutions of the target complexes in acetonitrile were prepared, diluted in a

phosphate buffer solution, incubated at 37 °C and the ultra violet spectrum modification monitored over different time frames.

Because the second series of gold(I) NHC (**2b**, **2c**) focused on ligand alteration replacing the chloride leaving group, complexes **2a**, **2b** and **2c** have been investigated for their stability in buffer solution (see figures 5.8, 5.9 and 5.10).

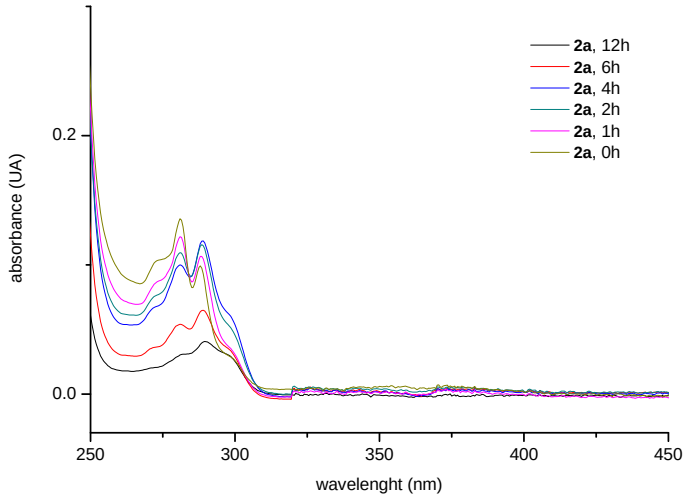

Figure 5.8: UV/Vis spectra of complex **2a** in buffer solution pH 7.0 incubated at 37 °C and at different time frames

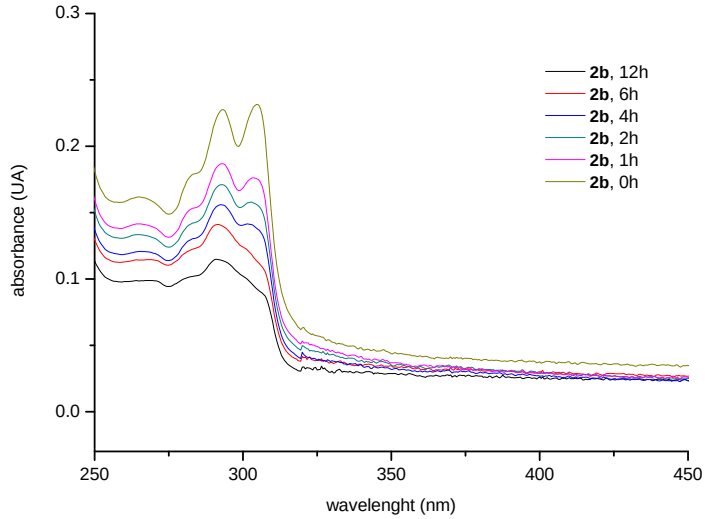

Figure 5.9: UV/Vis spectra of complex **2b** in buffer solution pH 7.0 incubated at 37 °C and at different time frames

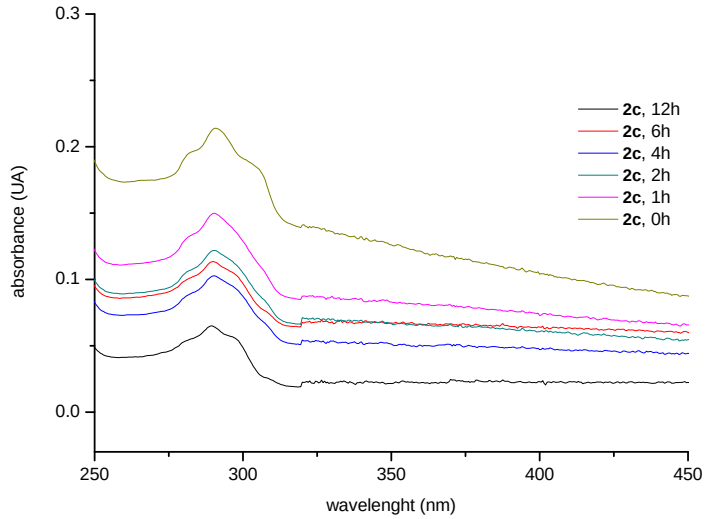

Figure 5.10: UV/Vis spectra of complex **2c** in buffer solution pH 7.0 incubated at 37 °C and at different time frames

The spectra do not show relevant changes in the UV/Vis profile within the first 2 - 4 h of incubation for **2a** and **2b**. A progressive decrease in absorbance has been noticed, especially for complex **2b** and **2c** that represent also the most hydrophobic of the series, and stands for the slow precipitation of the high concentrated complexes in buffer medium. After 6 h of incubation all the gold compounds presented changes the UV / Vis profile (more marked for **2a** and **2b**) suggesting that a ligand exchange reaction in buffer medium could take place.

6. Enzymatic studies

6.1 Background

The cell life is enabled by several biological processes that are not other than chemical reactions. Most of them require high activation energy in order to happen. Mammalian cells adopt two main related mechanisms to lower that energy: high internal temperature (37°C) and involvement of sub-cellular units called enzymes. An enzyme is a catalyst that enables not convenient reactions from one or more substrates to a product, not altering the equilibrium between substrates and products. The temperature, pH and specificity of a peptidic sequence called active site of the enzyme for the substrate reduce significantly the activation energy of the target process. The chemical reaction reaches quickly the equilibrium state (with an order of velocity millions fold greater than the uncatalyzed one) without consuming the enzyme.[176]

Between the 17th and the 19th century researchers started to observe the digestion of meat in the stomach, the fermentation of starch in plants or sugars in yeast. They did not correlate those processes with the life or organization of the cell in itself nor with the death or cellular decay. The structure, role and properties of enzymes were progressively established by the work of Nobel laureates such as Eduard Büchner, Stanley Northrop and David Chilton Philipps.[177]

Enzymes cover a large range of particules size from 62 amino acids to very large proteins constituted by many tertiary structures for an overall weight of many kDa. The modulation of the catalytic properties of an enzyme results in the specificity of the reaction which it catalyzes. Proteins use allosteric factors and cofactors to modulate that capacity. An allosteric factor is a molecule that binds in another place of the enzyme than the active site and increases or decreases the enzyme activity. A cofactor is a molecule that binds to the enzyme and provides important reactive elements (e.g. NADH, Fe center atom) without which the reaction could not take place. The active site itself is characterized by

an extreme stereo / regio and chemical specificity and in normal biological conditions has a small number of substrates. The spatial conformation and amino acids proximity are strictly related with the ΔG of the enzymatic reaction (see figure 6.1).[178]

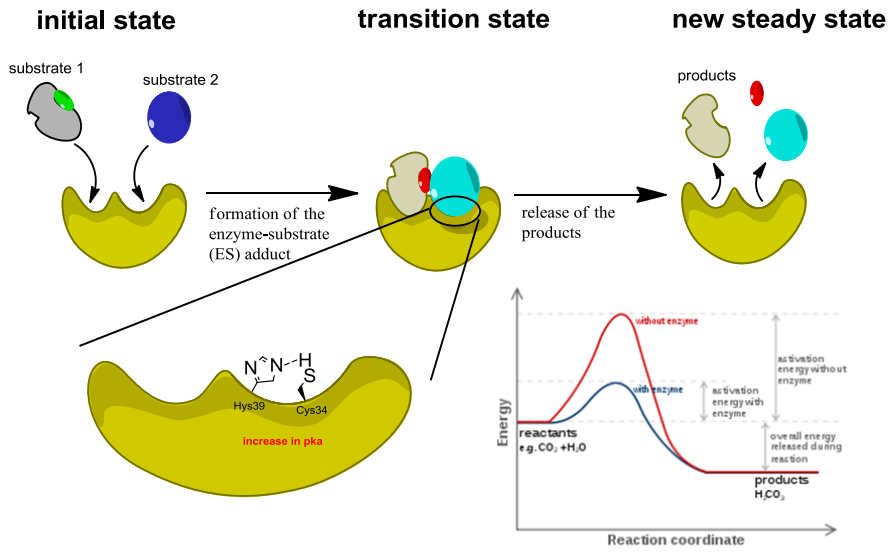

Figure 6.1: schematic representation of the active site reactions of an enzyme, chemical interaction favored by the proximity (e.g. serum albumin) and energetic curve of the enzymatic process; insert in the picture from *Wikipedia commons*, file: "Carbonic_anhydrase_reaction_in_tissue.svg"

The kinetic of the enzyme reactions were simplified by Henri Michaelis Menten at begin of the 20th century. Although further evidences underline the role of the enzyme environment, Michaelis-Menten kinetics are still at the base of modern enzymology. The core of the theory divides enzymatic reactions in many steps: the first equilibrium where the enzyme (E + S) and substrate are not in relation, the formation of the enzyme-substrate complex (ES), the chemical reaction that converts substrate in products (EP) and the release of them (E + P).[178] It is possible to have a single substrate reaction or a multi substrate reaction kinetic. Enzyme catalytic properties or activity does not follow a linear trend but is influenced by the substrate concentration displaying saturation kinetics. The velocity of the reaction, that is a measure of the affinity of the enzyme towards a target substrate, increases with the substrate concentration to reach a maximum when ES = E. It

represents the constant v_{max} also described by the Michaelis-Menten such as the concentration of substrate needed to reach half of v_{max} (K_m). The number of substrates that an active site can process over time is expressed as k_{cat} (or turnover number, $[S]/s^{-1}$). The enzymatic specificity or efficacy towards a substrate can, thus, be expressed as k_{cat}/K_m. When the enzymatic specificity reaches its theoretical maximum (10^{-8} – 10^{-9} $M^{-1}s^{-1}$), every collision of the enzyme with its substrate leads to catalysis.[178] Enzymes with this property are called kinetically perfect and the only parameter associated to them is the diffusion rate of the molecules in the medium.[178] For a single substrate enzymatic reaction the catalytic velocity of an enzyme will follow the equation presented below, assuming that the ES complex change over time is not minimal and tensing to zero and that the enzyme concentration is not changing over time.

single substrate

$$E + S \underset{k_{-1}}{\overset{k_1}{\rightleftharpoons}} ES \xrightarrow{k_2} E + P$$

$$v_0 = \frac{v_{max}[S]}{K_m+[S]} \quad \textit{where} \quad K_m = \frac{k_2 + k_{-1}}{k_1} \quad \textit{and} \quad v_{max} = k_{cat}[E]$$

Equation 6.1: Michaelis-Menten relation for single substrate kinetic

Some reactions are achieved by the walk-through an intermediate state. The Michaelis-Menten equation applied to single substrate intermediate catalysis is shown in equation 6.2.

single substrate and intermediate

$$E + S \underset{k_{-1}}{\overset{k_1}{\rightleftharpoons}} ES \xrightarrow{k_2} EI \xrightarrow{k_3} E + P$$

$$v_0 = k_{cat}\frac{[E][S]}{K_m^{'}+[S]} \quad \textit{where} \quad K_m^{'} = K_m\frac{k_3}{k_2+k_3} \quad \textit{and} \quad k_{cat} = \frac{k_2k_3}{k_2+k_3}$$

Equation 6.2: Michaelis-Menten relation for single substrate and intermediate kinetic

In multiple substrate reactions more than one substrate are concurring in the same enzymatic catalysis. When one substrate is kept constant the whole process can be reduced to a single substrate velocity kinetic. Another category of reaction is constituted by the random order multiple substrate reactions. They can be ternary when two substrates bind together to allow the formation of two products or with a ping-pong mechanism, in which the aggregation of the first substrate allows the formation of the first product and consequently the second substrate enables the formation of the second product.[176,178]

multiple substrate ternary reaction

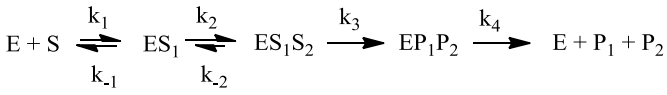

multiple substrate ping-pong reaction

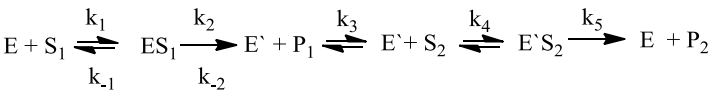

Equation 6.3: Michaelis-Menten relation for multiple substrates kinetic

All the enzymatic reactions cannot be efficiently described by Michaelis-Menten kinetics. Especially in the case of allosteric modulation it is possible that the ES adduct facilitates the formation of product increasing or decreasing the affinity of the enzymatic active site to the substrate (e.g. heme group). The Hill equation is often used to described such reactions where θ is the amount ligand that occupies the active sites of the enzyme, L free ligand, K_d the dissociation constant and n the Hill coefficient and described the affinity of ES for other S (see equation 6.4).[178]

In such cases the Michaelis-Menten equation needs to be integrated with the chemical kinetic orders equation that is used to determine the disappearance of substrate, the production of product and is a useful tool to predict metabolic processes.

$$\theta = \frac{[L]^n}{K_d + [L]^n}$$

Equation 6.4: Hill equation

6.2 Enzyme role in physiology and therapy

Non catalyzed reactions are characterized by a high energy demand or long span time frame. Enzymes enable these pathways with a convenient energy / time ratio, permitting the life of both simple and complex organisms. They are involved in almost all the cellular processes (motility, replication, internal communication, energy proceeds, transport, digestion etc.). A fine tuning up of their regulation results in homeostasis and maintenance of metabolic pathway functionality.[176,178]

Due to their enhanced reactivity, the active sites of the enzymes are an eligible target for specific inhibitors. The inhibition of the enzyme will result in a block of the process coordinated by the protein correlated often with severe consequences at cellular level. According to the Cleland categories, enzymatic inhibition can be divided in four types dependent on the alteration of v_{max} and K_m (see figure 6.2).[178]

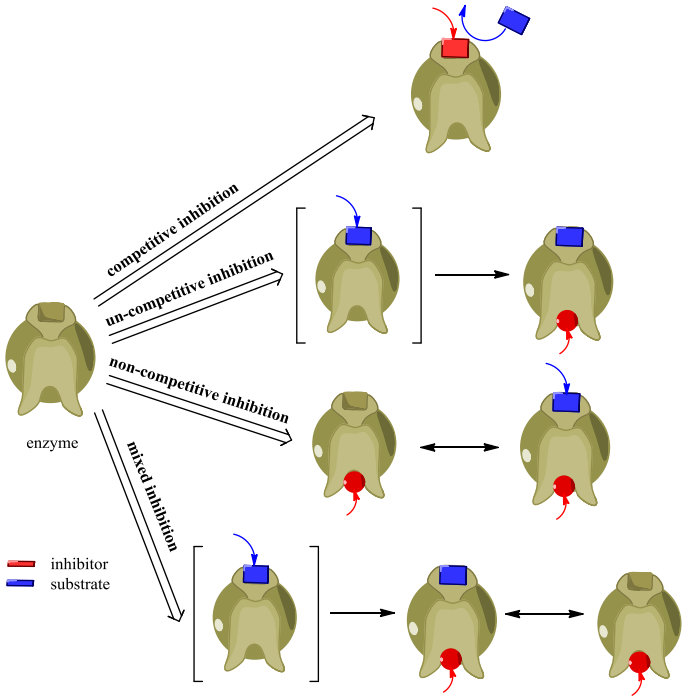

Figure 6.2: schematic representation of types of inhibition

In the competitive inhibition mode (the most diffuse one) substrate and inhibitor bind at the same site of the enzyme; in the uncompetitive inhibition mode the block of activity is reached when the inhibitor binds to the already preformed ES adduct; in the non competitive inhibition mode the inhibitor can bind to the free enzyme as well as to the ES complex but not in the active site; the mixed inhibition even if similar to the non competitive inhibition does not follow the Michaelis-Menten kinetic.[178]

Inhibition can be reversible or irreversible. In the reversible inhibition the binding between enzyme and inhibitor can be a dipole-dipole interaction, Van der Waals forces or hydrogen bond. The adduct EI (where I is the inhibitor) can be replaced by the substrate depending on exposure and concentration. In the irreversible inhibition the binding between enzyme and inhibitor is made by a covalent bond, with a consequent block of the active site functionality. The relation between v_{max} or K_m, inhibitor concentration and inhibition constant (K_i) is reported in the equation below.[178]

$$v_i = v_{max} + \Delta v_{max} \frac{[I']}{[I'] + K_i} \quad \textit{or related to } K_m \quad v_i = K_{max} + \Delta K_{max} \frac{[I']}{[I'] + K_i}$$

Equation 6.5: Michaelis-Menten inhibition correlation

Parallel to the Michaelis-Menten kinetics another important parameter is frequently used to describe the inhibition potential of a substance towards an enzyme: the inhibition concentration 50 (or half maximal inhibitory concentration, IC_{50}). The IC_{50} value indicates which concentration of an inhibitor is required to reduce the enzyme activity of the 50%. The IC_{50} can be related to the K_i as a measure of affinity of the substrate through the Cheng-Prusoff equation.[179]

$$K_i = \frac{IC_{50}}{1 + \frac{[S]}{K_m}}$$

Equation 6.6: correlation between IC_{50} value and K_i

Recently, beside the established anti-tumor approach some cancer cell lines demonstrated to over-express or under-express specific enzymes involved in the survival process. Examples of this preservation mechanism are the PI3K-AKT cascade, glutaminase, thioredoxin reductase, p38-α or monocarboxylate transferase.[180,181] The inhibition of over-expressed cellular components as therapeutic strategy stimulated in the last years many research groups to synthesize new potent and selective molecules to block key processes and induce tumor regression.

6.2 Thioredoxin reductase and the antioxidant network as anticancer targets

There is a difference of ten times fold in concentration between the reactive oxygen species (ROS) production in healthy cells towards cancer cells provoked by the increased metabolism connected to the pathology (DNA replication, movement and metastasis, un-differentiation).[61,182] To protect the biological structures from severe oxidative damage all the living organisms developed an intra-cellular system highly conserved among the species. The antioxidant network is a group of enzymes and relative substrates, working together to prevent, expel ROS and regenerate themselves.[180] Main enzymes belonging to this class are thioredoxin reductase (TrxR) and its substrate thioredoxin (Trx), glutathione reductase (GR) and its substrate glutathione (Glu), glutathione peroxidase (GPx), glutathione S-transferase (GST) and glutaredoxin reductase (GTR). The main ROS inactivation mechanism goes through a first Glu oxidation due to the high concentration of Glu in the cell (~10 mM). The ROS-Glu adduct will be afterwards expelled through specific protein channels or regenerate primarily through GR or GST.[164] Consequently also the concentrations of GR and GST are quite high. To regenerate the two enzymes less concentrated proteins have been involved: TrxR, GTR and GPx.[183] Interestingly, TrxR is strongly over-expressed in cancer cell. Its modulation and role elected TrxR as a possible efficient target in chemotherapy.[97,183,184-186]

TrxR is a ubiquitous NADPH dependent flavoprotein belonging to the family of the disulfide reductases.[185,187] There are two big families of TrxR, dependent on the cellular

evolution. The small TrxR (*s*TrxR) is present in prokaryotes and consists of two monomers both with an enzymatic active site and formed by three α-helices and two loops for an overall ~35 kDa of weight. All the structure is characterized by a high freedom degree that confers to the enzyme flexibility. It shows the so-called thioredoxin motif Cys-aa-Cys (where aa stand for 4 aminoacids) in the active site that through the disulfide bridge catalyzes the reaction. The large TrxR (*l*TrxR) is present in eukaryotes and consists of one NAPDH domain, one FAD domain, two monomeric regions composed by two α-helicies, one β-strand and in between an interface domain for an overall ~55 / 65 kDa of weight.[180] It possesses two catalytic sites respectively in the N-terminal and in the C-terminal of the protein. While both the active sites present a thioredoxin motif they differ just for one amino acid: in the N-terminal the bridge is between two cysteines but in the C-terminal one cysteine is replaced by a selenocysteine (see figure 6.3). The *l*TrxR present a quaternary structure more rigid than the *s*TrxR.[180]

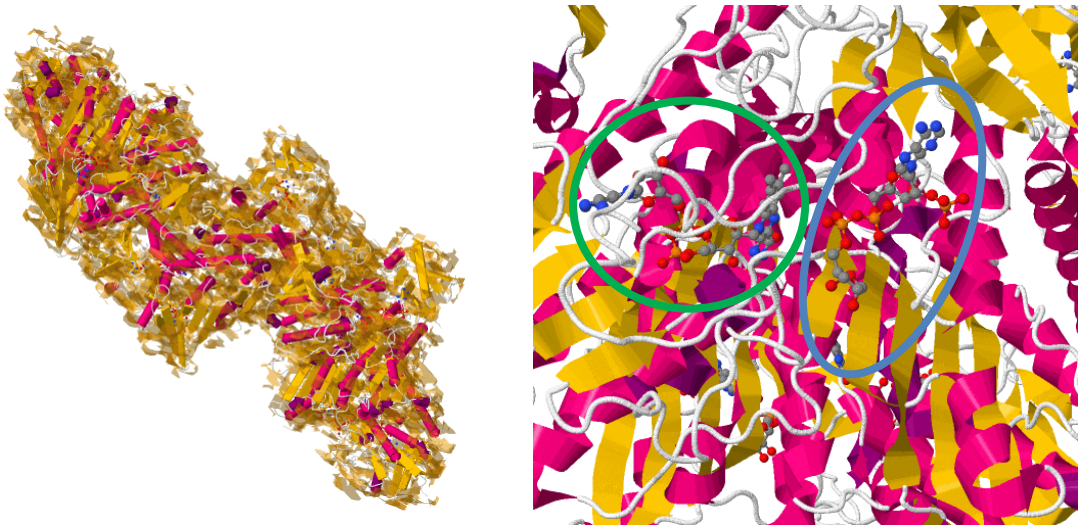

Figure 6.3: left) TrxR crystal structure worked out with proteinworkshop (taken from ref.188); right) particular of NADPH (blue) and FAD (green) binding site

In mammalian cells there are three types of TrxR. TrxR type 1 is present in the cytosol and has a central role in the regulation of the homeostasis. It regenerates Trx, Glu and GR and assists in the inactivation of ROS or small dangerous molecules (see figure 6.4).

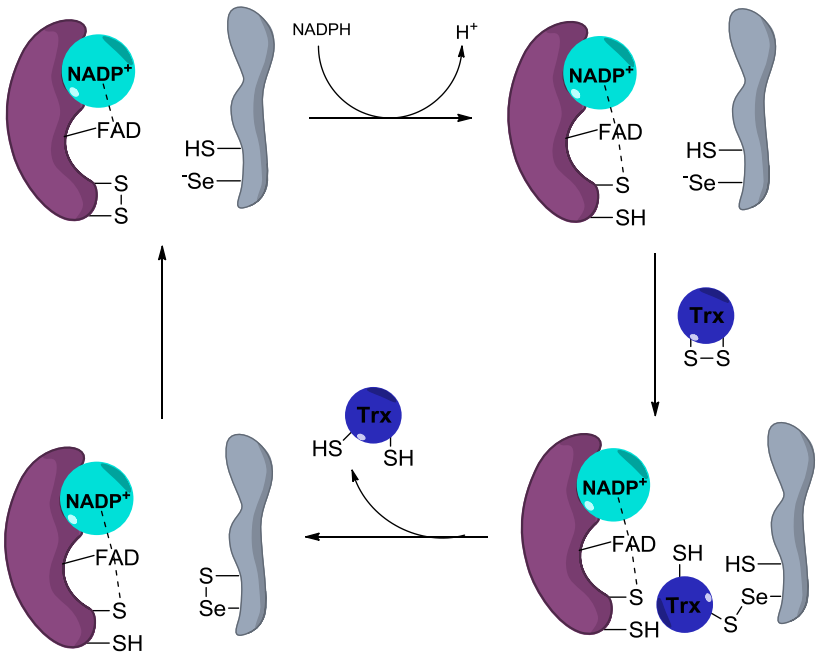

Figure 6.4: enzymatic mechanism of the Trx / TrxR system

TrxR type 2 is present on the membrane of mitochondria and plays an important role in cell survival. It concurs in the mechanism for the release of cytochrome *c*, apoptosome formation and apoptosis induction. TrxR type 3 is not largely expressed such as the other two subtypes and its role is still unclear.[189]

In the last decades the selective inhibition of TrxR arises as possible new effective anticancer strategy. Many reports are assessing that its inhibition produces a deep metabolic onset in cancer cells with an increment of ROS concentration, mitochondria dysfunction and cell death.[184,190,191] Gold complexes resulted to be the strongest TrxR inhibitors with IC_{50} in the low nanomolar range, 10 - 100 times fold more potent in comparison with organic compounds (e.g. PX12).[192] The selenocysteine present in the C-terminal active site of the enzyme has a pk_a 5.3 (cysteine just 8.1) and better coordination potential due to its Lewis base properties. Gold is a soft Lewis acid and its strong affinity for cysteine and moreover for selenocysteine determine an excellent selectivity. The inhibition of TrxR, such as main target for gold based therapy, has been evaluated and compared to the GR inhibition that possesses more than 75% of structural affinity in the active site with TrxR.[180]

6.3 TrxR and GR in situ inhibition by gold(I) NHC complexes[145,153]

The inhibition of the activity of the target enzyme TrxR and the structurally closely related GR by the NHC gold complexes **1a** - **4a**, **2b** – **2f**, **5c**, **5e** and the compounds **2** and **5** (as negative controls) as well as the gold(I) phosphine species Auranofin, chlorido triethylphosphine gold(I) (TEPG), and TPPG (as positive controls) was performed using the isolated enzymes. Whereas the non gold-containing compounds **2** and **5** were devoid of any activity against both enzymes, strong inhibitory effects against TrxR (IC_{50} values between 0.009 and 5.0 µM) and more moderate or no effects against GR (1.9 to > 100 µM) could be noted for all gold(I) complexes (see table 6.1).

	IC_{50} TrxR (µM)	IC_{50} GR (µM)	selectivity (x-fold)
auranofin	0.009 ± 0.000	15 ± 0.1	1666
TEPG	0.037 ± 0.005	7.9 ± 0.4	213
TPPG	0.256 ± 0.002	4.2 ± 0.7	16
2	>50µM	>50µM	n. a.
5	>50µM	>50µM	n. a.
1a	0.399 ± 0.040	30 ± 2.5	75
2a	0.361 ± 0.040	8.7 ± 0.0	24
3a	0.465 ± 0.006	9.3 ± 1.7	20
4a	4.01 ± 1.0	94 ± 15	23
2b	4.89 ± 1.15	> 100	> 20
2c	0.66 ± 0.02	2.60 ± 0.55	3.9
2d	0.034 ± 0.007	3.42 ± 1.62	101
2e	0.031 ± 0.001	2.55 ± 0.12	82
2f	0.113 ± 0.058	4.72 ± 0.53	42
5c	1.949 ± 1.020	49.9 ± 1.55	26
5e	0.019 ± 0.002	1.94 ± 0.24	102

Table 6.1: TrxR and GR in situ inhibition by Auranofin, TEPG and TPPG as positive controls (green), different free ligands (**2** and **5**, gray) and gold(I) NHC complexes (light blue: first series, blue: second series, dark blue: third series)

Overall, these results clearly demonstrate that the gold(I) center is necessary for the inhibition of the enzymes and support the assumption of the preferential binding to the selenocysteine residue present in the active site of TrxR. One striking feature observed in these enzymatic studies is the strong selectivity for TrxR over GR (see figure 6.5 for an example), which had been previously described for various gold phosphine derivatives and was also found for the here reported series of gold(I) NHC complexes.

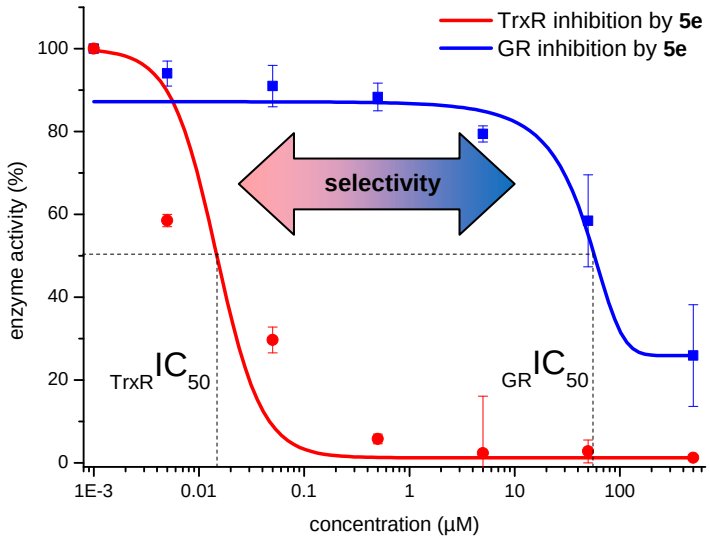

Figure 6.5: example of dose-response curves of the inhibition of TrxR and GR by complex **5e** and selectivity comparison

Moreover, the first series of complexes (**1a** – **4a**) demonstrated a good activity in the submicromolar concentration range, with the exception of the diphenylmethyl derivate **4a**, which exhibited a comparably low solubility in the used assay buffer that might explain its significantly lower activity.

The modification of the side chains at the benzimidazole core resulted in a minimal or no influence on the enzyme inhibition. The alteration of the second ligand at the gold atom (chlorido, NHC or phosphine), analyzed in the second series (**2b** and **2c**), produced interesting effects and changed the biological profile of the molecules. According with the theoretical data on BDEs (see chapter 4), the increase in the dissociation energy of

complex **2b** resulted in a decrease of reactivity towards TrxR and in a block of the activity towards GR, for which no inhibition could be determined up to the highest concentration used (100 µM). Complex **2c** was a good compromise between the phosphine and carbene class, demonstrating an enzymatic inhibition profile similar to other tested gold(I) NHCs (**1a** – **4a**) coupled with relative high BDE.

In general, higher activity was noted for the investigated gold(I) phosphine positive control derivatives (auranofin, TEPG and TPPG), which also represent a kinetically more reactive class of gold(I) complexes.

The coordination of the 1,3-diethylbenzimidazol-2-ylidene gold(I) rest with different phosphines (trimethyl, triethyl and triisopropyl) resulted in an outstanding activity with IC_{50} values in the low nanomolar range and an improvement in the selectivity towards TrxR in comparison with the precedent series (**1a** – **4a**, **2b** and **2c**). The activity was directly comparable to the hindrance and coordinative potential of the substituent (**2d** - **2f**, **2c**). Not bulky phosphine ligands inhibited the target enzyme TrxR more efficiently with an order of activity: **2c** < **2f** < **2e** < **2d**. The insertion of a methoxy group at the carbene core modulated the coordination at the NHC. The electron donor group increased the coordination potential of the carbene-metal bond, depressing the inhibitory activity of the triphenyl phosphine derivative **5c**. This chemical modification was not affecting the activity towards GR, influencing consequently the selectivity of the compounds. Especially for complex **5e** an exceptional activity and selectivity, in the range of the strongest gold base inhibitors, has been found. This profile is expected to be the result of the base activity of the triethylphosphine gold(I) moiety (see **2e** enzyme inhibition profile) and increment in selectivity due to the NHC-methoxy residue.

Overall, the SARs clearly demonstrated the importance of the gold(I) center to carry the activity as well as the ligands chemical properties to modulate it. While modifications at the side chains did not result in variation of the biological spectrum, the modulation of the chemistry of the ligands had a deep influence on the TrxR inhibition and selectivity. Gold(I) NHC phosphine complexes proved to be the most potent and selective molecules

of all the series. The insertion of an electron donor group as well as the minimization of the phosphine hindrance resulted in the most effective complex **5e** that for biological profile is almost comparable to other really potent TrxR inhibitors.

6.4 GPx in situ inhibition by gold(I) NHC complexes[153]

The presence of a selenocysteine in the active site of the interface domain of TrxR represented the reactive point of the protein and the specific target for gold complexes. The chemical difference between selenocysteine and cysteine is supposed to be the reason for the strong selectivity of the complexes towards this enzyme of the antioxidant network. TrxR is not the only seleno-protein present in the cell. Glutathione peroxidase (GPx) is another seleno-protein involved in the cellular protection against ROS. In order to study the selectivity between seleno-proteins the interaction between the gold(I) NHC complexes towards GPx was investigated (see table 6.2).[193]

	IC_{50} GPx (µM)	selectivity (GPx / TrxR)
2	> 100	---
2a	10.8 $^{\pm 0.95}$	30 fold
2b	> 100	>20-fold
2c	> 100	>150 fold

Table 6.2: GPx inhibition by **2a**, **2b** and **2c** and selectivity against TrxR

Representative complexes with a chlorido, a carbene and a phosphine as second ligand have been chosen and tested for their GPx activity. The enzyme was only inhibited by **2a** with an IC_{50} value approximately 30 fold higher than that observed with TrxR, which demonstrated that the compounds are not unspecific seleno-enzyme inhibitors. More interesting results showed **2b** and **2c**. Both the cationic compounds were not influencing

the activity of GPx at concentration up to 100 µM. The gold free ligand **2** was once more again inactive against GPx.

6.5 Disulfide reductase inhibition in cell lysates by gold(I) NHC complexes[145]

In order to evaluate the difference between the *in situ* / *in vitro* inhibition of the target enzymes, a cell lysates assay has been performed. HCT-116 coloncarcinoma cells were treated with different effective concentrations of complex **2a** for 18 h at 37 °C with the 5 % of CO_2. After the incubation the cells were pelletted, the membrane disrupted and the lysates collected. The disulfide reductases activity was determined according with the established condition for the *in situ* assay. The results indicated a clear effect of the gold complex on the reductases system with IC_{50} values one order larger in comparison with the *in situ* evaluation (see figure 6.6) but good comparable with the cytotoxic effects (see chapter 8).[194]

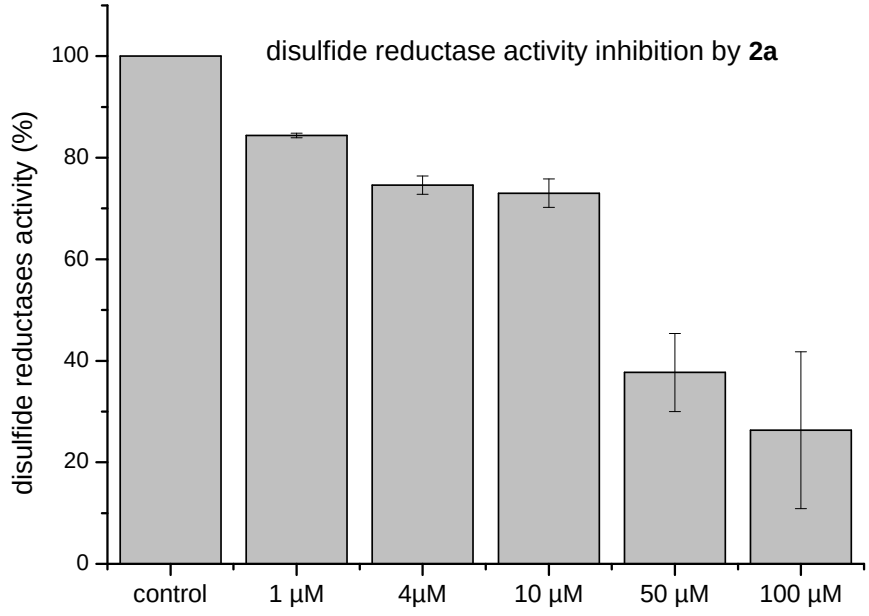

Figure 6.6: inhibition of disulfide reductases in HCT-116 cell lysates by **2a** after 18 h incubation at different concentrations

The results, in accordance with the antiproliferative activity, indicated that the enzyme inhibition has a central role to explain the activity of the complexes. Because GR and GPx are regenerated by TrxR, the hypothesis that a selective inhibition of that enzyme will produce a severe damage on the whole prevention system, having an impact on the cell homeostasis, is drastically enforced.[195]

7. Mass spectrometry investigations

MS experiments on the interaction of chlorido triphenylphosphine gold(I) with glutathione as well as the interaction of the gold(I) NHC carbenes with the selenocysteine containing decamer peptide were performed by Dr. Maria Stefanopoulou in the group of Prof. Dr. William Sheldrick, Lehrstuhl für Analytische Chemie, Ruhr-Universität Bochum, 44780 Bochum, Germany

MS experiments on the interaction of gold(I) NHC carbenes with the TrxR-containing-motif undecamer peptide were performed by Dr. Chiara Gabbiani in the group of Prof. Dr. Luigi Messori, Facoltá di Chimica, Universitá degli studi di Firenze, Via della Lastruccia 13, 50019 Sesto Fiorentino, Firenze, Italy

7.1 Background, importance and applications

Since the development of mass spectrometry (MS) by Goldstein in 1886 and Wien in 1899, MS analysis started to play a key role not only as mere molecule detecting tool but also as important method to perform high quality biological investigations such as proteomics and metabolomics.[196]

The principle at the base of MS analysis is the possibility for charged molecules to travel from an anode to channels of a perforated cathode in a low pressure medium. This flow can be deflected by the application of a magnetic field dependent on mass and charge of the molecules. The separation can be evaluated equating the Lorentz force law and the Second Newton law where *m* represents the mass, *Q* the charge, *a* the acceleration, *E* the electric field, *v* the velocity of the particle and *B* the magnetic field (see equation 7.1).

$$\left(\frac{m}{Q}\right) a = E + vB$$

Equation 7.1: relation between mass, electric field, magnetic field and charge of the particle

A MS measurement consists of the ionization of the target compound, its vaporization in the MS ion source and the carrying of the ionized molecules by an inert gas such as helium into the mass spectrometer under vacuum condition (see figure 7.1). In the spectrometer the ion flow will be deflected by the magnet, the magnitude of this deviation analyzed by a detector in form of scan (*m* / *Q*) of the molecules and increased by an amplifier.

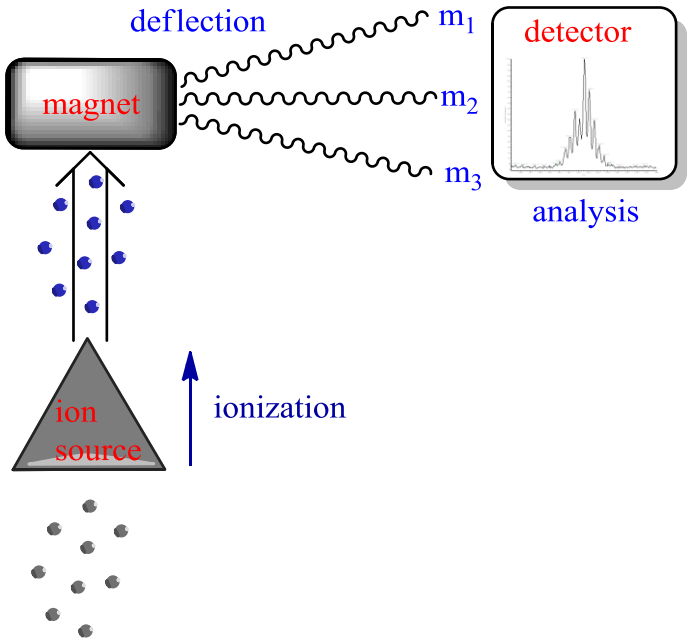

Figure 7.1: schematic representation of a MS analysis.

Ionization and MS-separation are key parameters to perform proper MS analysis. The molecules are deflected and detected according to their *m* / *Q* that is commonly replaced by the factor m / z where *z* = *Q* / *e* and relates to *Q* the dimensionless number of elementary charges *e*. A mass spectrometer can work in positive or negative modus.

Different ionization methods are involved for different sample types. Electron ionization (EI) and chemical ionization (CI) are providing normally a strong ionization suitable for organic compounds and involved gas chromatography (GC) as injection method. Typical liquid or solid phase samples are ionized with electron spray ionization (ESI when charged) or matrix assisted laser desorption ionization (MALDI). Inductively coupled plasma (ICP) source ionization is provided by an electric current provoked by radio

frequency magnetic field with a surrounding plasma coil, in which electrons are put in. ICP is a suitable technique for cations in really low concentrations or to determine metal traces. Fast atomic bombardment (FAB) ionization is obtained by the bombardment of the compounds inserted in a non-volatile matrix with a high energy electron beam. It represents a sort of ionization providing charged M^++H^+ ions. Quadrupole mass spectrometers (triple, linear or toroidal) are composed of 4 parallel rods that through specific radio frequency stabilize or destabilize compounds with the selected m / z. They work as a sort of analytic filter and are mainly involved in metabolomic and proteomic analysis. Tandem MS (MS / MS) operates a double fragmentation of a molecule. The ratio between mother MS and daughters MS provides high detection accuracy. Recently another kind of MS technique with high accuracy and sensitivity has been developed: orbitrap MS. Orbitrap works like a quadrupole with, at the end of the atoms fragmentation pathway, a spindle shaped electrode that allows the ion fragments to oscillate, prolonging their detectable time. The oscillation frequency produces current-images that will be translated into spectra through Fourier transformation where *f* is the frequency, *Q* the ion charge, *B* the magnetic field and *m* the mass of the molecule.

$$f = \frac{QB}{2\pi m}$$

Equation 7.2: relation between the frequency of the oscillation and the mass of the tested compound

MS analysis presents some advantages. High accuracy and sensitivity, the use of relatively low sample concentration, high reproducibility and the possibility to be coupled with other separation methods (e.g. GC, HPLC, electrophoresis or CE) resulted in a huge increase of application fields.[197,198] MS of big macromolecules as well as whole cell extracts make a new valuable tool to investigate biological processes available to the researchers.[199] One of the first investigations has been performed in 1958 when Andersson involved MS experiments to sequence the amino acidic more abundant peak

in a selected peptide.[200] Reproducibility and reliability of MS spectra have been used in pharmacokinetic studies to determine the rate of drug clearance in urine, the metabolization in liver or to quantify the accumulation of specific markers in tissue.[201] Specifically in the field of the proteomics, MS advantages resulted to be decisive.[202,203] Coupled with mild ionization techniques, two main methods are involved in protein characterization: top down and bottom up approaches. In the top down analysis whole proteins are ionized through MALDI or ESI and injected into a triple or linear quadrupole. In the bottom up technique proteins are previously lysed by proteolytic enzymes and analyzed by tandem MS according to a classical pattern called peptide mass fingerprint (PMF).

7.2 MS investigations on the interaction between TPPG and glutathione [145]

The inactivation by Glu seemed to play a key role in cell homeostasis. The gold(I) carbene complexes did not react with the tripeptide while gold(I) phosphine complexes (used as positive control) allowed the formation of significantly more than 100 % of the product TNB (see chapter 5). The data coming from the photometric assay and ^{31}P NMR studies suggested a possible further break down / oxidation reaction at the phosphine moiety and the formation of a DTNB–Glu / gold adduct. Because the results were still partially shaded, further studies on the kinetics of that DTNB–Glu / gold complex reaction have been required. Some reports are describing the possible non-enzymatic oxidation that could occur to the phosphine residue of Auranofin.[169] MS / MS investigations on the formation of triphenylphosphine oxide from chlorido triphenylphosphine gold(I) (TPPG) incubated with glutathione and DTNB have been performed. Clear spectra of the reaction mixture with significant signals were obtained (see figure 7.2). The data demonstrated the binding of the TPPG with TNB (695.24 m / z) and of the gold atom with both glutathione and DTNB (799.09 m/z), especially in the positive mode. The formation of the above mentioned triphenylphosphine oxide have been also confirmed in both the positive and the negative mode (316.36 and 316.07 m / z respectively). Overall the results

demonstrated that the phosphine moiety could undergo oxidation, supporting and clarifying the results previously described on the Glu interaction with gold complexes and DTNB (see chapter 5).

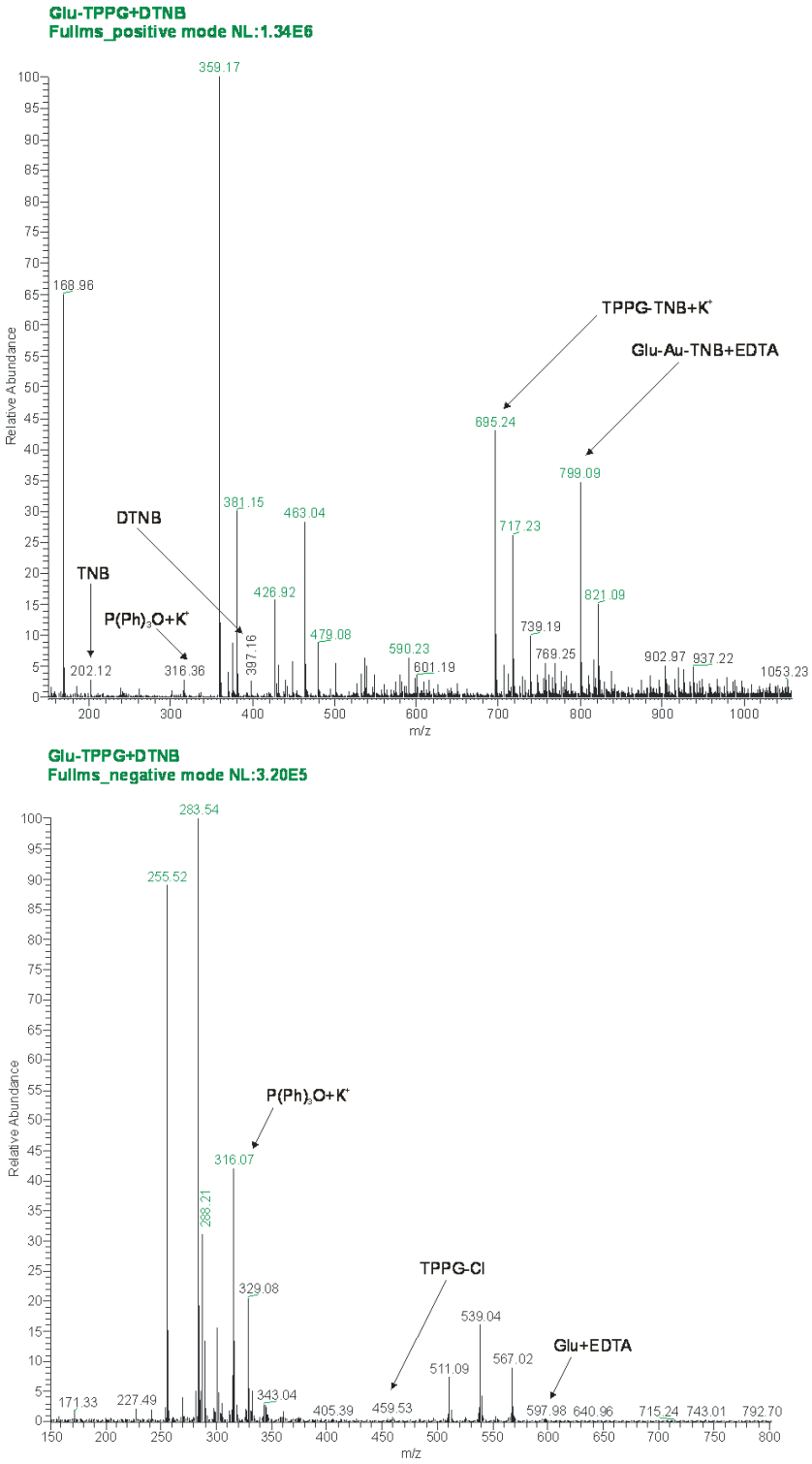

Figure 7.2: MS / MS spectra in positive (top) and negative (bottom) mode of $ClAuPPh_3$ incubated for 60 minutes with DTNB and glutathione at 40 °C; experiments performed by Dr Maria Stefanopoulou at the University of Bochum

7.3 Peptide interaction study

7.3.1 Interaction with a seleno-containing peptide[153]

To resemble the interaction with selenocysteine - containing enzymes a closely related selenocysteine - containing peptide (Ala-Gly-Sec-Val-Gly-Ala-Gly-Leu-Ile-Lys, AGUVGAGLIK) has been involved. Initial studies using chlorido triphenylphosphine gold(I) as a positive reference (data not shown) and the gold(I) NHCs **2a** – **2c** in full scan confirmed covalent binding of gold to the selenocysteine residue (see figure 7.3).

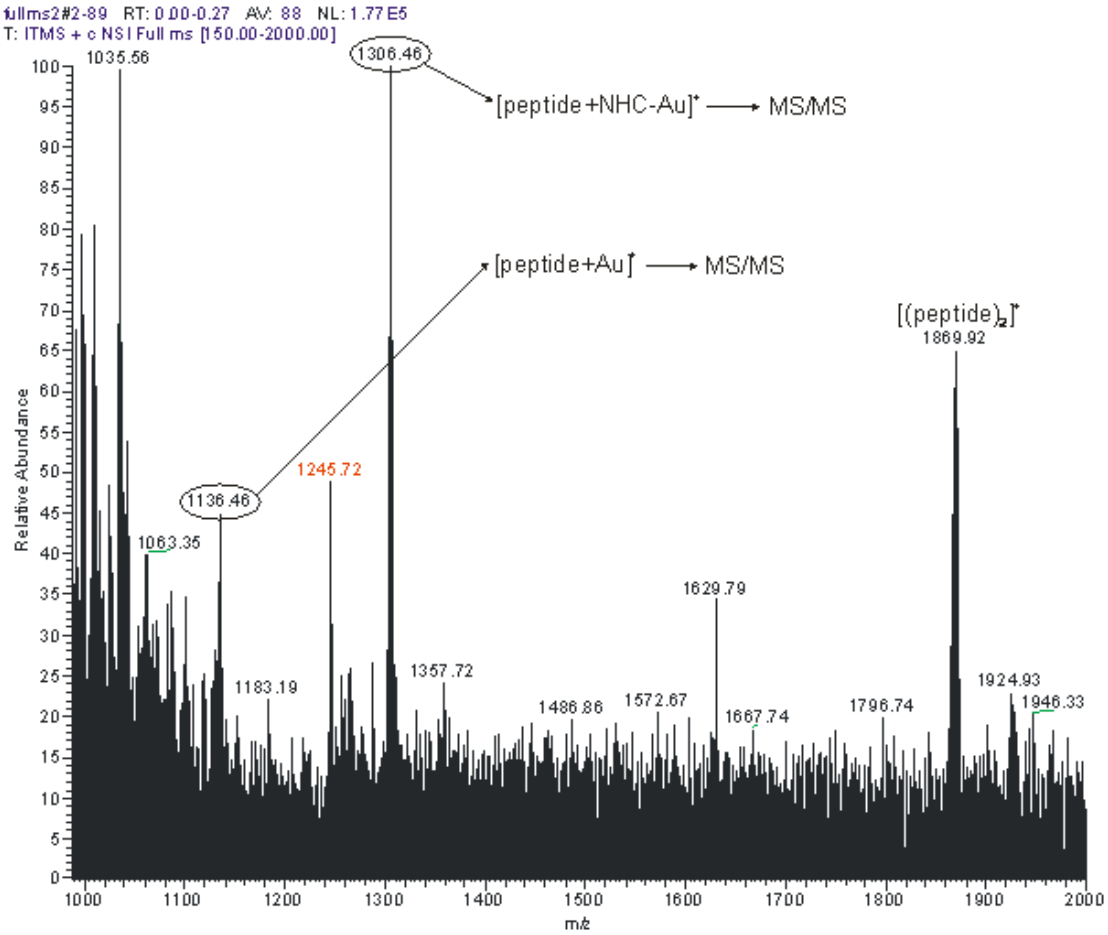

Figure 7.3: full scan of complex **2a** incubated for 48 h at 37 °C with the selenopeptide and localization of the covalent binding; experiments performed by Dr. Maria Stefanopoulou at the University of Bochum

Exposure of the seleno-peptide to complexes **2a**, **2b** and **2c** followed by MS ionization led in all the cases to molecular ions at *m / z* 1306 and 1134 corresponding to a gold

diethylbenzimidazol-2-ylidene fragment or a single gold ion being respectively attached to the peptide. MS / MS analysis of these molecular ions contained appropriate modified and unmodified series of b^+ (fragments containing selenocysteine) and y^+ (fragments containing cysteine) fragments ions that confirmed the selenocysteine residue as the major binding site (see figure 7.4 – 7.6). This indicated that covalent binding to selenium can indeed be expected to be the dominating mechanism of molecular interaction for the herein presented gold complexes.

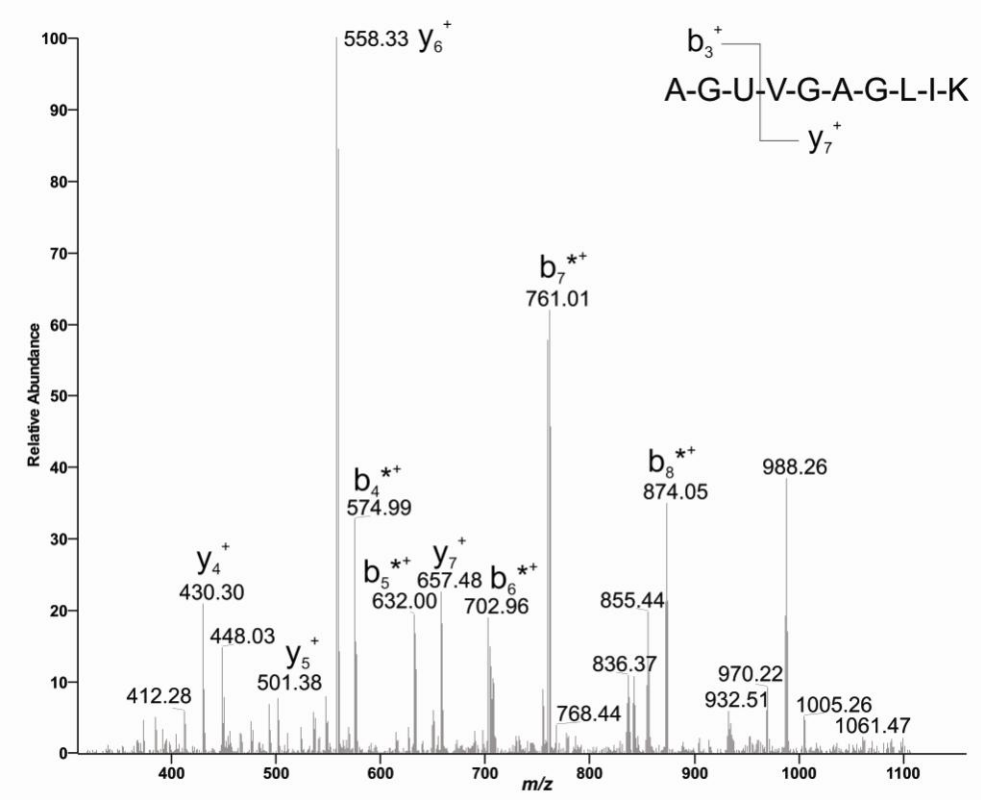

Figure 7.4: MS / MS spectra of complex **2a** incubated for 48 h at 37 °C with the selenopeptide and localization of gold bonded fragment(*); experiments performed by Dr. Maria Stefanopoulou at the University of Bochum

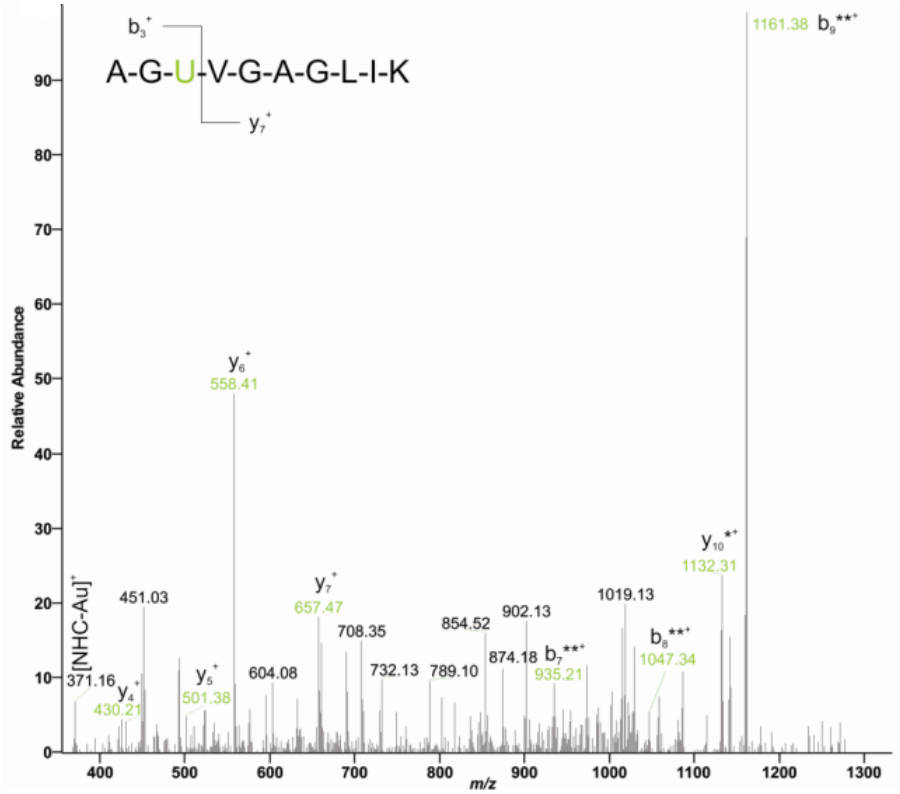

Figure 7.5: MS / MS spectra of complex **2b** incubated for 48 h at 37 °C with the selenopeptide and localization of the gold bonded fragment(*); experiments performed by Dr. Maria Stefanopoulou at the University of Bochum

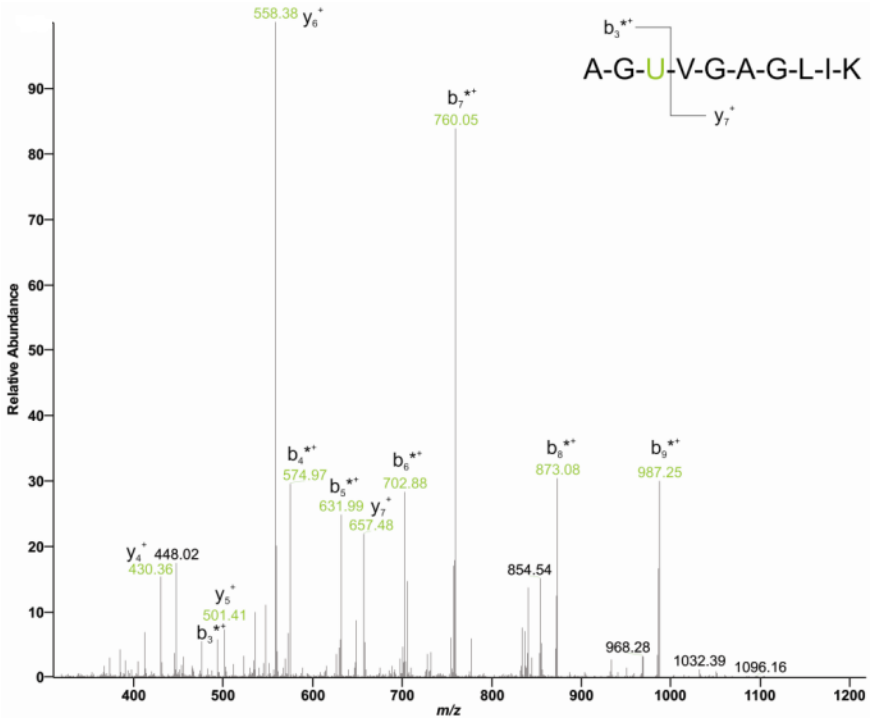

Figure 7.6: MS / MS spectra of complex **2c** incubated for 48 h at 37 °C with the selenopeptide and localization of the gold bonded fragment(*); experiments performed by Dr. Maria Stefanopoulou at the University of Bochum

7.3.2 Interaction with a seleno-containing peptide

The target enzyme TrxR possesses a characteristic amino acidic motif in its active site containing the selenocysteine. Thus, it was of interest to study the interaction of complexes **2a**, **2b** and **2c** with a selenopeptide mimicking the active site of TrxR. The seleno-dodecapeptide was prepared by solid phase peptide synthesis, following an established method present in the literature, and purified by reverse phase HPLC before to be tested by ESI-MS / MS in negative mode.[98] Preliminary full scan analysis of the dodecapeptide confirmed the presence of a main peak at 1181.3 m / z, corresponding to the peptide M^+ (data not shown).

Subsequently, the peptide was incubated for 20 minutes at room temperature with the gold complexes **2a** - **2c**, in a 3:1 molar ratio. The resulting ESI-MS spectra are shown in figure 7.7.

The obtained ESI-MS/MS spectra clearly showed the formation of different products matching the peptide-Au containing fragment for all the three gold carbene compounds **2a** – **2c**. Interestingly, for all the molecules the same MS fragment Au-NHC^+ bonded to the peptide could be detected. This result confirmed that the second ligand (NHC-Au-L) at the gold atom was mainly the leaving group of the compound. However, it resulted clear that the degree of peptide metalation and adduct formation differed in all three cases with the order of reaction **2c** < **2b** < **2a**. In fact, complex **2a** caused extensive peptide metalation with significant molecular peaks found at 1992.9, 1749.2, 1553.2 and 1379.3 *m / z*. Complex **2b** slightly metallated the dodecapetide while for complex **2c** just a very tiny and nearly negligible interaction was detected. In experiments with the dodecapeptide and Auranofin (as posivite control) an extensive peptide metallation has been observed as it is seen shown in figure 7.8

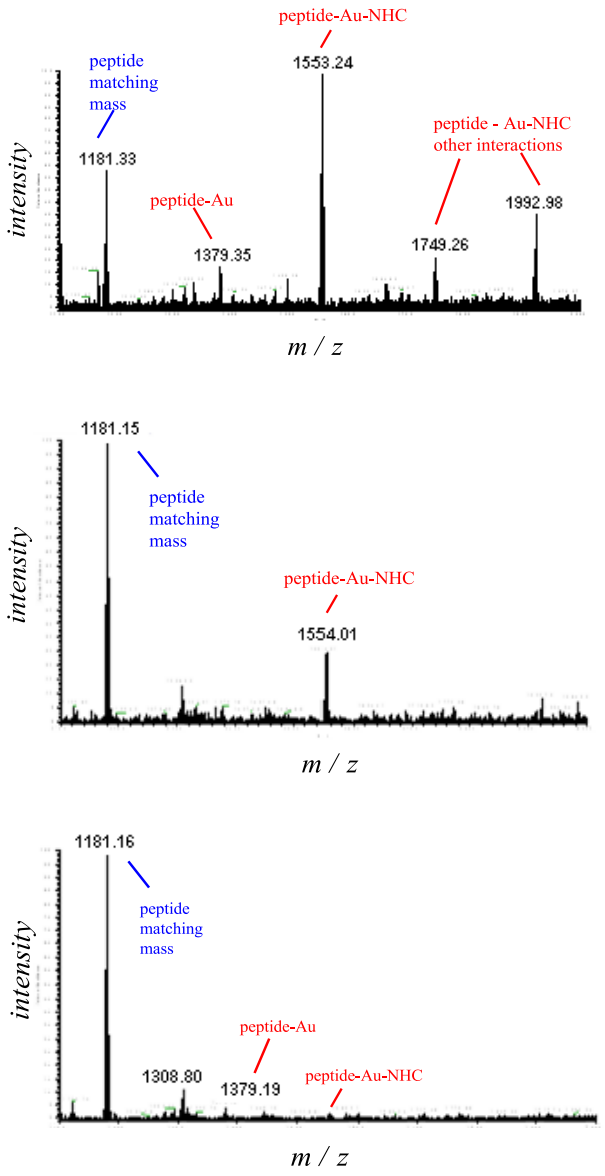

Figure 7.7: MS study of **2a** (top), **2b** (middle) and **2c** (bottom) incubated 20 minutes at room temperature with the seleno-dodecapeptide; experiments performed by Dr. Chiara Gabbiani at the University of Firenze

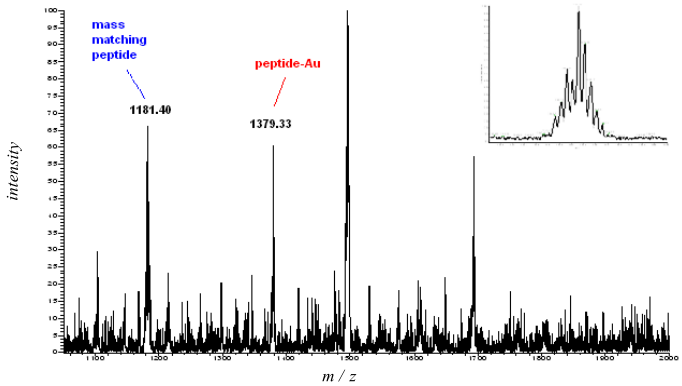

Figure 7.8: MS study of the interaction between Auranofin and the selenopeptide (with the Auranofin-peptide pattern): experiments performed by Dr. Chiara Gabbiani at the University of Firenze

7.4 Proteomics

Proteomics is the research branch which aims a detailed proteins study: their conformation, role and modification. Proteins are among the main bio-macromolecules present in the cell, having many roles, from the mere structural function to the most complicated regulators of metabolic pathways. Crucial feature of proteins is the spatial conformation obtained through internal bonds, Van der Waals forces and post-translational modifications like phosphorylation, acetylation or ubiquitination. These chemical modifications are strongly related to the protein activity.[204,205]

With the advent of Cisplatin, DNA became a main target for metal-based drug development. Intercalators, histone destabilizers, nucleotide analogues have been broadly investigated. Recently a different approach in cancer research caught on. In the last decades, tumor over-expressed enzymes started to play a central role as possible alternative therapeutics. Especially, gold complexes resulted phenomenal inhibitors of the disulfide reductases family with a high selectivity towards TrxR.

Proteomics is an important tool to evaluate not only the protein-mediated signalling pathways but even to study the chemical interaction of xenobiotics with target proteins. Due to the complexity of cell suspension contents, proper techniques are required to extract, separate and analyze specific proteins. The combination of the separation potential of multidimensional chromatography and identification and sequencing accuracy of mass spectrometry is a convenient and efficient tool to perform proteomic analysis. Multidimensional protein identification technology (MudPIT) is the combination of these two technologies, associated to a database searching system.[206-208]

The proteins separation is not performed by electrophoresis but by biphasic and triphasic microcapillary columns associated to a HPLC system and used as injection method. The direct interface of the source and the separation method provide a drastic implement in sensitivity, avoiding band broadening. The base of the chromographic separation takes advantage of the different hydrophilicity of the proteins. A proper cell lysis and solubilisation will give a protein mixture of charged (hydrophilic) and uncharged (lipophilic)

peptides. This mixture is separated depending on the affinity of the peptide to the pre-column / column. After a washing procedure, differential eluation will be used to bring the different peptidic fractions to the MS / MS system. The MS spectra are analyzed and compared to online bibliography from a protein database server (see figure 7.9).

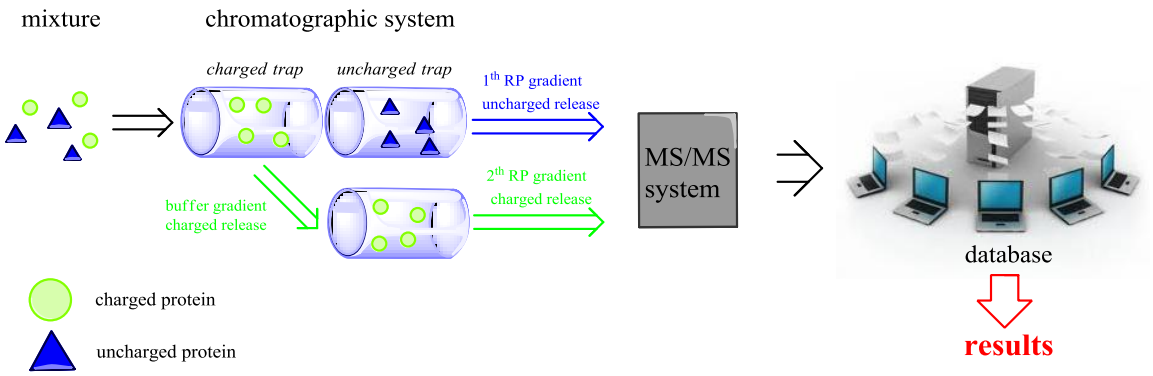

Figure 7.9: schematic representation of MudPIT working flow

MudPIT analysis has been performed for the selected gold complex **2b**. For comparative purposes, the incubation time was chosen to be 3 h (as well as for the uptake studies presented in chapter 9 and microarray experiments in chapter 10) and the concentration was set at 3 µM (as well as for the uptake studies and BIONAS data presented in chapter 10). A great number of peptides have been evaluated and significant alterations of the expression of the proteins are listed in table 7.1. The data show a large standard deviation, but even if they are not suitable for scientific publication they represent really interesting preliminary results of a proteomic studies of cellular protein expression regulation stimulated by a gold(I) NHC complex (**2b**).

A first sub-categorization of the proteins taken into consideration has been made. Four classes have been recognized: protein folding, phosphotransferase, DNA interaction and motility and transduction regulation (see figure 7.10). The protein folding process is responsible for the imprinting of the active protein shape.

The protein folding process is responsible for the imprinting of the active protein shape. The effect of **2b** on this class is really interesting. All the proteins investigated present a general under-expression.

Name of the Protein	Function	MuPIT result
Retinal Dehydrogenase I	oxidoreductase / Ras GTPase activator/ Vitamin A	up-regulated
Isoform C of Prelamin A/C	apoptosis/ oxidative stress / cell migration	up-regulated
Protein Disulfide Isomerase	cellredox homeostasis/ lipid & lipoprotein metabolic	down-regulated
Annexin A2 and isoform 2	heat-stress response/ angiogenesis	down-regulated
Histone H1.2-5	nucleosome assembly	up-regulated
Heat shock cognate	stress response/ regulation of transcription	down-regulated
X-ray complementing repair protein 6	DNA repair / transcription regulation	up-regulated
Elongation factor 2	protein biosynthesis	up-regulated
Protein disulfide isomerase A4	cell redox homeostasis (3 thioredoxin domains)	up-regulated
Pyruvate kinase isoenzyme M1 M2	glycolysis/ kinase/ transferase/ apoptosis	down-regulated
ATP synthase subunit alpha	H^+ transport/ respiratory electron transport chain	down-regulated
High mobility group protein B2	DNA damage/ DNA-RNA Pol. II transcription regulation	up-regulated
Calnexin	post-translational protein modification/ protein folding	down-regulated
mTrifunctional enzyme α	fatty acid metabolism/ lipid metabolism	up-regulated
nHeterogeneouesprotein M	mRNA processing/mRNA splicing	up-regulated
Adenilate kinase and isoforms	kinases/ transferases	up-regulated
cActin 1-2	cytoskeleton/ 'de novo' posttranslational protein folding	down-regulated
60S ribosome L10a	mRNA translational elongation/ termination	up-regulated
neuroblast AHNAK	nervous system development	up-regulated
Aspartyl/aspargyl β hydrolase and isoforms	oxidoreductase	down-regulated
Neutral α glucosidase AB	protein folding/ post-translational protein modification	down-regulated
Plectin and isoforms	cellular component disassembly involved in apoptosis	up-regulated
Myosin	motility	down-regulated

Table 7.1: proteins with a significant change in expression, obtained from MCF-7 lysates treated with 3 µM of **2b**; experiments performed by Dr. Maria Stefanopoulou at the University of Bochum

This could be explained by the good reactivity of the gold center atom that is able to bind free cysteines provoking consequently a strong misfolding of the structures. The phosphotransferase class is composed of a series of peptides in charge to transfer a phosphate moiety from a protein to another. This is one of the main mechanisms for the

translation of internal cellular signals. The translation of the signal induces protein biosynthesis, replication as well as apoptosis. **2b** presented a different effect on the various proteins investigated with a marked under-expression tendency. The data are in good agreement with the microarray results presented in chapter 10. The DNA interaction class is formed by a group of peptides which interacts DNA or RNA and ribosomes, induce cell death or survival stimuli. All the proteins analyzed presented a marked over-expression. This effect could be the symptom of a cellular answer which aims to compensate the stress provoked by **2b**. Proteins controlling the motility and regulating the transduction have been categorized under a single class because of the extreme variable effect of the gold complex on them. Overall, a general under-expression has been noted probably provoked by the ongoing stress and proximal apoptosis that modifies the plasma membrane and alters RNA protein transduction.

Protein folding (down)

Protein disulfide isomerase (PDI & A4)

Heat shock cognate (Hsc71)

Calnexin (CNX)

Neutral α glucosidase AB

Phospho-transferase (down)

Elongation factor 2 (EF2)

Pyruvate kinase isoenzyme M1 M2 (PK)

ATP synthase subunit alpha (ATPase-α)

Adenilate kinase andf isoforms (AK)

Aspartyl/aspargyl β hydrolase

DNA interaction (up)

Histone H1.2-5 (RdH2-5)

High mobility group protein B2 (HMG2)

X-ray complementing repair protein 6 (XCR6)

N-Heterogeneous protein M

60S ribosome protein L10a

Motility & transduction regulation (down)

cActin 1-2 (Act)

Isoform C of Prelamin A/C (ICPr)

Annexin A2 (AnnA2)

Plectin and isoforms

Myosin and Isoforms

Figure 7.10: protein classes monitored via MudPIT analysis; experiments performed by Dr. Maria Stefanopoulou at the University of Bochum

8. Antiproliferative effects

Experiments on resistant cell lines, DNA fragmentation and LDH release were performed by Liliane A. Onambele from the research group of Prof. Dr. Aram Prokop, department of Paedriatric Oncology, Childrens Hospital Cologne, Amsterdamer Strasse 59, 50735 Cologne

Experiments on the resistant healthy HFF cell line were performed by Dr. Hamed Alborzinia, apoptosis induction by Dr. Igor Kitanovic from the research group of Prof. Dr. Stefan Wölfl, Institut für Pharmazie und Molekulare Biotechnologie, Ruprecht-Karls-Universität Heidelberg, Im Neuenheimer Feld 364, 69120 Heidelberg

*Experiments on the resistant healthy HEK-293 cell line for complex **2a** cell line were performed by Dr. Yvonne Geldmacher from the research group of Prof. Dr. William S. Sheldrick, Lehrstuhl für Analytische Chemie, Ruhr-Universität Bochum, 44780 Bochum, Germany*

8.1 Introduction

The life of a cell is enabled by a great number of metabolic processes. A complicated physiology provides nutrients and energy, regulates the stress answer and coordinates its replication. The alternation of all these phases constitutes the cell cycle that is mainly subdivided in a mitotic phase (M), the final step that leads to division and an inter-phase (I) in which the cell grows and prepares the replication step.[176] The inter-phase could be divided into growth (G) sub-phases. In the G_1 phase the cell increases its metabolism, growing up until a maximum and then switches to the S phase in which the replication of DNA occurs. In the G_2 phase the cell still marginally grows and all the mechanism needed for the mitosis are prepared.[176] Finally the cell enters in the M terminal phase and mitosis

occurs. A cell that naturally leaves the normal cell cycle and hold its mitotic process is named quiescient or senescient (G_0 phase).[176]

There are several checkpoints during the cell cycle that control survival and replication (for example factors like p53 or p38 play a key role in both the G_1-checkpoint and G_2-checkpoint). An alteration of the checkpoints or differentiation in cell cycle could induce carcinogenesis. Under normal conditions cell survival is highly controlled and regulated. Strong homeostatic mysregulation and cellular stress induce processes of programmed cell death (especially in eukaryotes). There are three main types of programmed cell death: apoptosis, paraptosis / autophagy and necrosis.[176,209-212]

Apoptosis is a complicated metabolic multi-pathway that leads to cell death. It is composed by many factors, cascades and regulations. Almost 80 % of the apoptotic pathways converge to caspase 3 (Casp3) activation. Casp3 selectively cleaves Asp-aa-Asp sequences (where “aa” represents other different amino acids) contained in various proteins especially those constituting the cytoskeleton. Apoptosis presents some characteristic features like morphological changes, membranes blebbing, chromatin condensation and DNA fragmentation. It is a mediated cell death that occurs in not harsh conditions. It could be divided in two big categories: intrinsic or extrinsic apoptosis.[213,214]

The extrinsic apoptotic pathway is triggered by external factors like tumor necrotic factor (TNF) or Fas receptor interaction. They lead normally to the formation of adducts like TNF receptor-associated death domain (TRDD) or Fas / FasL (ligand) death inducing signaling complex (DISC) that activate caspase 8 and subsequently caspase 3. The intrinsic apoptosis is a mitochondria mediated pathway. It is provoked by different stimulation like oxidative stress, radiation, chemotherapy or internal communication pathways (p38, Hsp family). It works through the formation of apoptosome, release of Ca^{2+} cations into the cytosol, Bcl2 stimulation and activation of caspase 9 and caspase 3 (see figure 8.1).[215]

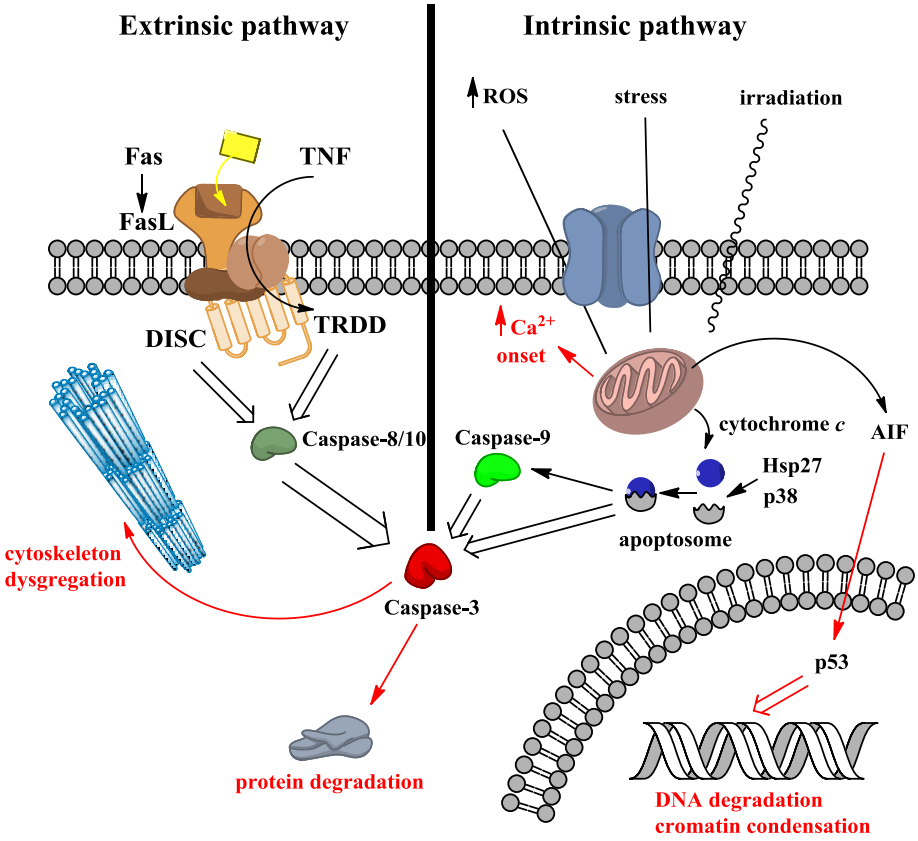

Figure 8.1: schematic representation of extrinsic (left) and intrinsic (right) apoptotic pathway

During paraptosis or autophagy the cell degrades its own organelles through lysosomial auto-digestion. The process is induced by a strong protein damage and misfolding that leads to uncontrolled lysosomiomal activity. The lysosome grows up and starts to digest important structures such as cytoskeleton or nucleus. The cell swells up presenting a preliminary characteristic vacuolation phase with extended encompassing of all the organelles and cellular structures and leading to internal cell digestion (see figure 8.2).[216]

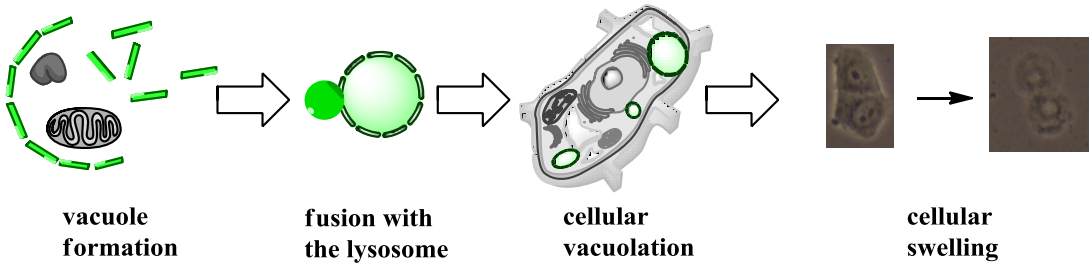

Figure 8.2: schematic representation paraptosis / autophagy

Necrosis is provoked by a strong onset of the cell homeostasis. While apoptosis is a metabolic pathway and presents some positive characteristic for the cell environment, necrosis is characterized by a fatal non metabolic process provoked by a strong external (infection, poison, etc.) or internal cellular stress (ROS, lysosome membrane damage, etc.). The plasma and internal membranes (like those of the mitochondria or nucleus) start a process of disintegration. The cellular components are lysed and the major osmotic misbalance provoked by the strong water penetration through the membrane dissociation lets the cell swell up (see figure 8.3).[176,212]

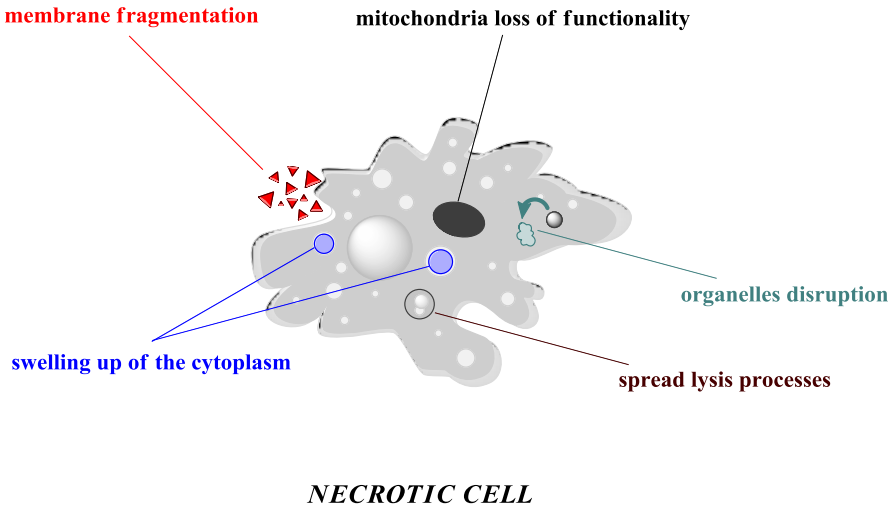

Figure 8.3: schematic representation of necrosis

Between these three cell death mechanisms, apoptosis induction and regulation provide a key tool to control the growth and health of the overall cell. A deviation from the normal cell cycle has been proven to be one of the causes of tumor formation. Cancer cells mutate and down-regulate effectors of programmed cell death like proliferation suppressor factors and start uncontrolled and undifferentiated replication processes. The high metabolic rate of malignant cells makes DNA replication more susceptible to failures. To control the potential dangerous exposure of the cell to this high metabolism, a strict network of signal translation pathways as well as enzyme networks has been largely

developed. These over-expressed components (e.g. anti-oxidant network, DNA-polymerases, kinases) are at the base of modern tumor therapy.[125]

8.2 Proliferation evaluation assays

In vitro antiproliferative effects provide a first basic screening to evaluate the possible anticancer properties of new drugs. A drug could have two different behaviors towards tumor: cytostatic and cytotoxic. Cytostatic is the property to block the replication of the cell without killing it directly. A substance with cytotoxic effect is able to provoke a strong onset in the metabolism that leads to cell death. A proper determination of the cytostatic / cytotoxic profile is required to start the characterization of new possible therapeutic agents.

One of the main parameters to monitor cell status is the membrane integrity. Because of its protection and regulation role, membrane porosity is a useful criterion to assess cell functionality. For example crystal violet is a dye able to penetrate the intact cell membrane, staining nucleoproteins and enabling to discriminate between living and damaged cells (see figure 8.4).[217] An increment in membrane permeation will enable specific dye to penetrate and stain also other intracellular components that will not be reached in normal conditions (e.g. in figure 8.4). For example, propidium iodide is a fluorometric dye that is uptaken into the cell only when the plasma membrane presents discontinuity, directly related to the apoptotic or necrotic processes.[218] Membrane homeostasis is experimentally controlled also by constituent sequestration. Lactate dehydrogenase is sequestered from the outside to the inside of the cell and its reaction could be monitored. Specific protease reactions are prohibited outside of the cell or when the cell is compromised. The measure of their activity is a useful parameter to control cell viability.[219] Also ATP based assays have been developed.[220] Reducing reactions could be also involved to determine cell proliferation. 3-(4, 5-Dimethyl-2-thiazolyl)-2, 5-diphenyl-2H-tetrazolium bromide (MTT) or resazurin are redox agents that are reduced by living cells to formazan (for MTT) or to fluorescent derivatives (for resazurin).[221] Recently, label-

free techniques have been developed to monitor living cellular populations. The determination of impedance as a measure of the cell morphological changes started to be an established procedure.[240] Cells are seeded on a gold-film electrode and the variation of the potential is studied.

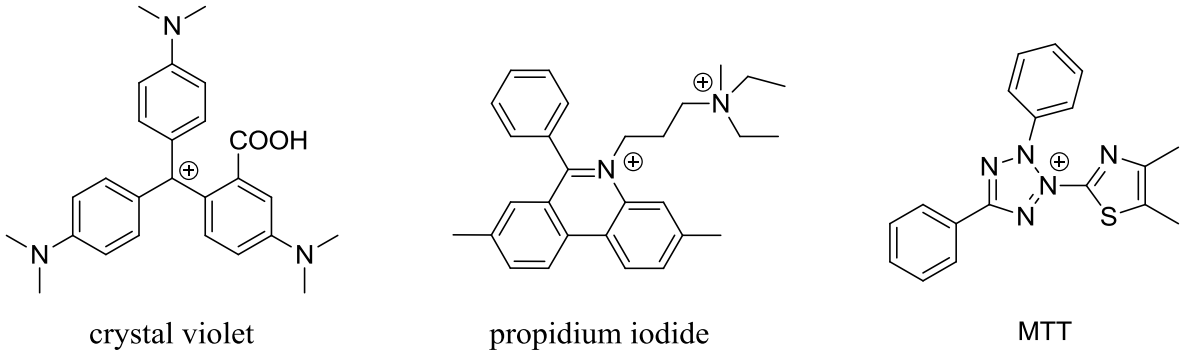

Figure 8.4: examples of cellular dyes

8.3 Effects on cell growth

8.3.1 Crystal violet and MTT staining[145,153]

The triggering of antiproliferative effects by the target new gold(I) carbene complexes was investigated in various tumor cell lines. A first screening of bioactivity has been conducted in two of the most common tumor cell lines with crystal violet assay: MCF-7 breast adenocarcinoma and HT-29 colon-carcinoma.

Relevant activities could be noted for all the complexes in these cell lines. The observed IC_{50} values (in the range of 0.11 - 13.3 μM) were generally within the same order of magnitude as noted for gold(I) phosphine species (IC_{50} values in the range of 1 - 5 μM in the used assay).[102] These results are in good agreement with other reports on bioactive gold carbene species, which reached activities in the low micromolar range.[109,112] The inactivity (IC_{50} values >100 μM) of the free benzimidazolium halides **2** and **5** confirmed that the gold center was necessary to obtain bioactive species.

Interestingly, the substitution of the chlorido leaving group in **2a** with the NHC and phosphine ligands in **2b** and **2c** led to an approximately 5 times fold increase in antiproliferative potency in MCF-7 cells as well as an approximately 15 fold increase in HT-29 cells.

Substance	IC_{50} HT-29 (µM)	IC_{50} MCF-7 (µM)
auranofin	2.6 ± 0.4	1.1 ± 0.3
TEPG	5.3 ± 1.9	3.2 ± 1.3
TPPG	4.2 ± 0.9	2.6 ± 0.1
2	> 100	> 100
5	> 100	> 100
1a	13.3 ± 4.4	7.5 ± 0.6
2a	6.4 ± 2.0	4.6 ± 0.0
3a	11.8 ± 1.9	10.2 ± 0.1
4a	12.3 ± 3.3	10.3 ± 0.7
2b	0.44 ± 0.13	0.81 ± 0.13
2c	0.40 ± 0.18	0.89 ± 0.40
2d	1.46 ± 0.19	0.74 ± 0.49
2e	8.85 ± 2.05	0.81 ± 0.07
2f	5.98 ± 1.78	0.59 ± 0.23
5c	6.23 ± 2.02	0.24 ± 0.01
5e	3.88 ± 1.51	0.11 ± 0.01

Table 8.1: antiproliferative effects of the new gold(I) carbene complexes on HT-29 human coloncarcinoma and MCF-7 human breast adenocarcinoma cell lines

An increase of the activity correlated with the change of the phosphine ligand was observed. A significant reduction of the cytotoxicity has been observed for the decrease of hindrance of the phosphine ligand (e.g. complex **2c** and complexes **2d** – **2f**). The data correlated well with already published information reporting the importance of lipophilic cations for the cellular uptake and the bioactivity.[112,149-151] A decrease in the phosphine lipophilicity will provoke a decrease in the cellular accumulation and weaker

anti-proliferative effects. An interesting preference of 2 – 35 times fold for MCF-7 against HT-29 cancer cells line has been observed for the third series of complexes (**2d** - **5e**). At this stage of the research an exhaustive explanation of the obtained selectivity cannot be explained. The role of lipophilic cations for the uptake and the selective delivery of the molecules (see chapter 9 and ref. 149) can play also a central role in explaining the obtained tendency. Also to be mentioned, MCF-7 display a larger size and estrogen receptors, differently to HT-29. But so far it was not possible to find a link between hormone-mediated cell answer and gold(I) NHC complexes. The insertion of an electron donor group on the carbene backbone deeply influenced the anticancer properties of the molecules that reached the lowest IC_{50} values (complex **5c** and **5e**). Another feature could be also observed in the dose-response curve, comparing for example complex **2a** and **2c**. For curve values above 0, there is just a block in replication and proliferation, while for curve values below 0 the target molecule is able to effectively kills the cells (even the seeded as control, before the complex treatment). **2a** (a neutral derivative) presented a cytostatic profile while **2c** (a lipophilic cationic derivative) resulted more aggressive displaying cytotoxic character (see figure 8.5).

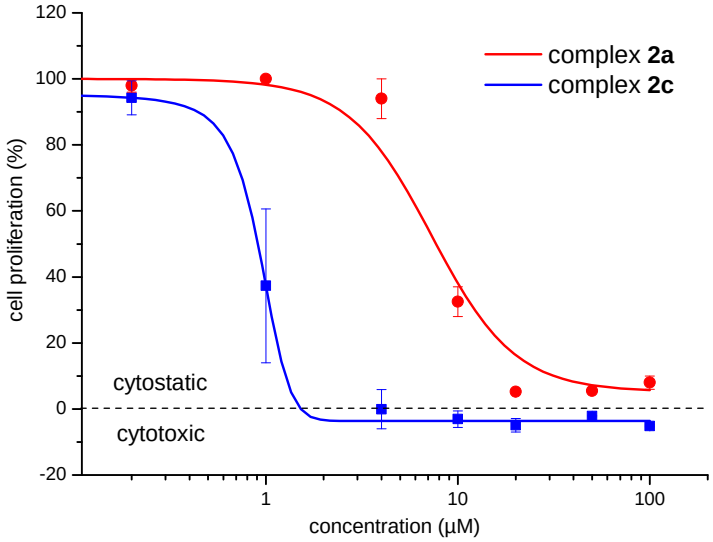

Figure 8.5: comparison between the antiproliferative properties (cytostatic / cytotoxic) of two chemically different gold(I) carbene complexes

Since the promising results revealed a remarkable activity in the range of benchmark anti-cancer compounds (e.g. tamoxifen, platinum derivatives[25,35]), it was of interest to study the activity of **1a** – **4a** towards other various cell lines. Other two cancers have been selected for further antiproliferative studies: HCT-116 colon-carcinoma and HEP-G2 hepato-carcinoma. Similar results have been observed for the other two target cell lines (with the exception of lower activity of **4a** in HCT-116 and HEP-G2 cells) (see table 8.2). The results clearly demonstrated the broad anticancer spectrum of the gold(I) NHCs.

Substance	IC_{50} HCT-116 (μM)	IC_{50} HEP-G2 (μM)
2	> 100	> 100
1a	6.7 $^{\pm 0.6}$	4.9 $^{\pm 0.8}$
2a	8.4 $^{\pm 2.2}$	11.2 $^{\pm 1.6}$
3a	10.0 $^{\pm 0.4}$	14.9 $^{\pm 3.9}$
4a	24.6 $^{\pm 2.8}$	60.7 $^{\pm 10.6}$

Table 8.2: antiproliferative properties of **1a** – **4a** towards HCT-116 human coloncarcinoma and HEP-G2 human hepatocarcinoma

In order to evaluate a possible selective effect of the gold(I) carbene compounds towards cancer cells, HEK-293 human embryonic kidney cells and HFF human foreskin fibroblast cells were used as a reference.

Selectivity towards cancer could not be confirmed for **1a** - **4a** and **2c** as comparative experiments in non tumorigenic cell lines (HEK- 293 human embryonic kidney cells and / or HFF human foreskin fibroblasts) afforded similar activities (IC_{50} values in the range of 7.6 - 32 μM). Interestingly, **2b** showed a slight preference towards cancer cells in comparison with HEK-293, with selectivity between 3 - 8 times fold (see table 8.3).

Substance	IC_{50} HEK-293 (µM)	IC_{50} HFF (µM)
2	> 100	> 100
1a	10.8 $^{\pm 1.1}$	12.2*
2a	10.3 $^{\pm 1.1}$	10.0*
3a	9.6 $^{\pm 3.5}$	8.9*
4a	32.0 $^{\pm 0.3}$	5.8*
2b	3.13 $^{\pm 0.5}$	n.d.
2c	0.41 $^{\pm 0.2}$	n.d.

Table 8.3: antiproliferative properties of **1a – 4a**, **2b** and **2c** towards HEK-293 immunized human embryonic kidney cells and HFF human foreskin fibroblast cells; *experiments performed by Dr. Hamed Alborzinia at the University of Heidelberg; ~ experiments performed by Dr. Yvonne Geldmacher at the University of Bochum

8.4 Video microscopic imaging[153]

The macro-morphology of MCF-7 cells was monitored in video microscopic imaging experiments. The cells were treated with an effective concentration (close to the IC_{50}) of complex **2a** (5.0 µM), **2b** and **2c** (both 1.0 µM) for 14 h and the changes in overall cell biomass are shown in figure 8.8 (pictures selected at 2, 6 and 10 h).

While just a sporadic rounding, detaching dying of single cells has been observed for the chlorido derivative **2a** (comparable with the untreated control), the cationic gold(I) NHCs (**2b** and **2c**) induced a strong and fast reduction of cell layer. This was accompanied by an alteration of cell morphology and cell swelling starting after approximately 8 - 10 hours of incubation. Overall these data confirmed again that for **2a** cell growth inhibition is mostly related to an inhibition of cell proliferation (cytostatic effect) whereas for the cationic species **2b** and **2c** also direct cytotoxic effects play a major role.

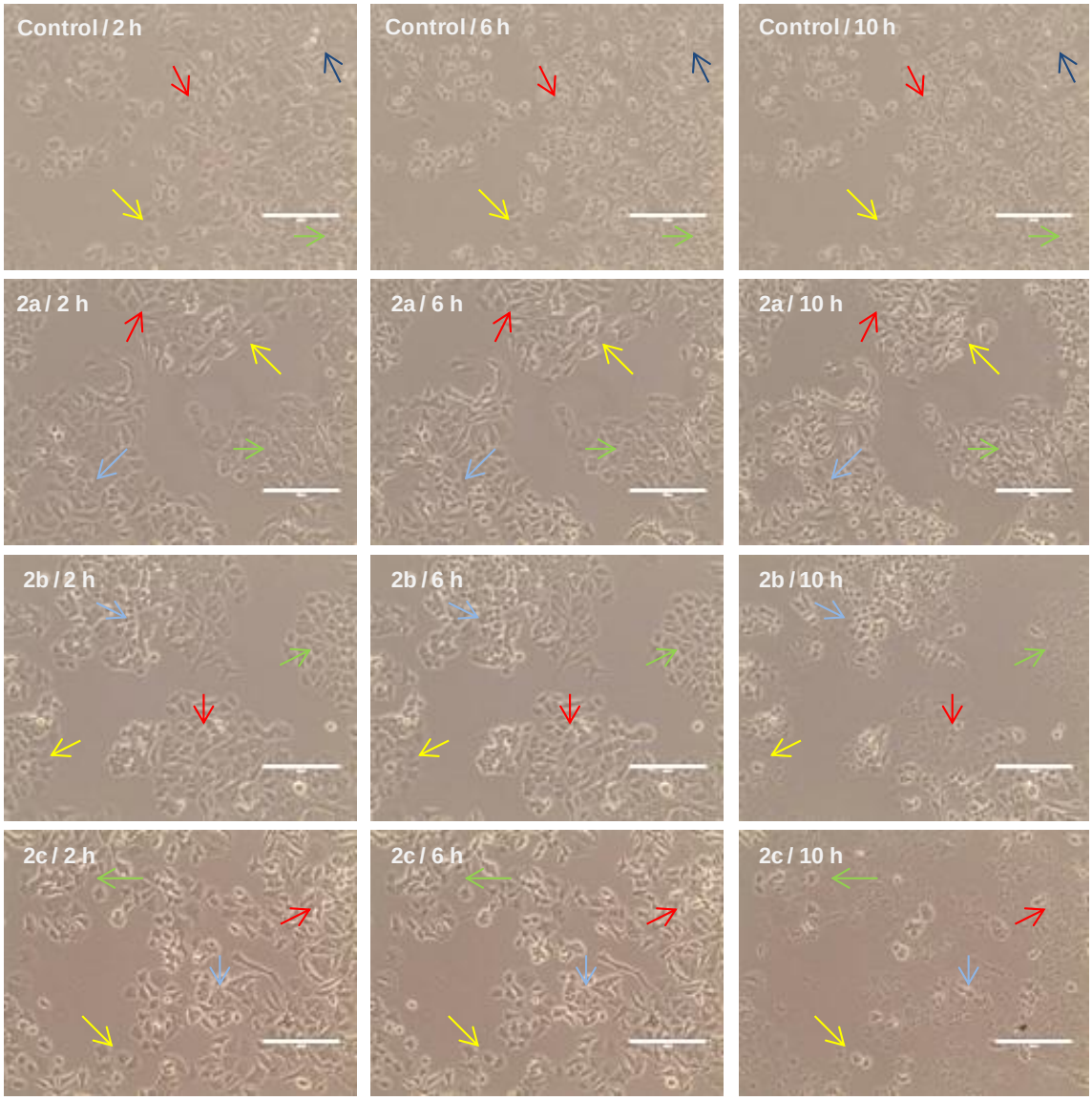

Figure 8.8: video imaging experiments of MCF-7 cancer cells treated with gold(I) NHC complexes for 14 h; from top to the bottom: control, **2a**, **2b**, and **2c**; from left to right) 2 h, 6 h, 10 h; the white bar represents a 200 µm scale

8.3.2 LDH sequestration and DNA fragmentation[145]

Short exposure (2 h) lactate dehydrogenase (LDH) release experiments (see figure 8.6) at higher concentrations (>10 µM) of **2a** showed a relevant loss of cell vitality, which indicated that first effects took place within a rather short time frame. In overall correlation with its inactivity in the proliferation experiments (see Table 8.2), **2** did not influence cell viability in this assay up to the highest concentration investigated (100 µM).

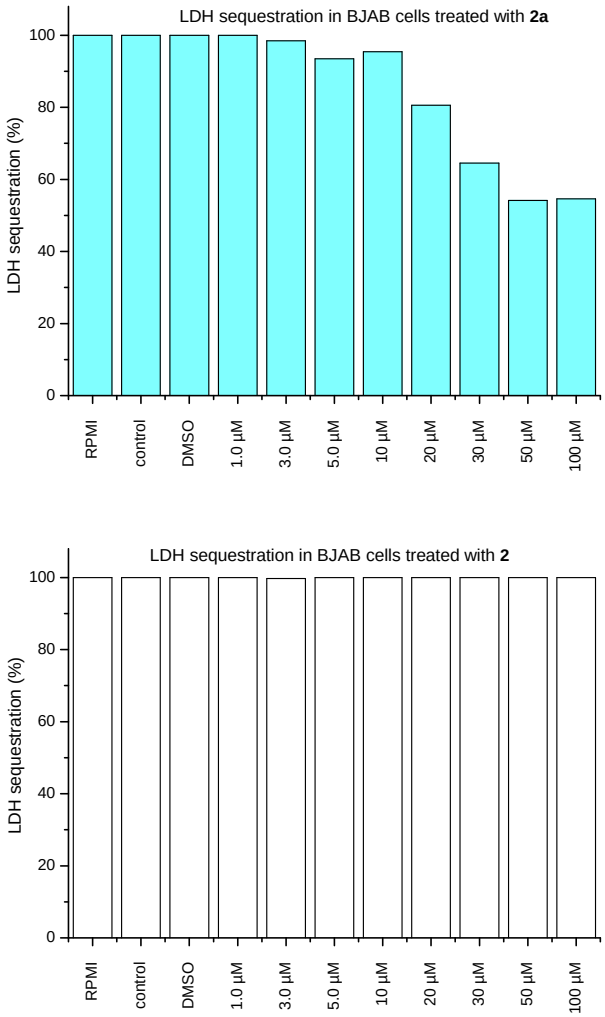

Figure 8.6: LDH sequestration experiments on BJAB cancer cells treated with different concentration of complex **2a** (top) and **2** (bottom) for 1 h; experiments performed by Liliane A. Onambele at the Children Hospital of Köln

Additionally, DNA fragmentation experiments were performed with the selected complex **2a** as the DNA integrity is another important marker for apoptosis. **2a** strongly increased DNA fragmentation after 72 h of exposure in a concentration dependent manner (see figure 8.7). The data are in overall good agreement with the proliferation inhibition assay. The organic ligand **2** did not influence the DNA integrity excepted for a really mild effect at 100 µM, emphasizing the importance of the metal atom for the bioactivity. Analogous results have been observed in experiments with Jurkat cells.

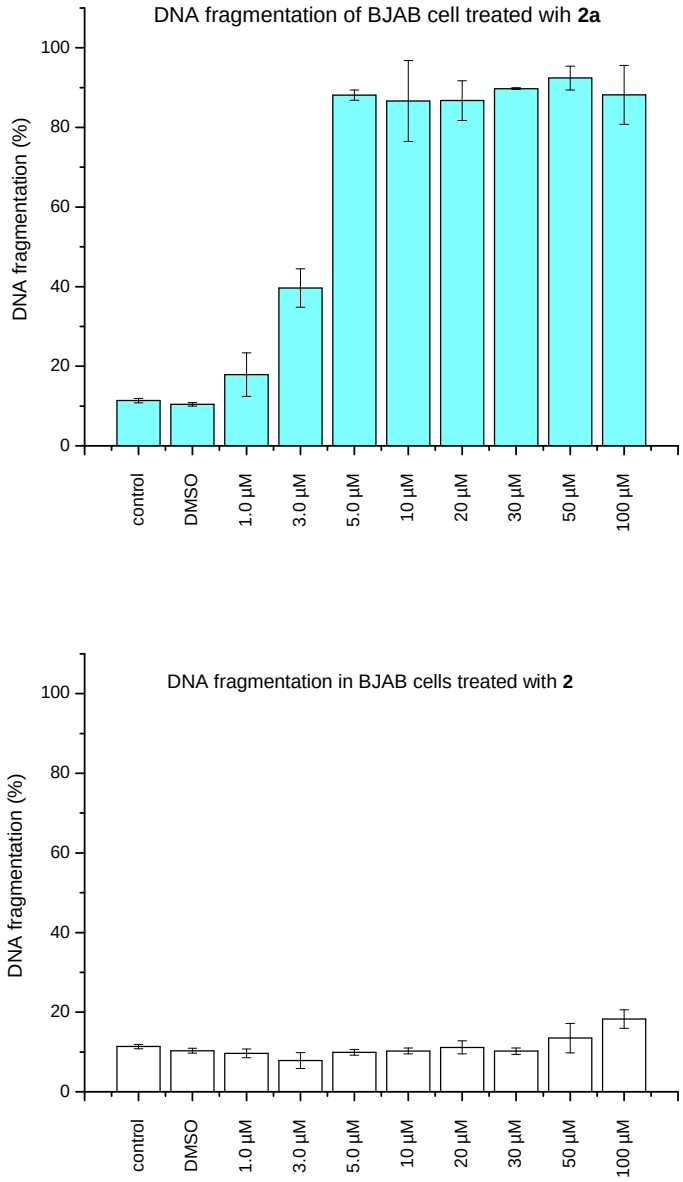

Figure 8.7: Influence of **2a** (top) on DNA fragmentation and viability in BJAB cells. **2** (bottom) showed only minor effects in both assays; experiments performed by Liliane A. Onambele at the University of Köln

8.5 Apoptosis or necrosis induction studies[145,153]

Experiments on the apoptosis and / or necrosis inducing activity of the new gold(I) carbene complexes were investigated in Jurkat leukemia cells using the annexin V / propidium iodide (PI) assay. During an onset capable to induce apoptosis, the negatively charged phophatidylserines present on the inner layer of the plasma membrane partially

migrate to the outer layer. The membrane, maintaining integrity, acquires symmetry and enables the binding with annexin V. When the membrane is completely compromised with relative necrosis induction, PI molecules are also allowed to penetrate into the cell. Both the dyes could be monitored through fluorescence-activated cell sorting technique (FACS analysis) and, dependent of the plasma membrane degradation degree, apoptosis and necrosis could be distinguished.[218] A selected complex per each different carbene class synthesized (**2a** as a chlorido, **2b** as a dicarbene and **2c** as a phosphine) underwent apoptosis / necrosis studies.

2a influenced vital cells accompanied by a significant relative increase of necrotic cells and a low percentage of apoptotic cells in a concentration dependent manner. Complex **2b** induced apoptosis in concentrations above 1.0 μM with cells in the early and late stages of the apoptotic process. Similarly, **2c** induced apoptosis in concentrations above 0.5 μM, however, leading to drastically more pronounced effects with most of the cells reaching the late apoptotic stages (see figure 8.8).

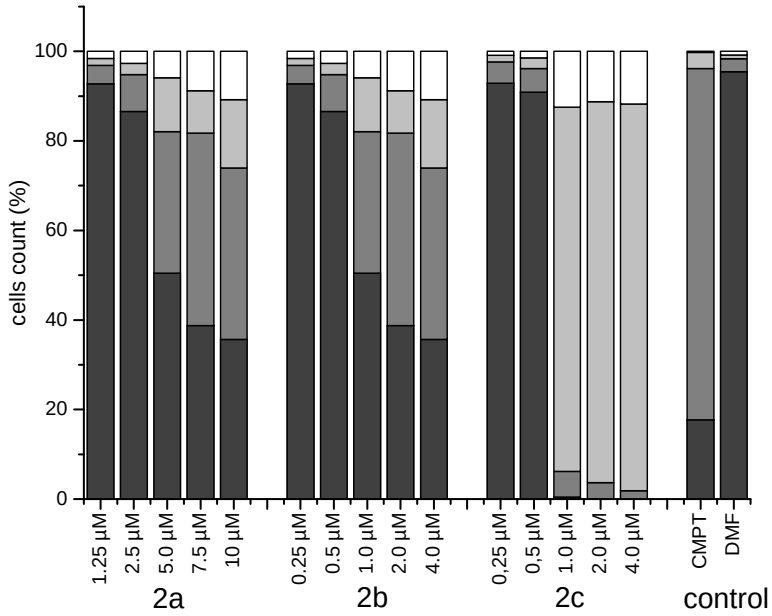

Figure 8.8: apoptosis / necrosis studies performed with annexin V / PI method and FACS instrumentation: black column = viable cells, dark grey column = early apoptotic cells, light grey column = late apoptotic, white column = necrotic cells; experiments on **2a** performed by Dr. Igor Kitanovic at the University of Heidelberg

8.6 Effect on resistant cell lines[145]

Drug resistance phenomena have a major impact on current therapy regimens and cause frequent treatment failures. The major reasons are found with alterations in drug transport processes or the up / down regulation of relevant metabolizing enzymes or molecular targets, thus causing a complex multi-factorial event. Novel compounds with different chemical structures and biological properties in some cases can address these highly relevant issues.[222]

To complete the antiproliferative properties evaluation of the target gold(I) NHC complexes the effects of **2a** on the apoptosis induction in wild type (grey color) and doxorubicin, daunorubicin, and vincristin resistant BJAB and Nalm-6 leukemia cells (blue color) have been studied (see figures 8.9 – 8.11). Western blot studies confirmed the over-expression of P-glycoprotein, proving the acquired resistance mechanism (see figure 8.12). The lower the apoptotic degree, the weaker is the effect of the complex on the cell line. The most marked effects of **2a** were observed in daunorubicin resistant Nalm-6 cells, where **2a** caused in the whole investigated concentration range (1.0 - 15.0 µM) the same extent of DNA fragmentation as in the respective wild type cells. In daunorubicine resistant Nalm-6 cells as well as in doxorubicine resistant 7CCA cells similar anti-proliferative effects to those obtained in wild type cells were observed at concentrations above 7.5 µM of **2a**. In the vincristin resistant cell types of BIBO and Nalm-6 cells, however, the resistance effects could only be partially reversed.

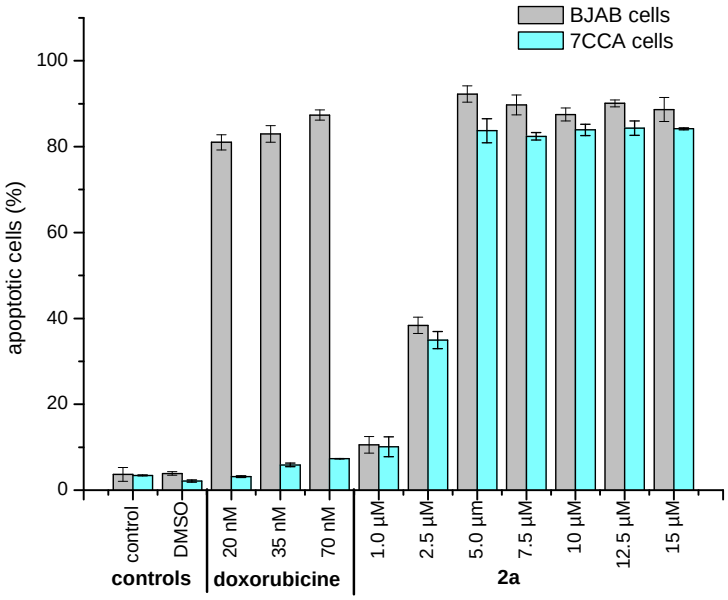

Figure 8.9: effect of complex **2a** (DNA fragmentation) on wild type BJAB cells and doxorubicine resistant 7CCA cells after 72 h incubation; experiments performed by Liliane A. Onambele at the Children Hospital of Köln

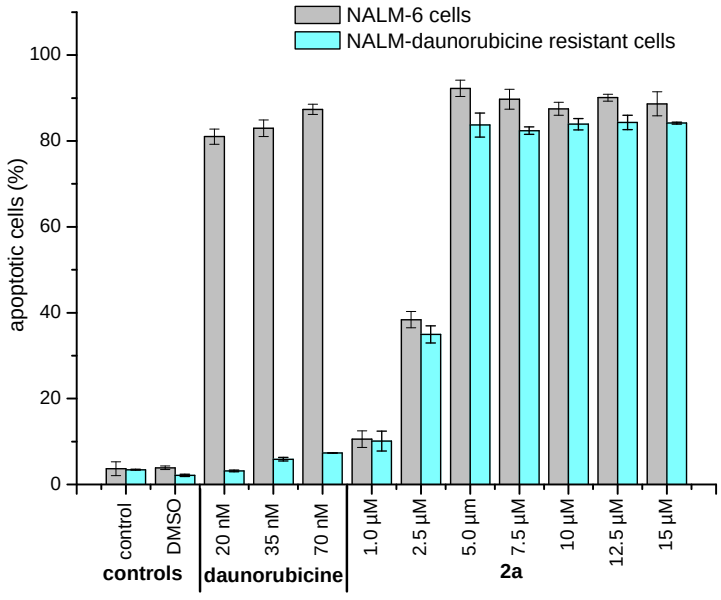

Figure 8.10: effect of complex **2a** (DNA fragmentation) on wild type NALM-6 cells and daunorubicine resistant NALM-Dau-res cells after 72 h incubation; experiments performed by Liliane A. Onambele at the Children Hospital of Köln

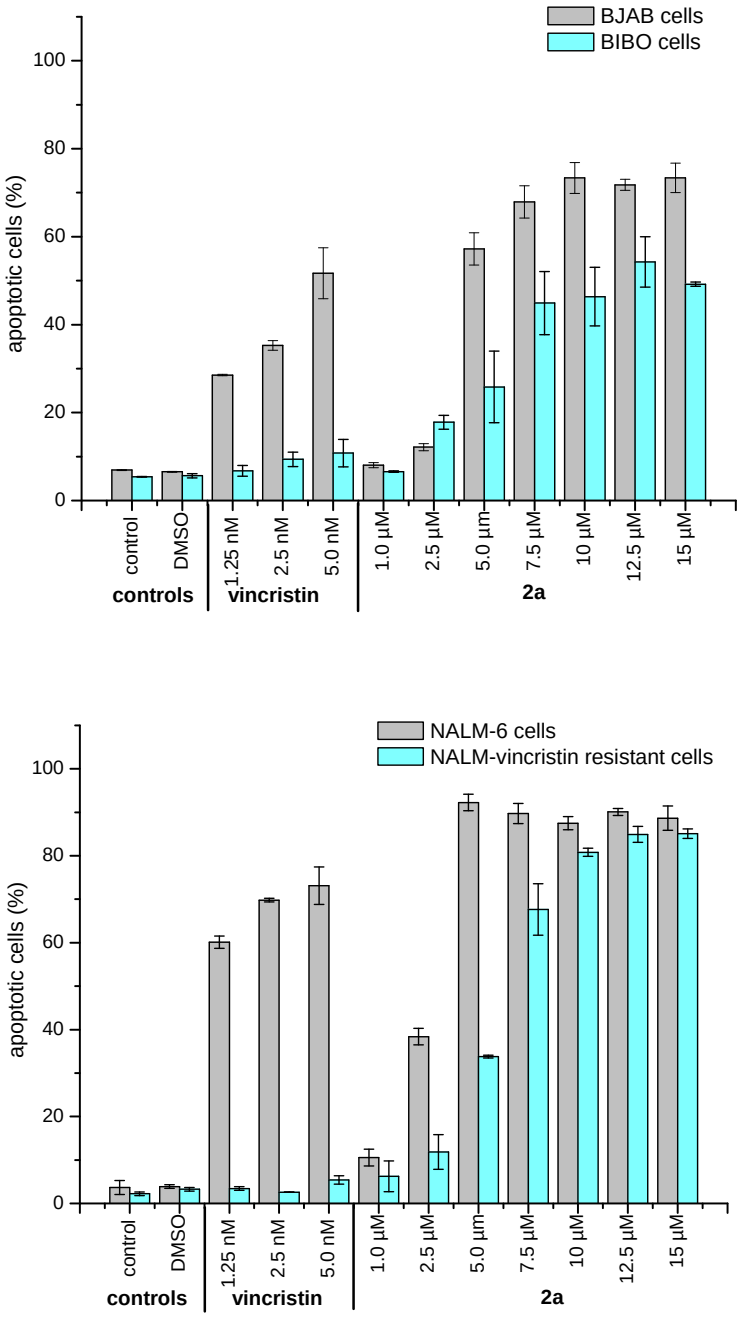

Figure 8.11: effect of complex **2a** (DNA fragmentation) on wild type BJAB (up-grey) and NALM-6 (down-grey) cells and vincristin resistant BIBO (up-blue) and NALM-Vin-res (down-blue) cells after 72 h incubation; experiments performed by Liliane A. Onambele at the University of Köln

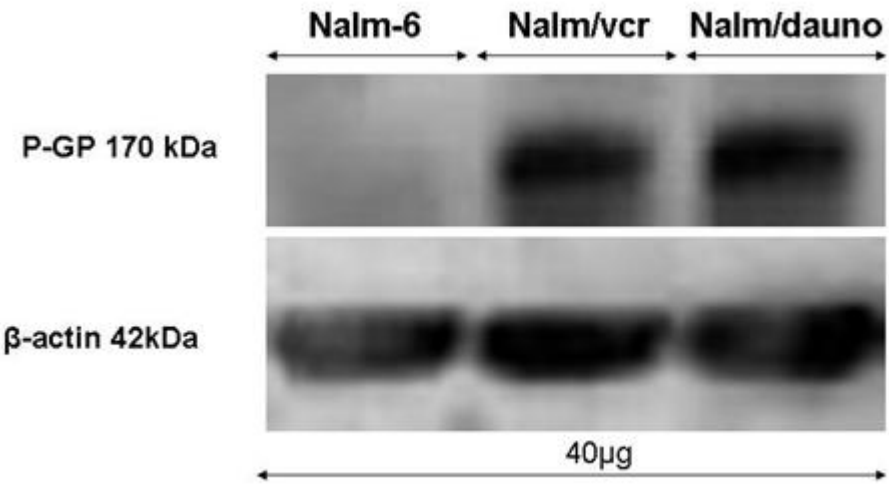

Figure 8.12: western blot experiment confirming the expression of the P-GP complex and acquired resistance; experiments performed by Liliane A. Onambele at the Children Hospital of Köln

9. Biodistribution studies

9.1 Introduction

Cells need a controlled environment to survive and grow. During evolution and differentiation all living organisms developed a complex membranes system. The plasma membrane represents a feature shared by bacteria, fungi as well as plants or mammalian cells. It consists of an amphiphilic phospho-lipidic double strand presenting, at the peripheral part, hydrophilic phosphate heads and, on the internal part, the hydrophobic alkylic chains of fatty acids.[223] Membranes are forming a lipidic double layer conglomerate characterized by an impermeable barrier that separates two compartments: inside and outside.[223] Because of the efficiency of this separation, the micelle unit is plenty used in nature and forms the basis structure of all cells. To preserve this separation and coordinate the exchange of information and nutrients with the outside, the membrane needs to develop specific mechanisms to regulate molecule traffic. The cells elaborated a sophisticated system to regulate this exchange called membrane transport. It is based on selectively controlled internal concentration and permeability of some solutes through chemical properties or specific channels. The efflux of molecules can be concentration or electrochemical gradient dependent. If substances proceed in the direction of these two parameters then the permeation is facile and does not need energy. If it flows against the gradient than specific energy-dependent mechanisms are required. The electrochemical properties form a membrane potential, which is controlling internal processes (stress answer, communication) and favors the diffusion of cations through the membranes.[150] A membrane penetration that reduces the free energy of the system is named simple or passive diffusion through the phospholipids. This process is dependent on the size, charge, concentration and hydrophobicity of the solute. When energy is needed the cells developed a sophisticated channel system to control the transport. The phospholipidic bi-layer is embedded with a lot of membrane proteins that through osmotic balance or ATP

involvement regulate the solutes efflux. The osmotic control favors the release or uptake of molecules through uniport, symport or antiport mechanisms, co-adjuvated by co-transporters, solutes or just coupling a favorable reaction to a high-energy required reaction.[176,178] For example, ATP-dependent channels use the ATP → ADP conversion to overcome the energetic barrier of specific uptake (see figure 9.1).

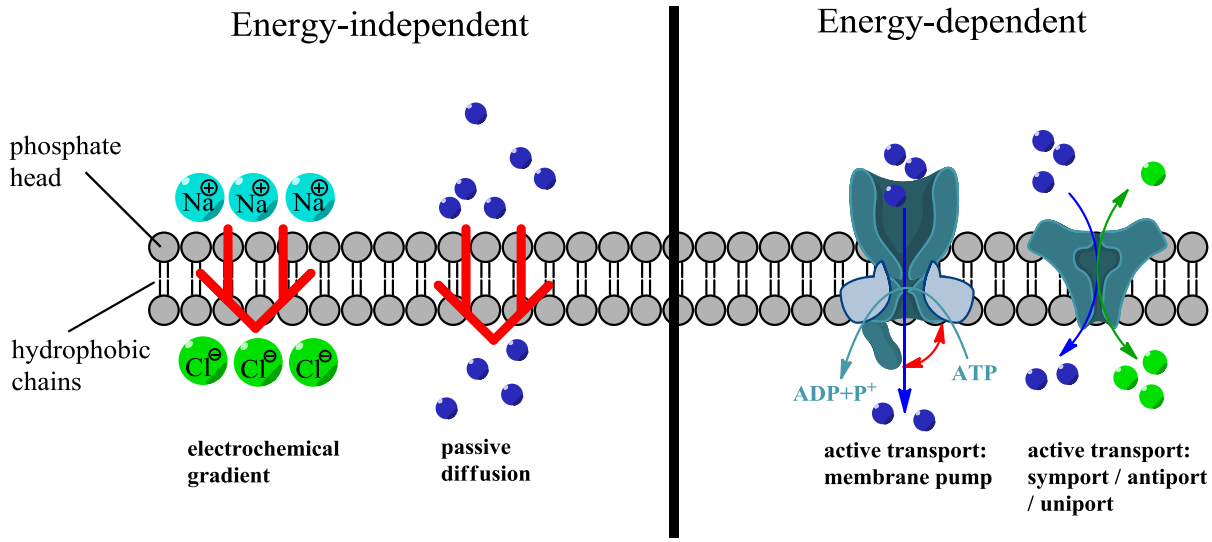

Figure 9.1: schematic representation of the cellular penetration mechanism

While a small number of solutes penetrate through passive diffusion, the majority of essential elements needed by the cell are regulated by protein channels.

A key principle that regulates membrane transport proteins is the exchange of free energy between two vicinal compartments. The Gibbs free energy variation (ΔG) of a system composed by two regions characterized by two different concentrations of the same analyte (C_1 and C_2) is regulated by the simplified equation 9.1. In it *n* represents the mole number (often calculated for 1 mole), *R* is the universal gas constant (*R* = 8.314 $J K^{-1} mol^{-1}$) and *T* is the absolute temperature. If C_2 is lower than C_1, ΔG will be negative and the whole process (e.g. analyte migration) will not require energy (till the equilibrium point $C_2 = C_1$). This is the principle at the base of passive diffusion.

$$\Delta G = -nRTln\frac{C_2}{C_1}$$

Equation 9.1: Gibbs energy variation relate to the chemical equilibrium, of two compartment with concentration C_1 and C_2

If the migration is thermodynamically prohibited, the system requires energy addition. This is the case of pump membrane transports. Pumps are normally ATPase dependent trans-membrane proteins. The hydrolysis of ATP to ADP provides enough energy to overcome the contrary electrochemical or concentration gradient and transport specific solutes into the cell.[176]

To enable an unfavorable process, a second transport can be coupled to the first one. The overall energy of the system will change following equation 9.2 where, in the case of an electrochemical gradient, $\Delta G^{ex} = zF\Delta P^{-1}$ where z is the number of elementary charges (or electrons) involved in the reaction, F is the Faraday constant ($9.649*10^4$ C mol$^-$1) and ΔP the membrane potential according to the Nernst equation (assuming n = 1).

$$\Delta G = -RTln\frac{C_2}{C_1} + \Delta G^{ex}$$

Equation 9.2: two system-transport energy relation

A negative ΔG^{ex} will affect the whole equilibrium of the system, encouraging the penetration of positive charged molecules. This is the principle at the base of the co-transport channels. If the coupled transport flows in the same direction of the target solute then the channel will be a symporter, while in the contrary case the protein will be an antiporter. If the protein is directly binding the solute and regulating its cell access without the use of other molecules or ions then it is called uniporter.[176]

Since for the most therapeutic compounds the cellular uptake is a key step to trigger acitivity a detailed study of the molecule biodistribution is required to properly define the drug profile.

9.2 Biodistribution

Monitoring the pathway of a drug, from intake to the target, is a key point to define its medical suitability.[225] The nature of the drug (e.g. synthetic or plant extract) and the different biological environments encountered by the therapeutic before reaching its target represent a major problem with which researchers have to deal. The substance must be dissolved in a water based medium, penetrate from the blood to the connective tissue and interstitial liquid, then to the cellular barriers (like plasma membranes) and finally explicit its action.[39,225] During this pathway, compounds change from hydrophilic to hydrophobic conditions, different pH, different pressures and gradients. Many parameters play a role to overcome the body elimination and reach the target. The drug structure should provide a good solubility to dissolve in water, medium or blood. Lipophilicity will increase the passive diffusion through cellular membrane. Some reports indicated that the presence of characteristic structures (e.g. amino-acid sequence for mitochondria) could also induce a specific delivery.[226] In 1997 Christopher A. Lipinski enunciated the so called “rule of five” which should regulate the administration, distribution, metabolization and escretion conditions (ADME). A compound should respect at least three of those four parameters: to have at maximum 5 hydrogen-bond donors or 10 acceptors, a molecular weight of 500 g / mol or less and a maximum log *P* of 5.[227]

A proper drug design should always take in consideration or even plan the compounds biodistribution and accumulation. Especially for metal complexes, a useful technique is available to quantify even small amounts of metal in biological samples: atomic absorption spectroscopy.

9.3 Atomic absorption spectroscopy

Discovered in the 19th century by Bunsen and Kirchhoff and improved in the 20th century by Walsh, atomic absorption spectroscopy (AAS) is an analytical technique to qualify and quantify specific elements in a sample.[228-230] The principle at the base of the method is that a certain atom irradiated with a specific energy and wavelength stimulates the electrons of the outer shield to reach the excited state. The amount of energy required is characteristic for each electron transition and element. The absorbance is quantified following the Lambert-Beer law. Through the Lambert-Beer law it is possible to correlate the transmission of the light with its absorption coefficient.

$$\boldsymbol{A = \log_{10} T} \quad \text{where} \quad \boldsymbol{T = 10^{-\alpha l}} \quad \text{and thus} \quad \boldsymbol{A = \alpha l}$$

Equation 9.3: Lambert-Beer law

The absorption coefficient is a measure of the cross-section of the cuvette analyzed and the molar absorbidity. Once measured the absorbance with photometer will be possible to determine the concentration of the substance, keeping constant the cross section parameter. Since each substance dissolved in constant concentration in a known medium gives a specific spectrum of absorbance, the variation of the spectroscopic profile will correspond to a compounds chemistry alteration.

AAS measurements allow the determination of more than 70 elements of the periodic table.[228-230]

The instrumentation is composed by an injector, an atomizer, a radiation source and a spectrometer (see figure 9.2).

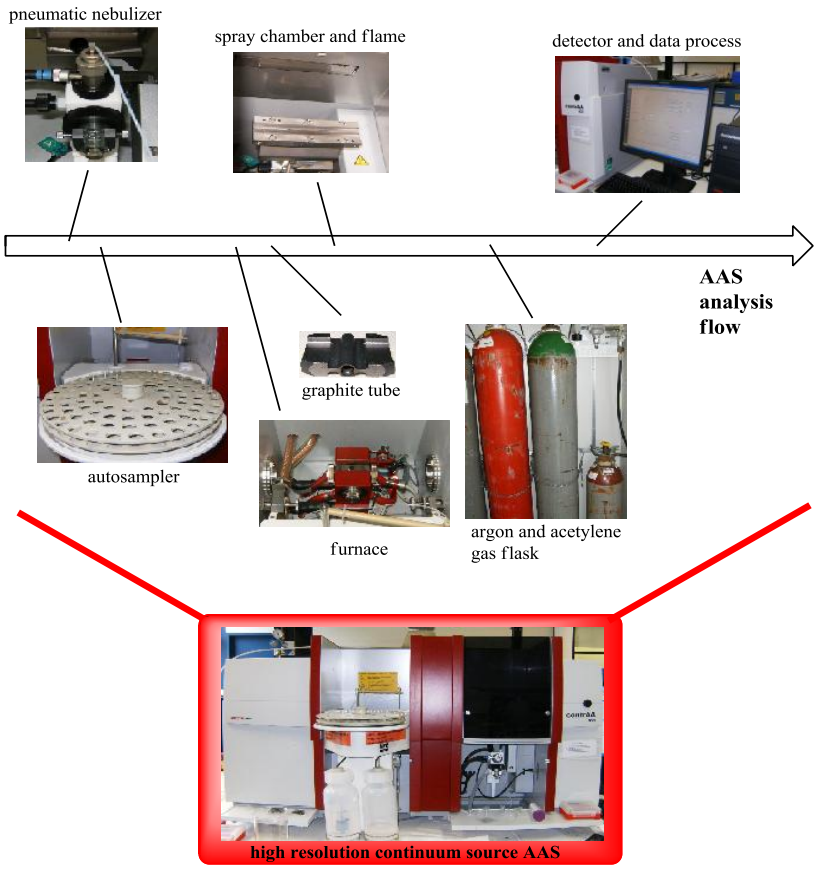

Figure 9.2: schematic representation of AAS instrumentation and workflow

There are two main injectors, dependent on the atomization type: simple pneumatic nebulizer injector or nebulizer-autosampler. Once that the probe is injected it needs to be atomized (reduced to its atoms) and analyzed. There are two main instrumentations: flames or electro-thermal atomizers. Flame atomizers consist of an O_2-acetylene or N_2O-acetylene flame and reach 2300 – 2700 °C. The sample is aspirated to a spray chamber and conditioned through a fine filter, that allows just small particles (<10 µm), to the flame that is crossed by the radiation beam. Electro-thermal atomizers involved characteristic trails called graphite tubes. This technique allows the analysis of different kinds of samples (liquid or solid) with an increment in selectivity of 2 – 3 time folds in comparison with the flame atomizers.[231] The graphite tube is heated and the solvent or matrix is removed by drying and pyrolysis steps. Then, the atomization occurs and the elements are quantified. The radiation source is producing the excitation required for the analysis. It

can be a linear or a continuum source. The linear source (LS AAS) provides energy for a specific element transition. The typical LS AAS lamp is a hollow cathode lamp (e.g. deuterium) that contains at the cathode traces of the target atom with an optimal working range of 190 – 320 nm. Continuum source (CS AAS) covers the entire spectral range and must be coupled with a high resolution monochromator. A full spectrum view enables the evaluation of background effects with a range of 190 – 900 nm and an analytic window of 2 nm. Because high radiation energy is needed, Xenon short arc lamps that can work in hot spot mode are required (for a resolution of 2 pm). The spectrometer is the final part of the instrumentation. It can be of two types: medium resolution and high resolution. The usual LS AAS detector is emitting a single narrow line and is capable to filter (through a monochromator) a band pass in a range of 0.2 – 2 nm. In CS AAS the detector is emitting a continuum beam to cover the whole spectrum and a high resolution monochromator (or double monochromator in the newest versions) is required. An important feature of the high resolution AAS is the possibility of a 3D – signal, which enables information also about the noise or matrix impurities.

Although AAS presents a high sensitivity, notable problems of interference and calibration subsist. To solve those effects, all the measurements meet mathematical corrections. Both AAS methods (LS and CS) need a calibration curve to standardize and quantify the area under the curve (AUC) and determine the amount of sample. The main interference effect is produced by the interfering lines from the analysis background. While there are just few and narrow absorption lines for single atoms, absorption lines of molecules are more abundant. The overlap of atomic lines by molecular lines produces erroneous spectra quantification. The principal reason for this absorption error is just a partial pyrolysis and the quantification of matrix-element adducts. Another common problem is provoked by a particle able to irradiate, creating a false positive. LS AAS does not allow many background corrections. Mainly, standardization occurs through a sequential measurement of whole sample signal (sample + background) followed by a background signal. Background correction are operated also using a secondary lamp (deuterium

correction method) or applying a magnetic field at the atomizer (Zeeman correction method). Concrete methods to determine lines overlap are not possible. In CS AAS few pixel are used to determine absorption. The rest of the free-pixel is involved in background calculations that are mathematically performed by the software. The full scan of CS AAS allows the measurement of all the background spectra, their storing and correction through a least-square algorithm to evaluate different possible structure and even atom line overlap.

9.4 Cellular uptake determination by AAS

AAS analysis is characterized by high sensitivity and enables quantification of target atoms in the ng range. Many reports demonstrated the suitability of AAS to determine metallic elements content, especially in biological samples.[224,232] CS AAS can be involved in lysates analysis due to its discrimination capability between background (like matrix effect, molecular lines) and element quantification.

Gold determination by AAS presents some advantages. ICP-MS is nowadays the most sensitive method to determine gold traces in a sample but has relevant analysis costs. AAS is a relative cheap technique that does not require complicated sample preparation. The limit of detection of gold is 2 ng / mL, still enough sensitive for biological determinations.[228,229] The peak shape of the gold line is sharp and defined (see figure 9.3).

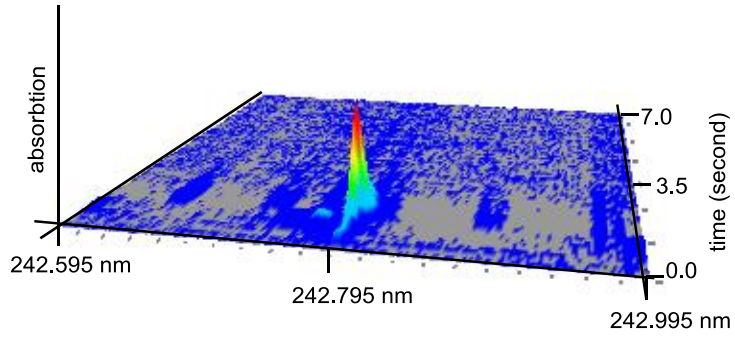

Figure 9.3: example of a gold signal determined by AAS

The main absorption line of gold is at 242.8 nm and does not collide with other important lines present in biological sample (just a minor interference could come from vanadium). Moreover, many recent reports described efficient methods for the gold determination in cell lysates.[224,232] Consequently, AAS proved to be a valuable technique for the determination of the gold content in the cell after the treatment with the target gold(I) NHC complexes.

To prepare the probes, MCF-7 cancer cells were incubated with an effective concentration of the gold complexes (referred to the cytotoxicity values, see chapter 8) of 3 µM. The experiments were conducted in a time dependent and comparative manner. After incubation the cells were trypsinized, the pellet collected and the lysis operated with a dounce homogenizator in a hypertonic solution or by freeze and thaw cycles. Protein quantification was performed according to the Bradford assay.[233] Aliquot of the sample for AAS analysis were finally prepared adding to the solution Triton X and HNO_3.

9.4.1 Gold uptake into whole cells: influence of the ligand type [153]

As reported in the previous chapters, the chemical properties could deeply influence the biological profile of the molecules. Since the carbene represented a strong coordinative ligand conferring high coordination potential to the gold(I) complexes, it was of interest to study the variation of cellular uptake in relation with the second ligand (L = -Cl, -NHC, or PPH_3) at the gold atom.

Three compounds underwent time-dependent uptake study into the MCF-7 cancer cell line. Complex **2a** is a rather lipophilic neutral compound that could easily penetrate through the plasma membrane by simple passive diffusion. Complex **2b** and **2c** are positively charged but also lipophilic species. For these, properties similar to that observed with delocalized lipophilic cations (DLC) could be expected. This includes an increased accumulation due to the coupled effect of concentration gradient (simple diffusion) and electro-chemical gradient (electric migration from the membrane outer-layer to the inner-layer). Consequently, the cellular uptake as well as the biodistribution of the

complexes **2a** – **2c** has been evaluated by atomic absorption spectroscopy. Cell uptake studies with serum free and serum containing fetal calf serum (FCS) medium (for its interference properties, see chapter 5) have been performed in parallel (see figure 9.4 – 9.6). In the experiments with serum free cell culture medium the gold uptake increased in the order **2a** < **2b** ≤ **2c** and the complexes reached stable cellular levels within the first 2 - 4 hours of incubation. The presumable DLC character notably increased the uptake of **2b** and **2c**, more markedly for the phosphine derivative that presents a higher reactivity (see BDEs, glutathione interaction and albumin binding studies in chapter 5). The presence of serum did not significantly affect the cellular uptake of **2b**, which had shown a rather low affinity for binding albumin. For **2a** and **2c**, which had shown higher protein binding ability, the cellular gold levels in the presence of serum were decreased indicating that protein binding negatively influenced the uptake of these two gold complexes with a profile comparable to what was reported for Auranofin. This effect was more marked for **2c**.

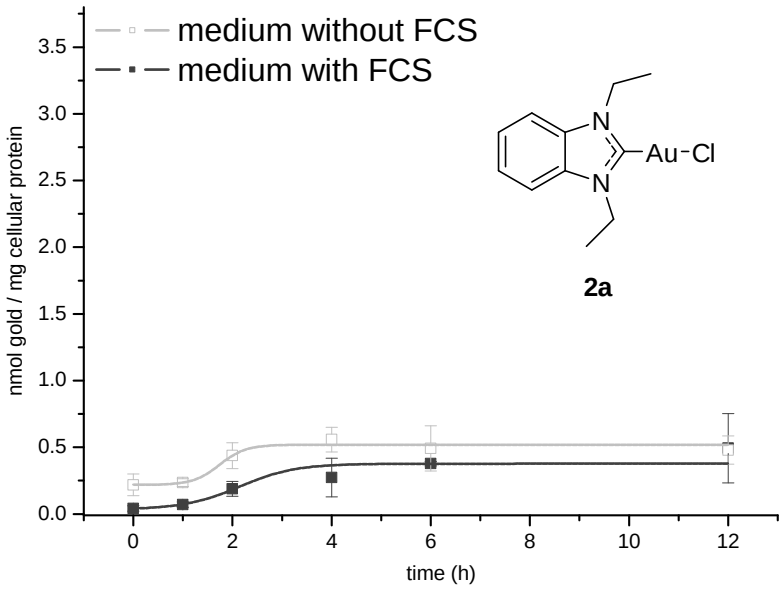

Figure 9.4: cellular uptake of complex **2a** in MCF-7, performed in serum free or serum containing FCS medium

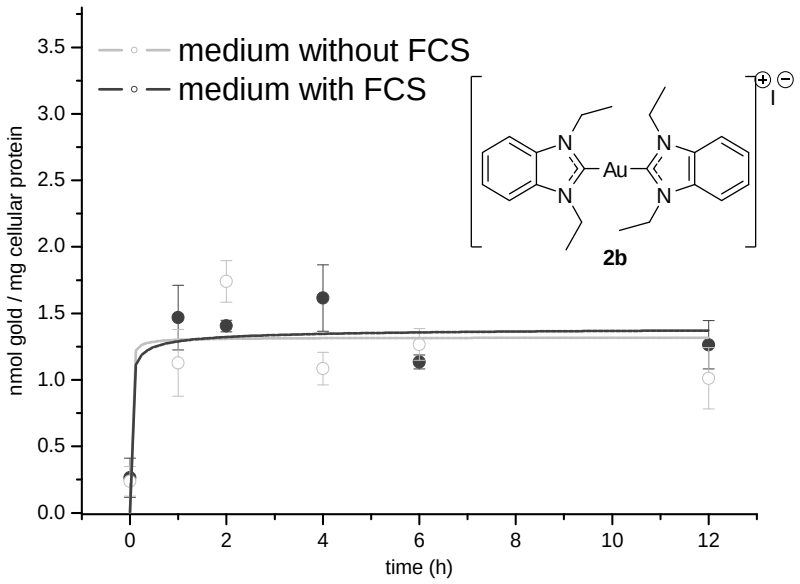

Figure 9.5: cellular uptake of complex **2b** in MCF-7, performed in serum free or serum containing FCS medium

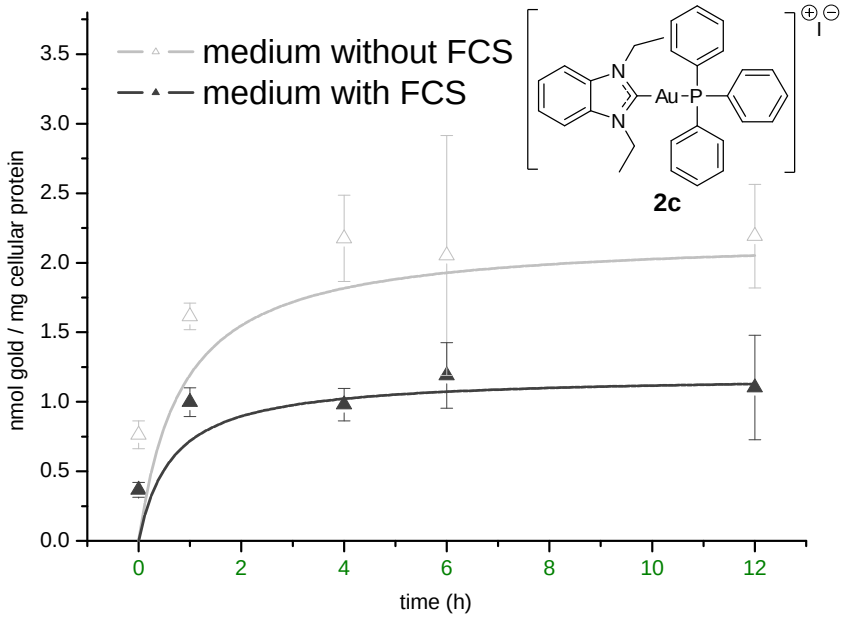

Figure 9.6: cellular uptake of complex **2c** in MCF-7, performed in serum free or serum containing FCS medium

9.4.2 Gold uptake into isolated mitochondria and cytosol: influence of the ligand type [153]

Due to the electrochemical gradient, an increment in cellular membrane penetration has been noticed, especially for the cationic compounds. Once taken up into the cell the complexes could be influenced by an analogous effect produced by the compartment membranes. It has been studied that for substances presenting the DLC character a migration effect to the peripheral zone of the cell (from the cytosol to the external membranes) could be expected.[150] This migration would drive the complexes in contact with the inner side of the plasma membrane or with the outer side of the organelle membranes. Recent studies described the strong effect of gold species on the mitochondria metabolism.[112,115] The lipophilic cation character and the presence of the gold atom could produce an increased or even selective delivery into this cell compartment.

For these reasons, the uptake of **2a** – **2c** into mitochondria isolated from MCF-7 cells exposed to 3 µM of the complexes was evaluated (see figure 9.7).

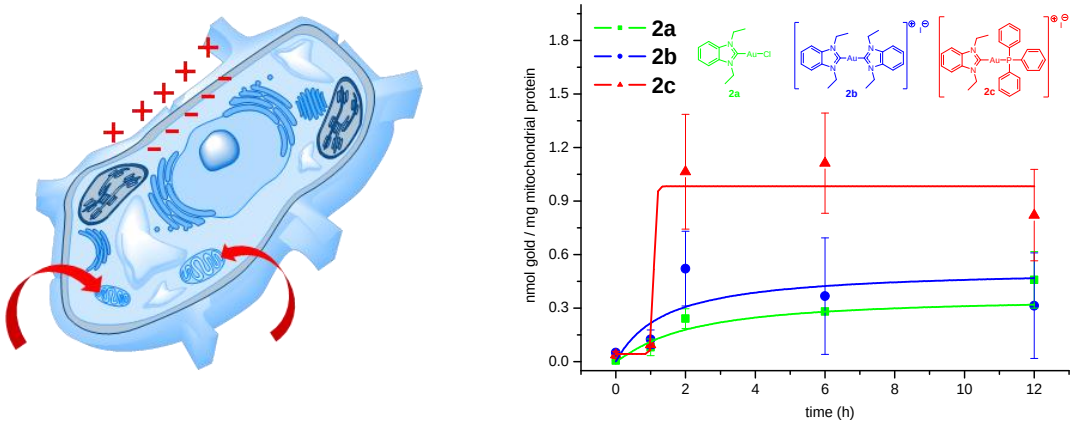

Figure 9.7: left) cell model with highlighted electro-chemical gradient and mitochondria delivery; right) time dependent mitochondrial uptake of 3 µM **2a** – **2c** in the MCF-7 cancer cell line

To avoid effects of albumin or other serum components the experiments were done using serum free cell culture media. The gold levels increased in the order **2a** ≤ **2b** << **2c** and similar to the overall uptake studies stable levels were obtained within the first four hours of exposure. The result indicated an exceptionally high mitochondrial uptake of **2c**. In part this can be related to its high whole cellular uptake and its lipophilic cationic character. However, based on the results above a similar strong uptake of **2b** could have been expected. The presence of a cation in a broad delocalized lipophilic system showed to be an important feature to improve membrane permeation.

During the isolation procedure of the mitochondria additional cytosolic fractions were obtained and were also investigated for their gold content. The gold levels in these samples were comparably low (see figure 9.8), implicating that the uptake into the mitochondria may be a major pathway for the cellular biodistribution of the complexes.

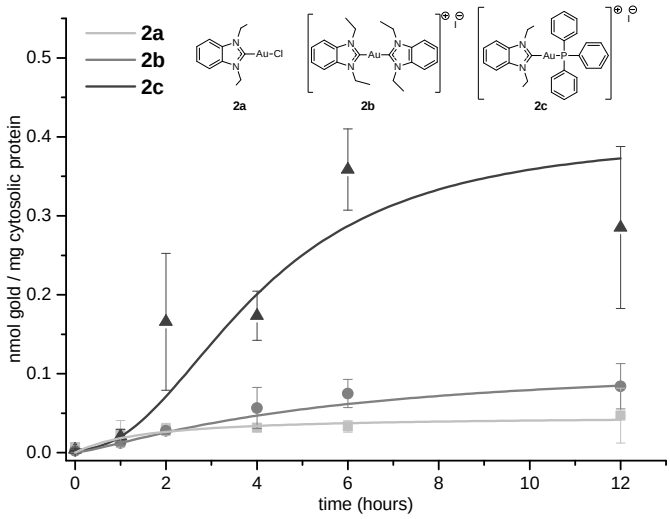

Figure 9.8: time dependent cytosolic uptake of 3 µM **2a** – **2c** in the MCF-7 cancer cell line

9.4.3 Gold uptake into whole cells: influence of the residues at the P atom

Since complex **2c** showed outstanding mitochondrial uptake properties coupled with a good TrxR inhibition (see chapter 6) a series of new gold(I) carbene phosphine complexes has been synthesized. The coordination of the different phosphine residues is expected to

have a different influence on the chemical properties and a deep affection on the cellular uptake.

To establish the impact of the phosphine ligand on the molecule permeation through the cell membranes, the new compounds underwent cellular uptake investigations. MCF-7 cells were treated with complexes **2d** – **2f** for a time span of 0 - 6 h at a concentration of 3 µM and were compared with the data obtained with **2c**. For all the molecules a similar profile to that observed for **2c** could be expected. The compounds accumulated in the cell with the order **2d** ≤ **2e** < **2f** << **2c**, reaching a maximum value within 4 h of incubation, in good agreement with the previous results (see figure 9.9). The P-aromatic system of complex **2c** was a key feature and enabled an uptake ~3 times fold greater than that obtained for the other phosphines (**2d**- **2f**).

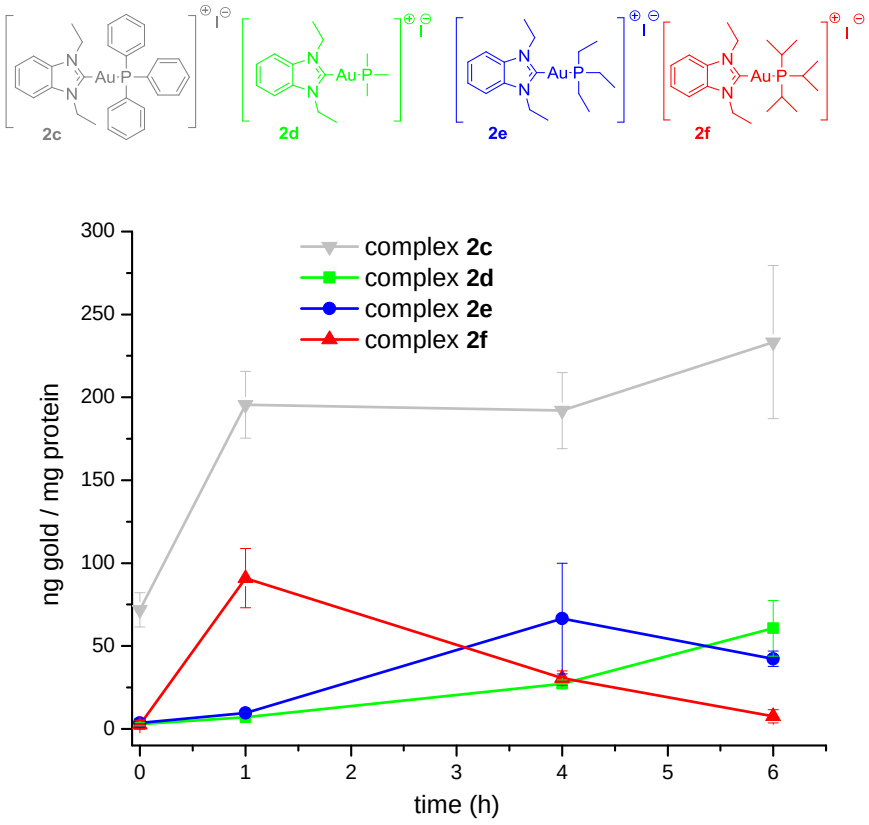

Figure 9.9: time dependent cellular uptake of 3 µM **2d** – **2f** in MCF-7 cancer cell line compared with the uptake of **2c**

10. Cell metabolism studies

*Experiments on ROS induction by **2a** were performed by Dr. Igor Kitanovic, Bionas measurements of **2a** by Dr. Hamed Alborzinia, MMP, cytochrome c release and oxygen consumption by Suzan Can and ELISA microarray by Pavlo Holenya from the research group of Prof. Dr. Stefan Wölfl, Institut für Pharmazie und Molekulare Biotechnologie, Ruprecht-Karls-Universität Heidelberg, Im Neuenheimer Feld 364, 69120 Heidelberg*

10.1 Cell metabolic pathways

The metabolism includes all those cellular activities that allow survival and growth. It is divided in two main processes: catabolism and anabolism.[176,178] Catabolism covers all the reactions that process organic material in order to provide energy. The most common catabolic reactions are basely redox, breaking down of organic macromolecules (e.g. glycogen lysis) or water and photoreactions. For example, glycolysis is one of the main catabolic processes that produce energy from carbohydrate molecules, pyruvate and then acetyl coenzyme A (AcetylCoA).[176,178] Fatty acids are processed in glycerol, proceeding into the glysolysis cycle, and their alkylic chains by oxidation. Amino acids are de-aminated and, through oxidation, converted into metabolites of the citric acid cycle.[176,178] In eukaryotes all the catabolic processes lead to the formation of AcetylCoA, the starting point of the Krebbs cycle and mitochondrial oxidative phosphorylation. In the latter energetic process, electrons are moved from molecules to oxygen. The high proton concentration formed by the reaction is pumped out from the mitochondria, creating an electrochemical gradient that is coupled with a non favorite process to form adenosine-tri-phosphate (ATP, the main energy molecule of the cell). Moreover, during the oxidative phosphorylation NAD^+ / $NADP^+$, a key molecule for all the metabolic processes and homeostasis regulation, is reconverted to NADH / NADPH due to the H^+ production and gradient.[178]

Anabolism includes all those processes that form cellular components using the energy produced during the catabolism. It is divided in three main phases: monomer formation, monomer activation through ATP involvement and monomer assembly (see figure 10.1 for a schematic representation of the metabolism).

Metabolic processes play also a key role in homeostasis regulation. Due to the variety of species and substances the cell cannot metabolize all the molecules. Some of them are harmful for the overall metabolism and could damage important structures or enzymes. The cell developed specific detoxification mechanisms to counteract the xenobiotic stress. Normally a first redox reaction is coupled with water coordination and termed with the modified substance extrusion through specific efflux channels. The cell itself produces dangerous species during its catabolic or anabolic processes. For example, a high rate of the cellular respiration stimulates the formation of reactive oxygen species (like peroxides or oxygen radicals). These molecules are able to induce severe oxidative damage. The cell answer involves a conjugated system called antioxidant network, formed by many enzymes, cofactors and substrates (see chapter 6).[234,235]

The cell represents a dynamic system influenced by environmental conditions as well as by internal processes. To control and coordinate this complicated mechanism, a fine tuning of the metabolism is required. There are two main levels of metabolic regulation. The intrinsic metabolic regulation is provided by the cellular monitoring, inducing or inhibiting of cell components like enzymes, substrates or products dependently on their cellular concentration (feedback mechanism). The extrinsic metabolic regulation answers directly to external stimuli (molecules as well electric potential of physical stress) from the environment or other cells.[176]

Especially targeted therapy in cancer research takes advantages of the deep understanding of cell metabolism. Some processes are drastically increased in cancer cells, resulting in an over-expression of enzymes that can become a selective target for chemotherapy.

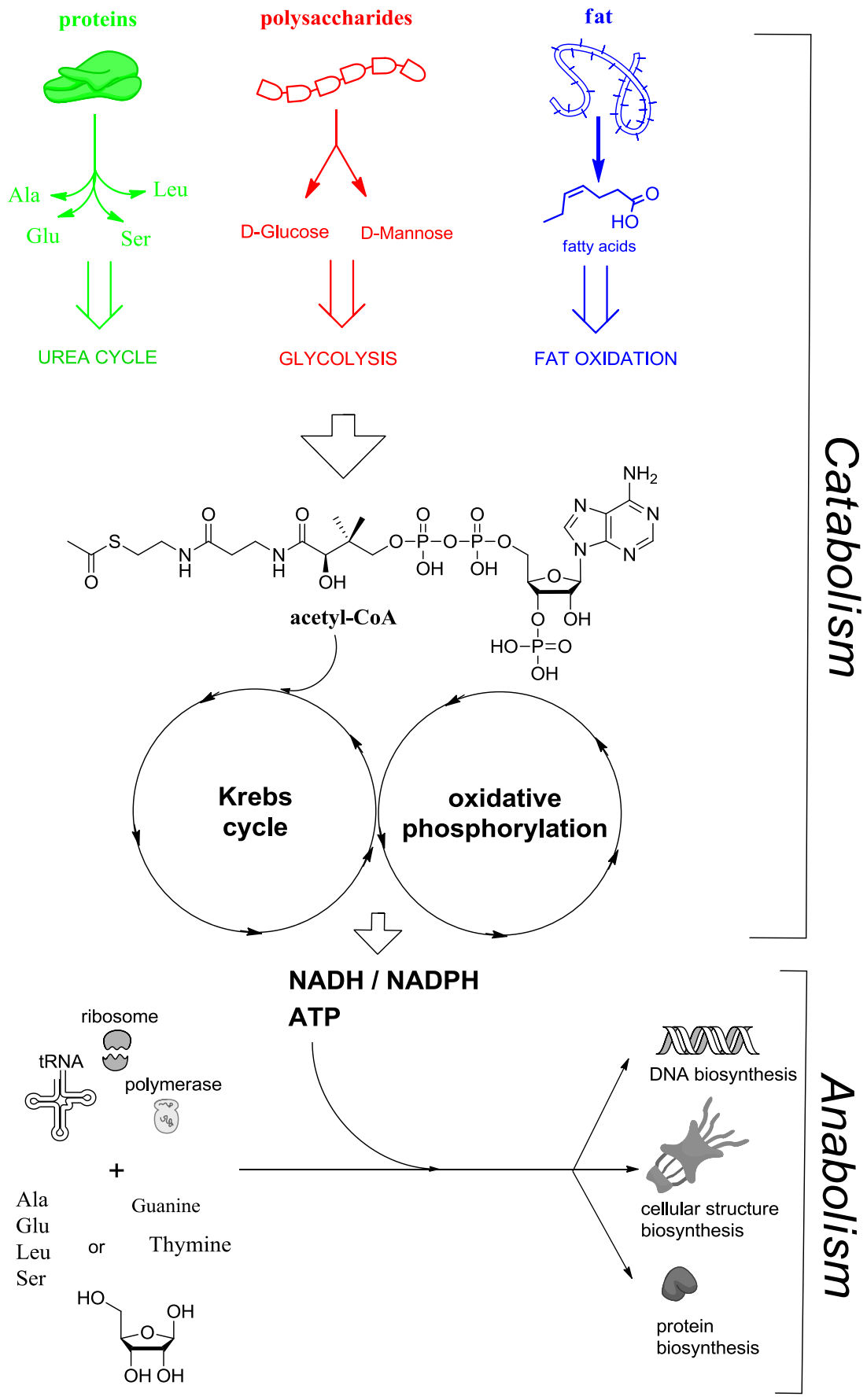

Figure 10.1: catabolic and anabolic processes schematic representation

10.2 Evaluation of reactive oxygen species (ROS) production[145,153]

ROS are largely products of the physiological mitochondrial cell metabolism and are negatively involved in cellular redox homeostasis. A high and uncontrolled concentration of ROS provokes DNA damage, lipoxidation of lipids with membrane lesions and proteins loss of functionality.[182] To control the cellular level of ROS and to avoid severe damage the cells developed an efficient enzymatic system called antioxidant network.[164,236-238] Belonging to this network are a series of enzymes and their substrates responsible for the detoxification and ROS extrusion. An alteration in its functionality allows a drastic increase of ROS concentration leading to cell death. Tumor cells present an increased metabolism and mitotic rate. The high energy demand of all the processes influences the ATP production in mitochondria and increments ROS concentration. Some reports indicate a significant difference of one order of magnitude between the internal ROS concentration of cancer cells in comparison with healthy ones.[61,239] This difference can be used to enhance the selectivity towards cancer cells or to sensitize and weaken their homeostasis.

Gold based molecules demonstrated to strongly inhibit the enzymes of the antioxidant network and especially with a high selectivity towards TrxR (see chapter 6). Since the inhibition of the cellular antioxidant network system can trigger a severe oxidative stress, it was of interest to study the production and cellular ROS content in cells treated with the gold(I) NHC carbene complexes. For this purpose three compounds have been selected, representing three different chemical categories of gold complexes: the chlorido derivative **2a**, the dicarbene derivative **2b** and the phosphine derivative **2c**.

In good agreement with the results of the proliferation assay, concentrations higher than 2.5 µM of **2a**, 1 – 2 µM of **2b** and **2c** strongly induced cellular ROS levels already after 24 h of incubation (see figure 10.2). In contrast, compound **2** (not containing the gold atom) did not trigger ROS production. This pattern correlates also well with the above notion that the gold compounds selectively affected the activity of the redox relevant enzyme TrxR and GR, whereas **2** had no effect on enzymatic activities (see chapter 6).

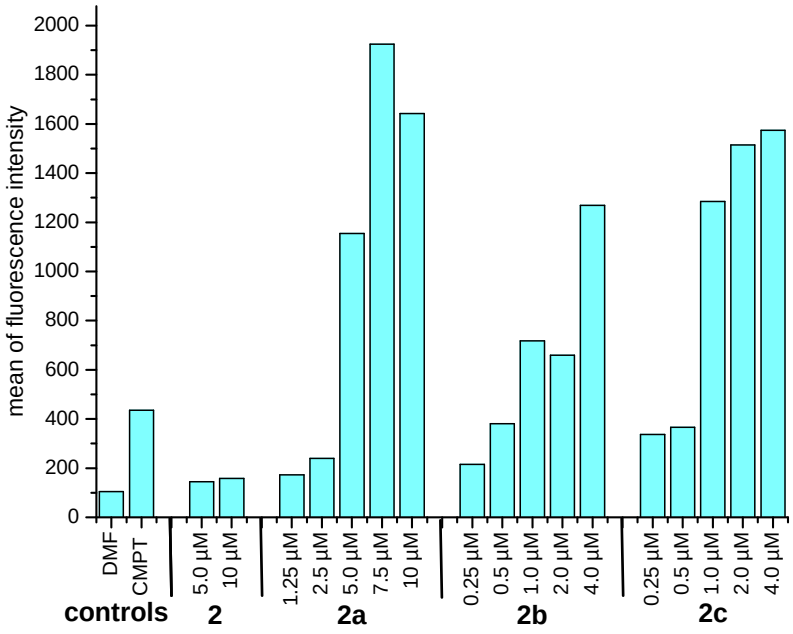

Figure 10.2: ROS induction in Jurkat cells incubated for 24 h with different concentrations of complex **2a - 2c** (DMF and 10 µM camptothecin, DMF and CMPT respectively) were used as negative and positive standard); experiments on **2a** performed by Dr. Igor Kitanovic at the University of Heidelberg

10.3 Metabolism alteration in living cell populations[145,153]

In the last decades an increasing number of methods started to deal with "online" monitoring of an *in vitro* system. Techniques like fluorescence microscopy or multi-sensor arrays have been established and started to play a role as routine analysis in research. Between these methods, the multi-sensor techniques were recently deeply involved in anticancer research.[240,241]

Bionas Discovery™ 2500 system is a scientific instrumentation that, through the involvement of up to 6 bio-modules and 6 sensors per bio-module, allows the tracking of several morphological and bio-energetical cellular pathways (see figure 10.3). The Bionas work flow is divided into three phases. In the adjustment phase medium free of substance flows on the chip to set the zero value. This first step is followed by a treatment phase in which the untreated medium is replaced with medium containing the compounds. At the

end, during a recovery the medium containing the substance is washed out by medium free of compounds.[240]

Figure 10.3: Bionas Discovery™ 2500 instrumentation: left) chip containing the different sensors on which the cells are seeded, right) workstation composed by medium carousels, six biomodules and calculation system; pictures taken from the official webpage *http://www.bionas-discovery.com*

For adherent cancer cells, the adhesion capacity and the membrane interaction between cells plays an important role in cell life. It allows nutrients and information exchange and confers a high resistance potential. A strong onset or apoptosis induction triggers a deep change in cell morphology as well as in cell-cell interactions. Since the gold(I) NHC complexes caused a metabolic onset (see chapters 6 and 8 and above) and induced apoptosis (see chapter 8), they underwent online analysis of impedance as a measure of cell morphology (see figure 10.4). The cells interact with the electric field produced by two sensors on the chip. Each variation of the field mirrors a variation of the shape or of the cell to cell contact. The impedance of the cells started to decrease in a concentration dependent manner after an exposure of approximately 7 h for all the gold compounds tested. The concentrations chose for the experiment were all close to the IC_{50} values of the complexes. The alteration of cell adhesion and cell-to-cell contacts were in good agreement with the uptake and anti-proliferative studies reported in chapter 8 and 9. Interestingly, the onset induced by the gold NHC complexes showed to be irreversible because no recovery has been observed after the treatment. Just a slight effect on

impedance could be noticed for compound **2**, demonstrating the importance of the gold center to achieve bioactive species.

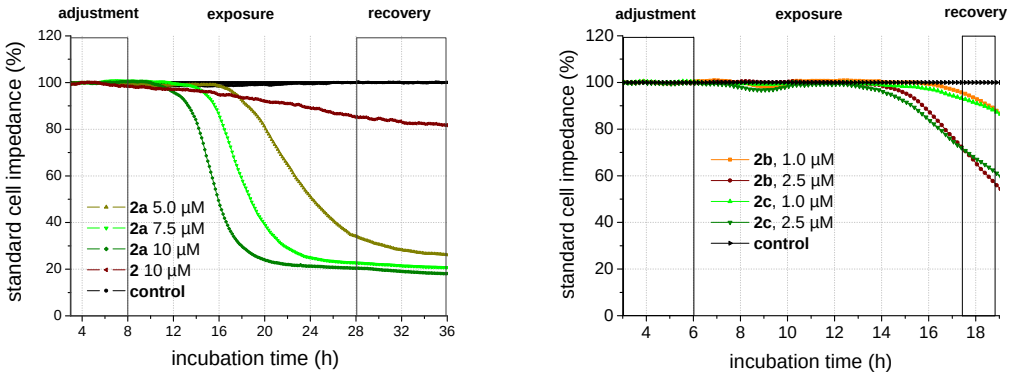

Figure 10.4: standard impedance modification in MCF-7 cancer cells treated with different concentrations of the compounds **2** and **2a** (left), **2b** and **2c** (right); experiments on **2a** performed by Dr. Hamed Alborzinia at the University of Heidelberg

The inter- and intra- cellular acidification rate is a measure of the cell catabolism and especially of the central energetic process of glysolysis. A dysregulation of the pH environment of the cell can be monitored by the chip sensors and will reflect a deep cellular onset. While **2b** and **2c** showed a minor effect on the acidification rate for an exposure time of almost 8 h, **2a** depressed drastically the process in a concentration dependent manner, which can be ascribed to the “dying” of the cells. The effect was not reversible once that the treated medium was replaced by medium free of substances and the cells washed for many hours. An initial increase in acidification is noticed within the first ≈ 4 h of treatment, suggesting an enhanced glycolysis to compensate for cellular stress. Once again **2** did not show to affect the analyzed parameter (see figure 10.5).

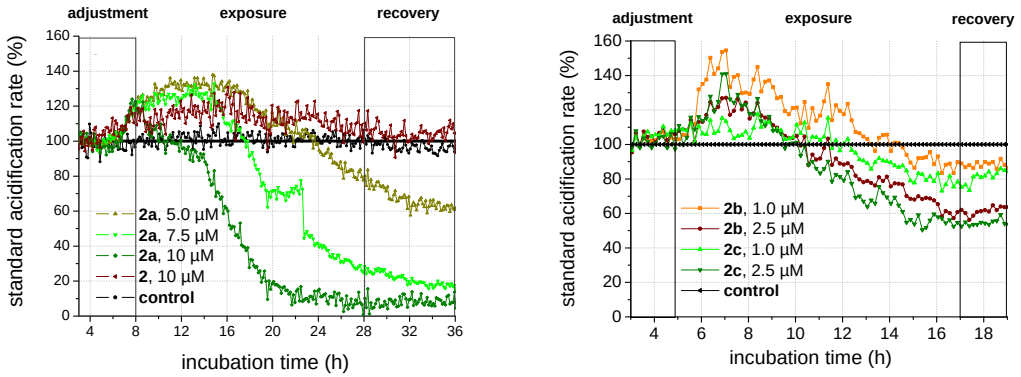

Figure 10.5: acidification rate of MCF-7 cancer cells treated with different concentrations of compounds **2** and **2a** (left), **2b** and **2c** (right) ; experiments on **2a** performed by Dr. Hamed Alborzinia at the University of Heidelberg

The respiration rate represents the major cell activity finalized to produce energy in form of ATP. In mammalian cells this process is in charge of the mitochondria that through the oxidative phosphorylation convert O_2 in water, CO_2 and ATP. During the experiment the cells seeded at the bottom of the chip were treated with cycles with flowing-medium rich or poor of oxygen. The variation in O_2 concentration could be monitored by the Bionas sensors.

The gold complexes showed a good uptake into the cell and a good delivery into mitochondria (especially for **2b** and **2c**) (see chapter 9). Consequently, the possible alteration of the respiration rate, as an index of mitochondria functionality, is a key parameter to describe the activity of the new gold(I) NHCs. All the complexes showed immediate effects (after just 1 - 3 h of incubation) reducing the oxygen consumption, and so probably stimulating the first glycolytic compensation effect in a concentration dependent manner. The aggressiveness of the gold compounds dysregulated intensively the respiration capacity not allowing any sort of recovery. As observed with the acidification rate and impedance, compound **2** did not affect also this parameter (see figure 10.6).

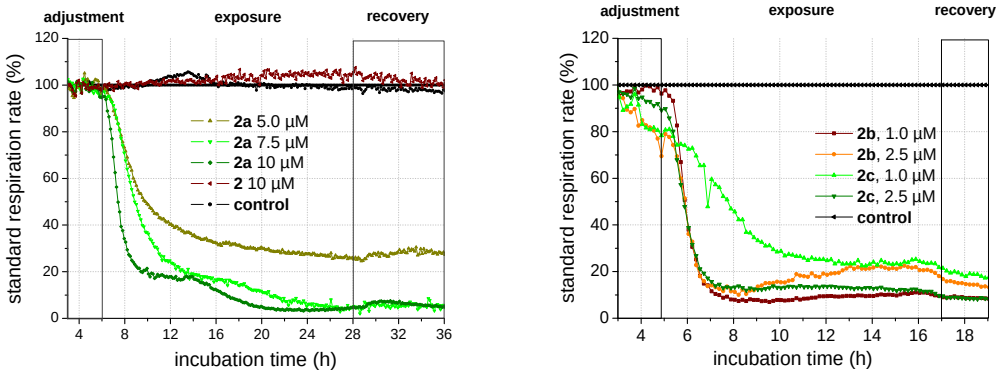

Figure 10.6: respiration rate of MCF-7 cancer cells treated with different concentrations of compounds **2** and **2a** (left), **2b** and **2c** (right) ; experiments on **2a** performed by Dr. Hamed Alborzinia at the University of Heidelberg

10.4 Influence on mitochondria metabolism[145,153]

The membrane encoded organelles called mitochondria have a central role in mammalian cell life. They provide energy, in the form of ATP through oxidative phosphorylation, and regenerate NADH / NADPH.[178] They play also a central role in cell homeostasis regulating the Ca^{2+} concentration, through its release and reuptake. Moreover, under cellular stress mitochondria allow the release of cytochrome *c* contributing to the formation of the apoptosome and activation of programmed cell death pathways.[150,242,243] The main mitochondrial activity is oxidative phosphorylation. When their metabolism is compromised a block of the respiration functionality is observed. The gold(I) NHC complexes demonstrated a good potential in altering the mitochondria homeostasis. They showed a good uptake into mitochondria, selective inhibition of TrxR and a strong influence on the respiration rate of the overall cell (see chapters 6 and 9). Thus, it was of interest to study the influence of the gold compounds on isolated mitochondria.

For this purpose, an assay measuring the oxygen consumption of isolated, functionally active mitochondria was applied. As expected, strong effects were observed in a concentration-dependent manner for all the three gold complexes (**2a** – **2c**). **2a** presented a remarkable activity, lowering the oxygen consumption in a concentration of 5.0 µM,

(close to the IC_{50} of the antiproliferative experiments, see chapter 8). The lipophilic cationic substances **2b** and **2c** presented a significantly stronger activity lowering respiration in concentrations as low as 0.1 µM and completely blocked respiration at 1.0 µM. The overall order of activity was **2a** < **2c** < **2b** (see figure 10.7).

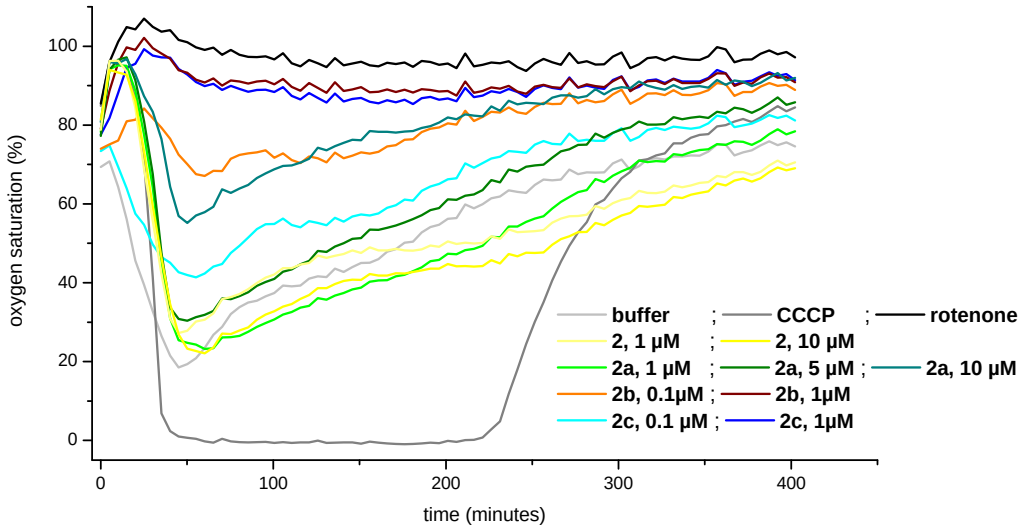

Figure 10.7: Respiration of freshly isolated mouse liver mitochondria. Mitochondrial activity leads to a decrease in oxygen saturation, which decreases over time (control). Inhibition of mitochondrial activity blocks oxygen consumption, resulting in continuous high oxygen concentration (rotenone, an inhibitor of respiratory chain complex I, positive control); decoupling of respiration by carbonyl cyanide 3- chlorophenylhydrazone (CCCP, positive control) leads to increased oxygen consumption. The gold complexes leads to a concentration-dependent inhibition of mitochondrial respiration while treatment with **2** shows no effect compared to the untreated control; buffer: positive control containing the organic solvent (DMF) but no compound, "respiration buffer": experiment without mitochondria; experiments performed by Suzan Can at the University of Heidelberg

The regulation of Ca^{2+} signaling and its release play a central role in the homeostasis of mitochondria and cells. The mitochondrial membrane potential (MMP) produced during oxidative phosphorylation largely contributes to its control and re-uptake. Hyperpolarization of the membrane leads to Ca^{2+} re-uptake while depolarization stimulates its release. A modification in the electrical properties of the membrane can

provoke an alteration in mitochondrial membrane permeability, the release of small mitochondria-derived activator of caspases (SMACs), the formation of the mitochondrial apoptosis-induced channel (MAC) and permeability transition pores (PTP), triggering programmed cell death.[150,242] Complexes **2a** – **2c** influenced the MMP in different ways (see figure 10.8). Complexes **2a** and **2c** induced after short incubation a strong hyperpolarization and after 8 h a small depolarization that can lead to Ca^{2+} release and possible activation of apoptotic processes. The effect was more pronounced for **2a**. In contrast to that, complex **2b** triggered an immediate and strong depolarization, which is in accordance with its exceptionally strong effects on mitochondrial respiration (see figure 10.7).

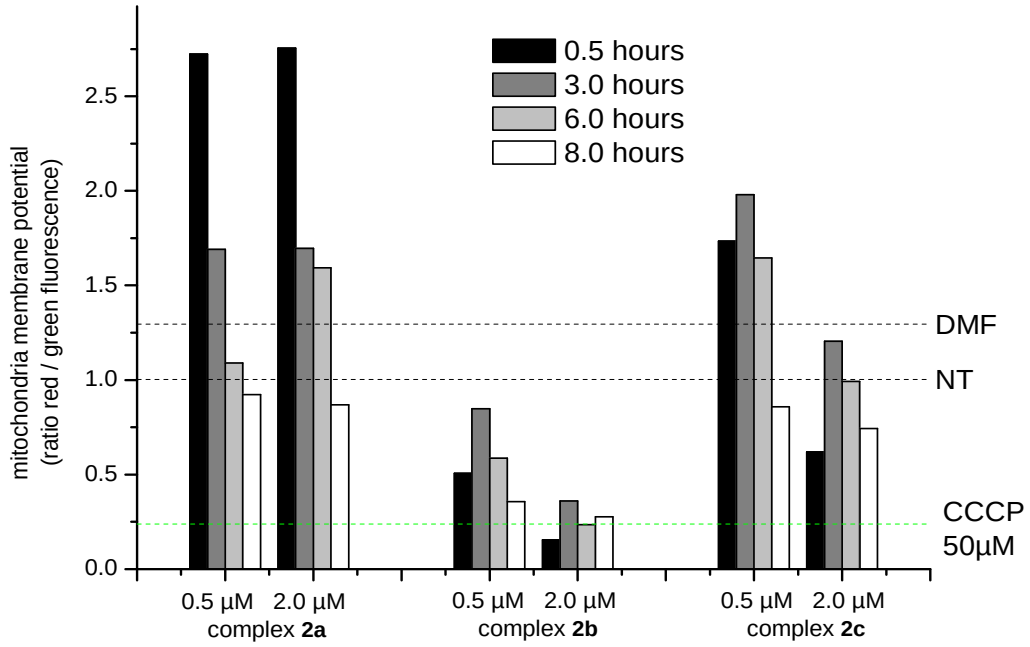

Figure 10.8: mitochondria membrane potential alteration provoked by the gold complexes: decoupling of respiration by carbonyl cyanide 3- chlorophenylhydrazone (CCCP dashed green line, positive control) leads to membrane depolarization, "DMF": buffer containing the organic solvent but no compound, "NT": not treated (experiment without solvent or compounds); experiments performed by Suzan Can at the University of Heidelberg

A strong onset of mitochondria homeostasis can also induce the release of cytochrome *c* as another possible apoptosis intermediate. Consequently, released cytochrome *c* levels were studied by Western blot experiments with mitochondria exposed to effective concentrations of **2a** – **2c**. However, the results do not indicate a contribution of the mentioned pathway, as no detectable levels of cytochrome *c* were present in the supernatants of the mitochondrial suspensions (with the exception of a marginally positive signal with 10 μM of **2a** (see figure 10.9).

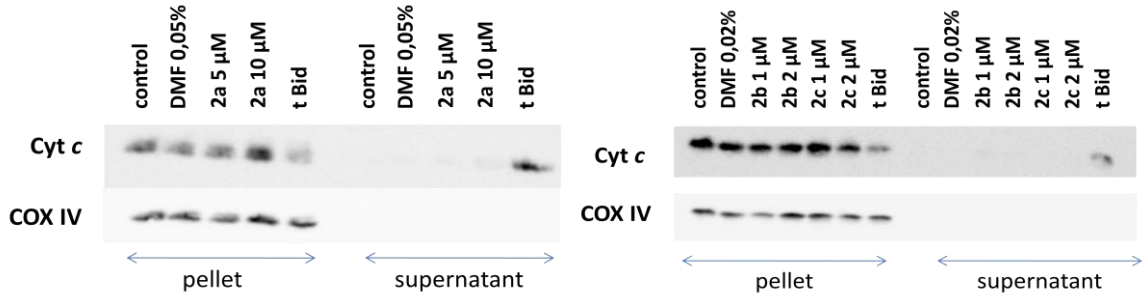

Figure 10.9: cytochrome *c* release of freshly isolated mouse mitochondria exposed to the gold complexes **2a** – **2c**. Mitochondria were treated with concentrations of **2a** – **2c** that had demonstrated a substantial impairment of respiratory effects. In all cases cytochrome *c* could be detected in the mitochondrial pellets but not in the respective supernatants. COX IV and truncated BH3 interacting domain death agonist (tBID) were used as positive controls; experiments performed by Suzan Can at the University of Heidelberg

10.5 Influence on protein kinases pathways

The regulation of serine-threonine protein kinases is a one of the main translational systems of the cell (e.g. mitogen activated protein kinase pathway, MAPK).[244] It is a signaling cascade that conveys information to effectors, translates signals and regulates the cellular answers phosphorylating or double-phosphorylating cytoplasmic components and nuclear transcription factors (see figure 10.10).[245] A cancer cell is characterized by a high metabolic degree that has to provide energy for mitosis and to react quickly against external and internal dangerous stimuli (e.g. reactive oxygen species ROS, inflammatory

stress). Monitoring these signaling systems provides useful information to understand better the cellular answer to anticancer drugs. Moreover, compounds that selectively interact especially with the MAPK cascade or related systems proved to be valuable as therapeutic agents in the control of malignant diseases.[246-248]

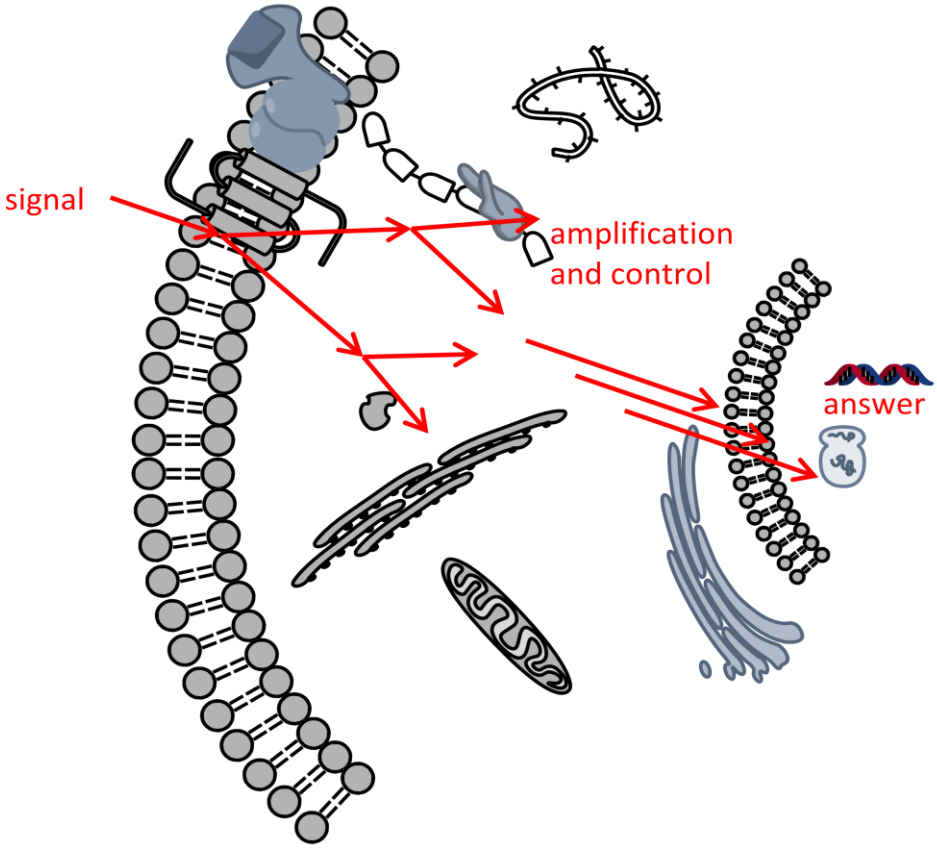

Figure 10.10: schematic representation of signal translation

Since the gold carbene complexes presented a different biological profile (e.g. enzyme inhibition, anti-mitochondrial effects), it was of interest to select some of them and screen their influence on the MAPK as well as on other important related signaling pathways (e.g. PI3K).[249] The signal pathways have been investigated with protein microarray technique.[250] With this method is possible to analyze simultaneously the expression of a wide number of proteins as well as their phosphorylation. A first antibody, specific for the phosphorylated or unphosphorylated target protein, is fixed directly on specific coated

slides used for the detection. The proteins are tagged with specific antigens, added to the slide where the specific sequence is recognized and the protein blotted on the antibody. Some following washing steps eliminate the non blot proteins from the slide and enable the effective treatment of the target protein with the secondary antibody. The detection is performed with a confocal high resolution microscope or scanner and analysis of the signal pattern by different multivariate statistical techniques.

A protein enzyme-linked immunosorbent assay microarray (ELISA-microarray, see reference 251) investigation has been performed on breast adenocarcinoma cancer cells (MCF-7) treated with different concentrations of **2b** and **2c** at different time frames. The tested proteins belonged to the MAPK cascade, to the PI3K signaling pathway or work in concert with them and can be divided in three groups: movement and adhesion regulating, energy regulating and stress regulating.

10.5.1 Movement and adhesion

Two proteins have been monitored concentration and time dependently: proto-oncogene tyrosine-protein kinase (Src) and focal adhesion associated protein kinase (FAK) (see figure 10.11). FAK and Src are controlling the MAPKs mediated adhesion and migration capacity that in cancer cells regulates the metastasis.[252,253]

Src is a protein which plays an important role in movement and proliferation and is correlated with the increase of invasiveness in cancer cells. Both gold(I) complexes did not show interactions with the exception of a small over-expression tendency of **2b** after 6 h of incubation.

FAK is responsible for cell adhesion and migration. It plays also a role in the nucleus ERK-dependent cascade (see below) promoting cell survival. **2b** promoted the under-expression of FAK in a time and concentration dependent manner and presented a stronger interaction than **2c**. The down-regulationphosphorylation of this protein can be associated to block of protein biosynthesis and alteration in the proliferation.[252]

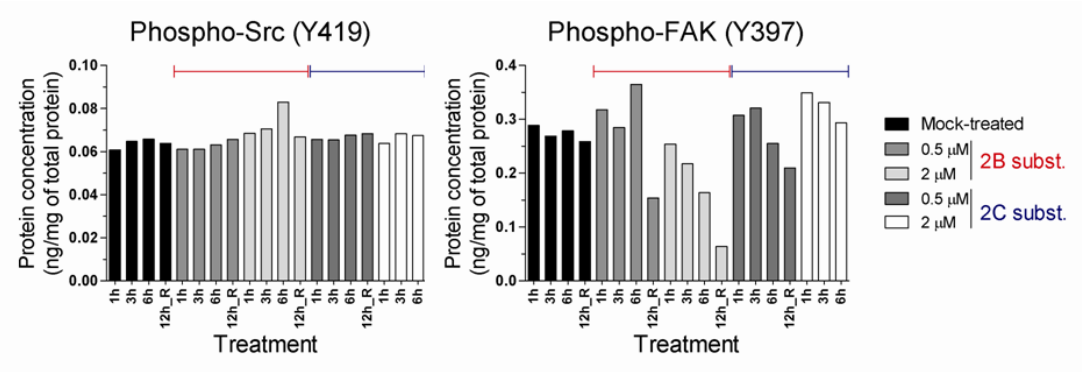

Figure 10.11: microarray phosphorylation results of movement and adhesion regulating proteins in MCF-7 cells incubated with **2b** and **2c** at different time frame and different concentrations; experiments performed by Pavlo Holenya at the University of Heidelberg

10.5.2 Energy and proliferation

Three proteins belonging to the cellular energy regulating signal pathway were monitored: 5` adenosine monophosphate-activated protein kinase (AMPK), mammalian target of rapamycin (mTOR) and glycogen synthase kinase 3β (GSK-3β) (see figure 10.12).[254-256]

AMPK plays a key role in cell energy homeostasis. It controls the fatty acid and cholesterol biosynthesis and glycogen oxidation. Stimulated by an increase of AMP, it is able to switch the cell from ATP consuming to ATP producing metabolism. The compounds depressed the phosphorylation of the target protein at concentrations below the IC_{50} values (related to the antiproliferative experiments, see chapter 8). At concentrations above the IC_{50} **2c** did not show any influence and **2b** kept a mild depression of its phosphorylation. The dysregulation of the energy compensation mechanism is associated with a perturbation in the cell cycle. These events are rapidly initiated and are referred to as short-term regulatory processes. They can be observed just for treatment concentrations that do not produce severe cell damage, explaining the minor effects noticed for high concentration.[254]

GSK-3β is a serine-threonine protein kinase with inhibiting function. It influences the activity of mTOR, the glycogen synthase pathway (together with AMPK) and it is

implicated in the cell response from damaged DNA. It regulates also the mitochondrial ERK fraction that prevents the protein transition pore (PTP) formation in mitochondria and apoptosis induction.[255] **2b** and **2c** influenced the level of phosphorylated GSK-3β after 12 h of incubation. Noteworthly, **2b** lowered drastically in a long-time incubation experiments the amount of pGSK-3β at a concentration of 2.0 µM.

mTOR is a key protein that integrates the upstream signals (e.g. AMPK) and translates them into the nucleus to promote protein biosynthesis and proliferation.[256] **2b** and **2c** did not interact with the mTOR functionality with the exception of a marked enzyme phosphorylation after 6 h incubation with **2b** (concentration dependent).

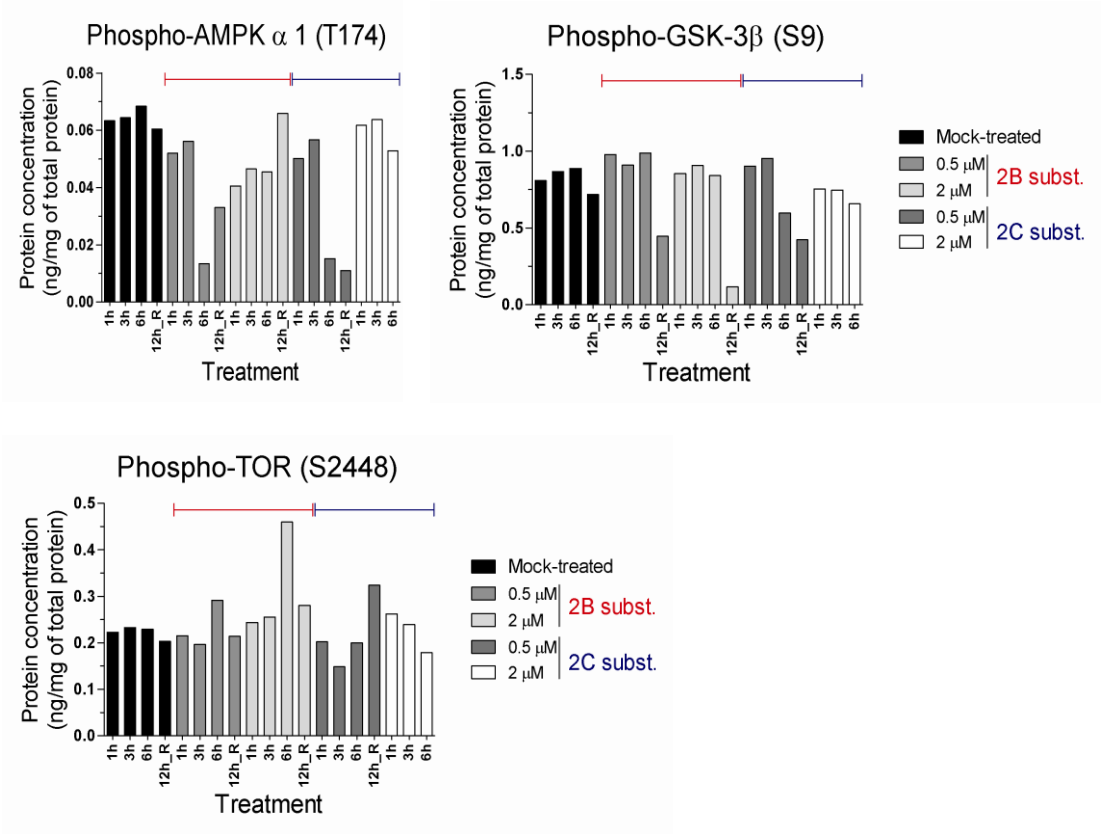

Figure 10.12: microarray phosphorylation results of energy and lipid oxidation regulating proteins in MCF-7 cells incubated with **2b** and **2c** at different time frame and different concentrations; experiments performed by Pavlo Holenya at the University of Heidelberg

10.5.3 Stress answer

Four proteins involved in the homeostatic cellular response and programmed cell death regulation have been investigated: MAPK-ERK-kinase (MEK1/2) and extracellular signal regulated kinase (ERK1, ERK2) for the survival and proliferation mechanism (see figure 10.13), heat shock protein 27 (Hsp27) and p38α mitogen protein activated kinase for the cellular stress answer (see figure 10.14).[246,257-259]

ERK (type 1 and 2) is activated by inflammatory stress or pleiotropic effectors. Its activation plays an important role in the control of gene expression involved in the cell division cycle, apoptosis, cell differentiation, and cell migration. The mitochondrial form prevents cancer cells from death altering the PTP formation. **2b** did not present relevant interaction on ERK-1 and ERK-2 with the exception of a mild increment in the phosphorylated forms with the highest concentration after 6 h of incubation. **2c** influenced the two ERK investigated similarly. While at 0.5 μM it did not show relevant activity, for dose above the IC_{50} value already after 1 h of incubation the protein is drastically phosphorylated (more than 10 times fold). The results suggested that the cell tried to compensate the dangerous stimulus but this response has been defeated by the cytoxic action of the complex. The effect of the gold(I) NHC complexes on the MEK-ERK kinases are shown in figure 10.13.

MEK1/2 kinase is a key protein with a central role in the MAPK pathway. It is activated by growth factors, Ca^{2+} level perturbation or inflammatory stress and mediates the activation of the ERK cascade leading to survival and proliferation response.[257] At 0.5 μM the gold(I) complexes stimulated its phosphorylation in a time dependent manner with effects more pronounced for **2b**. At 2.0 μM **2c** presented almost the same profile as for the low concentration used. **2b** induced a strong increase in phosphorylation (≈275% of the control), followed by a time dependent decrease (≈10% of control).

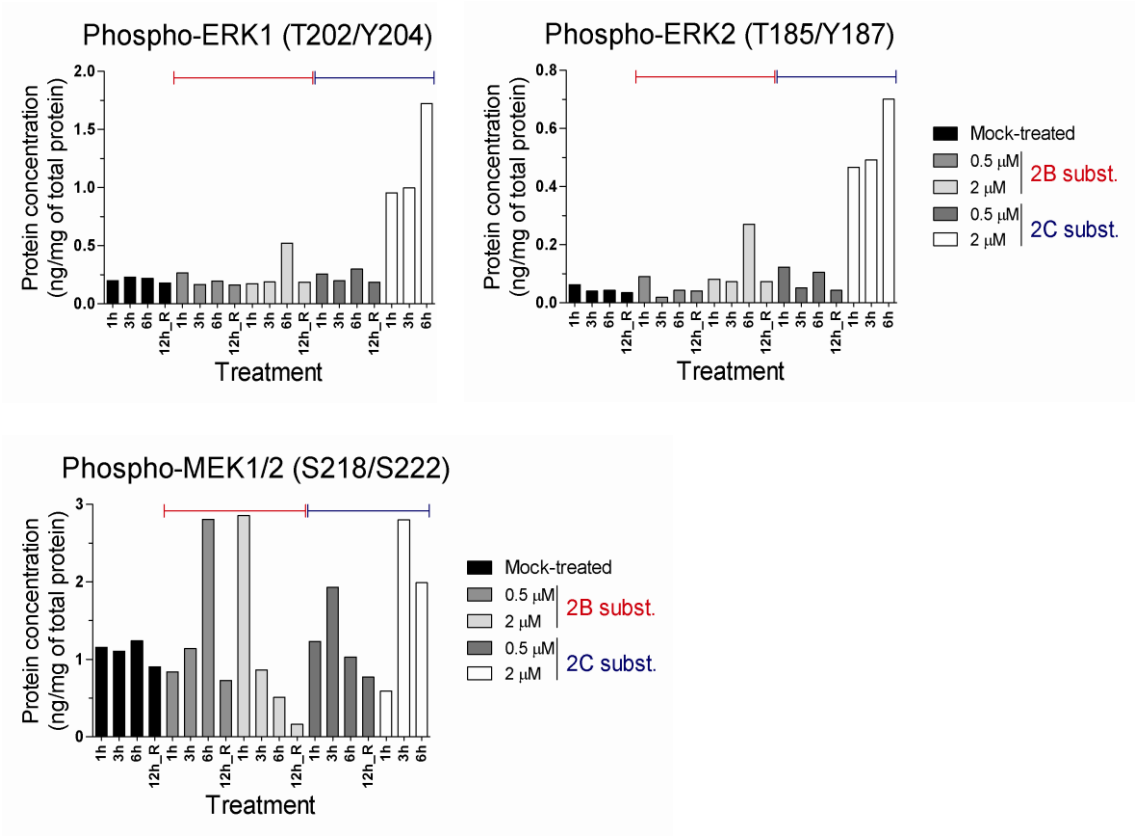

Figure 10.13: microarray phosphorylation results of translational mechanism regulating proteins in MCF-7 cells incubated with **2b** and **2c** at different time frame and different concentrations; experiments performed by Pavlo Holenya at the University of Heidelberg

Hsp27 provides thermotolerance in vivo, cytoprotection and supports the cell survival under stress conditions. It also modulates the ROS production raising glutathione levels. Hsp27 interacts also with the outer layer of the mitochondrial membrane interfering with the apoptosome, inhibiting the release of cytochrome *c*, SMACs production and procaspase / caspase-3 cascade activation.[246] High phosphorylated protein levels are in inverse relation with cell proliferation, metastasis and resistance to chemotherapy. Cellular levels of phosphorylated Hsp27 were not modified by a 0.5 µM treatment with the gold(I) complexes. Just an increment of the pHsp27 has been observed after 12 h incubation. However, the compounds presented interesting effects at high dosage. **2b**, at high concentration and after 6 h treatment, drastically increased the pHsp27 (~10 times fold

more than control) that was mainly reduced after 12 h. **2c** induced an increment in the phosphorylation of target protein gradually in a time dependent manner reaching also extreme high values (~8 times fold more than control). The results suggested a failure in the compensation mechanism of Hsp27 relatively to **2b** (antimitochondrial effects) and remarked the extreme stress induction caused by **2c** (TrxR inhibition, ROS stimulation and apoptosis induction).

p38α is the mayor regulator for inflammatory response. It is activated by many cellular stress factors including heat shock proteins, high osmotic stress, pro-inflammatory cytokines (such as IL-1 and TNF-α), DNA damage and ROS.[258] It is an essential effector of the programmed cell death pathway activation. It modulates Hsp27, GSK-3β, enhances the activity of ERK and down-regulates the proapoptotic protein Fas and Bax. Inhibition of p38α produces hyper-activation of proliferative stimuli. The gold(I) complexes presented a very different influence on the protein phosphorylation. Cells treated with **2b** showed a drastic decrease of pp38α even after 1 h of incubation. In contrast **2c** did not trigger strong effects.

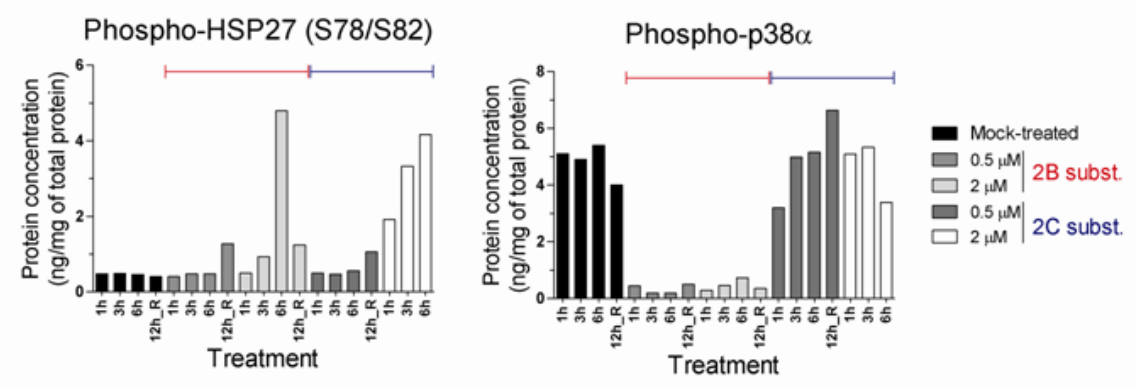

Figure 10.14: microarray phosphorylation results of cellular stress answer regulating proteins in MCF-7 cells incubated with **2b** and **2c** at different time frame and different concentrations; experiments performed by Pavlo Holenya at the University of Heidelberg

10.6 TrxR cellular expression

The control of the expression of specific enzymes enables the cells to react against internal as well as external stress. Elevated ROS levels induce the biosynthesis of the components of the antioxidant network (see chapter 6). TrxR has a key role in preventing ROS damage regenerating Trx, GR and glutathione peroxidase (GPx) or acting directly inactivating dangerous small molecules. Due to its vital function TrxR is over-expressed in cancer cells.[262,263] A strong internal onset can increase the need of the enzymes involved in the cellular protection and stimulate their further over-expression. The gold(I) NHCs demonstrated strong inhibitory activity towards TrxR. Thus, it was of interest to observe the modulation of the levels of TrxR by cancer cells. To monitor the proteins expression a technique called western blot is commonly used. Western blot is an immune-technique that through an electrophoretic separation enables the labeling of specific proteins and their detection. The cell lysate is firstly heated in order to denaturate the proteic fraction and loaded on an acrylamide gel. The proteins are electrophoretically separated and transferred on a spongy membrane to which is applied a first antibody that will recognize specific sequences of the target protein. After some washing steps the membrane is treated with a second antibody that recognizes the first antibody and is detectable through specific staining or chemiluminescence activation. In figure 10.15 a schematic representation of SDS-PAGE / western blot procedure is depicted.

Since the gold(I) phosphine derivatives are selective and strong TrxR inhibitors, it was of interest to study the expression of the target enzyme in cell lysates. MCF-7 cancer cells were treated with 3 µM concentration of selected gold(I) complexes and the TrxR expression was evaluated in a comparative manner by western blot analysis (see figure 10.16 and 10.17).

SDS-PAGE

conditions:
- protein denaturation at 95°C for 5 minutes acrylamide / bisacrylamide gel 8 %

- 70 V for 2 h electrophoretic run

- coomassie brilliant blue stain

protein visualization in fluorescence with UV filter at 590 nm

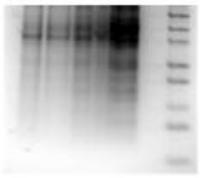

Westernblot

conditions:
- semidryblot system with destained membrane

- 1° antibody blot at 70 V for 7 min.; 2° antibody blot at 20 V for 9 minutes

- transfer glycine; methanol wash solution; ponceau red stain

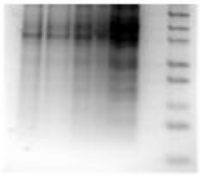

confirmation of protein run visualized in fluorescence with UV filter at 412 nm

CCD Camera Quantification

conditions:
- chemiluminescence substrate activation for 1 min

- preparation of the blot-sandwich

- Infinity Fusion® software calculations and western blot visualization

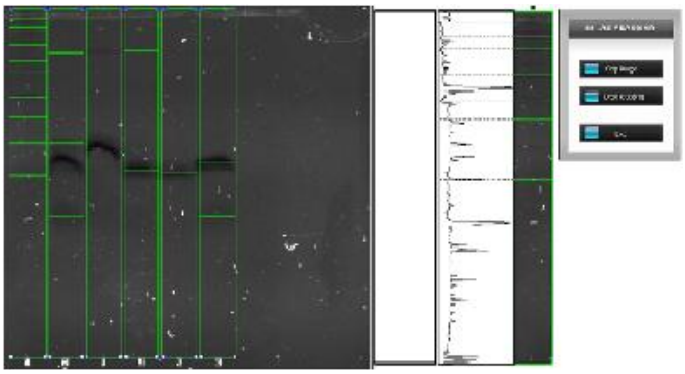

Figure 10.15: flow diagram of western blot experiment procedure

The electrophoresis showed the presence of marked bands in the range of 55-75 kDa, probably corresponding to the molecular weight of GR (55 kDa) and TrxR (55 - 65 kDa).

The western blot analysis indicated an influence of the compounds on the induction of TrxR. Interestingly, the control and complex **2f** presented expression analogies while complex **2d** and **2e** induced a clear strong over-expression of the target enzyme. The results are in good agreement with the inhibition studies on the isolated enzyme (see chapter 6) that assessed the order of enzyme inhibition **2d** = **2e** > **2f**. The results suggested a strong connection between the chemical properties (TEP, hindrance, lipophilicity, see chapter 3) of the phosphine moiety, the influence on TrxR and consequently the mode of action of the gold complexes.

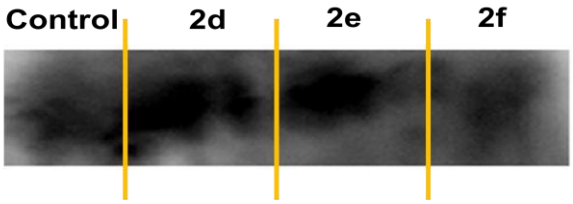

Figure 10.16: western blot analysis on MCF-7 cells treated 3 µM of complex **2d**, **2e** and **2f** for 3 h at 37°C / 5% CO_2; TrxR2 analysis: semi-dry blot of the substances on a nitrocellose membrane, marked with monoclonal mouse anti-TrxR2 antibody / anti-mouse 2° antibody phosphatase and visualized with a CCD camera in chemiluminescence mode; Control = lysate of untreated cells

11. Synopsis

A first series of chlorido *N*,*N*-disubstituted benzimidazol-2-ylidene gold(I) (**1a** – **4a**) was successfully synthesized and analytically characterized (see figure 11.1). The drug design was based on the combination of NHC coordination potential and structural analogy with a potent bioactive gold complex (GoPI).

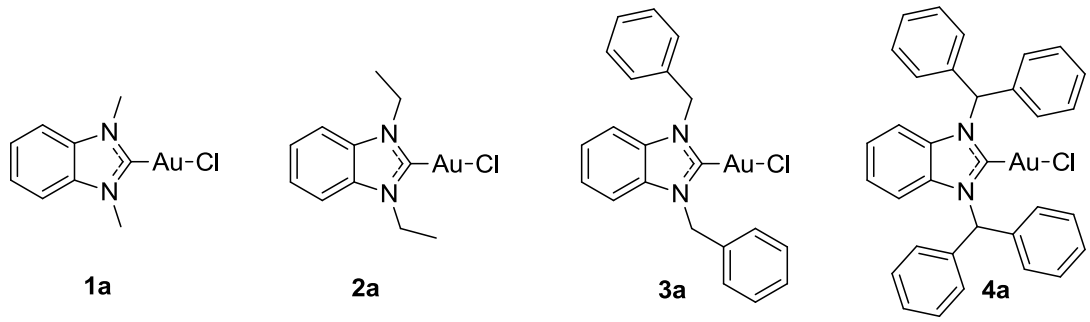

Figure 11.1: gold(I) NHC complexes of the first series

Key feature at the base of the drug design was the improvement of the stability of the gold compounds due to the carbene coordinative potential (in comparison with the more labile phosphine ligand, e.g. Auranofin) that enables trustable structure activity relationship (SAR) studies. Investigations on possible ligand exchange reactions at the carbene moiety under relevant biological conditions (high concentration of glutathione) confirmed the stability of the Au-NHC bond. Chlorido phosphine gold(I) derivatives (Auranofin, TEPG and TPPG), used as positive controls, displayed a characteristic two-step metabolization in presence of glutathione. It was indicated with NMR and MS *ad hoc* studies on TPPG that the first reaction, with the exchange of the chlorido ligand, is followed by a non enzymatic oxidation of the phosphine moiety. The results clearly attested the suitability of the gold(I) NHC complexes to perform reliable SARs in contrast with class of gold(I) phosphine complexes.

Studies on the inhibition of TrxR revealed a strong interaction between the complexes and the target enzyme. All the compounds strongly inhibited the activity of TrxR in situ in concentrations in the submicromolar range. The gold free *N*,*N*-diethyl-benzimidazolium iodide (**2**) did not show any activity up to the highest concentration tested (100 µM) attesting the importance of the gold atom to carry the activity. Studies on the inhibition of GR resulted in the minor interaction of **1a** – **4a** (in comparison with TrxR) with its active site containing a disulfide bridge (with IC_{50} values 20 - 75 fold higher than that for TrxR). The data clearly supported the hypothesis to inhibit selectively TrxR and its selenocysteine – cysteine pair, with a profile comparable to other gold(I) phosphine complexes (TEPG, TPPG), as described in the aim of the project (chapter 2). Unfortunately, the modification at the side chains of the benzimidazole core did not result in a difference in their activity.

In vitro anti-proliferative experiments showed an interesting cytostatic potential of the new molecules. The complexes were effective against different cancer cell lines (breast cancer, coloncarcinoma, hepatocarcinoma), displaying IC_{50} values in the low micromolar range (4.6 – 14.9, with the exception of **4a** probably due to solubility problems) well comparable with established anticancer drugs present on the market (e.g. Cisplatin). Unfortunately **1a** – **4a** did not demonstrate any selectivity in experiments with healthy and immortalized cell lines (HEK-293, HFF respectively). As observed in the enzymatic studies, the presence of the gold atom was a key feature to achieve activity (compound **2** was not active up to 100 µM).

Complex **2a** was chosen for a more detailed biological investigation. As expected, the interaction with the components of the antioxidant network (TrxR, GR) induced a drastic increase in ROS already after 24 h treatment with **2a** in a concentration dependent manner. At the same time frame, annexinV / PI experiments confirmed a high population of early and late apoptotic cells. For short time treatment (already after 2 - 3 h of incubation) an irreversible decrease in respiration rate was observed in living cell populations. The cells tried in vain to compensate the onset enhancing glycolysis as

demonstrated by BIONAS experiments on acidification rate. The failure of the cell compensative mechanisms and its homeostasis impairment was confirmed by the release of LDH, loss of DNA integrity and alteration of membrane functionality. Finally, experiments on doxorubicine, daunorubicine and vincristine resistant cell lines showed partial or significant overcoming of the resistance. Interestingly, all the biological effects were achieved with treatment concentration close to the IC_{50} value (for antiproliferative effects) of **2a**.

The hindrance and lipophilicity of the alkyl substituents at the nitrogens of the benzimidazole core, present in the first series, did not affect the overall activity of **1a** – **4a**. As a consequent and rational development of the project, it was of interest to study the alteration of the chemical environment of the gold center by replacing the chlorido ligand (second series of gold(I) NHCs). Two different ligands were chosen: a second NHC and a phosphine. The increase in coordination potential due to the backbonding and the overall positive charge of the designed molecules were expected to deeply influence the bioactivity. The two new gold(I) complexes were successfully synthesized and investigated in a comparative manner with the previous intensively tested **2a** (see figure 11.2).

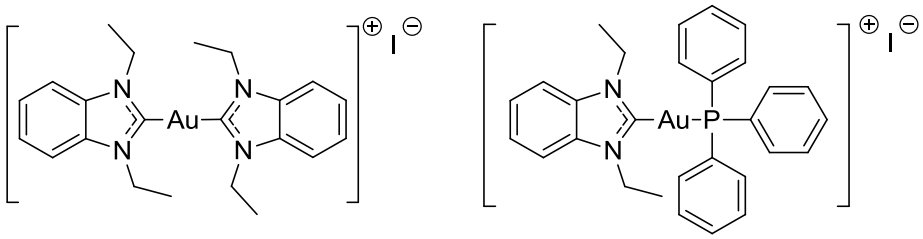

2b **2c**

Figure 11.2: gold(I) NHC complexes of the second series

DFT calculations for the binding between NHC-Au and the second ligand (-Cl, -NHC, -PPh_3) revealed different BDEs with an order of stability **2a** < **2c** < **2b**. The complexes

presented a good stability profile in glutathione inactivation experiments with just a partial lability of **2c** (due probably to oxidation of the phosphine residue). All the compounds showed an alteration in the UV profile after 2 – 4 h incubation in buffer solution, suggesting that a ligand exchange reaction in buffer medium could take place. Because many reports proved the binding of Auranofin with serum proteins and its impact on the complex pharmacodynamic, the interaction of **2a** - **2c** with bovine serum albumin has been investigated. Interestingly, the gold(I) NHC complexes demonstrated a different profile in close relation with the results obtained from the DFT calculations and presented the order of reactivity **2a** > **2c** >> **2b**. Especially **2b** showed just a really slight binding (< 20%) up to 6 h while **2a** and **2c** after 2 h showed already 50 – 60% of the gold binding to BSA.

In addition to the stability profile, also the TrxR inhibitory capacity was affected by the modification of the coordination sphere of the ligand. Complex **2a** and **2c** showed comparable effects with IC_{50} values in the submicromolar range. The TrxR inhibition of **2b** soared to 4.89 µM. The high BDE of the Au-NHC bond in **2b** depressed also the TrxR inhibition, for which a covalent binding modus between the gold atom and the selenocysteine is needed.

MS investigation confirmed for all the complexes the formation of a covalent bond between the gold center and representative peptides. The incubation of the gold NHC complexes with a decamer peptide containing a selenocysteine and a peptide mimicking the active site of TrxR revealed as the main binding modus the formation of a NHC-Au-Se-peptide or peptide-Sec-Au adducts.

In accordance with their BDEs, the new complexes differently interacted with GR. **2c** presented an inhibition profile and selectivity similar to **2a**. It was not possible to determine an IC_{50} value for **2b** (up to 100 µM, the highest concentration tested) against GR, which resulted to be the most selective compound synthesized.

Since the presence of a selenocysteine showed to be a key feature for the selectivity of the gold(I) NHCs, the inhibition of **2a – 2c** on GPx as another selenocysteine containing

enzyme involved in the antioxidant network has been investigated. Interestingly only complex **2a** (presenting a lower BDE and higher activity in experiments with BSA) inhibited GPx, in the same range of concentration as GR. For complex **2b** and **2c** no inhibition was determined up to 100 µM. The data clearly demonstrated the importance of the ligands to achieve an overall selective inhibition of TrxR.

Anti-proliferative studies in two different cancer cell lines assessed a ~ 5 - 10 times fold increase in activity for **2b** and **2c**, in comparison with the first series (**1a** – **4a**), with IC_{50} values in the submicromolar range. Interestingly, complex **2b** demonstrated also a preference towards cancer cells in comparison with immortalized HEK-293 (3 - 8 times fold). Video microscopic imaging of MCF-7 cells treated with the gold(I) NHC complexes underlined a spread cell swelling for complex **2b** and **2c** while complex **2a** showed just a sporadic reduction of biomass in comparison with the untreated control. These results were confirmed by irreversible effects on cell morphology observed with BIONAS instrumentation. All the results stand for the difference in anti-proliferative profile of the complexes: **2a** showed cytostatic properties, **2b** and **2c** were more aggressive than the chloride derivative (**2a**) demonstrating a cytotoxic profile.

The different antiproliferative properties between the complexes were related to the different chemical character of the molecules. The coordination of a neutral ligand, like a NHC or PPh_3, to the gold(I) benzimidazol-2-ylidene core produced a cationic substance with a broad lipophilic system. Many reports assessed the capacity of lipophilic cations to better penetrate the cellular membranes (due to the enhancement effect caused by the inner / outer electrochemical gradient) than neutral substances and even to accumulate in specific compartments like mitochondria. Biodistribution studies were conducted in a HRCS–AAS. The experiments were performed with serum containing or serum free medium, in order to evaluate the impact of serum proteins for the uptake of the complexes. In experiments without FCS the gold complexes were taken up into the cell with an order **2a** < **2b** << **2c** reaching a maximum already after 6 h. Experiments led with FCS clearly demonstrated the negative impact of the serum proteins interaction with the

complexes. With the exception of **2b**, the gold uptake of **2a** and **2c** was reduced with stronger effect for the latter one. The uptake order, for experiment with serum free medium, was **2a** < **2c** < **2b** indicating the key role of the chemical stability in good agreement with the BDEs and BSA interaction studies. As mentioned above, lipophilic cations can accumulate in organelles like mitochondria. Consequently, to complete the biodistribution profile the delivery of **2a** – **2c** into mitochondria was investigated. The order of accumulation was **2a** < **2b** << **2c** with the complexes reaching a maximum already after 4 – 6 h and highlighted the outstanding mitochondrial uptake of **2c**.

The uptake and lipophilic cationic character were at the base of the strong antimitochondrial profile shown by **2c** and especially by **2b**. The respiration rate of living cell population as well as oxygen consumption of isolated mitochondria was drastically reduced after short time incubation (less than 2 h). In particular **2b** already at 0.1 µM totally depressed the oxygen consumption. This effect has been confirmed by experiments on the mitochondrial membrane potential. While **2a** and **2c** interacted at high concentration with the MMP, **2b** already after short incubation time and low concentration drastically depolarized the mitochondrial membrane with increments of membrane permeability.

Apoptosis was confirmed by annexinV / PI assay. Especially **2c** showed a drastic increase (over 90%) of late apoptotic cells at concentration close to its IC_{50} value (relative to the antiproliferative studies). Experiments on cytochrome *c* release resulted negative, suggesting that the programmed cell death mechanism was cytochrome *c* - independent.

Moreover, also microarray analysis on the key signaling pathways (e.g. MAPK, PI3K) remarked the possible different mode of action of **2b** and **2c**. The latter presented a classical TrxR inhibition profile with activation of stress compensatory mechanisms (Hsp27, MEK1/2 – ERK cascade) but insufficient to restore homeostasis. **2b** showed a generalized influence on the different protein kinases, probably affecting the whole signal translation as confirmed by the proteomic studies. An extraordinary insight revealed the strong decrease in phosphorylation for the protein p38α by **2b**.

The study on the second series of gold(I) NHC complexes (**2a** – **2c**) clearly demonstrated how the pharmacodynamic pattern mainly was the consequence of several pathways related to the inhibition of TrxR but also the product of distinct effects against mitochondrial biochemistry as well as signaling pathway interaction not necessarily related to TrxR inhibition. The choice of a ligand instead of another deeply affected all the bioactivity as shown by the difference between neutral (**2a**) or cationic (**2b** and **2c**) complexes or even between cationic molecules with different coordination potential (**2b** / **2c**).

The combination of a NHC and a phosphine in **2c** proved to be a good compromise between good TrxR inhibition, metabolic onset induction and cellular uptake. Moreover, the gold(I) phosphine class represents the most investigated category of anticancer gold complexes. Since chemical variation of the gold ligands resulted in biodistribution and bioactivity modulation, it was of interest to synthesize a third series of gold(I) NHCs with different phosphine residues. The criterium behind the rational drug design was to modulate the coordination potential maintaining a lipophilic cationic system and the flexibility of the phosphines (e.g. possible ligand exchange reaction). According with the TEP as a parameter of the strength of the Au-P bond (and consequently influencing even the Au-NHC bond), a third series of gold(I) NHC phosphine complexes was successfully synthesized and characterized (see figure 11.3).

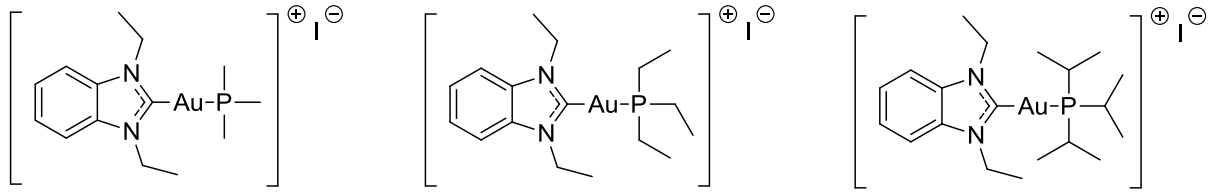

2d **2e** **2f**

Figure 11.3: gold(I) NHC complexes of the third series (part I, phosphine variation)

All the new gold(I) NHC phosphines strongly inhibited the target enzyme TrxR with an improvement in reactivity of ~3 – 10 times fold in comparison with the previous series. Interestingly, the same increment could not be observed for the GR inhibition, resulting in a strong increase of selectivity (~80-100 times fold for **2d** and **2e**, ~40 time fold for **2f** to ~4 times fold for **2c**). It was also possible to notice a representative size – inhibition correlation: the smaller the phosphine ligand, the better the TrxR inhibition (from ~30 nM for **2d** and **2e**, 113 nM of **2f** to 660 nM of **2c**). Unexpectedly, the data demonstrated the importance of the ligand to achieve not just a strong inhibition but even a remarkable selectivity for TrxR.

The remarkable activity of the new complexes towards TrxR influenced the whole homeostasis and regulation of the target enzyme. Preliminary western blot experiments on the expression of TrxR suggested a marked over-expression of the enzyme for treatment with **2d** and **2e** (with lower IC_{50} values, related to the enzyme inhibition studies) while for **2f** the intensity of the band was comparable to the control.

Anti-proliferative experiments assessed IC_{50} values for all the complexes in the high nanomolar range, in good correlation with the second series (**2b** – **2c**). The incoherence between the enzyme inhibition and the cytotoxic experiments was explained with the cellular uptake. Biodistribution experiments demonstrated how the phosphine hindrance and its lipophilicity influenced the accumulation. The smaller the phosphine ligand was the lower was the uptake into the cells.

Finally, it was of interest to study the influence of the donor properties of the carbene core through its modification. The addition of an electron-donor group at position 5 of the benzimidazol-2-ylidene scaffold affected the coordination potential of the NHC ligand to the gold atom. Triethylphopshine and triphenylphosphine were chosen as examples of a small residue at the phosphorus or a hindered P-ligand and the new complexes were successfully synthesized and characterized (see figure 11.4).

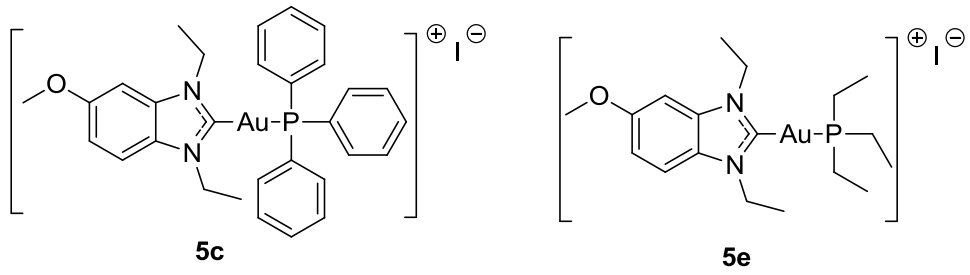

5c **5e**

Figure 11.4: gold(I) NHC complexes of the third series (carbene variation)

The alteration of the donor properties of the carbene deeply influenced the TrxR inhibition. For the triethylphosphine derivative (**5e**) the modification at the benzimidazol-2-ylidene scaffold slightly improved to ~2 times fold the already outstanding activity of its unsubstituted phosphine derivative (31 nM for **2e** and 19 nM for **5e**). Also the selectivity for TrxR increased from ~80 times fold of the analogous **2e** to ~100 times fold for **5e**, making it the most potent TrxR inhibitor of all the series. The electron donor effect in the triphenyl phosphine derivative **5c** did not significantly affect the inhibitory potential of the molecule in comparison with its unsubstituted analogous **2c**. However, similarly to **5e** the selectivity of the compound was increased from ~4 times fold for **2c** to ~26 times fold for **5c**.

All the modified NHC gold complexes demonstrated valuable antiprolifertive properties against HT-29 and especially MCF-7 cancer cell lines with IC_{50} values in the micromolar / submicromolar range. Cytotoxic activities followed the enzymatic trend, reaching the most potent value of all the complexes series synthesized (0.11 µM against MCF-7 for **5e**). The data strongly suggested that an electron donor moiety on the NHC backbone influences deeply the bioactivity, increases the enzyme inhibition and the selectivity towards TrxR as well as the antiproliferative properties.

Summarizing all, the here presented PhD thesis dealt with the therapeutical potential of gold(I) carbene complexes. The synthesis and full characterization of different compounds was successfully performed. A rational *modus operandi* stimulated all the further drug

designs. An intensive biological investigation highlighted the great potential of gold NHCs as anticancer agents. Features like TrxR inhibition, apoptosis induction, ROS stimulation, mitochondria metabolism interactions, uptake and anti-proliferative properties were successfully related to the chemical properties. The gold center carried the activity and it is at the base of the whole pharmacodynamic behavior of the complexes. Nevertheless, its chemical environment modulated the bioactivity profile. All the bioinvestigations presented here concurred to disclose the action mechanism of gold based therapeutics. It could be concluded that gold(I) NHC complexes represent a very interesting class of compounds and a possible alternative treatment to the classical platinum based therapy. Further, this study provided important evidence on their easy functionalization that enabled to investigate different SARs resulting in different bioactivity and stimulated the scientific research in the still niche-field of bioinorganic chemistry.

12. Materials and Methods

12.1 General

All the reagents and the solvents for synthetic purposes were used as received from Sigma Aldrich, Acros Organic, Fluka ChemPur, Invitrogen, Acrys or other suppliers.

Reagents, standards and compounds were weighted on a Sartorius CPA225D. ^{1}H-NMR, ^{13}C-NMR and ^{31}P-NMR were recorded on a Bruker DRX-400 AS NMR System, MS spectra were recorded on a Finnigan MAT 4515 (Thermo Electron Corp.). Elemental analysis was performed with a Flash EA112, Thermo Quest Italia (for all compounds undergoing biological evaluation the experimental values differed less than 0.5% from the calculated ones.). UV measurements were performed on a Specord 200 (Analytik Jena).

pH was assessed with a SevenEasy pH-meter (Mettler-Toledo). Sterilization was obtained in a LTA 2x3x4 autoclave (Zyrbus Technologies). Proper solubilization of lysates or complexes was achived through a Vortex Genie2 (ScientificIndustries) or an Ultrasonic Cleaner (VWR).

MCF-7 breast adenocarcinoma, HT-29 colon carcinoma, HCT-116 coloncarcinoma, HEP-G2 hepato carcinoma and HEK-293 human embryonic kidney healthy cells were maintained in DMEM High Glucose (PAA laboratories GmbH), supplemented with 50 mg / L gentamycin (US-Biological) and 10% (v/v) fetal calf serum (FCS, Biochrom AG) prior to use. Jurkat cells were cultured in RPMI 1640 supplemented with 10% (V/V) FCS. Purity of ≥ 95% of all synthesized compounds was confirmed by elemental analysis. All the cells were cultured in a Binder Incubator (Binder) or in a HeraCell240i CO_2 incubator (ThermoScientific). Experiments on cell under sterile conditions were led under a HeraSafeKS (ThermoScientific). Short and unsterile incubations were performed in a Vortemp56 (Labnet) or in a Inculine (VWR).

Cells were counted with a on C-Chip Neubauer Improve counting chamber (Biochrom AG) an optical microscope (Motic®) and videoimaging files recorded with EVOSxl microscope (AMG). Two plate shakers were used: a linear Titramax 1000 (Heidolph) and an orbital shaker PS-M3D (Grant-Bio).

Electrophoretic runs were performed on a MP-300V (Biozym) in a standard mini-electrophoresis chamber (BioStep). Western Blot analysises were led with iBlot semidry blotting system (Invitrogen) and the visualized with a CCD camera (Fusion Fx7, PeqLab).

All the photometric experiments (enzyme inhibitions, antiproliferative assay, protein quantification through Bradford method) were performed in a microplate reader (Victor x4, PerkinElmer).

Pellets for lysates or AAS analysis were obtained with two centrifuges: CompactStarCS4 (VWR) and CT15RE HIMAC (VWR). AAS analyses were performed in a high resolution continuum source electrothermal atomic absorption spectrometer (ContrAA 700, Analytik Jena).

12.2 Synthesis

12.2.1 General Procedure for Synthesis of the Benzimidazolium Halide Salts

Benzimidazole (1.0 mmol), 5-methoxybenzimidazole (1.0 mmol), the respective alkyl halogenide (3.0 mmol) and K_2CO_3 or Na_2CO_3 (1.0 mmol) were heated under reflux conditions in acetonitrile or toluene for 8 - 24 h. The solvent of the resulting suspension was removed under reduced pressure, and the residue was resuspended in dichloromethane and filtered to remove the formed potassium or sodium halogenide. The filtrate was evaporated under reduced pressure, the residue was resuspended in tetrahydrofuran or ethylacetate to remove the excess of halogenide and filtered to give the pure product.

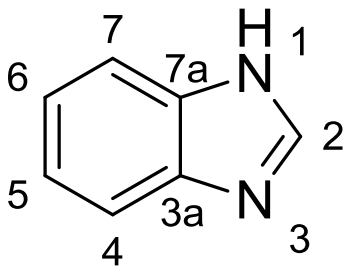

Figure 12.1: position number at the benzimidazole scaffold for the 1,3-dialkylbenzimidazolium halides

*1,3-Dimethylbenzimidazolium iodide (**1**)*

Benzimidazole (0.118 g, 1.0 mmol) was dissolved in acetonitrile and reacted with methyl iodide (0.187 mL, 3.0 mmol) under reflux condition for 8 h in presence of K_2CO_3 (0.138 g, 1.0 mmol); yield: 0.238 g (0.8 mmol, 87%); white powder; mp 217 °C; ^{1}H NMR (DMSO-d6): (ppm) 4.08 (s, 6H, CH_3), 7.71 (dd, 2H, ^4J = 3.2 Hz, ^3J = 6.3 Hz, $ArH_{4/7}$), 8.02 (dd, 2H, ^4J = 3.2 Hz, ^3J = 6.3 Hz, $ArH_{5/6}$), 9.64 (s, 1H, NHC); elemental analysis for $C_9H_{11}N_2I$ (% calculated/found): C (39.44/39.04), H (4.05/4.54), N (10.22/10.00).

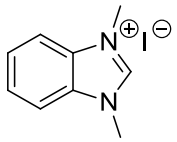

*1,3-Diethylbenzimidazolium iodide (**2**)*

Benzimidazole (0.118 g, 1.0 mmol) was dissolved in acetonitrile and reacted with ethyl iodide (0.241 mL, 3.0 mmol) under reflux condition for 8 h in presence of K_2CO_3 (0.138 g, 1.0 mmol); yield: 0.272 g (0.9 mmol, 90%); white powder; mp 240 °C; ^{1}H NMR (DMSO-d6): (ppm) 1.55 (t, 6H, J = 9.7 Hz, CH_3), 4.52 (q, 4H, J = 9.7 Hz, CH_2), 7.68 (dd, 2H, ^4J = 4.2 Hz, ^3J = 8.4 Hz, $ArH_{4/7}$), 8.10 (dd, 2H, ^4J = 4.2 Hz, ^3J = 8.4 Hz, $ArH_{5/6}$), 9.8 (s, 1H, NHC); ^{13}C NMR (DMSO-d6): (ppm) 14.1 (CH_3) 42.0 (CH_2) 113 ($ArC_{3a/7a}$) 126 (ArC_4) 130

(ArC_5) 141 (NHC); elemental analysis for $C_{11}H_{15}N_2I$ (% calculated/found): C (43.73/43.80), H (5.00/5.02), N (9.27/9.13).

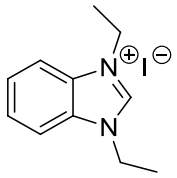

*1,3-Dibenzylbenzimidazolium bromide (**3**)*

Benzimidazole (0.118 g, 1.0 mmol) was dissolved in acetonitrile and reacted with benzyl bromide (0.357 mL, 3.0 mmol) under reflux condition for 8 h in presence of K_2CO_3 (0.138 g, 1.0 mmol); yield: 0.323 g (0.8 mmol, 76%); white powder; mp 150 °C; ^{1}H NMR (DMSO-d6): (ppm) 5.81 (s, 4H, CH_2), 7.46 (m, 10H, ArH), 7.64 (dd, 2H, ^4J = 3.1 Hz, ^3J = 6.3 Hz, $ArH_{4/7}$), 7.98 (dd, 2H, ^4J = 3.2 Hz, ^3J = 6.3 Hz, $ArH_{5/6}$), 10.12 (s, 1H, NHC); elemental analysis for $C_{21}H_{19}N_2Br$ (% calculated/found): C (66.30/65.41),H(5.26/5.20),N (7.36/6.79).

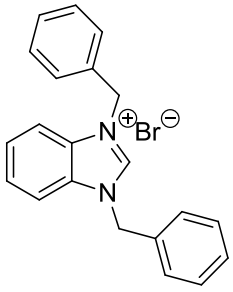

*1,3-Bis-(diphenylmethyl)benzimidazolium chloride (**4**)*

Benzimidazole (0.118 g, 1.0 mmol) was dissolved in acetonitrile and reacted with diphenyl-methyl chloride (0.608 g, 3.0 mmol) under reflux condition for 8 h in presence of K_2CO_3 (0.138 g, 1.0 mmol); yield: 0.462 g (0.8 mmol, 80%); white powder; mp 254 °C; ^{1}H NMR ($CDCl_3$): (ppm) 7.45 (m, 24H, ArH), 7.82 (s, 2H, CH), 10.68 (s, 1H, NHC); elemental analysis for $C_{33}H_{27}N_2Cl$ (% calculated/found): C (81.48/80.99), H (5.55/5.54), N (5.76/5.60).

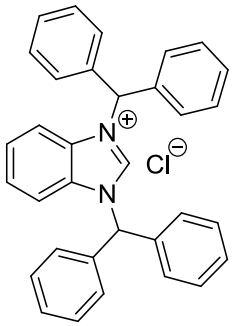

*1,3-Diethyl-5-methoxy-benzylimidazolium iodide (**5**)*

5-Methoxy-benzimidazole (0.74 g, 5.0 mmol) was dissolved in toluene and reacted with ethyl iodide (1.2 ml, 15.0 mmol) in presence of Na_2CO_3 (0.53 g, 5.0 mmol) for 24 h in reflux under vigorous stirring. The solvent of the resulting suspension was removed under reduced pressure, and the residue was resuspended in dichloromethane and filtered to remove the sodium bicarbonate. The filtrate was evaporated under reduced pressure, the residue was resuspended in tetrahydrofuran and filtered to give the pure product. Yield: 1.23 g (3.7 mmol, 74%) brown powder; ^{1}H NMR (DMSO-d_6): (ppm) 1.54 (m, 6H, CH_3), 3.92 (s, 3H, OCH_3), 4.48 (m, 4H, CH_2), 7.28 (dd, 1H, ^{3}J = 9.1 Hz, ^{4}J = 2.4 Hz, ArH_6), 7.61 (d, 1H, ^{4}J = 2.4 Hz, ArH_4), 7.97 (d, 1H, ^{3}J = 9.1 Hz, ArH_7), 9.68 (s, 1H, ArH_2); ^{13}C NMR (DMSO-d_6): (ppm) 14.2 (CH_3), 42.0 (CH_2), 56.3 (OCH_3), 96.0 (ArC), 114.4 (ArC), 116.4 (ArC), 125.2 (ArC), 132.1 (ArC), 140.6 (ArC_2), 158.6 (ArC_5); elemental analysis for $C_{10}H_{13}N_2O{\cdot}I$ (% calculated/found): C (43.39/43.55) H (5.16/5.20) N (8.43/8.41).

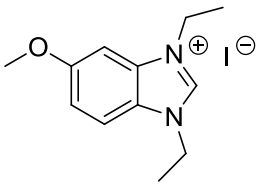

12.2.2 General Procedure for Synthesis of the Gold NHC Complexes

Series I

To achieve the chloride derivatives (**1a** – **4a**) the respective benzimidazolium salts (1.0 mmol) were treated with Ag_2O (0.5 mmol) under vigorous stirring in dichloromethane for 5 - 8 h. After the color change, dimethylsulfidegold(I) (1.0 mmol) was added and the reaction was stirred for another 10 h. The obtained suspension was filtered over Celite (281 nm), and the solvent was evaporated under reduced pressure to give the pure products.

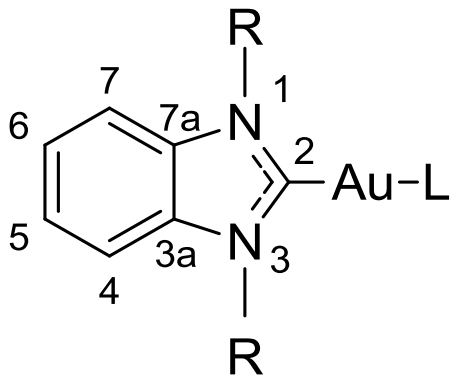

Figure 12.2: position number at the benzimidazole scaffold for the 1,3-dialkylbenzimidazol-2-ylidene gold(I) complexes

*Chlorido-(1,3-dimethylbenzimidazol-2-ylidene)gold(I) (***1a***)*

Dimethyl-benzimidazolium iodide (0.274 g, 1.0 mmol) was dissolved in dichloromethane and reacted with Ag_2O (0.116 g, 0.5 mmol) 5 h in reflux under vigorous stirring in the dark till color change then C_2H_6AuClS (0.295 g, 1.0 mmol) was added and the reaction additionally stirred for another 10 h. The product was purified under Celite column; yield: 0.095 g (0.3 mmol, 25%) yellow powder. ^1H NMR ($CDCl_3$): (ppm) 3.99 (s, 6H, CH_3), 7.46 (m, 4H, ArH); MS (EI): 378 $[M+H]^+$; elemental analysis for $C_9H_{10}AuClN_2$ (% calculated/found): C (28.55/28.56), H (2.60/2.69), N (7.40/6.98).

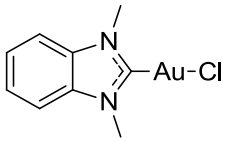

*Chlorido-(1,3-diethylbenzimidazol-2-ylidene)gold(I) (***2a***)*

1,3-Diethyl-benzimidazolium iodide (0.302 g, 1.0 mmol) was dissolved in dichloromethane and reacted with Ag_2O (0.116 g, 0.5 mmol) 5 h in reflux under vigorous stirring in the dark till color change then C_2H_6AuClS (0.295 g, 1.0 mmol) was added and the reaction additionally stirred for another 10 h. The product was purified under Celite column; yield: 0.122 g (0.3 mmol, 30%) pale-yellow powder. ^{1}H NMR ($CDCl_3$): (ppm) 1.55 (t, 6H, J = 5.9 Hz, CH_3), 4.54 (q, 4H, J = 9.8 Hz, CH_2), 7.46 (m, 4H, ArH); ^{13}C NMR ($CDCl_3$): (ppm) 15.4 (CH_3), 43.9 (CH_2), 111 (ArC_8), 124 (ArC_4), 132 (ArC_5), 177 (NHC); MS(EI) 406 $[M+H]^+$; elemental analysis for $C_{11}H_{14}AuClN_2$ (% calculated/found): C (32.49/32.03), H (3.47/3.38), N (6.89/6.91).

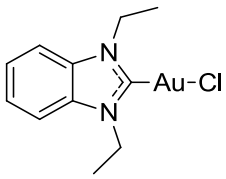

*Chlorido-(1,3-dibenzylbenzimidazol-2-ylidene)gold(I) (***3a***)*

1,3-Dibenzyl-benzimidazolium bromide (0.379 g, 1.0 mmol) was dissolved in dichloromethane and reacted with Ag_2O (0.116 g, 0.5 mmol) 5 h in reflux under vigorous stirring in the dark till color change then C_2H_6AuClS (0.295 g, 1.0 mmol) was added and the reaction additionally stirred for another 10 h. The product was purified under Celite column; yield: 0.265 g (0.5 mmol, 50%) white powder; ^{1}H NMR ($CDCl_3$): (ppm) 5.76 (s, 4H, CH_2), 7.35 (m, 14H, ArH). MS (EI): 530 $[M-H]^+$; elemental analysis for $C_{21}H_{18}AuClN_2$ (% calculated/found): C (47.52/47.72), H (3.42/3.58), N (5.28/5.25).

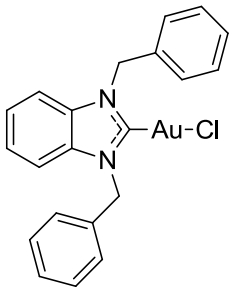

*Chlorido-[1,3-bis-(diphenylmethyl)benzimidazol-2-ylidene]gold-(I) (***4a***)*

1,3-Bis-diphenylmethyl-benzimidazolium chloride (0.487 g, 1.0 mmol) was dissolved in dichloromethane and reacted with Ag_2O (0.116 g, 0.5 mmol) 5 h in reflux under vigorous stirring in the dark till color change then C_2H_6AuClS (0.295 g, 1.0 mmol) was added and the reaction additionally stirred for another 10 h. The product was purified under Celite column; yield: 0.375 g (0.6 mmol, 55%); white powder; ^{1}H NMR ($CDCl_3$): (ppm) 7.05 (dd, 2H, ^4J = 3.5 Hz, ^3J = 6.5 Hz, $ArH_{4/7}$), 7.36 (m, 22H, ArH), 7.89 (s, 2H, CH); MS (EI) 682 $[M+H]^+$; elemental analysis for $C_{33}H_{26}AuClN_2$ (% calculated/found): C (58.03/57.75), H (3.84/3.87), N (4.10/3.87).

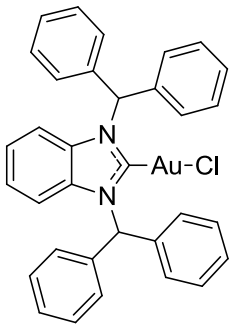

Series II

To achieve the dicarbene derivative (**2b**) the opportune salts (1.0 mmol) was dissolved in dichloromethane methanol (1 : 1) in presence of a K_2CO_3 (1.0 mmol) and reacted with the relative gold(I) chloride complex (**2a**) under vigorous stirring till the disappearing of the color and stirred for other 12 h. The solution was filtered to remove the K_2CO_3, evaporate

under reduced pressure and purified through column chromatography (silica column, eluent dichloromethane / methanol 97.5 / 2.5 %).

*[Bis-(1,3-diethylbenzylimidazol-2-ylidene)]gold(I) iodide (***2b***)*

Diethylbenzimidazolium iodide (0.151 g, 0.5 mmol) was dissolved in dichloromethane methanol (1 : 1) in presence of K_2CO_3 (0.069 g, 0.5 mmol), reacted with complex **2a** (0.203 g, 0.5 mmol) till color change and stirred for another 12 h. The carbonate was filtered off and the solvent removed under reduced pressure. The formed product was isolated by column chromatography (eluent: dichloromethane / methanol 97.5 / 2.5); yield: 0.202 g (0.3 mmol, 43%) white powder; ^{1}H NMR ($CDCl_3$): (ppm) 1.69 (t, 12H, J = 9.7 Hz, CH_3), 4.72 (q, 8H, J = 9.7 Hz, CH_2), 7.46 (dd, 4H, ^{4}J = 4.4 Hz, ^{3}J = 8.2 Hz, $ArH_{4/7}$), 7.58 (dd, 4H, ^{4}J = 4.4 Hz, ^{3}J = 8.2 Hz, $ArH_{5/6}$), ^{13}C NMR ($CDCl_3$): (ppm) 16.0 (CH_3), 44.2 (CH_2), 111.6 ($ArC_{3a/7a}$), 124.6 (ArC_4), 133.1 (ArC_5), 190.3 (NHC); MS(EI): 498 $[M\text{-}NHC]^+$, MS(ESI): 672 $[M]^+$, 545 $[M\text{-}I]^-$, elemental analysis for $C_{22}H_{28}AuN_4I$ (%calculated/found): C (39.18/39.08) H (4.48/4.22) N (8.31/8.06).

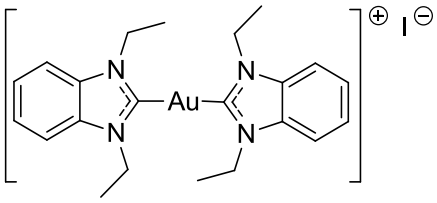

*[Triphenylphosphine-(1,3-diethylbenzylimidazol-2-ylidene)]gold(I) iodide (***2c***)*

Diethylbenzimidazolium iodide (0.151 g, 0.5 mmol) was dissolved in dichloromethane methanol (1 : 1) in presence of K_2CO_3 (0.069 g, 0.5 mmol), reacted with complex triphenyl phosphine gold(I) chloride (0.275 g, 0.5 mmol) till color change and stirred for another 8 - 10 h. The carbonate was filtered off and the solvent removed under reduced pressure. The substance was purified through liquid / liquid extraction with dichloromethane / water and the organic solvent was afterwards evaporated to give the pure product; yield: 0.228 g (0.3 mmol, 58%) white powder; ^{1}H NMR ($CDCl_3$): (ppm) 1.68 (t, 6H, ^{3}J = 9.7 Hz, CH_3),

4.71 (q, 4H, ^{3}J = 9.7 Hz, CH_2), 7.52 (m, 19H, ArH), ^{13}C NMR ($CDCl_3$): (ppm) 16.0 (CH_3), 44.2 (CH_2), 111.6 (ArC_8), 124.7 (ArC_4), 128.8 ($PArC_1$), 128.9 ($PArC_2$), 130.6 (ArC_5), 134.0 ($PArC_3$), 134.1 ($PArC_4$), 190.2 (NHC), ^{31}P NMR: (ppm) 32.5; MS (EI): 586 $[M\text{-}NHC]^+$, 498 $[M\text{-}PPh_3]^+$, MS (FAB): 760 $[M]^+$; elemental analysis for $C_{29}H_{29}AuN_2PI$ (% calculated/found): C (45.75/46.24) H (3.97/3.83) N (3.68/3.56).

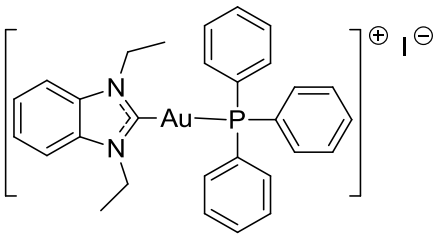

Series III

To achieve the gold phosphine complexes (**2c** – **2f**, **5c**, **5e**) the opportune benzimizadolium salt was dissolved in dichloromethane methanol (1 : 1) in presence of a Na_2CO_3 (1.0 mmol), heated at 50 °C for 15 minutes and then reacted with the relative tri-alkyl-phosphine gold(I) chloride (1.0 mmol) under vigorous stirring for 8 - 60 h. The solution was filtered to remove the K_2CO_3, evaporated under reduced pressure and purified through column chromatography (silica column, eluent dichloromethane / methanol 97.5 / 2.5 %) or washed with bidistilled water, redissolved in dichloromethane, treated with Na_2SO_4 for 2 h and the solvent evaporate under reduced pressure.

*[Trimethylphosphine-(1,3-diethylbenzylimidazol-2-ylidene)]gold(I) iodide (***2d***)*

1,3-Diethylbenzimidazolium iodide (0.060 g, 0.2 mmol) was dissolved in dichloromethane in presence of Na_2CO_3 (0.021 g, 0.2 mmol), heated 10 minutes at 50°C and reacted with trimethylphosphine gold(I) chloride (0.062 g, 0.2 mmol) under vigorous stirring for 60 h. The Na_2CO_3 was filtered off and the complex was purified through liquid / liquid extraction with dichloromethane / water, the organic solvent was afterwards evaporated and recrystallized in dichloromethane / hexane to give the pure product; yield: 0.057 g (0.1 mmol, 49%) white powder; ^{1}H NMR ($CDCl_3$): (ppm) 1.67 (br, 15H, PCH_3 / CH_3), 4.71 (q,

4H, J = 7.32 Hz, CH_2), 7.48 (dd, 2H, ^4J = 3.1 Hz, ^3J = 6.2 Hz, $ArH_{4/7}$), 7.60 (dd, 2H, ^4J = 3.1 Hz, ^3J = 6.2 Hz, $ArH_{5/6}$); ^{13}C NMR ($CDCl_3$): (ppm) 16.0 (PCH_3 / CH_3), 44.2 (CH_2), 111.6 ($ArC_{3a/7a}$), 124.8 ($ArC_{5/6}$), 133.0 ($ArC_{4/7}$), 189.9 (NHC); ^{31}P NMR ($CDCl_3$): (ppm) 39.3; MS (ESI): 574 $[M\text{-}I]^+$; m.p. 196°C; elemental analysis for $C_{14}H_{23}AuN_2P{\cdot}I$ (% calculated/found): C (29.28/29.66) H (4.04/4.06) N (4.88/5.00).

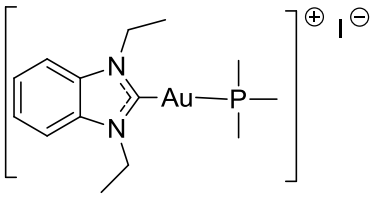

*[Triethylphosphine-(1,3-diethylbenzylimidazol-2-ylidene)]gold(I) iodide (***2e***)*

1,3-Diethylbenzimidazolium iodide (0.060 g, 0.2 mmol) was dissolved in dichloromethane in presence of Na_2CO_3 (0.021 g, 0.2 mmol), heated 10 minutes at 50°C and reacted with triethylphosphine gold(I) chloride (0.070 g, 0.2 mmol) under vigorous stirring for 60 h. The Na_2CO_3 was filtered off and the complex was purified through liquid / liquid extraction with dichloromethane / water, the organic solvent was afterwards evaporated and recrystallized in dichloromethane / hexane to give the pure product; yield: 0.073 g (0.1 mmol, 59%); white powder; ^1H NMR ($CDCl_3$): (ppm) 1.21 (br, 9H, PCH_3), 1.65 (t, 6H, J = 7.36 Hz, CH_3), 1.87 (br, 6H, PCH_2), 4.72 (q, 4H, J = 7.32 Hz, CH_2), 7.48 (dd, 2H, ^4J = 3.1 Hz, ^3J = 6.2 Hz, $ArH_{4/7}$), 7.57 (dd, 2H, ^4J = 3.1 Hz, ^3J = 6.2 Hz, $ArH_{5/6}$); ^{13}C NMR ($CDCl_3$): (ppm) 8.9 (PCH_3), 15.6 (CH_3), 17.8 (PCH_2), 44.2 (CH_2), 111.6 ($ArC_{3a/7a}$), 124.7 (ArC_4), 133.1 (ArC_5), 190.3 (NHC); ^{31}P NMR ($CDCl_3$): (ppm) 39.4; MS (EI): 489 $[M\text{-}I]^+$; m.p. 215°C; elemental analysis for $C_{17}H_{29}AuN_2P{\cdot}I$ (% calculated/found): C (33.13/33.44) H (4.74/4.61) N (4.55/4.29).

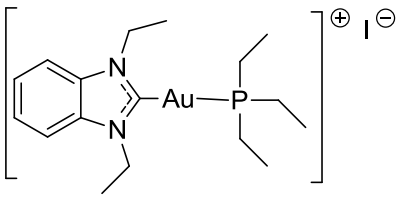

*[Triisopropylphosphine-(1,3-diethylbenzylimidazol-2-ylidene)]gold(I) iodide (***2f***)*

1,3-Diethylbenzimidazolium iodide (0.060 g, 0.2 mmol) was dissolved in dichloromethane in presence of Na_2CO_3 (0.021 g, 0.2 mmol), heated 10 minutes at 50°C and reacted with triisopropylphosphine gold(I) chloride (0.078 g, 0.2 mmol) under vigorous stirring for 60 h. The Na_2CO_3 was filtered off and the complex was purified through liquid / liquid extraction with dichloromethane / water, the organic solvent was afterwards evaporated and recrystalized in dichloromethane / hexane to give the pure product; yield: 0.071 g (0.1 mmol, 54%) white powder; ^{1}H NMR ($CDCl_3$): (ppm) 1.34 (br, 18H, PCH_3), 1.67 (t, 6H, J = 7.36 Hz, CH_3), 2.62 (br, 3H, PCH), 4.71 (q, 4H, J = 7.32 Hz, CH_2), 7.49 (dd, 2H, ^{4}J = 3.1 Hz ^{3}J = 6.2 Hz, $ArH_{4/7}$), 7.59 (dd, 2H, ^{4}J = 3.1 Hz ^{3}J = 6.2 Hz, $ArH_{5/6}$); ^{13}C NMR ($CDCl_3$): (ppm) 16.0 (CH_3), 20.3 (PCH_3), 20.6 (PCH), 44.2 (CH_2), 111.6 ($ArC_{3a/7a}$), 124.7 (ArC_4), 133.0 (ArC_5), 192.6 (NHC); ^{31}P NMR ($CDCl_3$): (ppm) 66.0; MS (ESI): 531 $[M\text{-}I]^+$; m.p. 174°C; elemental analysis for $C_{20}H_{35}AuN_2P{\cdot}I$ (% calculated/found): C (36.49/36.66) H (5.36/5.42) N (4.26/4.48).

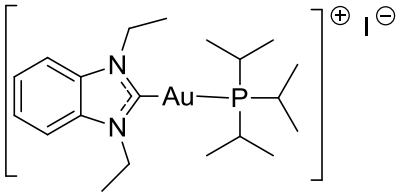

*[Triethylphosphine-(1,3-diethyl-5-methoxy-benzylimidazol-2-ylidene)]gold(I) iodide (***5e***)*

1,3-Diethyl-5-methoxy-benzimidazolium iodide (0.066 g, 0.2 mmol) was dissolved in dichloromethane in presence of Na_2CO_3 (0.021 g, 0.2 mmol), heated 10 minutes at 50°C and reacted with triethylphosphine gold(I) chloride (0.070 g, 0.2 mmol) under vigorous stirring for 60 h. The Na_2CO_3 was filtered off and the complex was purified through liquid / liquid extraction with dichloromethane / water, the organic solvent was afterwards evaporated and recrystalized in dichloromethane / hexane to give the pure product; yield: 0.098 g (0.2 mmol, 76%) brown powder; ^{1}H NMR ($CDCl_3$): (ppm) 1.21 (br, 9H,

PCH_3), 1.64 (m, 6H, CH_3), 1.99 (br, 6H, PCH_2), 3.95 (s, 3H, OCH_3), 4.63 (q, 4H, J = 7.32 Hz, CH_2), 7.08 (dd, 1H, ^4J = 3.1 Hz, ^3J = 6.2 Hz, ArH_5), 7.09 (d, 1H, ^3J = 2.36 Hz, ArH_4), 7.46 (d, 1H, ^3J = 9.08 Hz, ArH_7); ^{13}C NMR ($CDCl_3$): (ppm) 8.9 (PCH_3), 16.0 (d, CH_3), 17.8 (PCH_2), 44.2 (d, CH_2), 56.4 (OCH_3), 95.1 (ArC_6), 112.2 (ArC), 114.1 (ArC), 127.4 (ArC_4), 134.1 (ArC_5), 158.1 (ArC_7), 189.3 (NHC); ^{31}P NMR: (ppm) 39.4; MS (ESI): 519 $[M^+\text{-}I]^+$; m.p. 210°C; elemental analysis for $C_{18}H_{31}AuN_2OP{\cdot}I$ (%calc./found): C (33.45/33.33) H (4.83/4.76) N (4.33/4.02).

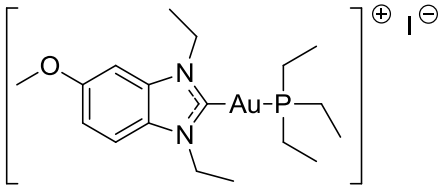

*[Triphenylphosphine-(1,3-diethyl-5-methoxy-benzylimidazol-2-ylidene)]gold(I) iodide (***5c***)*

1,3-Diethyl-5-methoxy-benzimidazolium iodide (0.066 g, 0.2 mmol) was dissolved in dichloromethane in presence of Na_2CO_3 (0.021 g, 0.2 mmol), heated 10 minutes at 50°C and reacted with chloridotriphenylphosphane gold(I) (0.099 g, 0.2 mmol) under vigorous stirring for 60 h. The solution was filtered to remove the Na_2CO_3, evaporated under reduced pressure and purified through column chromatography (silica column, eluent dichloromethane / methanol 97.5 / 2.5 %). Yield: 0.093 g (0.11 mmol, 59%) brown powder; ^1H NMR ($CDCl_3$): (ppm) 1.64 (m, 6H, CH_3), 3.95 (s, 3H, OCH_3), 4.60 (q, 2H, ^3J = 7.3 Hz, CH_2), 4.66 (q, 2H, ^3J = 7.3 Hz, CH_2), 7.45 (m, 18H, ArH); ^{13}C NMR ($CDCl_3$): (ppm) 16.0 (CH_3), 44.2 (CH_2), 56.5 (OCH_3), 95.1 (ArC), 112.2 (ArC), 114.2 (ArC), 127.3 (ArC), 128.8 (d, $PArC_{1'}$), 130.6 (d, $PArC_{2'}$), 132.2 (d, $PArC_{3'}$),133.9 (ArC), 134.1 (d, $PArC_{4'}$), 158.1 (ArC_5), 190.2 (ArC_2); ^{31}P NMR ($CDCl_3$): (ppm) 32.9; MS (ESI): 663 $[M\text{-}I]^+$; m.p. 202°C; elemental analysis for $C_{30}H_{31}AuN_2OP{\cdot}I$ (%calc./found): C (45.59/45.87) H (3.95/4.02) N (3.54/3.81).

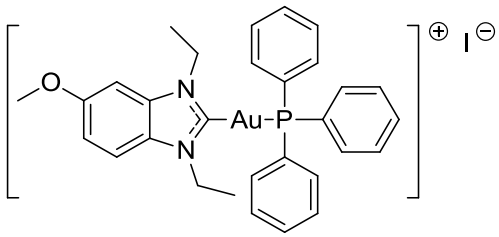

12.3 Computational chemistry[145]

Computational chemical studies on GoPI and TrxR active site were performed by Prof. Dr. Gerard Wolber, Institute of Pharmacy, Freie Universität Berlin, Königin-Luise-Strasse 2þ4, 14195 Berlin, Germany

The X-ray structure of GR complexed with the GoPI residue 2-(2-phenyl-3-pyridin-2-yl-4,5,6,7-tetrahydro-*2H*-isophosphoindol-1-yl)pyridine (PDB entry 1AAQ) was used and derived a 3D pharmacophore using the software LigandScout 3.0. LigandScout identified lipophilic contacts to Leu261, Leu183, and Ile175, which served as a basis for assumptions leading to the new compounds presented in this work. The 3D overlay of TrxR (2CFY) and GR (2AAQ) was performed using the molecular modeling package MOE (Molecular Operating Environment, version 2009.10, Chemical Computing Group, Montreal, Canada) and is based on a sequence alignment of the two proteins with a subsequent 3D overlay.

12.4 DFT Calculations[153]

DFT calculation were performed by Dr. Malte Kokoschka from the research group of Prof. Dr. William S. Sheldrick, Lehrstuhl für Analytische Chemie, Ruhr-Universität Bochum, 44780 Bochum, Germany

All calculations were performed using Gaussian 03 (Rev. E.01). Density functional theory (B3LYP) has been employed for all geometry and energy calculations. Geometries and zero point corrections were calculated using the Stuttgart RSC 1997 ECP (SDD) basis set on Au and the 6-31G(d) basis set on all other atoms. An ultragrid had to be employed for PPh_3 containing molecules to reach convergence. For the calculation of energies the diffuse basis sets aug-cc-pVDZ-PP on Au and aug-cc-pVDZ on all other atoms were used. The basis sets Stuttgart RSC 1997 ECP, aug-cc-pVDZ and aug-cc-pVDZ-PP have been obtained via the EMSL website Basis Set Exchange. The final energy values were corrected for the basis set superposition error using the counterpoise method according to Boys and Bernardi. To account for solvent effects the polarizable continuum model (IEF-PCM) was employed with ε=78.39 for water.[159-162] All Illustrations of molecular structures obtained from ab-initio calculations were prepared using Chemcraft.

12.5 Stability experiments

12.5.1 Stability in buffer solution

Stock solutions of **2a** – **2c** were prepared in acetonitrile and diluted with phosphate buffered saline (8.0 g NaCl, 1.0 g Na_2HPO_4, 0.15 NaH_2PO_4, 0.2 KCl, 0.2 KH_2PO_4, dissolved in 1.0 L) to a concentration of 100µM. The solutions were incubated at 37°C at different time frames and UV/Vis spectra were taken with a Specord 200 (AnalytikJena AG) spectrometer.

12.5.2 Interaction between the gold complexes and glutathione[145,153]

The metal complexes were prepared as stock solutions in dimethylformamide (DMF) and diluted with potassium phosphate buffer pH 7.0 to achieve a final concentration of 500 µM (DMF: 0.2% V/V). 25 µL of 250 µM aqueous solutions of reduced glutathione were added each to 25 µL of the respective potassium phosphate buffer solution (containing the

compounds or only the DMF vehicle as control) and 25 µL 100 mM aqueous EDTA solution pH 7.5 and the resulting solutions were incubated with moderate shaking in a 96-well plate at 37 °C for 20 or 60 min. To each well, 200 µL of reaction mixture (1000 µL reaction mixture consisted of 620 µL potassium phosphate buffer pH 7.0, 80 µL 100 mM EDTA solution pH 7.5, and 300 µL distilled water) were added, and the reaction was started with the addition of 25 µL of a 20 mM ethanolic solution of DTNB. After proper mixing, the formation of 5-TNB was monitored in a microplate reader (Perkin-Elmer Victor X4) at 405 nm. For each tested compound, the non interference with the assay components was confirmed by a negative control experiment using a glutathione free solution. Results are presented as means of two independent experiments.

12.5.3 ^{31}P-NMR experiments on TPPG interaction with glutathione and DTNB[145]

0.03 g (0.1 mmol) of glutathione were dissolved in 10 mL of methanol and 0.1 g (0.2 mmol) of triphenylphosphine gold(I) chloride (TPPG) dissolved in 5 mL dichloromethane : methanol (1 : 1) were added. The resulting solution was stirred at 40°C for two hours. Then 0.15 g (0.38 mmol) of DTNB dissolved in 15 mL of methanol were added and the solution was stirred vigorously for another hour. The solvent was evaporated and the yellow powder dried overnight. The powder was dissolved in aceton and two aliquots were prepared in NMR tubes: one containing the probe and one containing the probe with a mixture of triphenylphosphine oxide and TPPG (1:1, 0.3 mmol) as positive controls.

12.5.4 Binding to albumin[153]

The gold(I) complexes were prepared as stock solutions in dimethylformamide to achieve a final concentration of 3.0 mM. 440 mg of bovine serum albumin (BSA, Sigma Aldrich) were dissolved in 11.0 ml cell culture medium. 11 µL of the gold complex stock solutions were added to the BSA containing medium and incubated at 37°C in the dark under gentle shaking. After 0, 1, 2, 4, 6 and 24 h an 250 µL aliquot thereof was taken, treated with 500 µL of cold (-20°C) ethanol and stored at -20°C for 2 h to allow precipitation of the protein

fraction. Afterwards the solution was centrifuged at 400 g for 5 minutes at 4°C, 400 µL of the supernatant were taken, treated with 40 µL HNO_3 13% and the gold content was measured by atomic absorption spectroscopy (see table 12.1). The percentage of gold bonded to albumin was calculated thereof. Results are given as the means and error of repeated two independent experiments.

Step	Temp. (°C)	Rate (°C)	Hold (sec)
Drying	80	10	40
Drying	105	7	30
Drying	120	15	20
Drying	500	50	30
Pyrolysis	700	200	20
AZ zeroing	700	---	5
Atomization	1800	1500	6
Cleaning	2400	500	7

Table 12.1: graphite furnace program for the determination of gold traces in biological samples with AAS

12.5.5 Atomic absorption spectroscopy[153]

Gold contents were measured with a graphite furnace high resolution continuum source atomic absorption spectrometer (contraAA 700, Analytik Jena AG) at 242.795 nm according to a recently described method with minor modifications in the graphite furnace temperature program.[224,232] Matrix matched calibration with gold standard solutions (Fluka) was used as calibration mode. Probes were injected at a volume of 20 µL into graphite wall tubes. The mean absorbances of duplicate injections were used throughout the study.

12.6 Enzymatic experiments

12.6.1 TrxR / GR Inhibition Assay[145,153]

To determine the inhibition of TrxR and GR an established microplate reader based assay was performed with minor modifications.[168] For this purpose commercially available rat liver TrxR and baker yeast GR (both from Sigma-Aldrich) were used and diluted with distilled water to achieve a concentration of 2.0 U/mL. The compounds were freshly dissolved as stock solutions in DMF. To each 25 µL aliquots of the enzyme solution each 25 µL of potassium phosphate buffer pH 7.0 containing the compounds in graded concentrations or vehicle (DMF) without compounds (control probe) were added and the resulting solutions (final concentration of DMF: max. 0.5% V/V) were incubated with moderate shaking for 75 minutes at 37°C in a 96 well plate. To each well 225 µL of reaction mixture (1000 µL reaction mixture consisted of 500 µL potassium phosphate buffer pH 7.0, 80 µL 100 mM EDTA solution pH 7.5, 20 µL BSA solution 0.05%, 100 µL of 20 mM NADPH solution and 300µL of distilled water) were added and the reaction started by addition of 25 µL of an 20 mM ethanolic DTNB solution. After proper mixing, the formation of 5-TNB was monitored with a microplate reader (Perkin Elmer VictortmX4) at 405 nm in 10 s intervals for 6 minutes. The increase in 5-TNB concentration over time followed a linear trend ($r^2 \geq 0.99$) and the enzymatic activities were calculated as the slopes (increase in absorbance per second) thereof. For each tested compound the non interference with the assay components was confirmed by a negative control experiment using an enzyme free solution. The IC_{50} values were calculated as the concentration of compound decreasing the enzymatic activity of the untreated control by 50% and are given as the means and error of 3 - 6 independent experiments. The whole inhibition assay work flow is showed in figure 12.3.

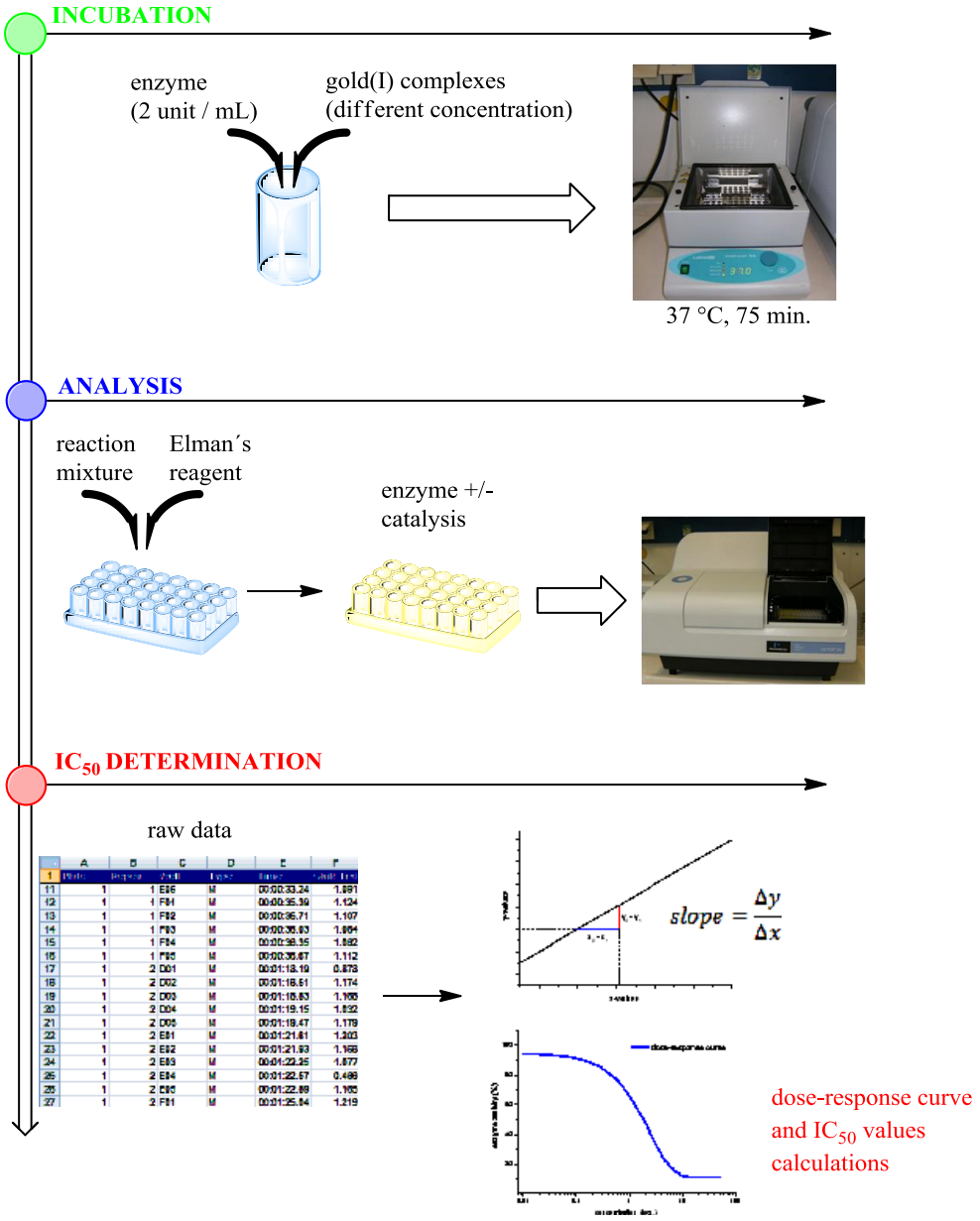

Figure 12.3: flow diagram of enzyme inhibition assay procedure

12.6.2 GPx Inhibition Assay[153]

To determine the inhibition of GPx an established microplate reader based assay was performed with minor modifications.[102,193] For this purpose commercially available fetal bovine erythrocytes GPx (Sigma-Aldrich) was used and diluted with distilled water to achieve a concentration of 100 ng/mL. The compounds were freshly dissolved as stock solutions in DMF. To each 35 µL aliquots of the enzyme solution each 35 µL buffer pH 7.0 containing the compounds in graded concentrations or vehicle (DMF) without compounds

(control probe) were added and the resulting solutions (final concentration of DMF: max. 0.5% V/V) were incubated with moderate shaking for 75 minutes at 37°C in a 96 well plate. To each well 25 µL of a 4 U/mL GR solution in water and 200 µL of reaction mixture (1000 µL reaction mixture consisted of 600 µL Hepes/TRIS-HCl 1:1 50 mM buffer pH 7.0, 100 µL 50 mM EDTA solution pH 7.5, 100 µL 50 mM reduced glutathione solution, 100 µL of 50 mM NADPH solution and 100 µL of distilled water) were added and the reaction was started by addition of 25 µL of an 5 mM t-butylperoxide solution. After proper mixing, the reduction of NADPH was monitored with a microplate reader (Perkin Elmer VictorX4) at 340 nm in 10 s intervals for 1 minute. The decrease in NADPH concentration over time followed a linear trend ($r^2 \geq 0.99$) and the enzymatic activities were calculated as the slopes (decrease in absorbance per second) thereof. For each tested compound the non interference with the assay components was confirmed by a negative control experiment using a GPx/GR-enzyme free solution. The IC_{50} values were calculated as the concentration of compound decreasing the GPx activity of an untreated control by 50% and are given as the means and error of 3 independent experiments.

12.6.3 Disulfide reductase inhibition in cell suspensions[145]

HCT-116 cells were grown in a 75 cm^2 cell culture flask to a confluency of 75% at 37°C, 5% CO_2 and were then treated with different concentrations of **2a** for 18 h. The activity of disulfide reductases was measured in cell culture lysates using the Ellmans reagent. For this purpose cells were trypsinized and centrifuged at 3000 g for 5 min. The obtained pellets were washed with PBS pH 7.4 and treated with 3.0 mL lysis buffer (Tris-HCl 10 mM, NaCl 10mM, $MgCl_2$ 10mM, pH 7.4) for 10 minutes. Homogenisation was performed with a Dounce homogenisator (20 strokes) and an aliquot of 1.0 mL of a 1.0 M sucrose solution was added to the resulting lysate. The activity of cellular disulfide reductases in an 50 µL aliquot of this solution was monitored at 405 nm according to the TrxR/GR inhibition assay described in the main text (the reaction mixture and DTNB solution were added to the aliquots, the other procedures were essentially the same as described in the

main text). The resulting values were corrected for the protein contents (measured by the Bradford method) of the respective cellular lysates. The final results were expressed as percentage of an untreated control and the IC_{50} value was calculated thereof.

12.7 Mass spectrometry studies

MS-studies on TPPG reaction with glutathione and on the decamer peptide were performed by Dr. Marilena Stefanopoulou from the research group of Prof. Dr. William S. Sheldrick, Lehrstuhl für Analytische Chemie, Ruhr-Universität Bochum, 44780 Bochum, Germany

12.7.1 MS/MS stability studies on the phosphine degradation of TPPG[145]

The reaction was performed analogously as presented above (chapter 12.5.3) excepted for that a 20 mM KH_2PO_4 pH=6.0 buffer solution was used instead of the potassium phosphate buffer pH 7.0 solution. ESI-MS and MS/MS spectra were taken directly after addition of DTNB with a Finnigan LTQ XL mass spectrometer (Thermo Electron Corp., San Jose, CA, USA), which was operated in the positive and negative ion mode with a capillary temperature of 200 ºC and a spray voltage of 1.8 kV. Delivery to the mass spectrometer was performed at a flow rate of 1.0 $\mu L \cdot min^{-1}$. The relative collision energy for collision-induced dissociation was set at 35%.

12.7.2 Binding studies with a selenopeptide[153]

The substances were dissolved in 10% acetonitrile to a concentration of 5 mM and incubated at 37°C for 48 hours with a selenium-containing decamer AGUVGAGLIK at a molar ratio of complex-to-peptide of 5:1. The peptide was previously treated at a 1:5 ratio with dithiothreitol for 1 h. ESI-MS and MS/MS spectra were recorded with a Finnigan LTQ XL mass spectrometer (Thermo Electron Corp., San Jose, CA, USA), which was operated

in the positive ion mode with a capillary temperature of 200 ºC and a spray voltage of 1.8 kV. Direct injection of samples into the mass spectrometer was performed at a flow rate of 1.0 $\mu L \cdot min^{-1}$. The relative collision energy for collision-induced dissociation was set at 35%.

MS-studies on undecamer peptide were performed by Dr. Chiara Gabbiani from the research group of Prof. Dr. Luigi Messori, Facoltá di Chimica, Universitá degli studi di Firenze, Via della Lastruccia 13, 50019 Sesto Fiorentino, Firenze, Italy

12.7.3 Interaction with a TrxR motif mimicking undecamer peptide

The selected peptide acetyl-SGGDILQSGCUG-NH_2 was treated with each of the three gold compounds **2a**, **2b** and **2c**, in a 3:1 molar ratio. Treatment was performed for 20 minutes at room temperature; then solutions were analysed by ESI-MS. ESI-MS spectra were recorded by direct injection at a 5 ml min^{-1} flow rate in a LCQ Advantage ion trap (Thermo, San Jose, California), equipped with a conventional ESI source. The specific conditions used for these experiments were as follows: the spray voltage was 4.0 kV, the capillary voltage was 1.7 V and the capillary temperature was kept at 270 °C. Sheath gas was set at 25 (arbitrary units) whereas auxiliary gas was kept at 0 (arbitrary units). All ESI spectra were elaborated using Xcalibur software (Thermo).

*Multidimensional protein identification technology experiments on complex **2b** were performed by Dr. Marilena Stefanopoulou from the research group of Prof. Dr. William S. Sheldrick, Lehrstuhl für Analytische Chemie, Ruhr-Universität Bochum, 44780 Bochum, Germany*

12.7.4 MudPIT analysis[206]

MCF-7 cells were cultured in a 175 cm^2 flask at 37°C under 5% CO_2 with 20 mL of culture medium (DMEM 4.5 g/L glucose, with L-glutamine, supplemented with 50 mg/L

gentamycine and 10% (V/V) FCS) till the 85% of confluence. Stock solution of 3.0 mM of complex **2b** in DMF was freshly prepared and diluted with culture medium supplemented with 10% (V/V) FCS or with serum free medium (final concentration of DMF: 0.1% v/v). The cell culture medium of the flasks was replaced with medium containing complex **2b** and incubated for 3 h at 37°C / 5% CO_2. The intact cell pellets were collected after trypsinisation (trypsin 0.05%) and centrifugation (3000 g, 5 min.). The cell pellet was send to the group of Prof. Sheldrick at the Ruhr-Universität Bochum for MudPIT analysis.

Multidimensional protein identification technology uses a biphasic microcapillary column packed with reversed phase (RP) and strong cation exchange (SCX) high performance liquid chromatography grade materials to load a complex protein mixture gained from the treatment of cell extracts with proteases.[206] The column is coupled with a quaternary HPLC arrangement, which in turn is connected directly to a tandem mass spectrometer. Thus the column acts as an ion source for the spectrometer. Peptides are eluted off of the biphasic microcapillary column by applying consecutive salt steps of increasing salt concentrations followed by a reverse phase gradients. This procedure is repeated till the whole peptide mixture is depleted by the SCX-phase. Depending on the composition of the peptide set, 10 to 15 salt steps can be applied. Peptides are directly ionized and the collision induced dissociation (CID) fragment ions are directed in the tandem MS where they are analyzed. A tandem MS is capable of fragmenting peptides in a predictable way which allows for the correlation of experimental tandem mass spectral data of peptides with the theoretical constructed tandem mass spectra (MS / MS) via the SEQUEST algorithm.[206] The SEQUEST algorithm is incorporated in the "BioWorks™" and "Proteome Discoverer" software. On a first step the protein sequence database of the studied biological unit or individual protein of interest is loaded on the software and theoretic MS / MS spectra are generated from the theoretic expected protein segments depending on the appropriate cleavage conditions. The experimental MS and MS / MS data are subsequently submitted. When the search starts SEQUEST chooses automatically 500 candidates extracted peptides that are in best agreement with the precursor mass of each

experimental MS / MS spectrum. A preliminary scoring analysis takes place where each one of the 500 peptides is scored according to the b- and y- type continuity (target MS / MS fragmentation) and the presence of immonium ions, as Eidhammer et al explained in their book.[264] SEQUEST is adapted for the identification of post-translational modifications or other kind of dynamic modifications (e.g. for chemical derivatisation). The initial segment selection step is changed so that the sequences with a mass equal or lower (in relation with a given threshold) than the precursor can be selected. In a case of a lower mass all different possible combinations of the considered modifications are added to it, and the resulting predicted mass is compared to the experimental precursor mass. If the masses are equal the segment is retained for comparison, using the residue masses for the potentially modified residues (experimental part extracted and reelaborated from reference 162).

12.8 Biodistribution experiments

12.8.1 Uptake into cells[153]

MCF-7 breast cancer cells were grown until at least 80% confluence in 75 cm^2 cell culture flasks. Stock solutions of 3.0 mM of the gold complexes in DMF were freshly prepared and diluted with culture medium supplemented with 10% (V/V) FCS or with serum free medium (final concentration of DMF: 0.1% v/v). The cell culture medium of the flasks was replaced with medium containing the substances and incubated for 0, 1, 2, 4, 6, and 12 h at 37°C / 5% CO_2. The intact cell pellets were collected after trypsinisation (trypsin 0.05%) and centrifugation (3000 g, 5 min.). Cell pellets were lysed with a 1000 µL Tris-HCl buffer (Tris-HCl 10 mM, NaCl 10mM, $MgCl_2$ 10 mM, pH 7.4) in a pre-chilled dounce homogenisator on ice. For cellular uptake studies an aliquot of 20 µL was removed for protein quantification by Bradford method, 100 µL of the lysate were treated with 10 µL of

triton X100 1% and investigated by AAS (see above). Results were expressed as nmol gold / mg protein as mean and error of two independent experiments.

12.8.2 Bradford assay for the determination of protein content in lysate samples

To determine the protein content of a sample the Bradford reagent was been prepared as described in literature.[233] 250 mg of ServaBlue G were dissolved in 250 mL ethanol 96%, 500 mL H_3PO_3 86% and 250 mL of bidistilled H_2O and kept at -20 °C. Freshly prepared solutions were obtained distilling the stock solution 1 : 5 with bidistilled H_2O. 200 µL were pipetted in a 96-wells plate, added with 20 µL protein solutions, the reaction allowed for 20 minutes at room temperature and the absorbance read at 595 nm in a microplate reader. Bovine serum albumin was used as standard to quantify the samples. For values out of the calibration range an opportune 1 : 10 or 1 : 20 dilutions of the sample were operated. Results were expressed as mean and error of two series of two repetitions of independent experiments.

12.8.3 Uptake into mitochondria and cytosol[153]

MCF-7 breast cancer cells were grown until at least 80% confluence 175 cm^2 cell culture flasks. Stock solutions of 3.0 mM of the gold complexes in DMF were freshly prepared and diluted with culture medium supplemented with 10% (V/V) FCS or with serum free medium (final concentration of DMF: 0.1% v/v). The cell culture medium of the flasks was replaced with medium containing the substances and incubated for 0, 1, 2, 4, 6, and 12 h at 37°C / 5% CO_2. The intact cell pellets were collected after trypsinisation (trypsin 0.05%) and centrifugation (3000 g, 5 min.). Cell pellets were lysed, the mitochondrial fraction and cytosolic fraction were isolated and collected using the Thermo Scientific mitochondria isolation kit for cultured cells (batch number 89874) according to the manufacturer instructions with minor modification. The cytosolic fraction was used as obtained from the kit isolation. The mitochondrial fraction was dissolved in 1000 µL of water. An aliquot of 20 µL was removed from the end-fractions for protein quantification by the Bradford method.

Aliquots of 100 µL were taken, treated with 10 µL of triton X100 1% and investigated by AAS. 100 µL of cytosolic fraction were directly treated with 10 µL of triton X100 1% and investigated by AAS. Results were expressed as nmol gold / mg protein as mean and error of two independent experiments.

12.9 Antiproliferative experiments

*Experiments on immortalized healthy HEK-293 cells for complex **2a** were performed by Dr. Yvonne Geldmacher from the research group of Prof. Dr. William S. Sheldrick, Lehrstuhl für Analytische Chemie, Ruhr-Universität Bochum, 44780 Bochum, Germany*

12.9.1 Antiproliferative effects in MCF-7, HT-29, HCT-116, HEP-G2 and HEK-293 cells[145,153]

The antiproliferative effects in MCF-7, HT-29, HCT-116, HEP-G2 and HEK-293 cells after 72 h (HT-29, HCT-116 and HEK-293) or 96 h (MCF-7 and HEP-G2) exposure to the gold complexes were evaluated according to a procedure already described in the literature. For the experiments the compounds were prepared freshly as stock solutions in DMF and diluted with the cell culture medium to the final assay concentrations (0.1% V/V DMF). The cells were cultured in a 75 cm^2 flask with 10 mL of cell culture medium. A volume of 100 µL of 10000 cells / mL medium (MCF-7, HEP-G2 and HEK-293) or 4500 cells / mL (HT-29 and HCT-116) were seeded in 96-well plates and incubated for 48 h (HT-29 and HCT-116) or 72 h (MCF-7, HEP-G2 and HEK-293) at 37°C under 5% CO_2. Afterwards, the medium was removed and replaced with medium containing the substances in different concentrations. The cells were exposed to the complexes for 72 h (HT-29 and HCT-116) or 96 h (MCF-7, HEP-G2 and HEK-293). The medium was removed, the cells washed with PBS and stained with 100 µL 0.02% crystal violet for 30 min. The excess of crystal violet was removed, the plates were washed with water, dried, 180 µL of 70% ethanolic

solution were added to each well, and the plates were read at 595 nm in a microplate reader (VictorX4, PerkinElmer) after 3 – 4 h of gently shaking. The IC_{50} values were calculated as the concentrations reducing proliferation of untreated control cells by 50% and are given as the means and error of two independent experiments (each performed with n=6) (see figure 12.2 for a schematic representation.

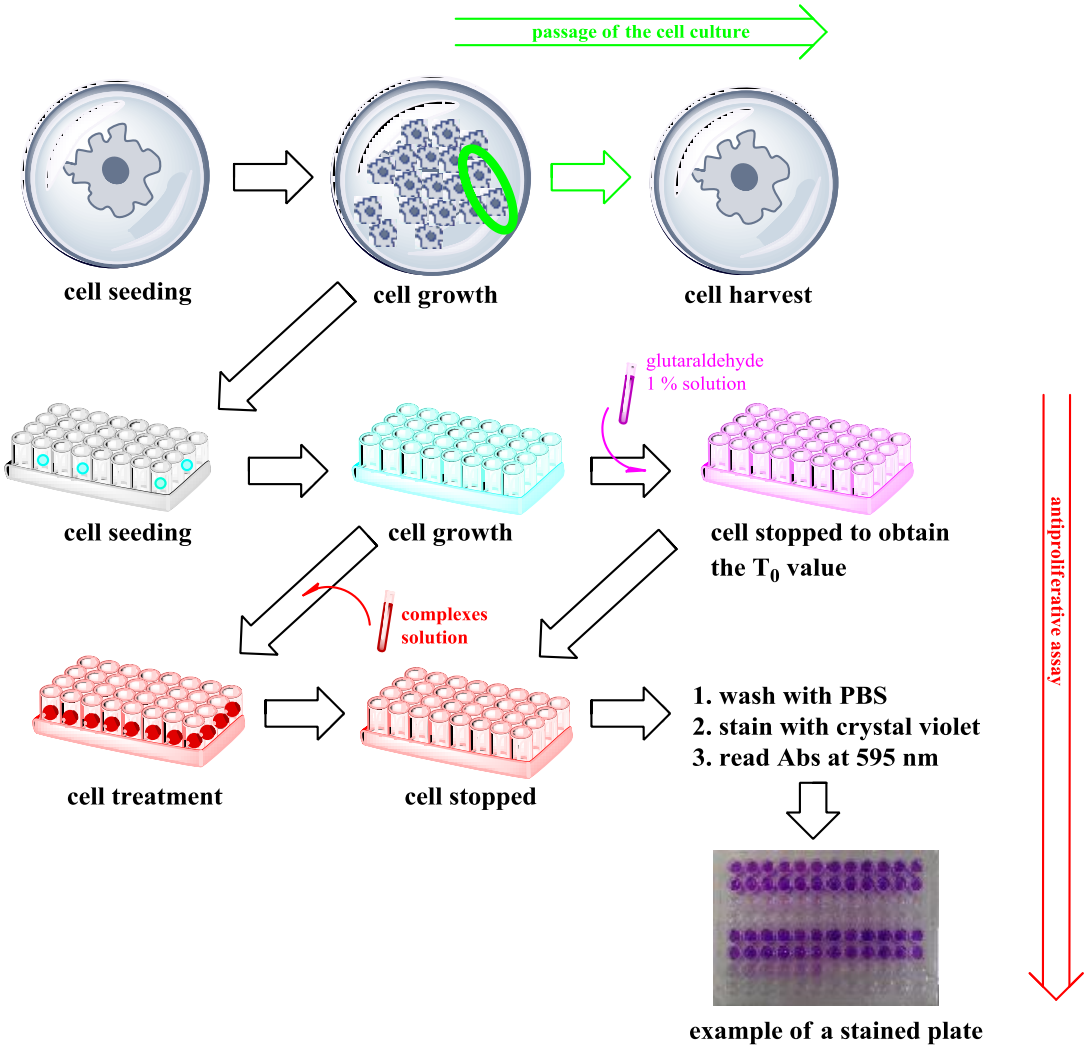

Figure 12.4: flow diagram of antiproliferative assay procedure

12.9.2 Phase contrast video microscopic imaging

MCF-7 cells were grown in phenolred free medium (DMEM 4.5 g/L glucose, with L-glutamine, supplemented with 50 mg/L gentamycine and 10% (V/V) FCS) in a 22.1 cm^2

tissue culture dish until approximately 60% confluency. The medium was replaced with 4.0 mL phenolred free medium containing 5.0 µM of **2a**, or 1.0 µM of **2b** or **2c** (0.1 % V/V DMF) or only the DMF vehicle as a control. The tissue culture dish was placed under a EVOSxl digital microscope and pictures were subsequently taken in 5 min intervals for 14 h.

*AnnexinV / PI experiments for **2a** were performed by Dr. Igor Kitanovic from the research group of Prof. Dr. Stefan Wölfl, Institut für Pharmazie und Molekulare Biotechnologie, Ruprecht-Karls-Universität Heidelberg, Im Neuenheimer Feld 364, 69120 Heidelberg*

12.9.3 Annexin V/PI Staining[145,153]

Jurkat cells were treated with the indicated concentration of the substance for 48 h, collected, and stained with Annexin V-FITC (eBioscience) according to the manufacturer recommendation. Briefly, approximately 5.0 x 10^5 cells were resuspended in 50 µL of Annexin V staining buffer (10 mM HEPES, 140 mM NaCl, and 2.5 mM $CaCl_2$, pH 7.4), 2.5 µL of AnnexinV-conjugate, and 1.25 µL of PI solution (1 mg/mL) were added and the probes were incubated in the dark at room temperature for 15 min. Signal intensity was analyzed using a FACS Calibur (Becton Dickinson) and CellQuest Pro (BD) analysis software. Excitation and emission settings were 488 nm, 515-545 nm (FL1 channel) for Annexin V-FITC and 564-606 nm (FL2 channel) for PI. Experiments were repeated with comparable results.

Experiments on resistant cell lines, DNA fragmentation and LDH were performed by Liliane A. Onambele from the research group of Prof. Dr. Aram Prokop, department of Paedriatric Oncology, Childrens Hospital Cologne, Amsterdamer Strasse 59, 50735 Cologne

12.9.4 LDH Release Assay[145]

After incubation with different concentrations of **2** and **2a** for 2 h, LDH released by BJAB cells was measured in cell culture supernatants using a cytotoxicity detection kit from Boehringer Mannheim (Mannheim, Germany). The supernatants were centrifuged at 300g for 5 min. Cell-free supernatants (20 µL) were diluted with 80 µL of PBS and 100 µL of reaction mixture were added. Then, the time-dependent formation of the reaction product was quantified photometrically at 490 nm. The maximum amount of LDH activity released by the cells was determined by lysis of the cells using 0.1% Triton X-100 in culture medium and was set as 100% cell death.

12.9.5 Measurement of DNA Fragmentation[145]

Apoptotic cell death was determined by a modified cell cycle analysis, which detects DNA fragmentation at the single cell level. For measurement of DNA fragmentation cells were seeded at a density of 1 x 10^5 cells / mL and treated with different concentrations of **2** and **2a**. After 72 h of incubation, cells were collected by centrifugation at 30 g for 5 min, washed with PBS at 4 °C, and fixed in PBS / 2 % (V/V) formaldehyde on ice for 30 min. After fixation, cells were incubated with ethanol / PBS (2:1, V/V) for 15 min, pelleted, and resuspended in PBS containing 40 µg / mL RNase A. After incubation for 30 min at 37 °C, cells were pelleted again and finally resuspended in PBS containing 50 µg / mL PI. Nuclear DNA fragmentation was then quantified by flow cytometric determination of hypodiploid DNA. Data were collected and analyzed using a FACScan (Becton Dickinson, Heidelberg, Germany) equipped with the CELLQuest software. Data are given in % hypoploidy (subG1), which reflects the number of apoptotic cells.

12.10 Effect on cell metabolism

Experiments on isolated mitochondria MMP, cytochrome c release and oxygen consumption were performed by Suzan Can from the research group of Prof. Dr. Stefan Wölfl, Institut für Pharmazie und Molekulare Biotechnologie, Ruprecht-Karls-Universität Heidelberg, Im Neuenheimer Feld 364, 69120 Heidelberg

12.10.1 Isolation of mouse liver mitochondria[145,153]

Mitochondria were isolated according to described procedures with minor modifications. Mouse (wildtype, C57BL/6) liver mitochondria were isolated by Dounce homogenization and differential centrifugation. The entire isolation process took place in isolation buffer (300 mM trehalose, 10 mM HEPES-KOH pH 7,7, 10 mM KCl, 1 mM EGTA, 1 mM EDTA, 0.1% fatty acid free BSA). The homogenate was centrifuged for 5 min at 1000 g and 4°C. The supernatant was collected and centrifuged for 2 min at 13000 rpm and 4°C. The mitochondrial pellet was resuspended in a small volume of isolation buffer and the last centrifugation step was repeated. After resuspending the final mitochondria pellet in isolation buffer the protein content was estimated by Bradford Assay.

12.10.2 Measurement of mitochondrial oxygen consumption[145,153]

The measurement was performed using OxoPlate® (PreSens, Germany), 96-well plates which contain an immobilized oxygen sensor at the bottom of each well. Fluorescence is measured in dual mode, excitation 540 nm and emission 650 nm, with reference emission 590 nm. The signal ratio 650 nm / 590 nm corresponds to the oxygen partial pressure. The calibration of the fluorescence reader is performed using a two-point calibration with oxygen-free water (1 % Na_2SO_3) and air-saturated water with an oxygen partial pressure corresponding to 0 % and 100 % respectively. 18 µg of freshly isolated mitochondria were suspended in 100 µL of respiration buffer (25 mM sucrose, 100 mM KCl, 75 mM mannitol,

5 mM $MgCl_2$, 10 mM KH_2PO_4, 0.5 mM EDTA, 10 mM TRIS, 0.1% fatty acid-free BSA, pH 7.4) containing 10 mM pyruvate, 2 mM malate, 2 mM ADP and 0.5 mM ATP to activate oxidative phosphorylation. Fluorescence was measured continuously for 400 min with kinetic intervals of 5 min by a Tecan Safire^2 (Tecan, Maennedorf, Switzerland) microplate reader at 37°C. During the measurements the plates were sealed with a breathable membrane (Diversified Biotech, Boston, MA). Additional controls were 5 µM rotenone (Sigma-Aldrich) as inhibitor of respiratory chain complex I and 1 µM CCCP (carbonyl cyanide 3-chlorophenylhydrazone, Sigma-Aldrich) as uncoupling agent, capable of increasing electron flow through the respiratory chain thereby increasing the oxygen consumption. Experiments were repeated with comparable results.

12.10.3 Mitochondrial membrane potential ($\Delta\psi_m$)[153]

Jurkat cells were cultivated in RPMI (PAA) with 10% FCS (PAA) at 37°C, 5% CO_2 and 95% humidity. 2.5 x 10^5 Jurkat cells were seeded in cell culture plates and treated with the indicated compounds for 0.5, 3, 6 and 8 hours. Cells were then stained with 500 nM JC-1 (5,5,6,6-tetrachloro-1,1,3,3-tetraethylbenzimidazolylcarbocyanineiodide, Sigma-Aldrich) for 15 min at 37°C, collected and analyzed using a FACSCalibur (Beckton Dickinson) and CellQuest Pro analysis software (Beckton Dickinson). Excitation and emission settings were 488 nm, 515-545 nm (FL1 channel) for JC monomers and 564-606 nm (FL2 channel) for JC aggregates. Experiments were repeated with comparable results.

*Experiments on ROS induction for **2a** were performed by Dr. Igor Kitanovic from the research group of Prof. Dr. Stefan Wölfl, Institut für Pharmazie und Molekulare Biotechnologie, Ruprecht-Karls-Universität Heidelberg, Im Neuenheimer Feld 364, 69120 Heidelberg*

12.10.4 ROS formation[145,153]

Jurkat cells were cultivated in standard conditions and cells were incubated with the compounds for 24h as indicated. After incubation cells were collected, centrifuged at 0.2 g (1500 rpm) and resuspended in FACS buffer (D-PBS, Gibco, + 1 % BSA, PAA). Cell suspensions were treated with DHE (dihydroethidium, SIGMA, 5 µL of 5 mM stock solution per 1.0 ml of cell suspension containing 10^6 cells) at room temperature in the dark for 15 min, washed one more time with FACS buffer and immediately analysed using a FACS®Calibur (Becton Dickinson) and CellQuest Pro (BD) analysis software. Excitation and emission settings were 488 nm and 564–606 nm (FL2 filter), respectively. Important note: although DHE is known to interact only with superoxide anion, the intensity of fluorescence is commonly considered as a reflection of total intracellular ROS. Experiments were repeated with comparable results.

*Bionas measurement for **2a** were performed by Dr. Hamed Alborzinia from the research group of Prof. Dr. Stefan Wölfl, Institut für Pharmazie und Molekulare Biotechnologie, Ruprecht-Karls-Universität Heidelberg, Im Neuenheimer Feld 364, 69120 Heidelberg*

12.10.5 Effects on cell metabolism[145,153]

Online measurement of cell metabolism and morphological changes was done using a Bionas 2500 biosensor chip system (Bionas, Rostock, Germany). The metabolic sensor chips (SC 1000) include ion-sensitive field-effect transistors to record pH changes, a Clark type electrodes to monitor oxygen consumption, and interdigitated electrode structures to measure impedance under the cell layer. Approximately 1.5 x 10^5 (150000 cell / chip) of MCF-7 cells were seeded directly onto each sensor chip in 450 µL of DMEM (PAA, E15-883) with penicillin/streptomycin and 10% (v/v) FCS (PAA) and incubated at 37°C, 5% CO_2, and 95% humidity for 24 h. The cell number used resulted in approximately 80-90% confluence of the cells on the chip surface after 24 h. This was the starting condition for online monitoring. Sensor chips with cells were then transferred to the Bionas 2500

analyzer in which medium is continuously exchanged in 8 min cycles (4 min exchange of medium and 4 min without flow), during which the parameters were measured. The running medium used during analysis was DMEM (PAN Biotech GmbH, Aidenbach, Germany) without carbonate buffer and only weakly buffered with 1 mM Hepes and reduced FCS (0.1%). For drug activity testing, the following steps were included: (1) 5 h equilibration with running medium (RM), (2) drug exposure with substances freshly dissolved in medium at indicated concentrations and indicated incubation time, (3) a drug free step in which cells are again fed with running medium without substances, and (4) at the end of each experiment, the cell layers are removed by adding 0.2% Triton X-100 to obtain basic signal without living cells on the sensor surface as a negative control.

12.10.6 Protein electrophoresis

To separate the different proteins a SDS-PAGE analysis has been established. The compounds were freshly dissolved in stock solution of 3 mM in DMF and MCF-7 cells were treated with a concentration of 3 µM for 3 h at 37°C / 5% CO_2. Cells were trypsinized, the whole pellets collected and lysed with 500 µL RIPA buffer (150 mM NaCl, 1.0% Triton X100, 0.5% Na-deoxycholate, 0.1% SDS, 50 mM TRIS at a 8.0 pH) containing 0.05% of a proetase inhibitor cocktail (batch P8340, Sigma Aldrich) in a pre-chilled dounce homogenizator (60 strokes). The solutions were centrifugated at 4°C, 13800 g for 20 minutes and the supernatants were collected. An aliquot of 20 µL of the sample was used for protein quantification by the Bradford method and the protein content in the probes normalized by dilution with distilled water. Aliquots of 10 µL of the normalized sample were added with 5 µL deionized water and 5 µL of sample loading buffer (batch number NP0007, Invitrogen). The proteins were denaturated at 95°C for 5 minutes under gentle shaking and 8.5 µL loaded on the mini-gel (8X8 mm). SDS-PAGE was performed as follows: separation gel 8% (4.0 mL 30% acryl-bisacrylamide mix, 3.8 mL 1.5 mM TRIS separation buffer pH 8.8, 150 µL 10% SDS, 150 µL 10% of ammonium persulfate (APS), 9 µL N,N,N',N'-

Tetramethylethylendiamine (TEMED) and 6.9 mL deionized H_2O), loading gel (670 µL 30% acryl-bisacrylamide mix, 500 µL 1.5 mM Tris loading buffer pH 6.8, 40 µL 10% SDS, 40 µL 10% APS, 4 µL TEMED and 2.7 mL deionized H_2O), running buffer (batch number NP0002, Invitrogen), 70 V for 2 h. For protein detection the gels were rinsed with deionized water twice and stained with a 0.25% solution of Coomassie Brilliant Blue for 1 h in a shaker. The excess of Coomassie Brilliant Blue was then washed off twice with deionized water. A first destaining solution (500 mL methanol, 100 mL ice acetic acid, 400 mL deionized water) was applied to the gel for 1 h and washed twice with deionized water. The step was repeated twice. A second destaining solution (165 mL ethanol absolute, 50 mL ice acetic acid, 785 mL deionized water) was applied to the gel for 2 h, then washed off with deionized water and applied again for 10 h. The gel was analyzed by a CCD camera (Fusion Fx7, Peqlab) in fluorescence modus with a white epi-low light and a UV-visible filter and the MW calculations were performed with the Infinity Fusion® software.

12.10.7 Western blot analysis of TrxR2 expression

To determine the TrxR2 expression a western blot assay has been established. Stock solutions of anti-TrxR2 were diluted 1 : 5 in deionized water and again 1 : 100 with the diluents provided in the kit (batch number CB7110, Invitrogen) quickly before use. To blot the membrane and block the 1° and 2° antibody a semi-dry blotter module as been used (iBlot™ module, Invitrogen). The experiment has been performed according to the manufacture guide with minor modification (iBlot® Western detection kit batch numbers IB7010 and IB7210, Invitrogen). The membrane was analyzed by chemiluminescence in a CCD camera (Fusion FX7, Peqlab) with an exposure time of 30 – 120 second. The RF distances were calculated with the Infinity Fusion® software.

Western blot experiments on Pgp expression Experiments were performed by Liliane A. Onambele from the research group of Prof. Dr. Aram Prokop, department of Paedriatric Oncology, Childrens Hospital Cologne, Amsterdamer Strasse 59, 50735 Cologne

12.10.8 Western blot analysis of Pgp expression[145]

Nalm-6 cells and its vincristin and daunorubicin resistant sublines were washed twice with PBS and lysed in buffer containing 10 mM Tris / HCl, pH 7.5, 300 mM NaCl, 1 % Triton X-100, 2 mM MgCl2, 5 µM ethylenediamino tetraacetic acid (EDTA) and one protease inhibitor cocktail tablet (Roche Diagnostics, Germany). Protein concentration was determined using the bicinchoninic acid assay from Pierce (Rockford, IL, USA) and equal amounts of protein (40 µg per lane) were separated by SDS-PAGE. Then, immunoblotting of protein onto nitrocellulose membranes (Schleicher and Schuell, Dassel, Germany) was performed. After blotting, the membrane was blocked for 1 h in PBST (PBS, 0.05 % Tween-20) containing 5 % non-fat dry milk and incubated with the Monoclonal Anti-P-Glycoprotein (Sigma-Aldrich, Saint-louis, USA) for 1 h. After the membrane had been washed three times in PBST, the Anti-Mouse IgG-HRP (Promega, Madison, USA) was applied for 1 h. Finally, the membrane was washed in PBST again and protein bands were visualized using the ECL enhanced chemiluminescence system (Amersham Buchler, Braunschweig, Germany).

ELISA microarray experiments were performed by Pavlo Holenya from the research group of Prof. Dr. Stefan Wölfl, Institut für Pharmazie und Molekulare Biotechnologie, Ruprecht-Karls-Universität Heidelberg, Im Neuenheimer Feld 364, 69120 Heidelberg

12.10.9 Microarray[251,265]

The phosphoprotein specific microarray analysis was based on the platforms ArrayTubeTM and ArrayStripTM (Alere Technologies, Jena, Germany). The Array-TubeTM system is a 1.5-mL reaction vial where a 3 mm x 3mm glass microarray with a

spotted area of 2.4 mm x 2.4mm is mounted onto the bottom. The Array- StripTM system comprises a micro-titer plate size strip of eight wells with microarrays of 4.2mm_4.2mm and a spotting area of 3.4mm x 3.6mm. The microarrays utilize a sandwich ELISA format in which tyramide signal amplification (TSA) technology amplifies colorimetric signals. The microarrays were prepared using a proprietary robotic microarray contactprinter (Alere Technologies) to deliver nanoliter volumes of specific capture antibodies onto epoxy-modified glass chips. Capture antibodies were printed without any detergents in four different concentrations (0.01 – 0.6 mg/mL) in Dulbecco's PBS (D-PBS) (Invitrogen, Carlsbad, CA, USA) containing 5 mM trehalose. Spots were deposited in three copies with different localization on chips to improve statistical readout quality. Each capture antibody was spotted with its own spotting capillary suited for both spotting and storage. After manufacturing, antibody microarrays were sealed under argon atmosphere into non-transparent bags and stored at 41°C until usage. We used commercially available optimized isotype specific capture antibodies and biotinylated phospho-specific detection antibodies developed for classical sandwich ELISAs (DuoSets IC kits, R&D Systems, Minneapolis, USA). Phosphorylated forms of seven human/mouse/rat signaling proteins in the focus of our interest, that is GSK-3β (S9), p38α (T180/Y182), ERK1 (T202/Y204) and ERK2 (T185/Y187) can be detected by our phosphoprotein-specific ArrayTube^{TM} microarrays. ArrayStrip^{TM} microarray analysis was designed to simultaneously detect these and ten additional phosphorylated proteins: ATM (S1981), MEK1/2 (S218/S222), p53 (S15), Src (Y419), mTOR (S2448). These phosphoproteins are known to be involved in different signaling pathways regulating cell survival and proliferation. Both microarray formats also contain an antibody pair against paxillin. Microarray calibration was performed with recombinant phosphoprotein standards (R&D Systems). For measurements, the following protocol was established. First, microarray surface was blocked with 200 mL of blocking buffer (1% BSA, 0.05% sodium azide in D-PBS, pH 7.2–7.4) at 231 °C for 90 min in horizontal tube shaker Thermomixer^{TM} (Eppendorf, Hamburg, Germany). All the following incubation / washing steps were carried out in the

ThermomixerTM under identical conditions. Blocking buffer was replaced with 10 mL of sample solution containing recombinant calibration standards in diluent buffer (1 mM EDTA, 0.5% Triton X-100, 5 mM sodium fluoride, 1.0 M urea in D-PBS, pH 7.2–7.4) applied directly onto the glass chip, and microarrays were incubated for 60 min. After incubation, microarrays were washed three times for 5 min with 200 mL washing buffer (0.05% Tween-20 in D-PBS, pH 7.2–7.4) and further incubated with 10 mL detection cocktail containing 18 biotin-labeled detection antibodies (R&D Systems) for 60 min. Concentration of detection antibodies was first adjusted according to manufacturer's recommendation and further diluted (1 : 20) for preparation of detection cocktail. Three additional washing steps were performed prior to detection. Bound detection antibodies were visualized in two steps: first, incubation with 100 mL streptavidin–HRP conjugate (R&D Systems) for 30 min to allow biotin–streptavidin binding, followed by three washing steps; second, addition of 100 mL of TrueBlueTM (KPL, Gaithersburg, MD, USA) containing 3,30,5,50-tetramethylbenzidine (TMB) to start the dye precipitation reaction. The resulting precipitation patterns were recorded by transmission measurements with the Arraymate^{TM} reader (Alere Technologies). The resulting pictures were analyzed automatically using PARTISAN IconoClust^{TM} software (Alere Technologies) with defined scripts for the different microarray layouts. The software identified processed spots and measured mean values of the spots (MV) as well as the local background (BG). Normalized signal intensities (NSI) were calculated by the equation NSI51–MV/BG.

13. References

[1] Papac R. J., *Origins of cancer therapy*, Yale Journal of Biology and Medicine, (**2001**), *74*, 391-398.

[2] Hajdu S. I., *A note from history: landmarks in history of cancer, part 1*, Cancer, (**2011**), *117*, 1097-1102

[3] Montazeri A., *Quality of life data as prognostic indicators of survival in cancer patients: an overview of the literature from 1982 to 2008*, Health and Quality of Life Outcomes, (**2009**), *7*, 102

[4] Jemal A., Bray F., Ferlay J., Ward E., Forman D., *Global Cancer Statistics*, CA Cancer Journal for Clinicians, (**2011**), *61*, 69-90

[5] Anand P., Kunnumakkara A. B., Sundaram C., Harikumar K. B., Tharakan S. T., Lai O. S, Sung B., Aggarwal B.B., *Cancer is a preventable disease that requires major lifestyle changes*, Pharmaceutical Research, (**2008**), *25*, 2097-2116

[6] Merlo L. M. F., Pepper J. W., Reid B. J., Maley C. C., *Cancer as an evolutionary and ecological process*, Nature Reviews on Cancer, (**2006**), *6*, 924-935

[7] Croce C. M., *Oncogenes and cancer*, The New England Journal of Medicine, (**2008**), *358*, 502-511

[8] Rao A. R., Motiwala H. G., Karim O. M, *The discovery of prostate-specific antigen*, British Journal of Urology International, (**2008**), *101*, 5-10

[9] Gulati A. P., Domchek S. M., *The clinical management of BRCA1 and BRCA2 mutation carriers*, Current Oncology Reports, (**2008**), *10*, 47-53

[10] Beckmann E. C., *CT scanning the early days*, British Journal of Radiology, (**2006**), *79*, 5-8

[11] Duffy M. J., Crown J., *A personalized approach to cancer treatment: how biomarkers can help*, Clinical Chemistry, (**2008**), *54*, 1770-1779

[12] Irby R. B., *Epidermal growth factor receptor revisited: prognostic marker or target for therapy?*, Cancer Biology and Therapy, (**2010**), *10*, 422-424

[13] Draoui N., Feron O., *Lactate shuttles at a glance: from physiological paradigms to anti-cancer treatments*, Disease Models and Mechanisms, (**2011**), *4*, 727-732

[14] Richard Nixon, National Cancer Act of 1971, source: National Cancer Institute (**1971**)

[15] Filler A. G., *The history of development and impact of computed imaging in neurological diagnosis and neurosurgery: CT, MRI and DTI*, Nature Precedings, (**2009**), doi:10.1038/npre.2009.3267.5

[16] Begley S., *This is no way to cure cancer*, Newsweek magazine of May 25, (**2007**)

[17] Begley S., *We fought Cancer … and Cancer won*, Newsweek magazine of September 5, (**2008**)

[18] L. S. Goodman L. S., Wintrobe M. W., Dameshek W., Goodman M. J., Gilman A., *Nitrogen Mustard Therapy Use of Hydrochloride, M.-bis B.-chloroethyl, Beta-chloroethyl for Hodgkin´s disease, lymphosarcoma, Leukemia and Certain Allied in Miscellaneous Disorders*, Journal of American Medicinal Association, (**1984**), *251*, 2255-2261

[19] Farber S., Diamond L.K., Mercer R.D., Sylvester R.S., Wolff J., *Temporary remission in acute leukemia in children produced by folic and antagonist 4-aminopteroyl-glutamic acid (aminopterin)*, The New England Journal of Medicine, (**1948**), *238*, 787-793

[20] Burchenal J.H., Ellison R.R., Murphy M.L., Karnofsky D.A., Sykes M.P., Tan C., Mermann A. C., Yuceoglu M., Myers W. P. L., Krakoff I., Alberstadt N., *Clinical studies on 6-mercaptopurine*, Annals New York Academy of Sciences, (**1954**), 359-368

[21] Longley D. B., Harkin D. P., Johnston P. G., *5-Fluorouracil: mechanisms of action and clinical strategies*, Nature Reviews Cancer, (**2003**), *3*, 330-338

[22] Johnson I. S., Armstrong J. G., Gorman M., Burnett J. P., *The vinca alkaloids: a new class of oncolytic agents*, Cancer Research, (**1963**), *23*, 1390-1427.

[23] Pommier Y., Leo E., Zhang H., Marchand C., *DNA topoisomerases and their poisoning by anticancer and antibacterial drugs*, Chemistry and Biology, (**2010**), *17*, 421-433

[24] Domarkas J., Dudouit F., Williams C., Qiyu Q., Banerjee R., Brahimi F., Jean-Claude, B. J., *The combi-targeting concept: synthesis of stable nitrosoureas designed to inhibit the epidermal growth factor receptor (EGFR),* Journal of Medicinal Chemistry, (**2006**), *49*, 3544-52

[25] Jordan V. C., *Tamoxifen: a most unlikely pioneering medicine*, Nature Reviews on Drug Discovery, (**2003**), *2*, 205-213

[26] Lao Romera J., Puertolas Hernández T. J., Peláez Fernández I., Sampedro Gimeno T., Fernández Martínez R., Fernández Pérez I., Iranzo González Cruz V., Illarramendi Manas J. J., Garcera J. S., Ciruelos G. E. M., *Update on adjuvant hormonal treatment of early breast cancer*, Advances in Therapy, (**2011**), *28*, 1-18

[27] Harris H., *The birth of the cell*, reviewed by Straus F. H., Perspectives in Biology and Medicine, (**2002**), *45*, 633-639

[28] Druker B. J., Lydon N. B., *Lessons learned from the development of an abl tyrosine kinase inhibitor for chronic myelogenous leukemia*, Journal of Clinical Investigation, (**2000**), *105*, 3-7

[29] Rafique S., Idrees M., Nasim A., Akbar H., Athar A., *Transition metal complexes as potential therapeutic agents*, Biotechnology and Molecular Biology Reviews, (**2010**), *5*, 38-45

[30] Hiller J,"*History of gold*", source: www.onlygold.com

[31] Lloyd N. C., Morgan H. W., Nicholson B. K., Ronimus R. S., *The composition of Ehrlich's salvarsan: resolution of a century-old debate*, Angewandte Chemie International Edition, (**2005**), *44*, 941-944

[32] J. Forestier, *Rheumatoid arthritis and its treatment with gold salts - results of six years experience*, Journal of Laboratory Clinical Medicine, (**1935**), *20*, 827-840

[33] Shaw III C.F., *Gold-Based Therapeutic Agents*, Chemical Reviews, (**1999**), *99,* 2589-2600

[34] Rosemberg B., Van Camp L., Krigas T., *Inhibition of cell division in Escherichia coli by electrolysis products from a platinum electrode*, Nature, (**1965**), *205*, 698-699

[35] Sleijfer D. T., Meijer S., Mulder, N. H., *Cisplatin: a review of clinical applications and renal toxicity*, Pharmazeutisch Weekblad, (**1985**), *7*, 237-244.

[36] Rosemberg B., Van Camp L., Trosko J.E., Mansour V.H., *Platinum Compounds: a New Class of Potent Antitumor Agents*, Nature, (**1969**), *222*, 385-386

[37] Loskotová H., Brabec V., *DNA interactions of cisplatin tethered to the DNA minor groove binder distamycin*, European Journal of Biochemistry / FEBS, (**1999**), *266*, 392-402

[38] Shanta D., Lippard S.J., *Current status and mechanism of action of platinum-based anticancer drugs*, Cap 3: Bioinorganic Medinical Chemistry, (**2011**), editor: Wiley-VCH, ISBN: 9783527326310

[39] Klein A.V., Hambley T.W., *Platinum drug distribution in cancer cells and tumors*, Chemical Reviews, (**2009**), *109*, 4911-4920

[40] Wang D., Lippard S. J., *Cellular processing of platinum anticancer drugs*, Nature Reviews Drug Discovery, (**2005**), *4*, 307-320

[41] Dos Santos N.A.G., Carvalho Rodrigues M.A., Martins, N.M., Dos Santos A.C., *Cisplatin-induced nephrotoxicity and targets of nephroprotection: an update*, Archives of Toxicology, (**2012**), *86*, 1233-1250

[42] Makrilia N., Syrigou E., Kaklamanos I., Manolopoulos L., Saif M.W., *Hypersensitivity reactions associated with platinum antineoplastic agents: a systematic review*, Metal-based Drugs, (**2010**), 1-11

[43] Bryce N. S., Zhang J. Z., Whan R. M., Yamamoto N., Hambley T. W., *Accumulation of an anthraquinone and its platinum complexes in cancer cell spheroids: the effect of charge on drug distribution in solid tumour models*, Chemical Communications, (**2009**), 2673-2675

[44] Desoize B., *Metals and metal compounds in cancer treatment*, Anticancer Research, (**2004**), *24*, 1529-1544

[45] Gautier A., Cisnetti F., *Advances in metal-carbene complexes as potent anti-cancer agents*, Metallomics, (**2012**), *4*, 23-32

[46] Bruijnincx P.C.A., Sadler P.J., *New trends for metal complexes with anticancer activity*, Current Opinion in Chemical Biology, (**2008**), *12*, 197-206

[47] Jungwirth U., Kowol C. R., Keppler B. K., Hartinger C. G., Berger W., Heffeter, P., *Anticancer activity of metal complexes: involvement of redox processes*, Antioxidants & Redox Signaling, (**2011**), *15*, 1085-1127

[48] Bergamo A, Gaiddon C., Schellens J.H.M., Beijnen J.H., Sava G., *Approaching tumour therapy beyond platinum drugs: status of the art and perspectives of ruthenium drug candidates*, Journal of Inorganic Biochemistry, (**2012**), *106*, 90-99

[49] Blanck S., Geisselbrecht Y., Kräling K., Middel S., Mietke T., Harms K., Essen L.-O., Meggers E., *Bioactive cyclometalated phthalimides: design, synthesis and kinase inhibition,* Dalton Transactions, (**2012**), 9337–9348

[50] Zanellato I., Heldt, J.-M., Vessières, A., Jaouen, G., Osella, D., *Antiproliferative effect of ferrocifen drug candidates on malignant pleural mesothelioma cell lines*, Inorganica Chimica Acta, (**2009**), *11*, 4037–4042

[51] Dubar F., Egan T.J., Pradines B., Kuter D., Ncokazi K.K., Forge D., Pierrot C., Kalamou H., Khalife J., Buisine E., Rogier C., Vezin H., Forfar I., Slomianny C., Trivelli X., Kapishnikov S., Leiserowitz L., Dive D., Biot C., *The antimalarial ferroquine: role of the metal and intramolecular*, ACS Chemical Biology, (**2011**), *6*, 275-287

[52] Korfel A, Scheulen M.E., Schmoll H.J., Gründel O., Harstrick A, Knoche M., Fels L.M., Skorzec M., Bach F., Baumgart J., Sass G., Seeber S., Thiel E., Berdel W. E., *Phase I clinical and pharmacokinetic study of titanocene dichloride in adults with advanced solid tumors*, Clinical Cancer Research, (**1998**), *4*, 2701-2708

[53] Strohfeldt K., Tacke M., *Bioorganometallic fulvene-derived titanocene anti-cancer drugs*, Chemical Society Reviews, (**2008**), *37*, 1174-1187

[54] Patra M., Gasser G., Pinto A., Merz K., Ott I., Bandow J. E., Metzler-Nolte N., *Synthesis and biological evaluation of chromium bioorganometallics based on the antibiotic platensimycin lead structure*, ChemMedChem, (**2009**), *4*, 1930-1938

[55] Panzner M. J., Hindi K.M., Wright B.D., Taylor J.B., Han D.S., Youngs W.J., Cannon C.L. (2009). *A theobromine derived silver N-heterocyclic carbene: synthesis, characterization, and antimicrobial efficacy studies on cystic fibrosis relevant pathogens*, Daltons Transactions (**2009**), 7308-7313

[56] Geldmacher, Y., Splith, K., Kitanovic, I., Alborzinia, H., Can, S., Rubbiani, R., Nazif, M. A., Ott I., Wölfl S., Neundorf I., Sheldrick W.S, *Cellular impact and selectivity of half-sandwich organorhodium(III) anticancer complexes and their organoiridium(III) and trichloridorhodium(III) counterparts*, Journal of Biological Inorganic Chemistry, (**2012**), *17*, 631-646

[57] Rubner G., Bensdorf K., Wellner A., Kircher B., Bergemann S., Ott I., Gust R., *Synthesis and biological activities of transition metal complexes based on acetylsalicylic acid as neo-anticancer agents*, Journal of Medicinal Chemistry, (**2010**), *53*, 6889-6898

[58] Orpen A.G., Connelly N.G., *Structural systematics: the role of P-A .sigma.* orbitals in metal-phosphorus .pi.-bonding in redox-related pairs of M-PA3 complexes (A = R, Ar, OR; R = alkyl)*, Organometallics, (**1990**), *9*, 1206–1210

[59] Segal E., Pecq J.-B., *Role of ligand exchange processes in the reaction kinetics of the antitumor drug cis -diamminedichloroplatinum (II) with its targets*, Cancer Research, (**1985**), *45*, 492-498

[60] Blanck S., Maksimoska J., Baumeister J., Harms K., Marmorstein R., Meggers E., *The art of filling protein pockets efficiently with octahedral metal complexes*, Angewandte Chemie International Edition, (**2012**), *51*, 5244-5246

[61] Hagen H., Marzenell P., Jentzsch E., Wenz F., Veldwijk M.R., Mokhir A., *Aminoferrocene-based prodrugs activated by reactive oxygen species*, Journal of Medicinal Chemistry, (**2012**), *55*, 924-934

[62] Bergamo A., Sava, G., *Ruthenium complexes can target determinants of tumour malignancy*, Dalton transactions, (**2007**), 1267-1272

[63] Hiller J., "*Gold in the ancient world*", source: www.goldgold.com

[64] Eisler R., *Chrysotherapy: a synoptic review*, Inflammation Research: Official Journal of the European Histamine Research Society, (**2003**), *52*, 487-501

[65] Stillman J. M., "*Story of alchemy and early chemistry*", Kessinger Publishing, (**2003**), 1st version, ISBN 0766132307, 9780766132306

[66] Hashmi A.S.K., Hutchings G.J., *Gold catalysis*, Angewandte Chemie International Edition, (**2006**), *45*, 7896-7936

[67] Haruta M., *Gold rush*, Nature, (**2005**), *437*, 1098-1099

[68] Bond G. C., Sermon P. A., Wells G. B., Buchanan D. A., Wells P. B., *Hydrogenation over supported gold catalysts*, Journal of the Chemical Society: Chemical Communications, (**1973**), 5-6

[69] Bailie J. E., Hutchings G. J., *Promotion by sulfur of gold catalysts for crotyl alcohol formation from crotonaldehyde hydrogenation*, Chemical Communication, (**1999**), 2151-2152

[70] Corma A., Serna P., *Chemoselective, Hydrogenation of nitro compounds with supported gold catalysts*, Science, (**2006**), *313*, 332-334

[71] Ito H., Yajima T., Tateiwa J., Hosomi A., *First gold complex-catalysed selective hydrosilylation of organic compounds*, Chemical Communications, (**2000**), 981-982

[72] Nowotny Otto, *Die Geschichte von der Goldmedizin von der Antike über die Zeit der Alchemie bis zur Gegenwart, In Klaus Meyer (Hg): Die Schelenzstiftung IV*, Verlagsgesellschaft GmbH Stuttgart (**1989**-**2003**), S99-113

[73] Basilius Valentinus, Basilii Valentini Tractus chymicus de quinta essentia, Erfurt: Crusius, (**1738**), Bibliotek von der Pharmazie Braunschweig

[74] Michelspacher S., *Cabala, Speculum Artis & Naturae*, (**1616**), Augusta, Bibliotek von der Pharmazie Braunschweig

[75] Nobili S., Mini E., Landini I., Gabbiani C., Casini A., Messori L., *Gold compounds as anticancer agents: chemistry, cellular pharmacology and preclinical studies*, Medicinal Research Reviews, (**2009**), *30*, 550-580

[76] Foye W.O., Lemke T.L., Williams D.A., *Foye's principles of medicinal chemistry*, Lippincott Williams & Wilkins, (**2008**), 6th version, ISBN 978-0-7817-6879-5, 989-991

[77] Mirabelli C.K., Johnson R.K., Sung C.M., Faucette L., Muirhead K., Crooke S. T., *Evaluation of the in vivo antitumor activity and in vitro cytotoxic properties of auranofin a coordinated gold compound in murine tumor models*, Cancer Research, (**1985**), *30*, 32-39.

[78] Graham G.G., Champion G. D., Ziegler J.B., The *cellular metabolism and effects of gold complexes*, Metal-based Drugs, (**1994**), *1*, 395-404

[79] Stuhlmeier K.M., *The anti-rheumatic gold salt aurothiomalate suppresses interleukin-1beta-induced hyaluronan accumulation by blocking HAS1 transcription and by acting as a COX-2 transcriptional repressor*, Journal of Biological Chemistry, (**2007**), *282*, 2250-2258

[80] Shapiro D.L., Masci J.R., *Treatment of HIV associated psoriatic arthritis with oral gold*, Journal of Rheumatology, (**1996**), *23*, 1818-1820

[81] Mphahlele M., Papathanasopoulos M., Cinellu M.A., Coyanis M., Mosebi S., Traut T., Modise R., Coates J., Hewer R., *Modification of HIV-1 reverse transcriptase and integrase activity by gold(III) complexes in direct biochemical assay*s, Bioorganic & Medicinal Chemistry, (**2012**), *20*, 401-407

[82] Sun R.W.-Y., Yu W.-Y., Sun H., Che C.-M., *In vitro inhibition of human immunodeficiency virus type-1 (HIV-1) reverse transcriptase by gold(III) porphyrins,* ChemBioChem, (**2004**), *5*, 1293-1298

[83] Navarro M., *Gold complexes as potential anti-parasitic agents*, Coordination Chemistry Reviews, (**2009**), *253*, 1619-1626

[84] Navarro M., Castro W., Biot C., *Bioorganometallic Compounds with antimalarial targets: inhibiting hemozoin formation*, Organometallics, (**2012**), *41*, 6335-6349

[85] Micale, N., Cinellu, M. A., Maiore, L., Sannella, A. R., Severini, C., Schirmeister, T., Gabbiani, C., Messori L., *Selected gold compounds cause pronounced inhibition of Falcipain 2 and effectively block P. falciparum growth in vitro*, Journal of Inorganic Biochemistry, (**2011**), *105*, 1576–1579

[86] Navarro M., Gabbiani C., Messori L., Gambino D., *Metal-based drugs for malaria, trypanosomiasis and leishmaniasis: recent achievements and perspectives*, Drug Discovery Today, (**2010**), *15*, 1070–1078

[87] Fraser J.F., Bodman J., Sturgess R., Faoagali J., Kimble R.M., *An in vitro study of the anti-microbial efficacy of a 1% silver sulphadiazine and 0.2% chlorhexidine digluconate cream, 1% silver sulphadiazine cream and a silver coated dressing*, Burns, (**2004**), *30*, 35-41

[88] Fiori A.T.M., Lustri W.R., Magalhães A., Corbi P.P., *Chemical, spectroscopic characterization and antibacterial activities in vitro of a novel gold(I)–ibuprofen complex*, Inorganic Chemistry Communications, (**2011**), *14*, 738-740

[89] Ozdemir I., Temelli N., Günal S., Demir S., *Gold(I) complexes of N-heterocyclic carbene ligands containing benzimidazole: synthesis and antimicrobial activity*, Molecules, (**2010**), *15*, 2203-2210

[90] Cui Y., Zhao Y., Tian Y., Zhang W., Lü X., Jiang X., *The molecular mechanism of action of bactericidal gold nanoparticles on Escherichia coli*, Biomaterials, (**2012**), *33*, 2327-2333

[91] Cox A.G., Brown K.K., Arner E.S.J., Hampton M.B., *The thioredoxin reductase inhibitor auranofin triggers apoptosis through a Bax/Bak-dependent process that involves peroxiredoxin 3 oxidation*, Biochemical Pharmacology, (**2008**), *76*, 1097-1109

[92] Becker K., Gromer S., Schirmer R.H., Müller S., *Thioredoxin reductase as a pathophysiological factor and drug target*, European Journal of Biochemistry / FEBS, (**2000**), *267*, 6118-6125

[93] Sandalova T., Zhong L., Lindqvist Y., Holmgren A., Schneider G., *Three-dimensional structure of a mammalian thioredoxin reductase: implications for mechanism and evolution of a selenocysteine-dependent enzyme*, Proceedings of the National Academy of Sciences U.S.A., (**2001**), *98*, 9533-9538

[94] Bindoli A., Rigobello M. P., Scutari G., Gabbiani C., Casini A., Messori L., *Thioredoxin reductase: a target for gold compounds acting as potential anticancer drugs*, Coordination Chemistry Reviews, (**2009**), *253*, 1692-1707

[95] Casini A., Gabbiani C., Sorrentino F., Rigobello M. P., Bindoli A., Geldbach T. J., Marrone A., Re N., Hartinger C. G., Dyson P. J., Messori L., *Emerging protein targets for anticancer metallodrugs: inhibition of thioredoxin reductase and cathepsin B by antitumor ruthenium(II)-arene compounds*, Journal of Medicinal Chemistry, (**2008**), *51*, 6773–6781

[96] Casini A., Messori L., *Molecular mechanisms and proposed targets for selected anticancer gold compounds*, Current Topics in Medicinal Chemistry, (**2011**), *11*, 2647-2660

[97] Gabbiani C., Mastrobuoni G., Sorrentino F., Dani B., Rigobello M.P., Bindoli A., Cinellu, M.A., Pieraccini G., Messori L., Casini A., *Thioredoxin reductase, an emerging target for anticancer metallodrugs. Enzyme inhibition by cytotoxic gold(III) compounds studied with combined mass spectrometry and biochemical assays*, MedChemComm, (**2011**), *2*, 50-54

[98] Pratesi A., Gabbiani C., Ginanneschi M., Messori L., *Reactions of medicinally relevant gold compounds with the C-terminal motif of thioredoxin reductase elucidated by MS analysis*, Chemical Communications, (**2010**), 7001–7003

[99] Casini A., Guerri A., Gabbiani C., Messori L., *Biophysical characterisation of adducts formed between anticancer metallodrugs and selected proteins: new insights from X-ray diffraction and mass spectrometry studies*, Journal of Inorganic Biochemistry, (**2008**), *102*, 995–1006

[100] Ott, I., *On the medicinal chemistry of gold complexes as anticancer drugs*, Coordination Chemistry Reviews, (**2009**), *253*, 1670-1681

[101] Santini C., Pellei M., Papini G., Morresi B., Galassi R., Ricci S., Tisato F., Porchia M., Rigobello M.P., Gandin V., Marzano C., *In vitro antitumour activity of water soluble Cu(I), Ag(I) and Au(I) complexes supported by hydrophilic alkyl phosphine ligands*, Journal of Inorganic Biochemistry, (**2011**), *105*, 232-40

[102] Gandin V., Fernandes A.P., Rigobello M.P., Dani B., Sorrentino F., Tisato F., Björnstedt M., Bindoli A., Sturaro A., Rella R., Marzano C., *Cancer cell death induced by phosphine gold(I) compounds targeting thioredoxin reductase*, Biochemical Pharmacology, (**2010**), *79*, 90-101

[103] Rackham O., Nichols S.J., Leedman P.J., Berners-Price S.J., Filipovska A., *A gold(I) phosphine complex selectively induces apoptosis in breast cancer cells: implications for anticancer therapeutics targeted to mitochondria*, Biochemical Pharmacology, (**2007**), *74*, 992-1002

[104] Craig S., Gao L., Lee I., Gray T., Berdis A.J., *Gold-containing indoles as anticancer agents that potentiate the cytotoxic effects of ionizing radiation*, Journal of Medicinal Chemistry, (**2012**), 55, 2437-2451

[105] Meyer A., Bagowski C.P., Kokoschka M., Stefanopoulou M., Alborzinia H., Can S., Vlecken D.H., Wölfl S., Sheldrick W.S., Ott I., *On the biological properties of alkynyl phosphine gold(I) complexes*, Angewandte Chemie International Edition, (**2012**), *51*, 8895-8899

[106] Ott I., Qian X., Xu Y., Vlecken D.H.W., Marques I.J., Kubutat D., Will J., Sheldrick W.S., Patrick J., Prokop A., Bagowski C.P., *A gold(I) phosphine complex containing a naphthalimide ligand functions as a TrxR inhibiting antiproliferative agent and angiogenesis inhibitor*, Journal of Medicinal Chemistry, (**2009**), *52*, 763–770

[107] Deponte M., Urig S., Arscott L. D., Fritz-Wolf K., Réau R., Herold-Mende C., Koncarevic S., Meyer M., Davioud-Charvet E., Ballou D.P., William C.H., Becker K., *Mechanistic studies on a novel, highly potent gold-phosphole inhibitor of human glutathione reductase*, Journal of Biological Chemistry, (**2005**), *280*, 20628-20637

[108] Ray L., Katiyar V., Barman S., Raihan M.J., Nanavati H., Shaikh M.M., Ghosh P., *Gold(I) N-heterocyclic carbene based initiators for bulk ring-opening polymerization of l-lactide*, Journal of Organometallic Chemistry, (**2007**), *692*, 4259-4269

[109] Lemke J., Pinto A., Niehoff P., Vasylyeva V., Metzler-Nolte N., *Synthesis, structural characterisation and anti-proliferative activity of NHC gold amino acid and peptide conjugates*, Dalton Transactions, (**2009**), 7063-7070

[110] Baker M.V., Barnard P.J., Berners-Price S.J., Brayshaw S.K., Hickey J.L., Skelton B.W., White A.H., *Cationic, linear Au(I) N-heterocyclic carbene complexes: synthesis, structure and anti-mitochondrial activity*, Dalton Transactions, (**2006**), 3708-3715

[111] Ray S., Mohan R., Singh J.K., Samantaray M.K., Shaikh M.M., Panda D., Ghosh P., *Anticancer and antimicrobial metallopharmaceutical agents based on palladium, gold, and silver N-heterocyclic carbene complexes*, Journal of the American Chemical Society, (**2007**), *129*, 15042-53

[112] Hickey J.L., Ruhayel R.A., Barnard P.J., Baker M.V., Berners-Price S.J., Filipovska A., *Mitochondria-targeted chemotherapeutics: the rational design of gold(I) N-heterocyclic carbene complexes that are selectively toxic to cancer cells and target protein selenols in preference to thiols*, Journal of the American Chemical Society, (**2008**), *130*, 12570-12571

[113] Casini A., Hartinger C., Gabbiani C., Mini E., Dyson P.J., Keppler B.K., Messori L., *Gold(III) compounds as anticancer agents: relevance of gold-protein interactions for their mechanism of action*, Journal of Inorganic Biochemistry, (**2008**), *102*, 564–575

[114] Gabbiani C., Casini A., Messori L., *Gold(III) compounds as anticancer drugs*, Gold Bulletin, (**2007**), *40*, 73-81

[115] Che C.-M., Sun R.W.-Y., Yu W.-Y., Ko C.-B., Zhu N., Sun H., *Gold(III) porphyrins as a new class of anticancer drugs: cytotoxicity, DNA binding and induction of apoptosis in human cervix epitheloid cancer cells*, Chemical Communications, (**2003**), 1718-1719

[116] Tiekink E.R.T., *Anti-cancer potential of gold complexes,* Inflammopharmacology, (**2008**), *16*, 138-142

[117] Casini A., Cinellu M. A., Minghetti G., Gabbiani C., Coronnello M., Mini E., Messori L., *Structural and solution chemistry, antiproliferative effects, and DNA and protein binding properties of a series of dinuclear gold(III) compounds with bipyridyl ligands*, Journal of Medicinal Chemistry, (**2006**), *49*, 5524–5531

[118] Coronnello M., Mini E., Caciagli B., Cinellu M.A., Bindoli A., Gabbiani C., Messori L., *Mechanisms of cytotoxicity of selected organogold(III) compounds*, Journal of Medicinal Chemistry, (**2005**), *48*, 6761–6765

[119] Saggioro D., Rigobello M.P., Paloschi L., Folda A., Moggach S.A., Parsons S., Ronconi L., Fregona D., Bindoli A., *Gold(III)-dithiocarbamato complexes induce cancer cell death triggered by thioredoxin redox system inhibition and activation of ERK pathway*, Chemistry and Biology, (**2007**), *14*, 1128-1139

[120] Mendes F., Groessl M., Nazarov A., Tsybin Y.O., Sava G., Santos I., Dyson P.J., Casini A., *Metal-based inhibition of poly(ADP-ribose) polymerase the guardian angel of DNA*, Journal of Medicinal Chemistry, (**2011**), *54*, 2196-2206

[121] Martins A.P., Marrone A., Ciancetta A., Galán Cobo A., Echevarría M., Moura T.F., Re, N., Casini A., Soveral G., *Targeting aquaporin function: potent inhibition of aquaglyceroporin-3 by a gold-based compound*, PloS one, (**2012**), *7*, e37345

[122] Gabbiani C., Casini A., Messori L., Guerri A., Cinellu M. A., Minghetti G., Corsini M., Rosani C., Zanello P., Arca M., *Structural characterization, solution studies, and DFT calculations on a series of binuclear gold(III) oxo complexes: relationships to biological properties*, Inorganic Chemistry, (**2008**), *47*, 2368–2379

[123] De Luca A., Hartinger C.G., Dyson P.J., Lo Bello M., Casini A., *A new target for gold(I) compounds: glutathione-S-transferase inhibition by auranofin*, Journal of Inorganic Biochemistry, (**2012**), *119*, 38-42

[124] van Jaarsveld C.H., Jahangier Z.N., Jacobs J.W., Blaauw A., van Albada-Kuipers G.A., ter Borg E.J., Brus, H.L., Schenk Y., van Der Veen M.J., Bijlsma J.W., *Toxicity of anti-rheumatic drugs in a randomized clinical trial of early rheumatoid arthritis*, Rheumatology, (**2000**), *39*, 1374–1382

[125] Alessio E., *Bioinorganic Medicinal Chemistry*, WILEY-VCH Verlag GmbH & Co. KGaA, (**2011**) ISBN: 9783527326310, DOI: 10.1002/9783527633104

[126] Berners-Price S.J., Filipovska A., *Gold compounds as therapeutic agents for human diseases*, Metallomics, (**2011**), *3*, 863-873

[127] Iqbal M.S., Taqi S.G., Arif M., Wasim M., Sher M., *In vitro distribution of gold in serum proteins after incubation of sodium aurothiomalate and auranofin with human blood and its pharmacological significance*, Biological Trace Element Research, (**2009**), *130*, 204-209

[128] Shaw F., Isab A., lqb A., Hoeschele J.D., Staricl M., Locke L., Schulteis P., Xiao J., *Oxidation of the phosphine from the auranofin analog, triisopropylphosphine(2,3,4,6-tetra-O-acetyl-1-thio-.beta.-D-glucopyranosato-S)gold(I), via a protein-bound phosphonium intermediate*, Journal of American Chemical Society, (**1994**), *116*, 2254-2260

[129] Zhang X., Frezza M., Milacic V., Ronconi L., Fan Y., Bi C., Fregona D., Dou Q.P., *Inhibition of tumor proteasome activity by gold-dithiocarbamato complexes via both redox-dependent and -independent processes*, Journal of Cellular Biochemistry, (**2010**), *109*, 162-172

[130] Marzano C., Ronconi L., Chiara F., Giron M.C., Faustinelli I., Cristofori P., Trevisan A., Fregona D., *Gold(III)-dithiocarbamato anticancer agents: activity, toxicology and histopathological studies in rodents*, International Journal of Cancer, (**2011**), *129*, 487-496

[131] Tonissen K.F., Di Trapani G., *Thioredoxin system inhibitors as mediators of apoptosis for cancer therapy*, Molecular Nutrition & Food Research, (**2009**), *53*, 87-103

[132] Marzano C., Gandin V., Folda A., Scutari G., Bindoli A., Rigobello M.P., *Inhibition of thioredoxin reductase by auranofin induces apoptosis in cisplatin-resistant human ovarian cancer cell*s, Free Radical Biology & Medicine, (**2007**), *42*, 872-881

[133] de Frémont P., Marion N., Nolan S.P., *Carbenes: Synthesis, properties, and organometallic chemistry*, Coordination Chemistry Reviews, (**2009**), *253*, 862–892

[134] Hay C., Hissler M., Fischmeister C., Rault-Berthelot J., Toupet L., Nyulászi L., Réau R., *Phosphole-containing pi-conjugated systems: from model molecules to polymer films on electrodes*, Chemistry: a European Journal, (**2001**), *7*, 4222-4236

[135] Tolman C. A., *Steric effects of phosphorus ligands in organometallic chemistry and homogeneous catalysis*, Chemical Reviews, (**1977**), 77, 313-348

[136] Stanley P.G.G., Hall, C., *Organometallic Chemistry, lecture notes*, (**2006**), taken from : http://chem-faculty.lsu.edu/stanley/webpub/4571-full-notes-Fall-2008.pdf

[137] Bourissou D., Guerret O., Gabbaı P., Bertrand G., *Stable Carbenes*, Chemical Reviews, (**2000**), *100*, 39-91

[138] Schuster O., Yang L., Raubenheimer H.G., Albrecht M., *Beyond conventional N-heterocyclic carbenes: abnormal, remote, and other classes of NHC ligands with reduced heteroatom stabilization*, Chemical Reviews, (**2009**), *109*, 3445-3478

[139] Metzler-Nolte N., *Ab initio study of Arduengo-type group 13 carbene analogues*, New Journal of Chemistry, (**1998**), *22*, 793-795

[140] Fischer E.O., Maasböl A., *On the existence of a tungsten carbonyl carbene complex*, Angewandte Chemie International Edition, (**1964**), 3, 580–581

[141] Arduengo A.J., Harlow R.L., Kline M., *A stable crystalline carbene*, Journal of American Chemical Society, (**1991**), *113*, 361–363

[142] Raubenheimer H. G., Cronje S., *Carbene complexes of gold: preparation, medical application and bonding*, Chemical Society Reviews, (**2008**), *37*, 1998-2011

[143] Teyssot M.L., Jarrousse A.S., Manin M., Chevry A., Roche S., Norre F., Beaudoin C., Morel L., Boyer D., Mahiou R., Gautier A., *Metal-NHC complexes: a survey of anti-cancer properties*, Dalton Transactions, (**2009**), 6894–6902

[144] Bhatnagar A., Sharma P.K., Kumar N., *A review on "Imidazole": their chemistry and pharmacological potentials*, International Journal of PharmTech Research, (**2011**), *3*, 268-282

[145] Rubbiani R., Kitanovic I., Alborzinia H., Can S., Kitanovic A., Onambele L.A, Stefanopoulou M., Geldmacher Y., Wolber G., Prokop A., Sheldrick W.S., Wölfl S., Ott I., *Benzimidazol-2-ylidene gold(I) complexes are thioredoxin reductase inhibitors with multiple antitumor properties*, Journal of Medicinal Chemistry, (**2010**), *53*, 8608–8618

[146] Fremont P.D., Stevens E.D., Fructos M.R., Diaz-Requejo M.M., Perez P.J. Nolan S.P., *Synthesis, isolation and characterization of cationic gold(I) N-heterocyclic carbene (NHC) complexes*, Chemical Communications, (**2006**), 2045-2047

[147] Wang H.M.J., Chen C.Y.L., Lin I.J.B., *Synthesis, Structure, and Spectroscopic Properties of Gold(I)−Carbene Complexes*, Organometallics, (**1999**), *18*, 1216-1223

[148] Ricard L., Gagosz F., *Synthesis and Reactivity of Air-Stable N-Heterocyclic Carbene Gold (I)Bis(trifluoromethanesulfonyl) imidate Complexes*, Organometallics, (**2007**), *26*, 4704–4707.

[149] Modica-Napolitano J.S., Aprille J.R., *Delocalized lipophilic cations selectively target the mitochondria of carcinoma cells*, Advanced Drug Delivery Reviews, (**2001**), *49*, 63-70

[150] Sundelacruz S., Levin M., Kaplan D.L., *Role of membrane potential in the regulation of cell proliferation and differentiation*, Stem Cell Reviews, (**2009**), *5*, 231-46

[151] McKeage M.J., Berners-Price S.J., Galettis P., Bowen R.J., Brouwer W., Ding L., Zhuang L., Baguley B.C., *Role of lipophilicity in determining cellular uptake and antitumour activity of gold phosphine complexes*, Cancer Chemotherapy and Pharmacology, (**2000**), *46*, 343-350

[152] Baker M.V., Barnard P.J., Berners-Price S.J., Brayshaw S.K., Hickey J.L., Skelton B.W., White A.H., *Synthesis and structural characterisation of linear Au(I) N-heterocyclic carbene complexes: new analogues of the Au(I) phosphine drug Auranofin*, Journal of Organometallic Chemistry, (**2005**), *690*, 5625-5635

[153] Rubbiani R., Can S., Kitanovic I., Alborzinia H., Stefanopoulou M., Kokoschka M., Mönchgesang S., Sheldrick W.S., Wölfl S., Ott I., *Comparative in vitro evaluation of N-heterocyclic carbene gold(I) complexes of the benzimidazolylidene type*, Journal of Medicinal Chemistry, (**2011**), *54*, 8646–8657

[154] Tommasi I., Sorrentino F., *1,3-Dialkylimidazolium-2-carboxylates as versatile N-heterocyclic carbene–CO_2 adducts employed in the synthesis of carboxylates and α-alkylidene cyclic carbonates*, Tetrahedron Letters, (**2009**), *50*, 104-107

[155] Urig S., Fritz-Wolf K., Réau R., Herold-Mende C., Tóth K., Davioud-Charvet E., Becker K., *Undressing of phosphine gold(I) complexes as irreversible inhibitors of human disulfide reductases*, Angewandte Chemie International Edition, (**2006**), *45*, 1881-1886

[156] Gasser G., Ott I., Metzler-Nolte N., *Organometallic anticancer compounds*, Journal of Medicinal Chemistry, (**2011**), *54*, 3-25

[157] Jones T., Williams C. H., *The sequence of amino acid residues around reduction active disulfide in yeast glutathione*, Journal of Biological Chemistry, (**1975**), *10*, 3779-3784

[158] Debreczeni J.E., Johansson C., Kavanagh K., Savitsky P., Sundstrom M., Arrowsmith C., Weigelt J., Edwards A., Von Delft F., Oppermann U., *Crystall structure of thioredoxin reductase 1*, RCSB-PDB: 2CFY, DOI:10.2210/pdb2cfy/pdb

[159] Frisch M.J., Trucks G.W., Schlegel H.B., Scuseria G.E., Robb M.A.,Cheeseman J.R., Scalmani G., Barone V., Mennucci B., Petersson G.A., Nakatsuji H., Caricato M., Li X., Hratchian H.P., Izmaylov A.F., Bloino J., Zheng G., Sonnenberg J.L., Hada M., Ehara M., Toyota K., Fukuda R., Hasegawa J., Ishida M., Nakajima T., Honda Y., Kitao O., Nakai H., Vreven T., Montgomery J. A., Peralta J.E., Ogliaro F., Bearpark M., Heyd J. J., Brothers E., Kudin K. N., Staroverov V. N., Kobayashi R., Normand J.,Raghavachari K., Rendell A., Burant J.C., Iyengar S.S., Tomasi J., Cossi M., Rega N., Millam N.J., Klene M., Knox J.E., Cross J.B., Bakken V., Adamo C., Jaramillo J., Gomperts R., Stratmann R.E., Yazyev O., Austin A.J., Cammi R., Pomelli C., Ochterski J.W., Martin R.L., Morokuma K., Zakrzewski V.G., Voth G.A., Salvador P., Dannenberg J.J., Dapprich S., Daniels A.D., Farkas Ö., Foresman J.B., Ortiz J.V., Cioslowski J., Fox D. J., *Gaussian 03, Revision E.1*, (**2009**), Gaussian, Inc., Wallingford CT, source: www.gaussian.com

[160] Miertus S., Tomasi J., *Approximate evaluations of the electrostatic free-energy and internal energy changes in solution processes*, Chemical Physics, (**1982**), *65*, 239-245.

[161] Tomasi J., Mennucci B., Cammi R., *Quantum mechanical continuum salvation models*, Chemical Reviews, (**2005**), *105*, 2999-3093

[162] Hrusak J., Hertwig R., Schroeder D., Schwerdtfeger P., Koch W., Schwarz H., *Relativistic effects in cationic gold(I) complexes: a comparative study of ab initio pseudopotential and density functional methods*, Organometallics, (**1995**), *14*, 1284-1291

[163] Coffer T. Shaw C.F., Eidsness M.K., Watkins J.W., Elder R.C., *Reactions of Auranofin and Et_3PAuCl with bovine serum albumin*, Inorganic Chemistry, (**1986**), *25*, 333-339

[164] Ortega A.L., Mena S., Estrela J.M., *Glutathione in cancer cell death*, Cancers, (**2011**), *3*, 1285-1310

[165] Mohn C., Kalayda G.V., Häcker H.G., Gütschow M., Metzger S., Jaehde U., *Contribution of glutathione and MRP-mediated efflux to intracellular oxaliplatin accumulation*, International Journal of Clinical Pharmacology and Therapeutics, (**2010**), *48*, 445-447

[166] Leier I., Jedlitschky G., Buchholz U., Cole S.P.C., Deeley R.G., Keppler D., *ATP-dependent glutathione disulfide transport mediated by the MRP gene-encoded conjugate export pump,* Biochemical Journal, (**1996**), *314*, 433-437

[167] Hill K.E., McCollum G.W., Burk R.F., *Determination of thioredoxin reductase*, Analytical Biochemistry, (**1997**), *253*, 123-125

[168] Liu W., Bensdorf K., Proetto M., Abram U., Hagenbach A., Gust R., *NHC gold halidecomplexes derived from 4,5-diarylimidazoles: synthesis, structural analysis and pharmacological investigations as potential antitumor agents*, Journal of Medicinal Chemistry, (**2011**), *54*, 8605-8615

[169] Coffer M.T., Shaw C.F., Hormann A.L., Mirabelli C.K., Crooke, S.T., *Thiol competition for Et_3PAuS-albumin: a nonenzymatic mechanism for Et_3PO formation*, Journal of Inorganic Biochemistry, (**1987**), *30*, 177–187

[170] Rivory L.P., Pond S.M., Winzort D.J., *The influence of pH on the interaction of lipophilic anthracyclines with bovine serum albumin. Quantitative characterization by measurement of fluorescence quenching*, Biochemical Pharmacology, (**1992**), *44*, 2347-2355

[171] Artali R., Bombieri G., Calabi L., Del Pra A., *A molecular dynamics study of human serum albumin binding sites*, Farmaco, (**2005**), *60*, 485-495

[172] Kratz F., Warnecke A., Scheuermann K., Stockmar C., Schwab J., Lazar P., Drückes P., Esser N., Drevs J., Rognan D., Bissantz C., Hinderling C., Folkers G., Fichtner I., Unger C., *Probing the cysteine-34 position of endogenous serum albumin with thiol-binding doxorubicin derivatives. Improved efficacy of an acid-sensitive doxorubicin derivative with specific albumin-binding properties compared to that of the parent compound,* Journal of Medicinal Chemistry, (**2002**), *45*, 5523-5533

[173] Hein K.L., Kragh-Hansen U., Morth J.P., Jeppesen, M.D., Otzen D., Møller J.V., Nissen P., *Crystallographic analysis reveals a unique lidocaine binding site on human serum albumin*, Journal of Structural Biology, (**2010**), *171*, 353–360

[174] Lemma K., Berglund J., Farrell N., Elding, L.I., *Kinetics and mechanism for reduction of anticancer-active tetrachloroam(m)ine platinum(IV) compounds by glutathione*, Journal of Biological Inorganic Chemistry, (**2000**), *5*, 300-306

[175] Ishikawas T., Ali-Osman F., *Glutathione-associated cis-diamminedichloroplatinum (I1) metabolism and ATP-dependent efflux from leukemia cells*, Journal of Biological Chemistry, (**1993**), *268*, 20116-20125.

[176] Alberts B., D. Bray, Lewis J., Daff M., Roberts K., Watson J.D., *Biologia Moleculare della Cellula*, editor: Zanichelli, (**2005**), 5th version, ISBN 978-8808-20185-0

[177] Smith W.H., *A History of Science: in Five Volumes*. *Volume IV:* Modern Development of the Chemical and Biological Sciences*, (***1863-1943***),* from *http://etext.lib.virginia.edu/toc/modeng/public/Wil4Sci.html*

[178] Nelson D.L., Cox M.M., *I Principi di Biochimica di Lehninger*, editor: Zanichelli, (**2002**), 3rd version, ISBN978-0-7167-4339-2

[179]. Cheng Y.-C., Prusoff W.H., *Relationship between theinhibition costant (K_i) and the concentration ofinhibitor which causes 50 per cent inhibition (I_{50}) of an enzymatic reaction*, Biochemical Pharmacology, (**1973**), *22*, 3099-3108.

[180] Becker K., Gromer S., Schirmer R.H., Müller S., *Thioredoxin reductase as a pathophysiological factor and drug target*, European Journal of Biochemistry / FEBS, (**2000**), *267*, 6118-6125

[181] Kaelin W. G., Thompson C. B., *Q & A Clues from cell metabolism*, Nature, (**2010**), *465*, 3-5.

[182] Schumacker P.T., *Reactive oxygen species in cancer cells: live by the sword, die by the sword*, Cancer Cell, (**2006**), *10*, 175-176

[183] Arnér E.S.J., Holmgren A., *The thioredoxin system in cancer*, Seminars in Cancer Biology, (**2006**), *16*, 420–426

[184] Tonissen K.F., Di Trapani G., *Thioredoxin system inhibitors as mediators of apoptosis for cancer therapy*, Molecular Nutrition & Food Research, (**2009**), *53*, 87-103

[185] Holmgren A., Lu J., *Thioredoxin and thioredoxin reductase: current research with special reference to human disease*, Biochemical and Biophysical Research Communications, (**2010**), *396*, 120-124

[186] Pennington J.D., Jacobs K.M., Sun L., Bar-Sela G., Mishra M., Gius D., *Thioredoxin and thioredoxin reductase as redox sensitive molecular targets for cancer therapy*, Current Pharmaceutical Design, (**2007**), *1*3, 3368–3377

[187] Xu J., Li T., Wu H., Xu T., *Role of thioredoxin in lung disease*, Pulmonary Pharmacology & Therapeutics, (**2012**), *25*, 154-162

[188] Sandalova T., Zhong L., Lindqvist Y., Holmgren A., Schneider G., *Three-dimensional structure of a mammalian thioredoxin reductase: implications for mechanism and evolution of a selenocysteine-dependent enzyme*, Proceedings of the National Academy of Sciences U.S.A., (**2001**), *98*, 9533–9538

[189] Matsuzaka Y., Okamoto K., Mabuchi T., Iizuka M., Ozawa A., Oka A., Tamiya G., Kulski J.K., Inoko H., *Identification and characterization of novel variants of the thioredoxin reductase 3 new transcript 1 TXNRD3NT1*, Mammalian Genome, (**2005**), *16*, 41–49

[190] Anestål, K., Prast-Nielsen S., Cenas N., Arnér E.S., *Cell death by SecTRAPs: thioredoxin reductase as a prooxidant killer of cells*, PloS one, (**2008**), *3*, e1846

[191] Rigobello M. P., Scutari G., Folda A., Bindoli A., *Mitochondrial thioredoxin reductase inhibition by gold(I) compounds and concurrent stimulation of permeability transition and release of cytochrome c*, Biochemical Pharmacology, (**2004**), *67*, 689-696

[192] Welsh S.J., Williams R.R., Birmingham Newman D.J., Kirkpatrick D.L., Powis G., *The thioredoxin redox inhibitors 1-methylpropyl 2-imidazolyl disulfide and pleurotin inhibit hypoxia-induced factor 1 α and vascular endothelial growth factor formation 1*, Molecular Cancer Therapeutics, (**2003**), *2*, 235-243

[193] Little C., Olinescu R., Reid K. G., O'Brien P.J., *Properties and regulation of glutathione peroxidase*, Journal of Biological Chemistry, (**1970**), *245*, 3632-3636

[194] Arnér E.S., Zhong L., Holmgren A., *Preparation and assay of mammalian thioredoxin and thioredoxin reductase*, Methods in Enzymology, (**1999**), *300*, 226-239

[195] Karlenius T.C., Tonissen K.F., *Thioredoxin and cancer: a role for thioredoxin in all states of tumor oxygenation*, Cancers, (**2010**), *2*, 209–232

[196] Comuzzi B., Sadar M. D., *Proteomics analysis to identify novel therapeutic targets for the treatment of advanced prostate cancer*, Cellscience, (**2007**), *3*, 1-15

[197] Guidi F., Puglia M., Gabbiani C., Landini I., Gamberi T., Fregona D., Cinellu M.A., Nobili S., Mini E., Bini L., Modesti P.A., Messori L., *2D-DIGE analysis of ovarian cancer cell responses to cytotoxic gold compounds*, Molecular BioSystems, (**2012**), *8*, 985–993

[198] Fekete S., Veuthey J.-L., Guillarme D., *New trends in reversed-phase liquid chromatographic separations of therapeutic peptides and proteins: theory and applications*, Journal of Pharmaceutical and Biomedical Analysis, (**2012**), *69*, 9–27

[199] Messori L., Cubo L., Gabbiani C., Álvarez-Valdés A., Michelucci E., Pieraccini G., Ríos-Luci C., Leon L.G., Padron J.M., Navarro-Ranninger C., Casini A., Quiroga A.G., *Reactivity and biological properties of a series of cytotoxic PtI_2(amine)2 complexes, either cis or trans configured*, Inorganic Chemistry, (**2012**), *51*, 1717–1726

[200] Andersson C.O., *Mass spectrometry study on amino acid and peptide derivatives*, Acta Chemica Scandinavica, (**1958**), *12*, 1353

[201] Mechref Y., Hu Y., Garcia A., Hussein A., *Identifying cancer biomarkers by mass spectrometry-based glycomics*, Electrophoresis, (**2012**), *33*, 1755–1767

[202] Morelle W., Canis K., Chirat F., Faid V., Michalski J.-C., *The use of mass spectrometry for the proteomic analysis of glycosylation*, Proteomics, (**2006**), *6*, 3993–4015

[203] Nakazawa T., Yamaguchi M., Okamura T.-A., Ando E., Nishimura O., Tsunasawa S., *Terminal proteomics: N- and C-terminal analyses for high-fidelity identification of proteins using MS*, Proteomics, (**2008**), *8*, 673–685

[204] Garrigue-Antar L., Hartigan N., Kadler, K.E., *Post-translational modification of bone morphogenetic protein-1 is required for secretion and stability of the protein,* Journal of Biological Chemistry, (**2002**), *277*, 43327–43334

[205] Xu Y.-M., Huang D.-Y., Chiu J.-F., Lau A.T., *Post-translational modification of human heat shock factors and their functions: a recent update by proteomic approach,* Journal of Proteome Research, (**2012**), *11*, 2625–2634

[206] Stefanopoulou M., *Mass spectrometric analysis of the differential protein expression of living cell systems in the presence of metal-based antitumor compunds*, PhD thesis, (**2011**), Faculty of Chemistry and Biochemistry, Ruhr-University, Bochum, Germany

[207] Yates J. R., Ruse C.I., Nakorchevsky A., *Proteomics by mass spectrometry: approaches, advances, and applications*, Annual Review of Biomedical Engineering, (**2009**), *11*, 49–79

[208] Will J., Wolters D. A., Sheldrick W. S., *Characterization of Cisplatin binding sites in human serum proteins using hyphenated multidimensional liquid chromatography and ESI tandem Mass Spectomety*, ChemMedChem, (**2008**), *3*, 1696–1707

[209] Kerr J.F.R., Wyllie A.H., Currie A.R., Br J, *Apoptosis: a basic biological phenomen with a wide-ranging implication in tissue kinetics*, Cancer, (**1972**), *26*, 239-257

[210] Fésüs L., Demény M.Á., Petrovski G., *Autophagy shapes inflammation*, Antioxidants & Redox Signaling, (**2011**), *14*, 2233-2243

[211] Krysko D.V., Vanden Berghe T., D'Herde K., Vandenabeele P., *Apoptosis and necrosis: detection, discrimination and phagocytosis*, Methods, (**2008**), *44*, 205-221

[212] Torres Andon F., Fadeel B., *Programmed cell death: molecular mechanisms and implications for safety assessment of nanomaterials*, Accounts of Chemical Research, (**2012**), doi 10.1021/ar300020b

[213] Prado-Garcia H., Romero-Garcia S., Morales-Fuentes J., Aguilar-Cazares D., Lopez-Gonzalez J. S., *Activation-induced cell death of memory CD8+ T cells from pleural effusion of lung cancer patients is mediated by the type II Fas-induced apoptotic pathway*, Cancer Immunology and Immunotherapy, (**2012**), *61*, 1065–1080

[214] Högstrand K., Hejll E., Sander B., Rozell B., Larsson L.-G., Grandien A., *Inhibition of the intrinsic but not the extrinsic apoptosis pathway accelerates and drives MYC-driven tumorigenesis towards acute myeloid leukemia*, PloS one, (**2012**), *7*, e31366

[215] Rasola A., Bernardi P., *Mitochondrial permeability transition in Ca^{2+}-dependent apoptosis and necrosis*, Cell Calcium, *50*, (**2011**), 222-233

[216] Mora R., Abschuetz A., Kees T., Dokic I., Joschko N., Kleber S., Geibig R., Mosconi E., Zentgraf H., Martin-Villalba A., Regnier-Vigouroux A., *TNF-alpha- and TRAIL-resistant glioma cells undergo autophagy-dependent cell death induced by activated microglia*, Glia, (**2009**), *57*, 561-581

[217] Clark J.B., Webb R.B., *The site of action of crystal violet*, Stain Technology, (**1955**), *30*, 89–92

[218] Engeland M., Nieland L.J., Ramaekers F.C., Schutte B., Reutelingsperger C.P. *Annexin V-affinity assay: a review on an apoptosis detection system based on phosphatidylserine exposure*, Cytometry, (**1998**), *31*, 1-9

[219] Ponsoda X., Jover R., Castell J.V., Gomez-Lechon M.J., *Measurement of LDH activity in 96-well cultures: a rapid and automated assay for cytotoxic study*, Journal of Tissue Culture Methods, (**1991**), *13*, 21–24

[220] Bradbury D.A., Simmons T.D., Slater K.J., Crouch, S.P.M., *Measurement of the ADP : ATP ratio in human leukaemic cell lines can be used as an indicator of cell viability , necrosis and apoptosis*, Journal of Immunological Methods, (**2000**), *240*, 79–92

[221] Mosmann T., *Rapid colorimetric assay for cellular growth and survival: application to proliferation and cytotoxicity assays*, Journal of Immunological Methods, (**1983**), *65*, 55–63.

[222] Igney F.H., Krammer, P.H., *Death and anti-death: tumour resistance to apoptosis*, Nature reviews. Cancer, (**2002**), *2*, 277-288

[223] Singer S.J., Nicholson G.L., *The fluid mosaic model of the structure of the cell membrane*, Science, (**1972**), *125*, 720-731

[224] Ott I., Scheffler H., Gust R., *Development of a method for the quantification of the molar gold concentration in tumour cells exposed to gold-containing drugs,* ChemMedChem, (**2007**), *2*, 702-707

[225] Volpe D.A., *Application of method suitability for drug permeability classification,* AAPS Journal, (**2010**), *12*, 670–678

[226] Horton K.L., Stewart K.M., Fonseca S.B., Guo Q., Kelley S.O., *Mitochondria-penetrating peptides*, Chemistry & Biology, (**2008**), *15*, 375–382

[227] Lipinski C.A, Lombardo F., Dominy B.W., Feeney P.J., *Experimental and computational approaches to estimate solubility and permeability in drug discovery and development settings,* Advanced Drug Delivery Reviews, (2001), *46*, 3–26

[228] Welz B., Becker-Ross H., Florek S., Heitmann U., *High-Resolution Continuum Source AAS*, Wiley-VCH, (**1999**), 1st version, ISBN 3-527-30736-2

[229] Bings, N. H., Bogaerts A., Broekaert, J.A.C., *Atomic spectroscopy: a review*, Analytical Chemistry, (**2010**), *82*, 4653–4681

[230] Lewen N., *The use of atomic spectroscopy in the pharmaceutical industry for the determination of trace elements in pharmaceuticals,* Journal of Pharmaceutical and Biomedical Analysis, (**2011**), *55*, 653–661

[231] Nguyen-Van D., Radziuk B., Frech W., *A comparison between continuum- and line source AAS for speciation analysis of butyl- and phenyltin compounds*, Journal of Analytical Atomic Spectrometry, (**2006**), *21*, 708-711

[232] Scheffler H., You Y., Ott, I., *Comparative studies on the cytotoxicity, cellular and nuclear uptake of a series of chloro gold(I) phosphine complexes*, Polyhedron, (**2010**), *29*, 66-69

[233] Bradford M.M., *A rapid and sensitive method for the quantitation of microgram quantities of protein utilizing the principle of protein-dye binding*, Analytical Biochemistry, (**1976**), *72*, 248–54

[234] Schafer F.Q., Büttner G.R., *Redox environment of the cell as viewed through the glutathione disulfide / glutathione couple*, Free Radicals and Biological Medicine*,* (**2001**), *30*, 1191–1212

[235] Valko M., Leibfritz D., Moncol J., Cronin M.T.D., Mazur, M., Telser J., *Free radicals and antioxidants in normal physiological functions and human disease*, International Journal of Biochemistry and Cell Biol*ogy*, (**2007**), *39*, 44–84

[236] Lin C.-H., Lin P.-H., *Induction of ROS formation, poly(ADP-ribose) polymerase-1 activation, and cell death by PCB126 and PCB153 in human T47D and MDA-MB-231 breast cancer cells*, Chemico-Biological Interactions, (**2006**), *162*, 181–94

[237] Sander C.S., Chang H., Hamm F., Elsner P., Thiele, J.J., *Role of oxidative stress and the antioxidant network in cutaneous carcinogenesis*, International Journal of Dermatology, (**2004**), *43*, 326–335

[238] Kasapoglu M., Ozben T., *Alterations of antioxidant enzymes and oxidative stress markers in aging*, Experimental Gerontology, (**2001**), *36*, 209–220

[239] Kuang Y., Balakrishnan K., Gandhi V., Peng X., *Hydrogen peroxide inducible DNA cross-linking agents: targeted anticancer prodrugs*, Journal of the American Chemical Society, (**2011**), *133*, 19278–19281

[240] Alborzinia H., Can S., Holenya P., Scholl C., Lederer E., Kitanovic I., Wölfl S., *Real-time monitoring of cisplatin-induced cell death*, PloS one, (**2011**), *6*, e19714

[241] Schatzschneider U., Niesel J., Ott I., Gust R., Alborzinia H., Wölfl S., *Cellular uptake, cytotoxicity, and metabolic profiling of human cancer cells treated with ruthenium(II) polypyridyl complexes [Ru(bpy)2(N--N)]Cl2 with N--N=bpy, phen, dpq, dppz, and dppn*, ChemMedChem, (**2008**), *3*, 1104–1109

[242] Heerdt B.G., Houston M.A, Augenlicht L.H., *The intrinsic mitochondrial membrane potential of colonic carcinoma cells is linked to the probability of tumor progression*, Cancer Research, (**2005**), *65*, 9861–9867

[243] Crimi M., Esposti M.D., *Apoptosis-induced changes in mitochondrial lipids*, Biochimica et Biophysica Acta, (**2011**), *1813*, 551–557

[244] Zhang W., Liu H. T., *MAPK signal pathways in the regulation of cell proliferation in mammalian cells*, Cell Research, (**2002**), *12*, 9–18

[245] Meng F., Zhang H., Liu G., Miller F.R., Wu G., *Protein kinase contributes to oncogenic properties maintenance and resistance to poly (ADP-ribose)-polymerase-1 inhibition in breast cancer*, Neoplasia, (**2011**), *13*, 472–482

[246] Zhang Y., Shen, X., *Heat shock protein 27 protects L929 cells from cisplatin-induced apoptosis by enhancing Akt activation and abating suppression of thioredoxin reductase activity*, Clinical Cancer Research, (**2007**), *13*, 2855–2864

[247] Tanbk K., Li X., Zheng M. Q., Rozanski G. J., *Role of apoptosis signal-regulating kinase-1-c-Jun K^+ channel remodeling of the failing heart: regulation by thioredoxin*, Antioxidant and Redox Signaling, (2011), *14*, 25-35

[248] Rovida E., Sbarba P.D., *p38 and cancer; Yang gets Yin*, Cancer Biology and Therapy, (**2008**), *7*, 1241–1242

[249] Kim N.-H., Oh M.-K., Park H. J., Kim I.-S., *Auranofin, a gold(I)-containing antirheumatic compound, activates keap1/Nrf2 signaling via Rac1/iNOS signal and mitogen-Activated protein kinase activation*, Journal of Pharmacological Sciences, (**2010**), *113*, 246–254

[250] Hatjiharissi E., Ngo H., Leontovich A.A., Leleu X., Timm M., Melhem M., George D, Lu G., Ghobrial J., Alsayed Y., Zeismer S., Cabanela M., Nehme A., Jia X., Moreau A.S., Treon S.P., Fonseca R., Gertz M. A., Anderson K.C., Witzig T.E., Ghobrial I., *Proteomic analysis of waldenstrom macroglobulinemia*, Cancer Research, (**2007**), *67*, 3777–3784

[251] Holenya P., Kitanovic I., Heigwer F., Wölfl S., *Microarray-based kinetic colorimetric detection for quantitative multiplex protein phosphorylation analysis,* Proteomics, (**2011**), *11*, 2129–2133

[252] Naik M.U., Naik, U.P., *Calcium-and integrin-binding protein regulates focal adhesion kinase activity during platelet spreading on immobilized fibrinogen,* Blood, (**2003**), *102*, 3629–3636

[253] Bartscht T., Lehnert H., Gieseler F., Ungefroren H., *The Src family kinase inhibitors PP2 and PP1 effectively block TGF-beta1-induced cell migration and invasion in both established and primary carcinoma cells*, Cancer Chemotherapy and Pharmacology, (**2012**), *70*, 221–230

[254] Jin J., Mullen T.D., Hou Q., Bielawski J., Bielawska A., Zhang X., Obeid L.M., Hannun Y. A., Hsu Y. T., *AMPK inhibitor Compound C stimulates ceramide production and promotes Bax redistribution and apoptosis in MCF7 breast carcinoma cells*, Journal of Lipid Research, (**2009**), *50*, 2389–2397

[255] Kozikowski A.P., Gaisina I.N., Petukhov P.A., Sridhar J., King L.T., Blond S.Y., Duka T., Rusnak M., Sidhu A., *Highly potent and specific GSK-3b inhibitors that block tau phosphorylation and decrease a-synuclein protein expression in a cellular model of Parkinson ' s Disease*, ChemMedChem, (**2006**), *1*, 256–266

[256] Iqbal M. A., Bamezai R.N., *Resveratrol inhibits cancer cell metabolism by down regulating pyruvate kinase M2 via inhibition of mammalian target of rapamycin,* PloS one, (**2012**), *7*, e36764

[257] Gardner A.M., Vaillancourt R.R., Lange-Carter C.A., Johnson G.L., *MEK-1 Phosphorylation by MEK Kinase , Raf , and Mitogen-activated Protein Kinase: Analysis of Phosphopeptides and Regulation of Activity*, Molecular Biology of the Cell, (**1994**), 193–201

[258] Chen J., Sidhu A., *The role of D1 dopamine receptors and phospho-ERK in mediating cytotoxicity. Commentary,* Neurotoxicity Research, (**2005**), *7*, 179–181

[259] Hui L., Bakiri L., Mairhorfer A., Schweifer N., Haslinger C., Kenner L., Komnenovic V., Scheuch H., Beug H., Wagner E.F., *p38alpha suppresses normal and cancer cell proliferation by antagonizing the JNK-c-Jun pathway*, Nature Genetics, (**2007**), *39*, 741–749

[260] Hynes J., Wu H., Pitt S., Shen D.R., Zhang R., Schieven G.L., Gillooly K.M., Schuster D.J., Taylor T.L., Yang X., McIntyre K.W., McKinnon M., Zhang H., Marathe P.H., Doweyko A.M., Kish K., Kiefer S.E., Sack J.S., Newitt J.A., Barrish J.C., Dodd J., Leftheris K., *The discovery of (R)-2-(sec-butylamino)-N-(2-methyl-5-(methylcarbamoyl) phenyl) thiazole-5-carboxamide (BMS-640994)-A potent and efficacious p38alpha MAP kinase inhibitor*, Bioorganic & Medicinal Chemistry Letters, (**2008**), *18*, 1762–1767

[261] Duffy J.P., Harrington E.M., Salituro F.G., Cochran J.E., Green J., Gao H., Bemis G.W., Ghotas E., Galullo V.P., Ford P.J., Germann U.A., Wilson K.P., Bellon S.F., Chen G., Taslimi P., Jones P., Huang C., Pazhanisamy S., Wang Y.-M., Murcko M.A., Su M.S.S., *The discovery of VX-745: a novel and selective p38 kinase inhibitor*, ACS Medicinal Chemistry Letters, (**2011**), 2, 758–763

[262] Sakurai A., Yuasa K., Shoji Y., Himeno S., Tsujimoto M., Kunimoto M., Imura N., Hara S., *Overexpression of thioredoxin reductase 1 regulates NF-kappa B activation*, Journal of Cellular Physiology, (**2004**), *198*, 22–30

[263] Gasdaska J. R., Harney J. W., Gasdaska P.Y., Powis, G., Berry M.J., *Regulation of human thioredoxin reductase expression and activity by 3-untranslated region selenocysteine insertion sequence and mRNA instability elements*, Journal of Biological Chemistry, (**1999**), *274*, 25379–25385

[264] Eidhammer I., *Computational methods for mass spectrometry proteomics*, John Wiley & Sons, (**2007**), 1st version, ISSBN 978047072430904707243 07

[265] Holenya P., Heigwer F., Wölfl S., *KOMA: ELISA-microarray calibration and data analysis based on kinetic signal amplification*, Journal of Immunological Methods, (**2012**), *380*, 10–15